

CRANFIELD UNIVERSITY

J KELVIN

EVAPORATION IN FEN WETLANDS

SCHOOL OF APPLIED SCIENCES

PhD THESIS
2011

Supervisor: T. Hess
June 2011

CRANFIELD UNIVERSITY

SCHOOL OF APPLIED SCIENCES

PhD THESIS

2011

J KELVIN

Evaporation in fen wetlands

Supervisor: T. Hess

June 2011

This thesis is submitted in partial fulfilment of the requirements for the degree of Doctor of Philosophy

© Cranfield University 2011. All rights reserved. No part of this publication may be reproduced without the written permission of the copyright owner.

Abstract

Wicken Fen represents a remnant of the once extensive peat fenlands of East Anglia, which survived large-scale drainage efforts intended to bring land into agricultural production due to its importance within the local economy and subsequently as a site of interest to scientists. Wicken Fen is managed so as to conserve a variety of habitats lost as a result of drainage and therefore does not represent a truly natural environment. Traditional management practices on Sedge Fen, the largest part of Wicken Fen, involve maintaining a 3 – 4 year harvesting cycle and controlling soil water levels. Previous hydrological studies of Wicken Fen have determined that soil water levels are strongly influenced by precipitation and evapotranspiration. The evaporative flux at Sedge Fen is commonly estimated by using meteorological data within empirical formulae such as the Penman Monteith equation owing to measurement difficulties. Furthermore, there has been little investigation of the evaporative loss from fens within the UK. This study aims to investigate the evaporative loss from Sedge Fen so as to better inform hydrological management and to describe evapotranspiration estimation techniques which may be employed at other fen sites. Eddy covariance measurements demonstrated that evapotranspiration from Sedge Fen was typically less than reference evapotranspiration estimates. Evapotranspiration estimates may be improved by consideration of surface parameters which can be described using meteorological data. Meteorological differences existed between Sedge Fen and the surrounding area, resulting in differing evapotranspiration estimates depending on where data was collected. Evapotranspiration measurements were used within a simple water budget model of Sedge Fen and demonstrated the lateral movement of soil water, a hydrological flux previously assumed to be of little consequence within the hydrological balance of Sedge Fen.

Acknowledgements

I would like to acknowledge the Natural Environment Research Council (NERC) as the main sponsors of this research. NERC have also provided me with access to facilities and expertise at the Centre for Ecology and Hydrology (CEH), without which this project would not have been possible. Particular thanks are owed to Dave McNeil and Geoff Wicks for acquiring and assembling the various instrumentation systems and teaching me what I needed to know in a very short space of time. Jon Finch and Jon Evans provided additional instruments which contributed to this study. I am indebted to Charlie Stratford and Adam Sutcliffe for giving up their time to help with installing, upgrading and dismantling the instrumentation at the field sites. I'm also grateful for the efforts of Jimmy McClelland and James Evans in providing the means to travel to Wicken Fen.

The National Trust staff and volunteers at Wicken Fen provided continual support and advice throughout the project. Owen Mountford provided the initial contact with the National Trust and was always happy to share his extensive knowledge of the fen. Martin Lester assisted greatly with the siting and installation of the instrumentation systems at Wicken Fen and provided additional data used within this study. I hope that the findings of this work are of some small use by way of recompense.

Cranfield University was another invaluable source of equipment and advice. I am grateful to Pat Bellamy and Monica Rivas-Casado for providing statistical advice. The Thesis Committee provided regular feedback and encouragement, and I would

like to thank Stephen Evans, Brian McIntosh, Adrian Yallop and Mick Whelan for their contributions.

Hourly water level data were provided by Francine Hughes (Anglia Ruskin University), Peter Stroh (Anglia Ruskin University), The Environment Agency (Anglian Region) and the National Trust at Wicken Fen. I am grateful to these individuals and organisations for allowing me to use their data within this study.

Thanks are also due to Ross Morrison of the University of Leicester. Over the past two years, Ross has gladly shared his experiences of working with an eddy covariance system, and the insights he has gained as a result. I hope my advice has been of equal use, and would like to wish Ross well with the remainder of his project.

I am particularly grateful to my supervisors, Mike Acreman (CEH) and Tim Hess (Cranfield University) for continued support and feedback on everything from research ideas to thesis drafts. Paul Burgess and Richard Harding also helped to keep me on the straight and narrow throughout the project.

Finally, I would like to thank my (long-suffering) family and friends without whose generosity, patience and support I would never have been able to start, never mind finish, this project.

Table of Contents

List of Figures.....	vii
List of Tables.....	xi
Chapter 1: Introduction and Overview.....	1
1.1. Wicken Fen.....	1
1.2. Aims and Objectives.....	12
1.3. Research Questions.....	13
1.4. Thesis Structure.....	16
Chapter 2: Introduction to Wetland Evapotranspiration.....	18
2.1. Wetlands.....	18
2.2. Evaporation.....	25
2.3. Wetland Evapotranspiration.....	32
Chapter 3: Instrumentation, Data Collection and Processing.....	35
3.1. Introduction.....	35
3.2. The Eddy Covariance System.....	35
3.3. The Automatic Weather Station.....	56
3.4. Relative Humidity Stations.....	62
3.5. Stomatal Resistance Measurements.....	63
3.6. Leaf Area Index.....	65
Chapter 4: The Surface Energy Budget at Sedge Fen.....	66
4.1. Introduction.....	66
4.2. Methods.....	71
4.3. Results.....	75
4.4. Discussion.....	101
4.5. Conclusions	109

Chapter 5: Surface Controls on Evapotranspiration at Sedge Fen.....	111
5.1. Introduction.....	111
5.2. Methods.....	115
5.3. Results.....	124
5.4. Discussion.....	146
5.5. Conclusions	154
Chapter 6: Sedge Fen Microclimate	156
6.1. Introduction.....	156
6.2. Methods.....	159
6.3. Results.....	163
6.4. Discussion.....	175
6.5. Conclusions	181
Chapter 7: The Hydrology of Sedge Fen.....	182
7.1. Introduction.....	182
7.2. Methods.....	186
7.3. Results.....	192
7.4. Discussion.....	206
7.5. Conclusions	214
Chapter 8: Conclusions.....	216
8.1. Answering the Research Questions.....	216
8.2. Conclusions.....	223
8.2. Recommendations for Further Research.....	225
References.....	228
Appendix A: Eddy Covariance System Comparison.....	241
A.1. Introduction.....	241

A.2. Methods.....	242
A.3. Results.....	246
A.4. Conclusions	250
Appendix B: The Penman-Monteith Equation.....	254
Appendix C: The Hargreaves Radiation Formulae.....	256
Appendix D:Relative Humidity Probe Comparison.....	257
D.1. Introduction.....	257
D.2. Methods.....	257
D.3. Results.....	258
D.4. Conclusions	261

List of Figures

Figure 1.1: The Fenlands of East Anglia.	1
Figure 1.2: Map of Wicken Fen.	2
Figure 1.3: Wicken Fen and the surrounding area	9
Figure 2.1: Generalised wetland water budget.	24
Figure 2.2: Schematic representation of evaporation.	26
Figure 3.1: Schematic representation of incoming and outgoing energy fluxes at the Earth's surface.	36
Figure 3.2: Schematic diagram representing the operating principle of the HFP01 soil heat flux plate.	43
Figure 3.3: Schematic diagram illustrating the operating principles of the sonic anemometer.	45
Figure 3.4: Schematic diagram illustrating the operating principles of the IRGA.	47
Figure 4.1: Schematic representation of flux source areas.	67
Figure 4.2: Example flux source area prediction demonstrating relative contribution to flux from distance x m upwind of instrumentation according to Schuepp <i>et al</i> (1990)	72
Figure 4.3: Surface energy fluxes recorded at Sedge Fen by the eddy covariance system for: a) 2009 and; b) 2010.	78
Figure 4.4: Net long wave and short wave radiation fluxes at Sedge Fen, 2009.	79
Figure 4.5: Residual energy at Sedge Fen, 2009 and 2010.	91
Figure 4.6: Ranges of latent heat flux and actual evapotranspiration estimates derived by the apportioning of residual energy described in section 4.2.3 for: a) 2009 and; b) 2010.	96

Figure 5.1: Relationship between surface energy absorption and reference evapotranspiration	127
Figure 5.2: Mean weekly actual and reference evapotranspiration estimates for: a) 2009 and; b) 2010.	129
Figure 5.3: Mean weekly albedo at Sedge Fen, 2009 and 2010.	131
Figure 5.4: Weekly mean surface resistance estimates for Sedge Fen: a) 2009 and; b) 2010.	138
Figure 5.5: Mean daily stomatal resistance data recorded by porometer for 2009 and 2010.	140
Figure 5.6: Leaf area index curve compiled from 2009 and 2010 LAI data.	143
Figure 5.7: Mean weekly actual, reference and Sedge Fen Penman Monteith evapotranspiration for: a) 2009 and; b) 2010.	145
Figure 6.1: Comparison of Hargreaves solar radiation estimates and eddy covariance solar radiation measurements.	166
Figure 6.2: Weekly mean temperature anomalies relative to Sedge Fen at: a) Adventurer's Fen and; b) Oily Hall.	167
Figure 6.3: 30-minute mean temperature anomalies relative to Sedge Fen at: a) Adventurer's Fen and; b) Oily Hall.	170
Figure 6.4: Weekly mean diurnal temperature range anomalies relative to Sedge Fen at Adventurer's Fen and Oily Hall.	171
Figure 6.5: Weekly vapour pressure anomalies relative to Sedge Fen at: a) Adventurer's Fen and; b) Oily Hall.	172
Figure 6.6: Weekly mean reference evapotranspiration anomalies relative to Sedge Fen at Adventurer's Fen and Oily Hall.	174
Figure 7.1: Map of Sedge Fen showing locations of dipwells.	187

Figure 7.2: Location of Sedge Fen automated rain gauge atop Wicken Fen Visitor's Centre.	188
Figure 7.3: Monthly water level range 1994 – 2008 and 2009 and 2010 monthly mean water levels at dipwell 9 on Sedge Fen.	193
Figure 7.4: Weekly mean surface resistance and water levels at Sedge Fen during a) 2009 and; b) 2010.	194
Figure 7.5: Comparison of rainfall data from Sedge Fen and Upware, 1996 – 2008.	196
Figure 7.6: Monthly rainfall range 1994 – 2008 and monthly rainfall totals for 2009 and 2010 at Upware.	198
Figure 7.7: Weekly mean actual evapotranspiration as derived by eddy covariance system and estimated evapotranspiration calculated as the residual of the water balance for: a) 2009 and; b) 2010.	200
Figure 7.8: Mean hourly water levels at Sedge Fen, April – September 2009 and 2010.	203
Figure 7.9: Daily specific yield at Sedge Fen, September 2009.	204
Figure A.1: Comparison of 30-minute averaged sensible heat fluxes from R3 eddy covariance system and: a) Original Windmaster system; b) Upgraded Windmaster system.	247
Figure A.2: Comparison of 30-minute averaged latent heat fluxes from R3 eddy covariance system and: a) Original Windmaster system; b) Upgraded Windmaster system.	248
Figure A.3: Cumulative evapotranspiration rates from the R3 system, original Windmaster system and upgraded Windmaster system.	249

Figure A.4: Comparison of 30-minute averaged sensible heat fluxes from original and upgraded Windmaster eddy covariance systems. 250

Figure D.1: Comparisons of vapour pressure anomalies relative to Sedge Fen using 2008 regressions (table 6.1) and 2011 regressions (table D.1) for: a) Adventurers Fen and; b) Oily Hall 260

List of Tables

Table 3.1: Table 3.1: Locations of relative humidity stations.	63
Table 4.1: Summary flux source area characteristics for different wind directions at Wicken Fen, 2009 – 10.	76
Table 4.2: Monthly mean and standard deviation of daily net radiation fluxes at Sedge Fen, 2009 and 2010.	81
Table 4.3: Monthly mean and standard deviation of daily ground heat fluxes at Sedge Fen, 2009 and 2010.	83
Table 4.4: Monthly mean and standard deviation of daily sensible heat fluxes at Sedge Fen, 2009 and 2010.	85
Table 4.5: Monthly mean and standard deviation of daily latent heat fluxes at Sedge Fen, 2009 and 2010.	87
Table 4.6: Monthly mean and standard deviation of daily Bowen ratio at Sedge Fen, 2009 and 2010.	89
Table 4.7: Residual energy as proportion of available energy at Sedge Fen	92
Table 4.8: Monthly mean and standard deviation of daily residual energy at Sedge Fen, 2009 and 2010.	94
Table 4.9: Monthly mean and standard deviation of daily latent heat flux mid-point at Sedge Fen, 2009 and 2010.	98
Table 4.10: Monthly Bowen ratio mid points.	100
Table 5.1: Summary of stomatal resistance data collection periods.	122
Table 5.2: Monthly evapotranspiration estimates from eddy covariance data and reference evapotranspiration estimates from AWS data for Sedge Fen, 2009 and 2010.	125

Table 5.3: Monthly mean and standard deviation of albedo at Sedge Fen, 2009 and 2010.	133
Table 5.4: Monthly mean of zero plane displacement and roughness length at Sedge Fen.	134
Table 5.5: Monthly mean and standard deviation of aerodynamic impedance at Sedge Fen, 2009 and 2010.	136
Table 5.6: Results of Mann-Whitney U tests applied to meteorological variables taken on days of porometry measurements.	141
Table 5.7: Results of Pearson's product moment correlation coefficient applied to stomatal resistance and meteorological data recorded on days of porometry measurements.	142
Table 6.1: Results of comparison of half-hourly temperature and relative humidity data from HMP45Cs at Adventurers' Fen and Oily Hall, relative to that installed on Sedge Fen.	164
Table 6.2: Parameters used for calculating confidence intervals associated with the regressions detailed in table 6.1.	165
Table 6.3: Results of comparisons of daily mean temperature data from Adventurer's Fen and Oily Hall to that at Sedge Fen by means of the Mann-Whitney U test.	168
Table 6.4: Results of comparisons of daily mean vapour pressure data from Adventurer's Fen and Oily Hall to that at Sedge Fen by means of the Mann-Whitney U test.	173
Table 6.5: Summary of reference evapotranspiration data at all stations, 2009 and 2010.	175
Table 7.1: Summary of rain gauges.	189

Table 7.2: Results of comparison of monthly rainfall totals at Sedge Fen to the average of monthly rainfall recorded at Upware and Stretham.	196
Table 7.3: Mean monthly rainfall at Upware (1994 - 2008) and Cambridge (1971 – 2000).	197
Table 7.4: Monthly Evapotranspiration estimates from EC system and water balance.	201
Table 7.5: Hydrological fluxes during periods of zero net soil water level change.	202
Table 7.6: Actual evapotranspiration, water balance evapotranspiration estimates according to McCartney <i>et al</i> (2001) and revised water balance evapotranspiration estimates accounting for inflow and specific yield.	205
Table 8.1: Reference surface parameters and average values of surface parameters at Sedge Fen.	221
Table A.1: Eddy covariance system components.	244
Table A.2: Anemometer temperature calibration results.	245
Table A.3: Results of post-processing verification.	246
Table A.4: Results of comparison of cumulative daily evapotranspiration totals with R3 system.	250
Table D.1: Results of comparison of half-hourly temperature and relative humidity data from HMP45C probes at Adventurer’s Fen and Oily Hall relative to that installed on Sedge Fen.	258

Chapter 1

Introduction and Overview

1.1. Wicken Fen

This study focuses on work undertaken at Wicken Fen. Wicken Fen is within the East Anglian Region of the UK and is located approximately 10 km north east of Cambridge at $52^{\circ}18'N$, $0^{\circ}16'E$ (figure 1.1).

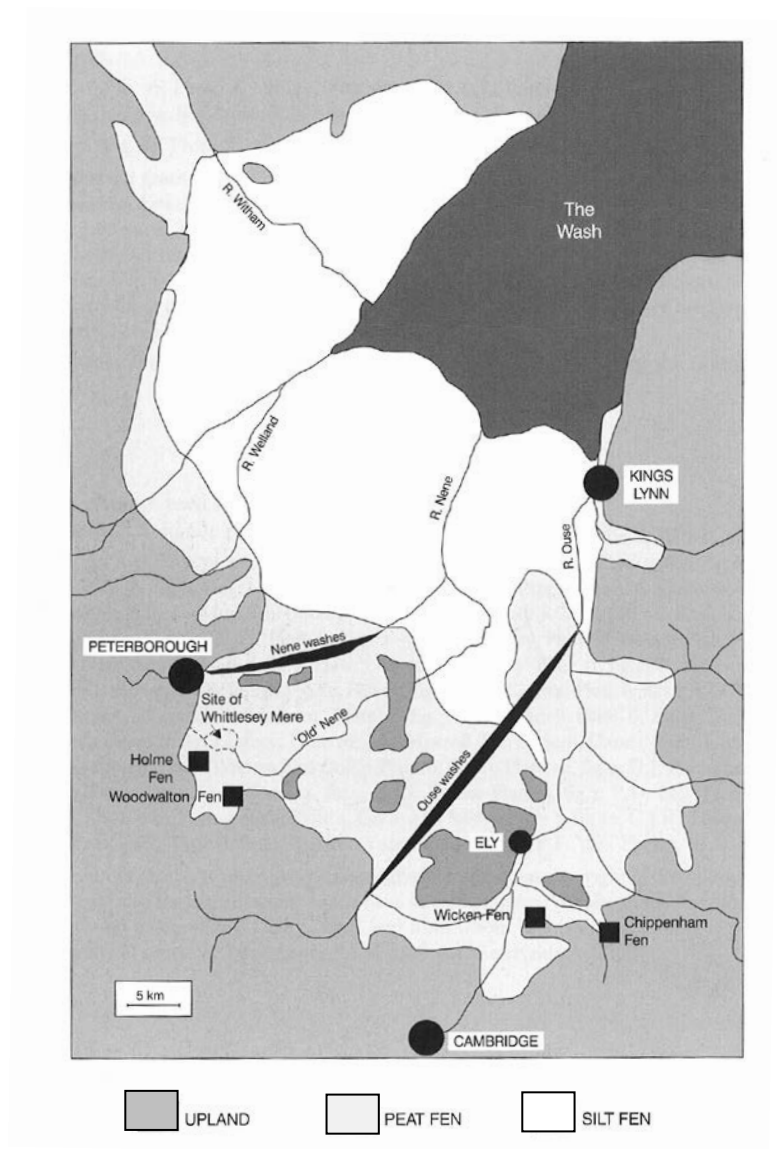


Figure 1.1: The fenlands of East Anglia (from Moore, 1997)

Wicken Fen is owned and managed by the National Trust. The site comprises several fenland vegetation communities, each representing a different stage of ecological succession. The lodes, ditches and meres at Wicken Fen are areas of shallow open water equivalent to early fenland conditions. Reed-beds are the next successional stage, and are found most extensively on Adventurer's Fen (figure 1.2). Further drying encourages the establishment of sedge communities typically found at Sedge Fen. The final stage of ecological succession is represented by the occurrence of woody vegetation as "carr" (scrub) or woodland, which may be found in limited extents on Verrall's Fen and on the margins of Sedge Fen. The diversity of communities maintained at Wicken Fen provides habitats for a wide range of insect and bird species.

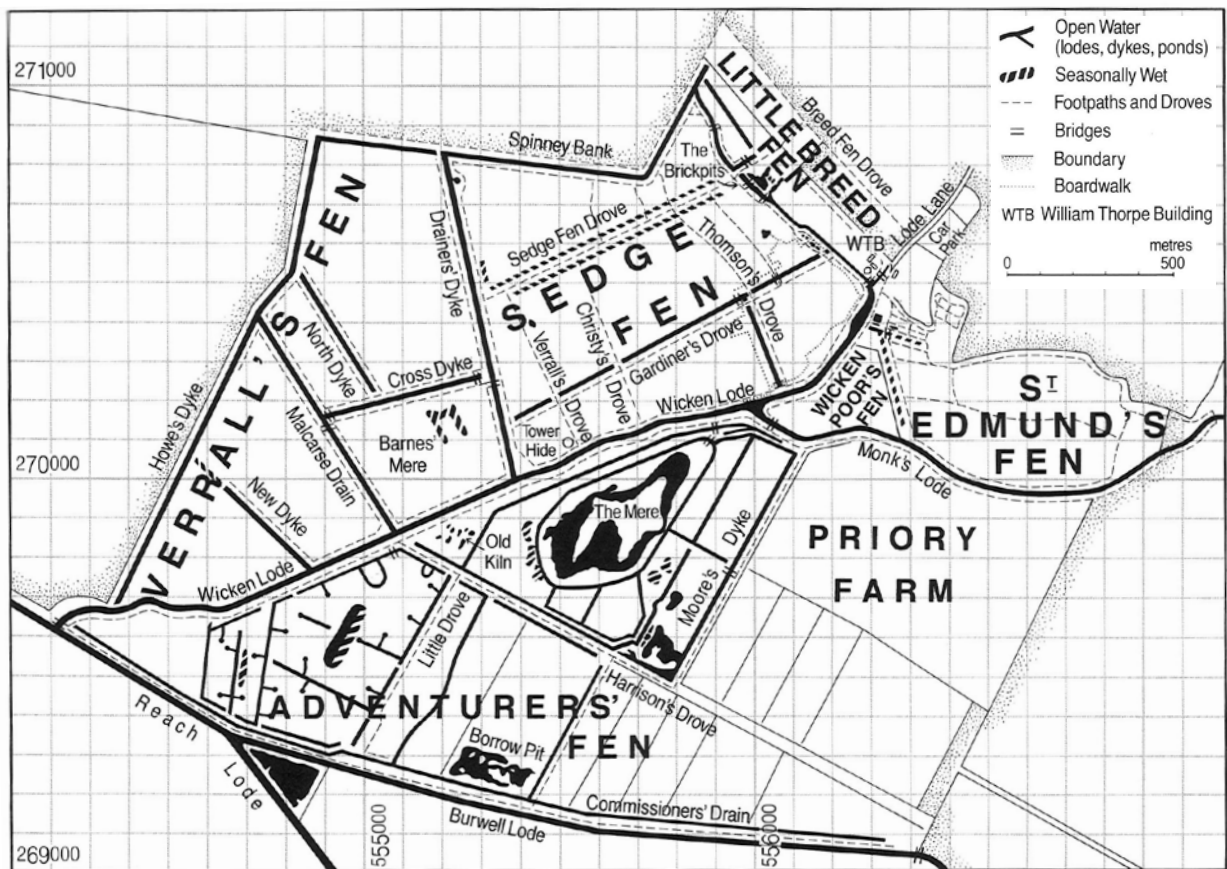


Figure 1.2: Map of Wicken Fen (from Friday, 1997)

1.1.1. History of Wicken Fen

Wicken Fen is located on the southerly margin of the formerly extensive East Anglian fenlands that formed between the uplands of Lincolnshire, Cambridgeshire, Suffolk and Norfolk. Regular flooding events from the sea and the Ouse, Nene, Welland and Witham rivers ensured the entire region remained waterlogged. The fenlands could originally be divided into two regions; the northerly area characterised by the deposition of marine silts from the regular incursion of seawater and the southern area consisting of peat soils formed by the decay of dead vegetation in the waterlogged conditions (Darby 1983; Moore, 1997).

The waterlogged conditions of the East Anglian Fens initially represented a barrier to large-scale human settlement. However, technological advances believed to have been first introduced to Britain by the Romans eventually permitted settlement and economic exploitation of the Fens. Initially, such activities were largely limited to the coastal regions which were drained and gradually expanded by reclaiming land from the sea. By approximately 1100 AD, the coastal regions of the northern siltlands were apparently prosperous. By contrast, large-scale habitation and transformation was not evident in the southern peatlands. What settlements there were generally existed on isolated islands of high ground and were dependent on the surrounding wetlands for resources. For example, Ely is located on high ground to the north of Wicken Fen and was dependent on eels as both a food source and trading commodity. Nevertheless, the peat fenlands largely experienced minimal economic exploitation despite providing vegetation for thatching, fish and wildfowl for food and peat for fuel (Darby, 1983).

Large-scale drainage of the peat Fens commenced in the 17th Century. Much of the Fenland was held as ecclesiastical property until the early 16th Century and religious orders managed their Fenland holdings so as to generate revenue, necessitating small-scale drainage schemes. The dissolution of the monasteries in 1539 resulted in much of the Fenland becoming property of the Crown, and it was subsequently divided between members of the ruling class as reward for service or sold to generate income for the Crown. As a consequence, piecemeal management practices led to a deterioration of the existing drainage infrastructure and thus a loss in the revenue generated from the landholdings. Large scale plans to drain the southern peatlands were first proposed by the Crown in 1620, although progress was interrupted by royal succession and the Civil War. Cornelius Vermuyden, a Dutch engineer with experience of undertaking large drainage projects, was appointed to devise and oversee the drainage of the peatlands. Vermuyden's plans called for the creation of an extensive drainage network including the straightening of natural watercourses and excavation of artificial channels so as to increase the rate at which water could be removed from the peat Fenlands. Work was complete in 1663 and the maintenance of the new infrastructure was written into law under the terms of the General Drainage Act. The drainage of the Fens chiefly resulted in agricultural improvements. Large areas of land had been bought into agricultural production and land values rose in response (Darby, 1983; Harris, 1953; Wentworth-Day, 1954).

However, keeping the newly generated agricultural land in production required ongoing works to resolve unforeseen problems arising from the original drainage scheme. Amongst these was the issue of peat shrinkage, resulting in a lowering of the peat surface due to the drying of the soil. Eventually the land surface to be drained

was at a lower level than the drains created to remove excess water. The solution was to pump water from agricultural land into Vermuyden's drainage network. This created a circular effect in which continued drainage resulted in further peat shrinkage, thus necessitating more efficient pumping mechanisms. Pumping technology was therefore forced to keep pace with these needs, resulting in successive shifts from widespread use of wind-driven pumps to steam-driven pumps and subsequently to modern electrically powered pumping mechanisms in order to maintain the removal of excess water from the reclaimed agricultural land (Darby, 1983; Wentworth-Day, 1954).

Despite the large-scale drainage of the East Anglian peat fens, Wicken Fen persists as an example of a peat wetland. However, it is important to note that this is not a natural landscape, rather one that reflects the retention of management practices that pre-date the drainage schemes. Early management efforts at Wicken Fen developed in response to the commodification of the vegetation found there, particularly sedge. Sedge was an important material within multiple sectors of the local economy, being used for thatching, fuel, domestic and agricultural litter and fodder. It is likely that the proximity of Wicken Fen to large population centres such as Ely and Cambridge meant that Wicken was an important source of sedge, whilst the draining of other sedge production sites in the region (such as Whittlesey Mere and Burwell Fen) served to enhance the importance of sedge production at Wicken Fen. Following failed attempts at preventing winter flooding at Wicken Fen as part of the wider drainage programme, the land was adjudged to be of little agricultural value and thus sedge harvesting continued in spite of the drainage efforts (Rowell, 1997; Wentworth-Day, 1954).

During the 19th Century the value of sedge began what was to ultimately prove a terminal decline. Wicken Fen appears to have survived the collapse of the sedge industry by becoming a site of interest to botanists and entomologists. Once again, the proximity to Cambridge – and in particular, the University of Cambridge – played an important role in the recognition of the value of Wicken Fen. The Fen became a study site for researchers from the University and regular field trips were established as part of Undergraduate studies. Undergraduates are also known to have used the Fen for leisure activities such as hunting. The increasing interest in the natural history of Wicken Fen culminated in the acquisition of portions of the Fen by individuals who subsequently bequeathed or sold their holdings to the National Trust. The National Trust first took ownership of part of Sedge Fen in 1899 and have since expanded their holdings to the present extent, managing the entire area for conservation purposes (Rowell, 1997; Wentworth-Day, 1954).

1.1.2. Conservation at Wicken Fen

Wicken Fen may therefore be considered to be of interest from both social and natural history perspectives, and both are promoted by the National Trust. The biota of Wicken Fen have long been studied, providing valuable historical records of ecological changes for a range of species. Consequently, Wicken Fen has acquired national and international recognition for its importance to conservation and has attained several designations intended to protect the Fen and ensure ongoing conservation efforts.

Wicken Fen was designated as a Site of Special Scientific Interest (SSSI) in 1983 under the Wildlife and Countryside Act 1981¹. The diversity of flora and fauna found at Wicken Fen was specifically cited as a reason for awarding SSSI status² (Lock *et al*, 1997). Corbet *et al* (1997) note that records of dragonflies have been made at Wicken Fen for more than 100 years, revealing that just over half of all native British species breed at Wicken Fen. The breeding success of these insect depends on the availability of open water, thus making the lodes, ditches and meres of Wicken Fen ideal locations for the conservation and study of dragonfly species.

The conservation value of Wicken Fen was further recognised by designation as a National Nature Reserve in 1993 and a Ramsar site in 1995. Recognition as a Wetland of International Importance under the terms of the Ramsar Convention was awarded as a result of the diverse habitats found at Wicken Fen, as well as for supporting endangered plant species such as the fen violet (*Viola persiciflora*) and vulnerable species such as milk-parsley (*Peucedanum palustre*). The occurrence of such species allows for scientific investigation with a view to expanding existing populations and informing re-introduction programmes at other sites. The fen violet is subject to such monitoring at Wicken Fen as part of a species recovery programme. Milk-parsley is the larval food plant of the swallowtail butterfly (*Papilo machaon britannicus*), and is thus important to ongoing monitoring of efforts to re-establish the swallowtail at Wicken Fen. Both of these projects are also cited within the Ramsar

¹ <http://jncc.defra.gov.uk/page-3614>

² http://www.sssi.naturalengland.org.uk/citation/citation_photo/1003251.pdf

notification for Wicken Fen³ (Corbet *et al*, 1997; Friday *et al*, 1997; Lock *et al*, 1997; Walters, 1997).

1.1.3. The Hydrology of Sedge Fen

The work reported within this study was undertaken on Sedge Fen (figure 1.2), and thus subsequent descriptions focus on this area of Wicken Fen.

Historically, Sedge Fen was subject to winter flooding from Wicken Lode whilst summer was typified by lower water levels. The installation of a sluice and pump at Upware, where the lode meets the River Cam (figure 1.3), in the 1940s has served to stabilise the lode levels and prevent the inundation of the Fen. Water is distributed across Sedge Fen via a network of open channels connected to Wicken Lode (figure 1.2). As well as water distribution, hydrological management at Sedge Fen has entailed water retention. Owing to peat shrinkage (section 1.1.1), the agricultural land to the north of Sedge Fen is at a lower elevation than the surface of Sedge Fen, thus permitting seepage of water from the Fen through Spinney Bank and Howe's Bank. This was incompatible with both the conservation objectives at Sedge Fen and agricultural interests, and so an impermeable membrane was installed along the northern boundary of Sedge Fen in the late 1980s so as to prevent this transfer of water (Friday and Rowell, 1997; Lock *et al*, 1997).

³ <http://www.wetlands.org/reports/ris/3UK091RIS2005.pdf>



Figure 1.3: Wicken Fen and the surrounding area. Locations of instrumentation used within this study are highlighted. © Crown Copyright/database right 2011. An Ordnance Survey/ EDINA supplied service.

The earliest investigations of the hydrological regime at Sedge Fen were undertaken by Godwin (1931), and demonstrated that soil water levels were lower in summer than winter. This variation was shown to be independent of the rainfall observed at Sedge Fen and of ditch water level fluctuations, leading Godwin (1931) to conclude that enhanced summer transpiration loss from the vegetated surface was the mechanism by which water levels were lowered. Further investigations by Godwin and Bharucha (1932) determined that ditch water levels influenced soil water levels in areas immediately adjacent to ditches, serving to stabilise soil water levels in these areas. The seasonal variation of soil water levels in areas removed from the ditch network therefore produces a seasonal variation in the shape of the water table, thus

the ditches serve as drainage channels during winter and irrigation channels during summer.

Subsequent investigations by Gowing (1977) and Gilman (1988) have served to confirm the findings of Godwin (1931) and Godwin and Bharucha (1932). The hydrological parameters therefore believed to determine soil water levels at Sedge Fen are precipitation, evapotranspiration and ditch water levels. However, since Godwin and Bharucha (1932) demonstrated that ditch water levels only influence soil water levels within narrow regions adjacent to ditches, this parameter is not believed to control soil water levels throughout most of the Fen. Sedge Fen is hydrologically isolated by the impermeable membrane within the northern boundary and a layer of impermeable clay beneath the peat layer (Friday and Rowell, 1997), thus precluding the exchange of water between Sedge Fen and the surrounding landscape by other means.

1.1.4. The Vegetation of Sedge Fen

The diverse vegetation communities of Wicken Fen persist due to ongoing human management, thus arresting the natural process of ecological succession (Godwin, 1929). In the case of Sedge Fen, the important management practices maintaining the vegetation community are the control of soil water levels and the implementation of an appropriate cutting regime.

The great fen sedge (*Cladium mariscus*) has historically been the dominant vegetation species at Sedge Fen, although the common reed (*Phragmites australis*) also occurs abundantly. *C. mariscus* can typically be found in waterlogged environments in which the roots are below the level of the water table. Oxygen is supplied to the submerged parts of the plant by means of diffusion through internal channels. Owing to the physiology of *C. mariscus*, the internal diffusion of oxygen is dependent on the depth to which it is submerged thus limiting it to areas of shallow water or waterlogged soil (Conway, 1936; 1938). *C. mariscus* would therefore have been capable of persisting despite the winter flooding once typical at Sedge Fen (section 1.1.3).

Traditional vegetation management practices at Sedge Fen developed in response to the commodification of the sedge, which was harvested for a variety of uses (section 1.1.1). Summer harvesting of 3 or 4 year old sedge became established as standard practice by the mid-15th Century, likely due to the preference of thatchers for sedge of such an age. This practice continued until the acquisition of Sedge Fen for conservation purposes in the late 19th Century. During the early 20th Century there was much debate regarding the appropriate cutting regime for sedge and a practice of winter cutting was implemented, although not strictly adhered to. This new management practice ultimately led to a decline in sedge and the colonisation of Sedge Fen by carr. Current harvesting practices are informed by this experience; following extensive carr clearance on Sedge Fen, a traditional management regime was once again implemented. Vegetation is currently harvested every 3 or 4 years. Sedge Fen is divided into numerous compartments which are cut in different years, thus producing a mosaic of vegetation stands of varying ages. This cutting regime

therefore preserves the vegetation community at Sedge Fen by arresting the process of natural succession (Lock *et al*, 1997; Rowell, 1997).

1.2. Aims and Objectives

The quantification of hydrological fluxes in wetland environments is important for the definition of accurate water budgets to inform effective continued management. Many hydrological fluxes are commonly measured, such as rainfall or soil water levels, and thus are much studied. However, quantification of the evaporative loss is inherently difficult owing to the gaseous state of the water involved. The evaporative flux has therefore typically been estimated according to empirical formulae or as the residual of the water budget if all other components are known.

Recent developments in instrumentation technology now permit the measurement of the evaporative flux using fast response sensors. However, the expertise and expense required to maintain such systems often makes them impractical for operational quantification of evaporative loss and so they are typically utilised for research applications. Nevertheless, such systems have been deployed in a range of wetland environments worldwide (Acreman *et al*, 2003; Lafleur and Roulet, 1992; Li *et al*, 2009; Kellner, 2001; Thompson *et al*, 1999). Within the UK, the evaporative loss from many wetland environments has been investigated using such systems, although no studies of the evaporative flux from fenlands exist within the literature.

The Fens of East Anglia are situated in one of the driest regions of the UK. In addition, there is competition within the region for available water resources from a large agricultural sector and an increasing population (Anglian Water, 2007). Given this relative scarcity of, and high demand for, water in East Anglia accurate quantification of hydrological fluxes for wetland management purposes is of enhanced significance for ongoing conservation efforts.

The aim of this research is therefore to improve the understanding of the evaporative flux from UK fens, with particular reference to Sedge Fen. The primary objective is to quantify the evaporative loss at Sedge Fen using the eddy covariance technique. These measurements will provide a benchmark against which evaporative loss estimates for Sedge Fen may be compared. Hydrological management is likely to be informed by estimates of evaporative loss, rather than measurements from sophisticated instrumentation. Therefore, a secondary objective is to evaluate such estimates relative to the eddy covariance data and to propose modifications if appropriate.

1.3. Research Questions

In order to fulfil the objectives detailed in the previous section, several research questions were proposed. The research questions are:

1. What is the energy balance at Sedge Fen?

The description of the energy balance will serve as a quality control procedure, highlighting any inconsistencies within the surface flux data generated by the eddy covariance system. Any inconsistencies identified within the flux data may be addressed and rectified, thus validating the latent heat flux data from which estimates of the evaporative loss are derived.

2. What is the actual evaporative loss from Sedge Fen?

The latent heat flux data gathered by the eddy covariance system may be used to derive actual evapotranspiration data. Evapotranspiration has never previously been measured at Sedge Fen, but rather has been estimated by standardised techniques or from water budget models. The evapotranspiration data from the eddy covariance system will therefore provide the first direct measurements of the evaporative flux at Sedge Fen.

3. How accurately can the evaporative loss at Sedge Fen be modelled?

The actual evapotranspiration data derived from the eddy covariance flux measurements provides a benchmark against which evapotranspiration estimates may be compared. This will allow an assessment of the accuracy of evapotranspiration estimation techniques at Sedge Fen.

4. What are the controls on the evaporative loss at Sedge Fen, and how can they be modelled?

Evapotranspiration estimation methods are based on parameterisations of those surface factors believed to exert an influence over the evapotranspiration flux. Such parameterisations may be standardised to represent a reference surface. Meteorological measurements taken at Sedge Fen may be used to model the surface characteristics of the Fen, permitting comparison with the reference surface parameters and demonstration of the control exerted by these factors on evapotranspiration estimates.

5. Does Sedge Fen experience a microclimate relative to the surrounding area which may affect estimates of the evaporative loss?

Previous studies have identified wetland microclimates. Comparison of meteorological measurements taken at Sedge Fen and in former arable land typical of the surrounding area determines whether such an effect can be observed at Sedge Fen. The existence of a wetland microclimate may have implications for wetland evapotranspiration estimates if meteorological data collected outside the wetland is assumed to be representative of the wetland.

6. How does the actual evaporative loss affect the current hydrological understanding of Sedge Fen?

Evapotranspiration is assumed to represent a major hydrological flux at Sedge Fen. The evapotranspiration flux measured by the eddy covariance system allows

the examination of the water budget using measurements of all the major terms within the conceptual water budget. This will permit evaluation of the present understanding of the hydrological functioning of Sedge Fen.

1.4. Thesis Structure

Chapter 2 provides an introduction to concepts such as the importance of quantifying the evaporative flux to wetland management. This provides the background context to the research described within the thesis.

Chapter 3 describes the instrumental systems and measurement techniques employed to gather the data upon which subsequent analyses are based. The eddy covariance system is of particular importance and so the underlying theory upon which this system is founded is outlined. Processing routines applied to the eddy covariance data are described so as to fully record all aspects relating to the manipulation of the data.

The analysis chapters collectively address the research questions defined in section 1.3. Chapter 4 describes the energy balance of Sedge Fen, therefore quantifying the evaporative loss from Sedge Fen and addressing research questions 1 and 2. Chapter 5 describes the measured evapotranspiration in greater detail and compares measured and estimated evapotranspiration. The surface characteristics at Sedge Fen are modelled and compared to those of the standardised reference surface. Thus chapter 5 addresses research questions 2, 3 and 4. Chapter 6 investigates whether a microclimate can be identified at Sedge Fen and therefore addresses research question

5. Chapter 7 investigates the water budget at Sedge Fen using the measured evapotranspiration data. Attempts are also made at improving evapotranspiration estimates for Sedge Fen based on water budget calculations. Chapter 7 therefore addresses both research questions 3 and 6.

The results of all analyses are discussed within the context of the research objectives in chapter 8 and recommendations are made regarding possible opportunities for further research arising from the findings of this study.

Chapter 2

Introduction to Wetland Evapotranspiration

2.1. Wetlands

2.1.1. Definition

A formal scientific definition of wetlands is a problematic concept. “Wetland” is a generic term intended to cover a range of ecosystems including swamps, mires, fens and bogs. However, recent developments in national and international legislation relating to wetland environments (see section 2.1.3) have highlighted the need to formally define the term “wetland” based upon rigorous scientific criteria (Acreman and José, 2000; Mitsch and Gosselink, 2000).

In order to define wetlands, characteristics common to all such environments that distinguish them from all other environments must be identified. Hydrology is the most important feature of wetland ecosystems, as reflected in the main components of the common wetland definitions listed by Mitsch and Gosselink (2000):

1. The presence of water, either at the surface or in the root zone.
2. Unique soil conditions differing from adjacent uplands
3. The presence of vegetation adapted to the wet conditions (hydrophytes) and absence of flood-intolerant species.

However, even these characteristics are not conducive to the formulation of an absolute definition of wetlands. The extent, depth and duration of flooding may vary

between wetlands and even within the same wetland from year to year. Wetlands may also be viewed as extensions of adjacent terrestrial and aquatic ecosystems, incorporating the characteristics of each and thus implying that wetlands have no separate identity. Problems also arise in using plant and animal species as indicators typical of wetlands. Species found in wetlands include those that have evolved to survive in both wet and dry conditions (Mitsch and Gosselink, 2000; Williams, 1990a).

The reduction of wetlands to the most basic components overlooks the interaction of the individual components that result in the creation of highly diverse and finely balanced ecosystems. Such interactions result in wetlands performing environmental functions, some of which may be translated into benefits to human society (see section 2.1.2). Any definition must therefore be suitably general, identifying the important features of a wetland without prescribing absolute criteria. An internationally recognised definition is that adopted by the Convention on Wetlands of International Importance:

“areas of marsh, fen, peatland or water, whether natural or artificial, permanent or temporary, with water that is static or flowing, fresh, brackish or salt including areas of marine water, the depth of which at low tide does not exceed 6 metres”

(Mitsch and Gosselink, 2000; p. 31)

Within such a definition, wetlands may be categorised according to location, hydrological features, characteristic ecosystem or a hierarchy incorporating these and

other criteria (Acreman and José, 2000; Bullock and Acreman, 2003; Mitsch and Gosselink, 2000; Williams, 1990a).

2.1.2. Wetlands and Human Society

Wetlands are found on every continent except Antarctica and in every climatic zone and are commonly estimated to account for approximately 6% of the Earth's land surface. Wetlands perform several important ecosystem functions that may be said to be important to the development and maintenance of human cultures and societies. The most notable such function is food production. The domestication of wetland ecosystems was first practiced by ancient human civilisations, and is still practiced so as to produce foodstuffs such as rice and crayfish. Wetland vegetation may provide building materials such as timber or reeds for thatching. Even wetland soils may be utilised to fulfil human needs. Many nations have a long history of extracting peat soils for use as a fuel. Several ancient civilisations sustained large settlements by creating water distribution networks dependent on wetlands. Wetlands may also function as recreational spaces for human societies, offering the populace the opportunity to participate in activities such as fishing and hunting for sport or conservation projects (Maltby, 1986; Mitsch and Gosselink, 2000; Wentworth-Day, 1954).

Despite the contribution of wetlands to human societies, such environments came to be perceived as wastelands with little intrinsic value. Mitsch and Gosselink (2000) identify several works of medieval literature which refer to wetlands in disparaging

terms. Similar references persist into 20th Century popular culture, implying the continuation of negative human attitudes regarding wetlands despite their provision of valuable ecosystem functions. Such attitudes may have arisen from the belief that the productivity of wetlands were insufficient to support rapidly developing societies, and were manifested in the human destruction of wetlands throughout this period of history so as to enhance the production functions beneficial to human societies. For example, within the British Isles during the early middle ages, an expanding population and economy placed increasing demands on the available land resources, notably in terms of demand for land for settlement and agriculture. The draining of the seemingly redundant wetlands provided additional land as well as apparently reducing the natural uncertainty of flooding. The trend of wetland reclamation continued throughout the medieval period, albeit interrupted by plague, economic recession and the dissolution of the estates and monasteries that funded much of the work. Over time, the drained wetlands gave rise to the expansion of arable agriculture and a rise in land values, thus creating an economic feedback that encouraged further wetland conversion. The rate of conversion also increased due to novel technologies such as wind-powered and, subsequently, steam-powered pumping mechanisms and tile drains. Throughout the early 20th Century, the UK government assumed control of drainage operations from local landowners, partly due to an agenda of national self-sufficiency likely influenced by the increasing impact of wartime blockades on food supplies that occurred in this period. As a result of historical wetland drainage, some of the UK's most productive agricultural land is located upon former wetlands; for example, the fens of East Anglia. It has been estimated that as much as 90% of UK wetlands have been lost since Roman times. Similar trends were prevalent in other nations. Within the United States, wetland drainage was accepted practice, leading to

the establishment of major cities such as Chicago and Washington, D.C. in part on drained wetlands. Such trends are not necessarily confined to economically developed nations. For example, Mexico City is located on the site of a lake and associated wetlands that have been drained as the result of human activity during the past 400 years (Mitsch and Gosselink, 2000; Hume, 2008; Maltby *et al*, 2011; Williams, 1990b).

2.1.3. Wetland Conservation, Restoration and Management

By contrast with the historical experience, the modern era has witnessed a trend towards the conservation and restoration of wetland ecosystems, driven by increasing awareness of the beneficial aspects of wetlands. The importance of wetlands was internationally acknowledged by the Ramsar Convention in 1971. This convention aimed to stimulate the international protection of wetlands as habitats for migratory fauna and for the benefit of human populations dependent on wetlands. Subsequent international agreements, such as the Convention on Biological Diversity and the European Water Framework Directive also encouraged the preservation and restoration of wetland ecosystems (Acreman and José, 2000; Acreman *et al*, 2007; Mitsch and Gosselink, 2000; Williams, 1990c).

The restoration of degraded wetlands and conservation of surviving wetlands requires dedicated management. Consideration must be given to the objectives of a particular wetland management scheme. Mitsch and Gosselink (2000) list a range of possible objectives of wetland management schemes, such as wildlife enhancement,

agricultural production and scientific inquiry. Where management seeks to attain multiple objectives, it must be acknowledged that some objectives may be mutually exclusive and so consideration must be given to the practicality of multipurpose management schemes. So as to assess whether management objectives are being achieved, wetlands require close monitoring in order to assess the effectiveness of the conservation and restoration practices employed. Within the UK, wetlands are typically owned and managed by government agencies such as Natural England, wildlife conservation organisations such as the Royal Society for the Protection of Birds or heritage bodies such as the National Trust and often have some form of legal designation as important conservation areas.

2.1.4. Wetland Hydrology

The hydrology of a wetland creates its unique physiochemical conditions, and thus wetland management is an exercise in hydrological management. Successful management therefore depends upon sufficient knowledge of the existing hydrological regime at a site as well as the regime required to satisfy the management objectives. The key hydrological parameter of a wetland is the water level which is a function of the capacity of a wetland to store water, being influenced by landscape morphology, local soil and geology and the balance between the inflows and outflows of water to and from the wetland. The balance between inflows and outflows is known as the water budget and is represented schematically in figure 2.1.

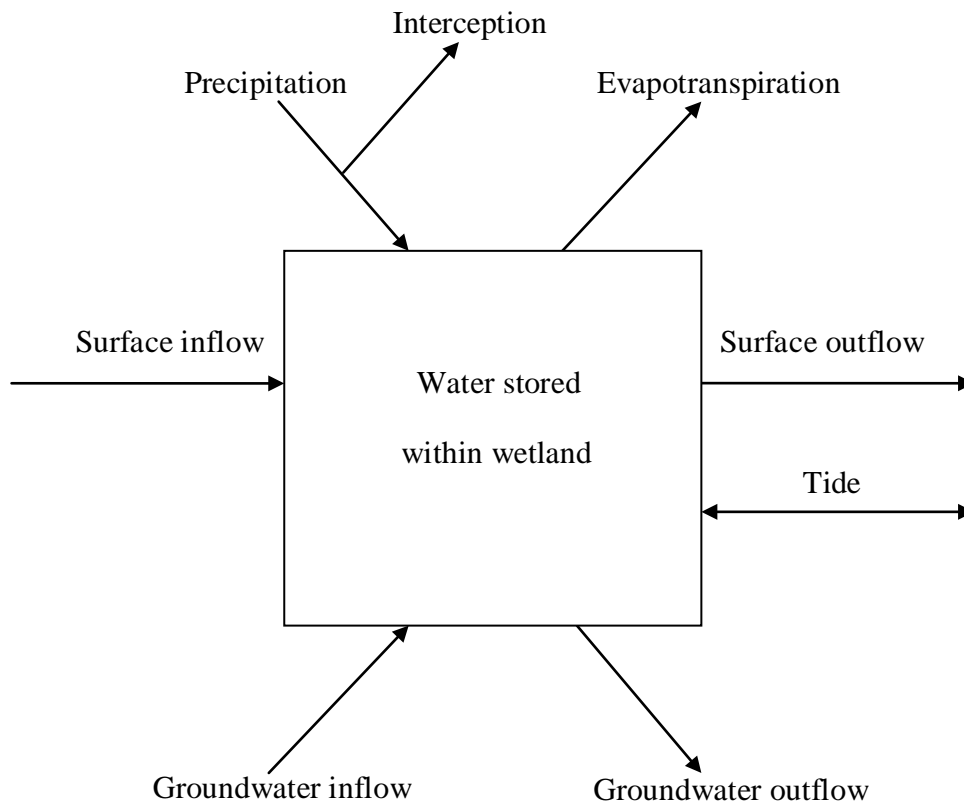


Figure 2.1: Generalised wetland water budget (Mitsch and Gosselink, 2000)

Wetland management may also involve the active manipulation of the water storage at a wetland by exercising control over either the inflows to or outflows from a site. For example, water levels within a wetland may be controlled using a network of surface ditches which water may be transferred to or removed from by sluices and pumps. Particular water levels will be defined by the management objectives and may be seasonally variable (Acreman *et al*, 2003; 2007; Duever, 1988; Gasca-Tucker *et al*, 2007).

2.2. Evaporation

Evaporation may be qualitatively described as the process by which a liquid is converted into a gaseous state (Ward and Robinson, 2000). This study is concerned with the evaporative process converting liquid water into water vapour. This section outlines the relevant physical theory describing the evaporative process and methods of evaporation measurement and estimation.

2.2.1. Physical Mechanisms of Evaporation

At the molecular level, evaporation is the exchange of water molecules between a water surface and the atmosphere, schematically illustrated in figure 2.2. Molecules in the liquid phase are in constant motion and thus possess kinetic energy. The addition of energy to the water body will therefore raise the kinetic energies of the constituent molecules. Those liquid molecules near the surface of the water body may attain sufficient energy to escape the liquid, thus attaining a gaseous state within the atmosphere immediately above the surface of the water body. The number of molecules escaping the water surface is related to the energy available to them (Shuttleworth, 1993; Wallace and Hobbs, 2006; Ward and Robinson, 2000).

Water vapour molecules within the atmosphere exert a pressure, known as the vapour pressure, which is additional to the atmospheric pressure. As the vapour pressure increases, water molecules may be returned to the liquid phase by the process of condensation. Evaporation may therefore be considered as the difference between the rates of vaporisation and condensation, and as such is controlled by the energy input

to a body of water and the atmospheric vapour pressure. If the vapour pressure increases to a critical value, the rates of vaporisation and condensation are equal and the air is said to be saturated. This critical vapour pressure is known as the saturation vapour pressure (Shuttleworth, 1993; Wallace and Hobbs, 2006).

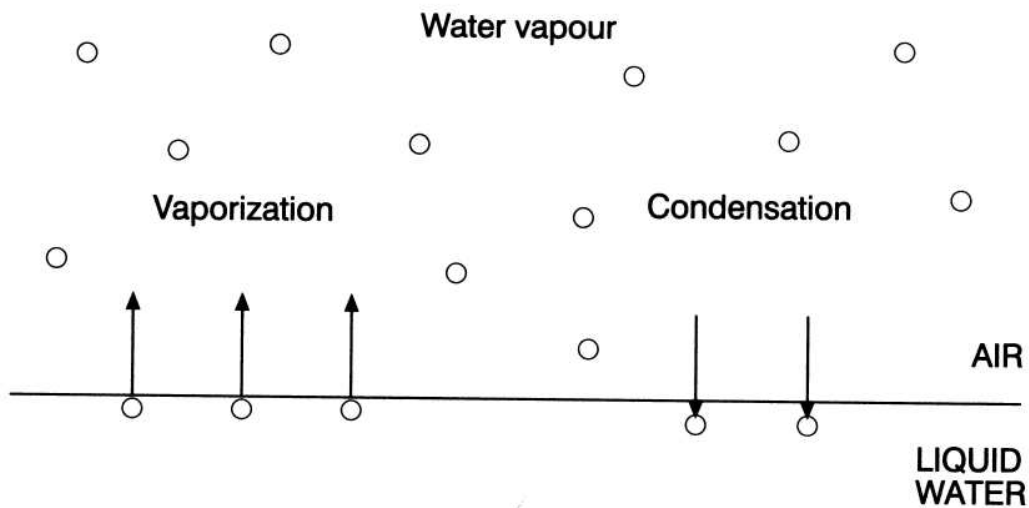


Figure 2.2: Schematic representation of evaporation (Ward and Robinson, 2000)

If water vapour molecules are removed from the atmosphere immediately above the water surface by a mechanism other than condensation, then the atmosphere will not attain saturation and evaporation may continue indefinitely. Water vapour is typically removed from the lowest layers of the atmosphere by means of turbulent transport. Turbulence may be thermally or mechanically generated. Thermally generated turbulence is associated with convection within the atmospheric boundary layer. Mechanically generated turbulence arises due to shear stress within the horizontal airflow. The surface exerts a frictional drag upon the wind, resulting in lower wind speeds nearer to the surface than at greater height. This vertical wind shear leads to an unstable flow comprised of turbulent eddies, which serve to transport momentum,

heat and water vapour vertically through the turbulence layer. The depth of the atmosphere through which the frictional influence of the surface acts depends upon the roughness of the surface, with rougher surfaces creating deeper turbulence layers. Thus the characteristics of the turbulence layer are a function of mean wind speed and surface roughness (Garratt, 1992; Oke, 1987; Shuttleworth, 1993; Ward and Robinson, 2000).

Several studies have borne out the theoretical understanding of the evaporative process outlined above. For example, the works of Eaton and Rouse (2001), Izadifar and Elshorbagy (2010) and Souch *et al* (1996) demonstrated correlations between evaporation and net radiation, whilst Lafleur and Roulet (1992) and Kellner (2001) identified correlations between available energy (defined as net radiation less ground heat flux) and evaporation. Such findings are consistent with the concept of evaporation being driven by the addition of energy to a body of water. Souch *et al* (1996) also demonstrated a positive relationship between vapour pressure deficit (defined as the difference between saturation vapour pressure and vapour pressure) and the water vapour flux. This evidence is consistent with the theoretical description of evaporation previously presented, suggesting that the atmospheric water vapour content controls the evaporation rate. However, it must be acknowledged that the atmospheric water vapour content is likely to be influenced by the evaporation rate, raising the possibility of a feedback in which high evaporation rates result in atmospheric saturation and thus the suppression of evaporation. Wind speed has also been shown to be positively correlated with water vapour fluxes by Souch *et al* (1996) and Izadifar and Elshorbagy (2010), providing observational verification of the theory

relating to the contribution of turbulent transport within the atmosphere to the evaporative flux.

2.2.2. Transpiration

Transpiration is the molecular diffusion of water vapour from within vegetation. Plants extract water from soil through their root networks and subsequently transport water throughout their internal tissues. Within leaves, water evaporates from cell walls, causing the air within the leaf to approach saturation. This water vapour diffuses into the atmosphere through leaf pores known as stomata since the atmospheric vapour pressure is typically lower than that inside the leaf. The primary function of stomata is to allow atmospheric carbon dioxide to enter the internal leaf tissues by diffusion, where it is utilised in photosynthesising nutrients. Thus transpiration may be regarded as an inevitable by-product of photosynthesis. Transpiration may be regulated by guard cells which may open or close the stomatal aperture in response to external environmental or internal physiological factors. The stomatal aperture is known to respond to irradiance, humidity, temperature, carbon dioxide concentration within the plant and leaf water status, although the precise nature of these responses are species dependent. Thus stomata operate to optimise the balance between the carbon dioxide uptake and water loss of a plant (Brutsaert, 2005; Jones, 1992; Monteith and Unsworth, 1990; Shuttleworth, 1993; Ward and Robinson, 2000).

Transpiration therefore represents an alternative process of molecular diffusion to that of evaporation described in section 2.1.1. On vegetated surfaces, these mechanisms may operate simultaneously to transfer water from the surface to the atmosphere. Differentiating the relative proportions of water transfer by evaporation and transpiration is extremely difficult, and so the two processes are collectively referred to as evapotranspiration. (Monteith and Unsworth. 1990; Shaw, 1994)

2.2.3. Evapotranspiration Measurement

Evapotranspiration may be measured as either the loss of liquid water from the surface or as the rate of gain of water vapour by the atmosphere. The former method assumes a closed hydrological system and quantifies the net loss of water from that system, based upon a water balance (by mass or volume) for the water in a specified volume. The most simplistic example of such methods is the evaporation pan, in which the open water evaporation may be measured as the residual of the water balance for the pan. However, errors may occur due to design, siting or leakage of the pan (Gangopadhyaya *et al*, 1966; Shuttleworth, 1993). Lysimeters are hydrologically isolated devices in which soil may be placed and planted with vegetation so as to measure water loss by monitoring the change in water storage within the lysimeter. The inclusion of a vegetated surface within lysimeters permits the measurement of evapotranspiration, although care must be taken to ensure the soil profile and vegetation canopy within the lysimeter are representative of the surface being studied. Consideration must also be given to the drainage of excess water percolating through the soil mass and the design of lysimeter walls, which may influence thermal exchange between the soil masses inside and outside the lysimeter and the dissipation

of incident solar energy (Aboukhaled *et al*, 1982; Gangopadhyaya *et al*, 1966). Evapotranspiration can also be estimated at the catchment scale in situations with extensive hydrological monitoring. However, considerations relating to estimates of area average precipitation and unmeasured seepage may lead to large errors in watershed scale evapotranspiration estimates based on water balance calculations (Shuttleworth, 1993).

Atmospheric vapour gain methods involve quantifying the flux of water vapour from the evaporating surface with micrometeorological instrumentation. The development of high-frequency instrumentation and increasingly powerful microprocessors during the 1970s allowed for evapotranspiration measurements based upon turbulent exchange within the near-surface atmosphere. Examples of these measurement techniques are the Bowen ratio method, in which evapotranspiration is determined from atmospheric water vapour and temperature profiles and measurements of surface energy fluxes, and the eddy covariance method, which is described in detail in chapter 3 (Shuttleworth; 1993; 2007).

2.2.4. Evapotranspiration Estimation

Prior to the development of micrometeorological instrumentation to directly measure evapotranspiration, techniques based upon the physical mechanisms known to influence evapotranspiration (sections 2.2.1 and 2.2.2) were developed to estimate water vapour loss. Such techniques were largely driven by the agricultural science community with the ultimate goal of determining the water requirements of crops, and

take the form of mathematical formulae in which the input variables are meteorological parameters which may be directly measured and for which historical records exist (Shuttleworth, 1993; 2007). Penman (1948) originally proposed what was subsequently referred to as the Penman method to estimate evaporation from an open water surface. Subsequent revisions of this technique incorporated the influences of a vegetated surface on the water vapour flux. Initially, the inclusion of an aerodynamic resistance term based on wind speed and canopy height attempted to account for the effects of a vegetation canopy on atmospheric turbulence and thus turbulent diffusion of water vapour away from the evaporating surface (Penman, 1956). A later revision of the Penman equation acknowledged the contribution of transpiration to the water vapour flux with the inclusion of a bulk surface resistance term, representing the regulation of the transpiration component of the water vapour flux by vegetation, producing the Penman-Monteith equation (Allen *et al*, 1998; Monteith 1965). The Penman-Monteith equation is presented in Appendix B.

Consideration of the Penman-Monteith equation (Appendix B) demonstrates that the value of evapotranspiration is a function of both meteorological and surface parameters. The surface parameters will depend on the vegetation community present at a site, since the aerodynamic properties of the surface are related to the height of the vegetation canopy (Appendix B) and the stomatal resistance to water vapour transfer is known to be species dependent (section 2.2.2). So as to eliminate the need to define surface parameters for all crops and stages of growth, a reference surface was defined by the FAO as:

“A hypothetical reference crop with an assumed crop height of 0.12 m, a fixed surface resistance of 70 s m^{-1} and an albedo of 0.23” (Allen *et al*, 1998).

The reference surface resembles an extensive, well watered and actively growing grass surface of uniform height. The parameters are based upon previous studies of the physiological and aerodynamic characteristics of grass. By utilising these parameters within the Penman-Monteith equation, the reference evapotranspiration, ET_0 (mm), may be defined for a specified period using meteorological data. Reference evapotranspiration estimates may be utilised in the derivation of evapotranspiration estimates for specific crops with the use of empirical crop coefficients, which represent the ratio of crop evapotranspiration to reference evapotranspiration (Allen *et al*, 1998).

2.3. Wetland Evapotranspiration

Evapotranspiration may be one of the major hydrological fluxes within wetland water budgets, as demonstrated by the findings of Gasca-Tucker *et al* (2007). This study highlights that the dominant hydrological fluxes within a UK wet grassland are those that occur naturally. A small proportion of the hydrological loss from wetlands may be attributable to human activity such as the abstraction of water for domestic or industrial use, although such fluxes are inherently quantifiable. Where wetlands are hydrologically isolated from groundwater flows by impermeable geological layers, the evapotranspiration may become the dominant loss of water from a wetland (Acreman and José, 2000). Wetlands tend to lose more water through evapotranspiration than other land types, such as forests, grasslands or arable land due to dense vegetation cover and saturated or inundated soils typical of wetland

environments (Bullock and Acreman, 2003). High evapotranspiration from wetlands can thus deplete water resources downstream, as demonstrated on the Nile downstream of the Sudd (Sutcliffe and Parks, 1999). The quantification of wetland evapotranspiration is therefore important to facilitate successful hydrological management of the wetland and to determine available water resources on the larger scale.

Previous studies have reported a range of evapotranspiration rates for different wetland environments. For example, sedge meadows in South Africa were found to evaporate between 0.6 and 9.8 mm d⁻¹ during the summer, whilst nearby reedbed evapotranspiration was found to be between 0.2 and 3.3 mm d⁻¹ during the same period (Smithers *et al*, 1995). Within the UK, extreme values for reeds of 13.39 mm d⁻¹ have been reported (Fermor, 1997), although lower values between 0.5 and 5 mm d⁻¹ were found for reedbeds by Peacock and Hess (2004). For UK wet grasslands typical maximum rates between 0.6 mm d⁻¹ during a very wet period to 6.4 mm d⁻¹ during a hot dry spell have been reported from the Pevensey Levels, Sussex (Gasca-Tucker and Acreman, 2000) and 1 to 5.5 mm d⁻¹ at Yarnton Mead, Oxfordshire (Gardner, 1991). Acreman *et al* (2003) reported evapotranspiration rates from a reedbed to be 14% higher than those of a nearby wet grassland over a five month period. Mould *et al* (2010) recorded up to 5.5 mm d⁻¹ from Otmoor floodplain in Oxfordshire.

A range of techniques has been employed to measure wetland evapotranspiration. Of the previously cited studies, Mould *et al* (in press) and Smithers *et al* (1995) used

diurnal water table fluctuations, Peacock and Hess (2004) relied upon a Bowen ratio energy balance system, whilst Acreman *et al* (2003) and Gardner (1991) each used the eddy covariance approach. Whilst scope exists for methodological inconsistencies to affect the comparability of the data collected by these studies, a direct comparison of Bowen ratio and eddy covariance systems demonstrates a good agreement between data gathered using these techniques (Thompson *et al*, 1999).

There is therefore some evidence to suggest that rates of actual evapotranspiration vary between different types of wetland environments. Acreman *et al* (2003) note that these differences may be attributable to the proportion of open water and aerodynamic characteristics of the vegetation canopy within a wetland. As yet, no investigations of evapotranspiration within UK fens have been reported within the literature.

Chapter 3

Instrumentation, Data Collection and Processing

3.1. Introduction

This chapter describes the theory and operation of the instrumentation systems used to collect the data upon which the analyses in this study are based. The procedures for the retrieval, processing, quality control and storage of data are also outlined.

3.2. The Eddy Covariance System

The eddy covariance system is the primary instrumentation system used within this study to estimate evapotranspiration from the surface energy flux.

3.2.1. Eddy Covariance Theory

Eddy covariance systems attempt to measure the components of the surface energy budget, which describes the partitioning of radiative energy input at the Earth's surface into separate fluxes. The relevant energy fluxes are represented schematically in figure 3.1.

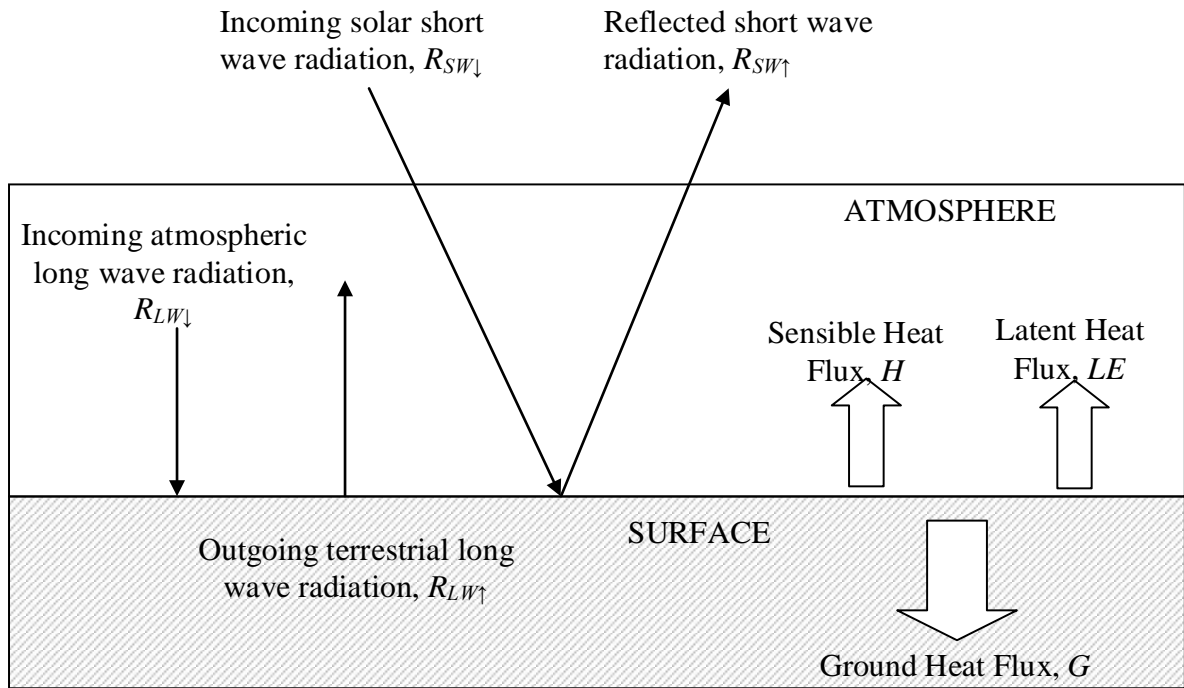


Figure 3.1: Schematic representation of incoming and outgoing energy fluxes at the Earth's surface. All fluxes are measured in units of W m^{-2} . Not to scale.

The radiative energy inputs to the surface are represented in figure 3.1 by the $R_{SW\downarrow}$ and $R_{LW\downarrow}$ terms and the outputs by the $R_{SW\uparrow}$ and $R_{LW\uparrow}$ terms. The shortwave input represents the solar radiation incident upon the surface, and a proportion of this radiation is reflected. Some of the incoming and reflected shortwave radiation is absorbed by the atmosphere and re-emitted as radiation of a longer wavelength, typically in the infra-red part of the electromagnetic spectrum. A proportion of the longwave radiation emitted by the atmosphere is incident upon the surface, where it is absorbed and re-emitted back into the atmosphere at infra-red wavelengths. Conventionally, incoming radiative fluxes at the surface are regarded as positive, whilst outgoing fluxes are regarded as negative. Collectively, the incoming and outgoing short- and longwave radiation fluxes at the surface are referred to as the net radiation flux, R_n , defined as:

$$R_n = R_{SW\downarrow} + R_{LW\downarrow} - R_{SW\uparrow} - R_{LW\uparrow} \quad (3.1)$$

where all terms are as defined in figure 3.1 and the units of measurement are W m^{-2} .

The net radiation input at the surface must be dissipated as other energy fluxes or stored at the surface so as to maintain a balance. The dissipative fluxes are the sensible, H , latent, LE , and ground, G , heat fluxes (all measured in units of W m^{-2}) in figure 3.1. The sensible heat flux describes the direct transfer of thermal energy between the surface and the atmosphere. The latent heat flux describes an indirect energy transfer in which energy is used to convert liquid water at the surface into a gaseous state (evaporation, see section 2.2) and thus also represents a mass transfer between surface and atmosphere. Both sensible and latent heat fluxes serve to initiate vertical convective motion within the atmosphere. The ground heat flux describes the conduction of energy between the surface and the underlying soil (Oke, 1987). Energy may also be stored within or released from the surface layer, ΔS (W m^{-2}), as described in section 3.2.3.3. Mathematically, the surface energy budget may be expressed as:

$$R_n = H + LE + G + \Delta S \quad (3.2)$$

where all terms are as previously defined and the units of measurement are W m^{-2} .

Energy fluxes may occur in either direction, thus a sign convention is adopted to describe the direction in which energy is being transferred. The net radiation term, R_n , is considered positive when the flux is towards the surface; i.e. the surface is gaining energy. The remaining terms are positive when the flux is away from the

surface; i.e. the surface is losing energy. A negative energy storage term, ΔS , indicates the release of energy stored within the surface layer.

Sensors exist for the measurement of the net radiation and ground heat flux terms within the surface energy budget (see section 3.2.2). An eddy covariance system offers the capability to measure the sensible and latent heat flux terms based on the theory presented below. The early development of eddy covariance systems is described by Swinbank (1951) and Dyer (1961). Swinbank (1951) employed hot wire anemometers and thermocouples to measure fluctuations in wind speed and air temperature, respectively, and presents a methodology by which such measurements may be used to define the sensible and latent heat fluxes. Swinbank's (1951) system recorded the fluctuations in atmospheric entities of interest as traces on paper charts, thus requiring manual derivation of the surface fluxes. Dyer (1961) successfully automated the calculation of fluxes and demonstrated good energy budget closure in unstable atmospheric conditions. Modern eddy covariance systems make use of advances in computer processing power to record high frequency fluctuations in atmospheric variables and compute surface fluxes.

The theory underpinning eddy covariance systems conceptualises atmospheric entities as comprising two components; a time averaged mean, \bar{s} , and a fluctuating value, s' .

The instantaneous value, s , of any variable may therefore be written as:

$$s = \bar{s} + s' \quad (3.3)$$

An air parcel may be considered as possessing three properties: mass (or density, ρ , (kg m^{-3}) when considered per unit volume); vertical velocity, w (m s^{-1}), and volumetric content of any entity, s . Taking each of these properties as being broken into constituent parts as in equation 3.3, the mean vertical flux density of an entity, S , is given by:

$$S = \overline{(\bar{\rho} + \rho')(\bar{w} + w')(\bar{s} + s')} \quad (3.4)$$

Equation 3.4 expands to:

$$S = (\overline{\bar{\rho}ws} + \overline{\bar{\rho}ws'} + \overline{\bar{\rho}w's} + \overline{\bar{\rho}w's'} + \overline{\rho'ws} + \overline{\rho'ws'} + \overline{\rho'w's} + \overline{\rho'w's'}) \quad (3.5)$$

Equation 3.5 can be simplified if the following assumptions are made:

- i) The average fluctuation of any property is, by definition, equal to zero;
- ii) Air density is constant in the lower atmosphere; and
- iii) The surface is uniform. This eliminates the concept of mean vertical velocity by conservation of mass.

Equation 3.5 may therefore be reduced to:

$$S = \overline{\rho w' s'} \quad (3.6)$$

Therefore the sensible heat flux, H (W m^{-2}), and the latent heat flux, LE (W m^{-2}), are given by:

$$H = \rho_a C_p \overline{w'T'} \quad (3.7)$$

$$LE = L_v \overline{w'\rho_v'} \quad (3.8)$$

where:

ρ_a = Air density (kg m^{-3})

C = Specific heat capacity of air at constant pressure ($1004.67 \text{ J K}^{-1} \text{ kg}^{-1}$)

p

T = Temperature ($^{\circ}\text{C}$)

L_v = Latent heat of vapourisation of water ($2.5 \times 10^6 \text{ J kg}^{-1}$)

ρ_v = Water vapour density (kg m^{-3})

and all other terms are as previously defined

3.2.2. Eddy Covariance Instrumentation

An eddy covariance system consists of multiple sensors making co-ordinated measurements of the data required for the derivation of all flux terms in the surface energy budget (equation 3.2). The eddy covariance system used within this study was composed of the following instruments:

- 1 x Kipp & Zonen CNR1 net radiometer
- 2 x Hukseflux HFP01 soil heat flux plates
- 1 x Gill R3-50 ultrasonic anemometer
- 1 x LiCor LI-7500 infra red gas analyser (IRGA)
- 1 x Vaisala HMP45C Relative Humidity and Temperature Probe
- 1 x Campbell Scientific CR3000 logger

The sonic anemometer and IRGA were used to derive the sensible and latent heat fluxes according to the theory presented in section 3.2.1. These instruments are capable of making high frequency (20 Hz) measurements so as to capture rapid fluctuations in the vertical velocity, temperature and vapour density.

3.2.2.1. CNR1 Net Radiometer

The CNR1 radiometer consists of four radiation sensors, allowing the measurement of the radiation terms on the right hand side of equation 3.1, thus permitting the derivation of net radiation (Campbell Scientific, 2008a).

The shortwave radiation is measured by a pair of CM3 pyranometers; one facing upward so as to measure incoming radiation, $R_{SW\downarrow}$ (W m^{-2}), and one facing downward to measure the reflected radiation, $R_{SW\uparrow}$ (W m^{-2}). Each pyranometer generates an electrical signal, V (mV), proportional to the intensity of shortwave radiation, R_{SW} (W m^{-2}), incident upon it. The shortwave radiation may therefore be derived according to equation 3.9 if the sensitivity of the pyranometer, S_{CNR1} ($\text{mV (W m}^{-2}\text{)}^{-1}$), is known.

$$R_{SW} = \frac{V}{S_{CNR1}} \quad (3.9)$$

The longwave radiation is measured by a pair of CG3 pyrgeometers; one facing upward so as to measure the atmospheric component, $R_{LW\downarrow}$ (W m^{-2}), and one facing downward to measure the terrestrial component, $R_{LW\uparrow}$ (W m^{-2}). As with the pyranometers, an electrical signal is generated by each pyrgeometer which is

dependent on the intensity of incident radiation. However, a correction must be applied to the CG3 data to account for the radiation flux attributable to the instrument itself, R_{LWCNR1} (W m^{-2}). This flux is directly related to the absolute temperature of the instrument, T_{CNR1} (K), by Stefan's Law:

$$R_{LWCNR1} = \sigma T_{CNR1}^4 \quad (3.10)$$

where Stefan's constant, $\sigma = 5.67 * 10^{-8} \text{ W m}^{-2} \text{ K}^{-4}$.

A temperature sensor is therefore integrated within the CNR1 to measure the instrument's temperature. Using the temperature data, the corrected longwave flux can be calculated as:

$$R_{LW} = \frac{V}{S_{CNR1}} + R_{LWCNR1} \quad (3.11)$$

It should be noted that the range of temperatures to which the CNR1 will be exposed is associated with greater spectral brightness (defined as power radiated per unit area per unit wavelength range) in the infra-red (longwave) region of the electromagnetic spectrum. The spectral brightness at short wavelengths generated by bodies radiating at such temperatures is negligible. Hence, the CNR1 temperature correction is only required for the longwave radiation.

The sensitivity, S_{CNR1} , of the CNR1 used within this study was determined by the manufacturers as being $9.8 * 10^{-3} \text{ mV (W m}^{-2}\text{)}^{-1}$. The CNR1 electrical outputs are converted into short- and longwave fluxes by the logger according to equations 3.9

and 3.11. These fluxes were subsequently used by the logger to calculate the net radiation flux according to equation 3.1. The CNR1 is mounted to the south of the eddy covariance mast to ensure no shadow is cast upon it at any time, thus maintaining the integrity of the radiation data.

3.2.2.2 HFP01 Soil Heat Flux Plate

The soil heat flux plates measure the ground heat flux term, G (W m^{-2}), in equation 3.2. Within each plate, a plastic filler acts as thermal resistance, thereby inducing a thermal gradient across the plate. This temperature gradient is measured by copper and constantan thermocouples connected in series, which generate an output voltage proportional to the temperature difference between the copper-constantan and constantan-copper joints. Connecting the thermocouples in series to form a thermopile serves to enhance the output signal. The heat flux across the plate will follow the temperature gradient (Campbell Scientific, 2008b). Figure 3.2 outlines the operating principles of the heat flux plates.

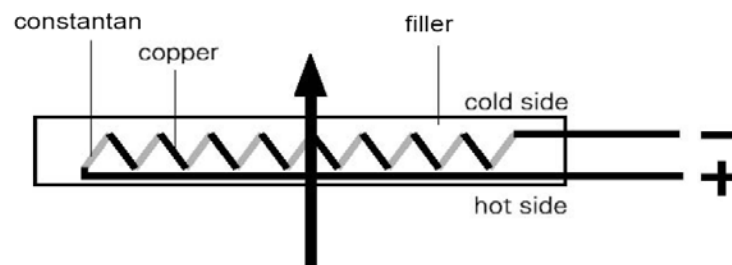


Figure 3.2: Schematic diagram representing the operating principle of the HFP01 soil heat flux plate (from Campbell Scientific, 2008b)

The output voltage, V (V), from each flux plate may be converted into ground heat flux, G (W m^{-2}), if the plate's unique sensitivity, S_{HFP01} ($\text{V (W m}^{-2}\text{)}^{-1}$), is known:

$$G = \frac{V}{S_{HFP01}} \quad (3.12)$$

The sensitivities, S_{HFP01} , of the heat flux plates attached to the eddy covariance system were determined by the manufacturers as being $6.16 * 10^{-2} \text{ V (W m}^{-2}\text{)}^{-1}$ and $6.05 * 10^{-2} \text{ V (W m}^{-2}\text{)}^{-1}$. The HFP01 electrical outputs are converted into ground heat fluxes by the logger according to equation 3.12.

It must be acknowledged that the heat flux plates have a limited level of accuracy owing to factors such as changing soil moisture content, disturbance of soil during installation of flux plates (both affecting soil thermal parameters) and contact between flux plate and soil. Each plate was installed by excavating an angled “shaft” within the soil and installing the flux plate horizontally at the bottom. The shaft was then backfilled so as to minimise disturbance to the soil profile and maximise the thermal contact between plate and soil. However, it is anticipated that the error range will be $\pm 10\%$ of the measured flux (Campbell Scientific, 2008b). Since the soil heat flux is typically the smallest of the surface energy fluxes, it is not believed that this potential error will significantly distort any energy balance calculations performed within this study.

3.2.2.3 R3-50 Ultrasonic Anemometer

The ultrasonic anemometer derives the horizontal, u and y , and vertical, w , air velocities (m s^{-1}) and air temperature, T ($^{\circ}\text{C}$) by measuring the times taken, t_1 and t_2

(s), for ultrasonic pulses to travel a known distance, l (m), between a pair of transducers (A_1 and A_2) and receivers (B_1 and B_2) as shown in figure 3.3.

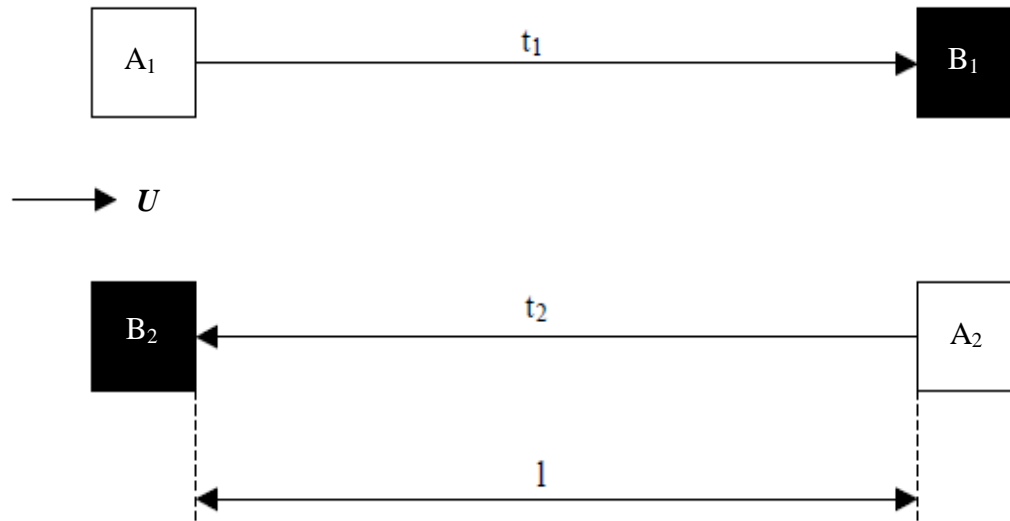


Figure 3.3: Schematic diagram illustrating the operating principles of the ultrasonic anemometer. (after Met Office, 1981).

Since an ultrasonic pulse propagates through a medium by inducing motion at the molecular level, any molecular motion occurring independently of an ultrasonic pulse will affect the pulse's travel time. Therefore, if the air is in motion and has velocity, U (m s^{-1}), along the axis of the pulse's motion the travel times of the ultrasonic pulse, t_1 and t_2 (s), will be a function of the speed of sound, c (m s^{-1}), and the velocity of the air along the axis of interest. Therefore:

$$t_1 - t_2 = \frac{l}{c + U} - \frac{l}{c - U} \quad (3.13)$$

$$U = \frac{l}{2} \left(\frac{1}{t_1} - \frac{1}{t_2} \right) \quad (3.14)$$

Applying equation 3.14 to multiple pairs of transducers and receivers yields separate velocities for each pairing. These velocities are subsequently transformed into u , v and w components representing velocities in the horizontal plane parallel and perpendicular to the air flow and in the vertical plane, respectively, by means of a transformation matrix based upon the physical dimensions of the anemometer (Cuerva *et al*, 2003).

The temperature, T (°C), may be derived from the measured speed of sound, c , by:

$$c = \frac{l}{2} \left(\frac{1}{t_1} + \frac{1}{t_2} \right) \quad (3.15)$$

$$T = \frac{c^2}{403} \quad (3.16)$$

(Gill Instruments, 2007; Met Office, 1981)

The ultrasonic anemometer was mounted atop a mast at a height of 3.94m above ground level. Measurements were taken at a frequency of 20 Hz (i.e. every 50 milliseconds). The calculations presented above are performed by the anemometer's on-board program (known as “firmware”) and are subsequently transmitted to the CR3000 logger for storage.

3.2.2.4 LI-7500 Infra-Red Gas Analyser

The infra-red gas analyser (IRGA) measures the water vapour density in the air, ρ_v (kg m^{-3}), by quantifying the attenuation of infra-red radiation by the water vapour present in the air. This instrument takes advantage of the tendency of water vapour to absorb radiation at a specific and unique wavelength (in the case of the IRGA used within this study, $2.59 \mu\text{m}$) and calculates the proportion of this radiation emitted by a source of known power, Φ_0 (W), measured by a detector, Φ , a known distance away. Air is allowed to pass between source and detector, thus any loss in power is attributable to absorption by water vapour within the air (figure 3.4).



Figure 3.4: Schematic diagram illustrating the operating principles of the IRGA.

Equation 3.17 demonstrates the quantitative treatment of this process, where z_v and s_v are instrumental calibration functions, P is atmospheric pressure (kPa), f_v is a calibration function derived using known molar vapour concentrations, and f_c is a cross-sensitivity correction function based on the carbon dioxide absorption, α_c , measured by the IRGA (Auble & Meyers, 1991; Crill *et al*, 1995; Li-Cor Biosciences, 2007).

$$\rho_v = Pf_v \left(\frac{1 - \left(\frac{\phi}{\phi_0} + f_c(\alpha_c) \right)^{z_v s_v}}{P} \right) \quad (3.17)$$

The IRGA is mounted adjacent to the ultrasonic anemometer so as to minimise the separation distance between the two sensors. The IRGA is mounted at an angle so as to prevent water drops remaining on the windows, thus reducing errors in the measurement of attenuated radiation. As with the ultrasonic anemometer, measurements are taken at a frequency of 20 Hz. The IRGA has a dedicated logger which derives the water vapour density data. This data is then transferred to and stored on the CR3000 logger.

3.2.2.5 HMP45C Relative Humidity and Temperature Probe

The relative humidity and temperature probe is used to collect data from which the air density, ρ_a (kg m^{-3}), is derived. This variable is a function of absolute temperature, T_k (K), and relative humidity, RH (%), and is used in the derivation of sensible heat according to equation 3.7. The air density may be calculated as:

$$\rho_a = \frac{e}{T_k R_v} + \frac{P - e}{T_k R_D} \quad (3.18)$$

where:

- e = Vapour pressure of air (kPa) – a function of T_k and RH
 - P = Atmospheric pressure (kPa)
 - R_v = Gas constant for water vapour ($4.63 \cdot 10^{-4} \text{ kPa m}^3 \text{ K}^{-1} \text{ g}^{-1}$)
 - R_D = Gas constant for dry air ($2.88 \cdot 10^{-4} \text{ kPa m}^3 \text{ K}^{-1} \text{ g}^{-1}$)
- and all other terms are as previously defined

The HMP45C probe is mounted within a URS1 radiation shield to ensure that the instrument is shaded from solar radiation. The shield is naturally aspirated so as to allow air to pass through the shield and across the sensor itself, thereby permitting the

measurement of ambient air temperature and relative humidity (Campbell Scientific, 2009a).

3.2.2.6 CR3000 Micrologger and Power Supply

The CR3000 logger co-ordinates the measurements of all the eddy covariance sensors. The logger program used within this study is written in CRBasic (Campbell Scientific's proprietary language). The program supplied as standard with the eddy covariance system was adapted to include the unique calibration constants for each sensor presented within this section. Measurements were taken at a frequency of 20 Hz from all instruments, and stored within the logger. 30 minute averages were calculated from the 20 Hz data.

A CFM100 CompactFlash Module was connected to the logger, permitting the writing of 20 Hz and 30 minute average data to a 2 GB CompactFlash card. This facilitated straightforward data retrieval. Data was read from the card into a portable tablet PC in the field using a CompactFlash card reader and was subsequently transferred to a backed-up files server at the earliest opportunity.

The power supply for the eddy covariance system comprises sixteen 12V batteries. So as to ensure a continuous supply of power, the power supply is recharged using an array of eleven Shell Solar SM55 solar panels and a Steca PR3030 solar charge regulator. Such a substantial power supply was intended to provide sufficient power during the winter months in order to permit the collection of data by the eddy

covariance system during this period. However, some data was lost to power failures, most notably in the late winter and early spring periods.

3.2.2.7. Location of Eddy Covariance System

The eddy covariance system was located within the area of Wicken Fen known as Sedge Fen (52.31°N, 0.28°E). This area is a managed wetland in which ground water levels are typically within 1 m of the surface throughout the year. The dominant vegetation community is the *Symphytum officinale* sub-community of *Phragmites australis*-*Peucedanum palustre* tall-herb fen (NVC classification S24c). Sedge Fen takes its name from the great fen-sedge, *Cladium mariscus*, which grows abundantly on this part of the Wicken Fen reserve (Friday and Harvey, 1997; Mountford *et al*, 2005).

The eddy covariance system was installed at Sedge Fen during June 2008. However, owing to a malfunction of the original ultrasonic anemometer the 2008 energy flux data was regarded as suspect and so was not used in this study. The malfunctioning anemometer was replaced in February 2009, and the data subsequently gathered was considered sufficiently reliable for inclusion within this study. A full description of the investigation of the anemometer malfunction is presented in Appendix A.

3.2.3 Eddy Covariance Data Processing

3.2.3.1. 20 Hz Data Processing

The 20 Hz data retrieved from the eddy covariance system was processed using EdiRe software (University of Edinburgh, 1999). A customised processing list was constructed to read the data and perform quality control tests prior to calculating fluxes and applying corrections.

The first stage of the quality control procedure ensured that the raw data were within realistic limits. These were defined as $\pm 20 \text{ m s}^{-1}$ for horizontal wind speed, $\pm 10 \text{ m s}^{-1}$ for vertical windspeed, between $-10 \text{ }^{\circ}\text{C}$ and $40 \text{ }^{\circ}\text{C}$ for temperature, between 5 mg m^{-3} and 1500 mg m^{-3} for atmospheric carbon dioxide density and between 0.1 g m^{-3} and 20 g m^{-3} for atmospheric water vapour density. If any of the 20 Hz data values lay outside these limits, the software assumed the data to be in error and omitted these values from subsequent analyses. For each half-hourly period, the mean horizontal wind speed and friction velocity were calculated. Fluxes were not derived for periods with a mean horizontal wind speed of less than 1 m s^{-1} or friction velocity less than 0.1 m s^{-1} so as to avoid large errors (Alavi *et al*, 2006).

The temperature, carbon dioxide and water vapour data were then “despiked” to remove short duration, large amplitude fluctuations that may result from random electronic noise. This is a statistical procedure in which each data point is compared to its neighbours so as to ensure consistency (Foken *et al*, 2004). If a data point

differed from its neighbours by more than ten standard deviations of the population mean, it was considered to be erroneous and was omitted from further processing.

The next stage of the quality control procedure was to apply stationarity tests to the covariances of vertical windspeed and temperature, carbon dioxide and water vapour. This test ensured that the average fluctuation of these properties was equal to zero; a key assumption within eddy covariance theory (see section 3.2.1.). Each half-hourly period was broken down into successive 5 minute intervals, and the mean covariance of each 5 minute interval was compared to that of the full 30 minute period. A mathematical treatment of this procedure is presented by Foken & Wichura (1996).

A co-ordinate rotation was required to ensure that the derived fluxes are perpendicular to the mean streamline plane. If the eddy covariance system is tilted from the perpendicular with respect to the mean streamline plane, the fluxes may be over- or underestimated depending on the angle of the tilt relative to the mean streamline as described by Lee *et al* (2004). A planar fit rotation was applied to the data so as to address this possible source of error. Rotation coefficients were determined according to the methodology described by Wilczak *et al* (2001) and using the three dimensional wind speed data for the entire study period. These coefficients were subsequently applied to the wind speed data prior to the derivation of average fluxes. The 30 minute average fluxes were then derived according to equations 3.7 and 3.8.

Sensor path length and sensor separation may result in the loss of high-frequency data and thus lead to underestimates of the mean fluxes (Wilson *et al*, 2002). The frequency response corrections detailed by Moore (1986) were derived and applied to the fluxes calculated according to equations 3.7 and 3.8.

When measuring turbulent fluctuations of atmospheric entities *in situ*, corrections must be made for density changes caused by the fluxes themselves. The input of heat or water vapour will cause expansion of the air, thus affecting the density of any given entity being measured. A full discussion and derivation of density corrections may be found in Webb *et al* (1980), although it is acknowledged that such corrections represent only a few percent of the fluxes derived in equations 3.7 and 3.8. The density corrections recommended by Webb *et al* (1980) were applied to the frequency response corrected surface fluxes.

3.2.3.2. Gap Filling of Flux Data

Owing to periodic power failures and the rejection of data according to the criteria described in section 3.2.3.1, the resultant eddy covariance flux time series is not continuous. For example, between 14th April and 31st December 2009 only 59% of the processed 30 minute average values are available. Between 9th April and 5th November 2010, 62% of the processed 30 minute average values are available. This is a common feature of eddy covariance time series data, although not widely reported within the literature. The proportion of gaps within the 2009 and 2010 data are at the

upper end of the ranges described by Alavi *et al* (2006), Foken *et al* (2004) and Mauder *et al* (2006). A strategy for infilling missing data must therefore be defined.

The technique described by Reichstein *et al* (2005) provides a methodology for the estimation of missing flux data. Missing data are replaced by the mean derived for the corresponding 30 minute period from previous and subsequent days for similar meteorological conditions. A processing routine for infilling data according to this method is available online¹, and was used to fill the missing latent heat flux data from the Wicken Fen eddy covariance system. The tool also provides estimates for missing solar radiation, sensible heat and air temperature data.

Missing reflected shortwave radiation data were estimated using the infilled solar radiation data and the albedo from the corresponding period of the preceding day. Missing net longwave radiation data were estimated according to the recommendations of Allen *et al* (1998). Terrestrial longwave radiation data were required to estimate the storage terms (section 3.2.3.3). Where terrestrial longwave data was missing, the atmospheric longwave radiation was calculated according to the recommendations of Crawford and Duchon (1999), using the Brunt approximation of the emissivity parameter as recommended by Wang and Liang (2009). The terrestrial longwave radiation was estimated by subtracting the atmospheric longwave radiation from the net longwave radiation.

¹ <http://gaia.agraria.unitus.it/database/eddyproc/>

3.2.3.3 Energy Storage Terms

Incoming energy may also be stored within or released from the surface layer, as represented by the ΔS term in equation 3.2. Although presented as a single term, energy is stored within the surface layer in several forms. Jacobs *et al* (2008) reviewed the energy storage mechanisms within the surface layer, and these may be summarised as:

- i. Photosynthesis, S_p : energy used by vegetation for sustenance
- ii. Air enthalpy change, S_a : energy stored within air beneath instrumentation
- iii. Crop enthalpy change, S_c : energy stored within vegetation canopy
- iv. Atmospheric moisture change, S_q : energy stored within water vapour beneath instrumentation
- v. Canopy dew water enthalpy change, S_d : energy stored within moisture in vegetation canopy.

All terms are measured in units of W m^{-2} .

Jacobs *et al* (2008) describe methods to calculate additional minor energy storage terms often overlooked in eddy covariance studies and report a significant improvement in energy budget closure for 30-minute averaging periods. Although Wilson *et al* (2002) note that these minor terms are likely to be negligible when integrated over longer timescales, they are considered within this study. The data required for the calculations presented by Jacobs *et al* (2008) were collected at Wicken Fen, and were infilled where necessary using the method described in section

3.2.3.2. It is only by considering all components of the energy budget that the accuracy of the energy fluxes, and thus the evaporation data, collected at Wicken Fen can be assessed.

3.2.3.4. Energy Budget closure

Eddy covariance systems are known to underestimate the surface fluxes, resulting in a residual energy term arising due to an imbalance between the two sides of equation 3.2 (Foken *et al*, 2004). Wohlfahrt *et al* (2009) present possible methods to force closure by apportioning the residual energy between the sensible and latent heat fluxes. Since this project is concerned with evapotranspiration estimates, the residual energy was apportioned to the latent heat flux. Whilst it remains unknown in which proportions the residual energy might be apportioned between the surface fluxes, this approach allows for the definition of an upper limit to the latent heat flux. In this manner, an uncertainty margin may be defined for the evapotranspiration estimates derived from the eddy covariance data.

3.3 The Automatic Weather Station

The automatic weather station consists of the following components:

- 1 x Didcot Instruments dry bulb platinum resistance thermometer
- 1 x Didcot Instruments wet bulb platinum resistance thermometer
- 2 x Didcot Instruments DWR-201 cup anemometer
- 1 x Didcot Instruments DWD-102 wind direction sensor

- 2 x Hukseflux HFP01 soil heat flux plates
- 1 x Vaisala HMP45C Relative Humidity and Temperature Probe
- 1 x Campbell Scientific CR1000 logger

3.3.1. Wet and Dry Bulb Platinum Resistance Thermometers

The platinum resistance thermometers (PRT) derive temperature from measurements of the resistance of a platinum element. The resistance of electric conductors is known to vary with temperature. Within the range of atmospheric temperatures, this relationship exhibits linear behaviour and may be expressed as:

$$R_T = R_0(1 + aT) \quad (3.19)$$

where:

R_T = Electrical resistance (Ω) at temperature T ($^{\circ}\text{C}$)

R_0 = Electrical resistance (Ω) at 0°C

a = Temperature sensitivity of conductor ($^{\circ}\text{C}^{-1}$)

The sensitivity term, a , is a constant dependent on the conductor used as the thermometer element. The conductor used within this study is constructed of platinum which is known to have a temperature sensitivity of 0.4°C^{-1} and a resistance, R_0 , of $100\ \Omega$ at 0°C . Hence, rearrangement of equation 3.19 allows the derivation of temperature from measurements of the resistance of the platinum element (DeFelice, 1998; Middleton & Spilhaus, 1953; Strangeways, 2003).

Two PRTs were attached to the AWS so as to permit the determination of relative humidity by the psychrometric method. One PRT measures the air temperature, T (°C), and is referred to as the dry bulb thermometer. The other PRT is covered by a moistened wick and is referred to as the wet bulb thermometer. The resulting wet bulb temperature, T_w (°C), is indicative of the cooling attributable to the evaporation of water from the wick, which is dependent on the proportion of water vapour in the atmosphere, i.e. the relative humidity. Using these measurements, the vapour pressure, e (hPa), may be determined as:

$$e = e_s - Ap(T - T_w) \quad (3.20)$$

where:

- A = Psychrometric coefficient ($\sim 0.667 \times 10^{-3} \text{ }^\circ\text{C}^{-1}$)
- p = Atmospheric pressure (hPa)

and the saturation vapour pressure, e_s (hPa), at T_w is:

$$e_s = 6.11 \exp\left(\frac{17.27T_w}{237.3 + T_w}\right) \quad (3.21)$$

Relative humidity, RH (%), may therefore be determined as

$$RH = \frac{e}{e_s} \quad (3.22)$$

(DeFelice, 1998; Strangeways, 2003).

In order to account for any systematic bias attributable to the PRT sensors attached to the AWS, both were calibrated in the laboratory by comparison with data from a precision thermometer. This revealed a linear relationship between the PRTs and the precision thermometer, requiring the dry bulb data to be adjusted by a coefficient of 1.001 and an offset of -3.1286 and the wet bulb data to be adjusted by a coefficient of 1.005 and an offset of -4.6514.

The PRTs were mounted within a naturally aspirated screen so as to prevent direct solar radiation affecting the temperature measurements. The wet bulb thermometer was covered by a cloth wick, the opposite end of which was immersed in a reservoir of distilled water incorporated within the screen, thus ensuring a constant supply of moisture to the wet bulb thermometer. The reservoir was topped up with distilled water during each visit to the field site (approximately every 2-3 weeks).

3.3.2. DWR-201 Cup Anemometers

The cup anemometers each consist of three evenly-spaced conical cups rotating about a vertical axis. When exposed to the wind the pressure exerted on the open side of the cups is greater than that on their backs, thus causing the cups to rotate. This response is independent of wind direction. If the cup speed is known, it may be used to derive the wind speed (Strangeways, 2003).

The cup speed is determined by counting the number of revolutions of the anemometer shaft in a known period of time. The shaft has a contact attached which

closes a switch each time a revolution is completed, sending an electronic pulse to the logger. The number of pulses, n , is therefore indicative of the cup speed (m s^{-1}) and may be used to determine the wind speed, u (m s^{-1}), by:

$$u = 0.3125n \quad (3.23)$$

where 0.3125 is the calibration constant of the anemometer determined by the manufacturers based upon wind tunnel tests (Wicks, pers. comm.).

The two anemometers were affixed to the AWS. The first was installed in June 2008 at a height of 3.08 m. The second was installed during June 2009 at a height of 2.59 m.

3.3.3. DWD-102 Wind Direction Sensor

The wind direction sensor consists of a wind vane connected to a circular resistance coil. As the vane responds to changes in wind direction, a contact attached to the shaft moves across the resistance coil. If the resistance coil is incorporated within a circuit, the fluctuations in voltage may be monitored and used to derive the resistance of the circuit, and thus the wind direction (Middleton & Spilhaus, 1953; Strangeways, 2003).

3.3.4. HFP01 Soil Heat Flux Plate

The soil heat flux plates attached to the AWS are the same model as attached to the eddy covariance system, and are described in section 3.2.2.2. The sensitivities,

S_{HFP01} , of the heat flux plates used attached to the AWS were determined by the manufacturers as being $6.09 * 10^{-2} \text{ V (W m}^{-2}\text{)}^{-1}$ and $6.07 * 10^{-2} \text{ V (W m}^{-2}\text{)}^{-1}$. The HFP01 electrical outputs are converted into ground heat fluxes by the logger according to equation 3.12.

3.3.5. HMP45C Relative Humidity and Temperature Probe

The relative humidity and temperature probe attached to the AWS is the same model as attached to the eddy covariance system, and is described in section 3.2.2.5.

3.3.6. CR1000 Micrologger and Power Supply

The CR1000 logger co-ordinates the measurements of all the AWS sensors and stores the resulting outputs. The logger program used within this study is written in CRBasic (Campbell Scientific's proprietary language). The program was adapted from a standard AWS program to include the unique calibration constants for each instrument presented within this section. Measurements were taken at intervals of 10 seconds from all instruments, and stored within the logger. 30 minute and daily averages were calculated from this data.

A CFM100 CompactFlash Module was connected to the logger, permitting the writing of 30 minute and daily average data to a 1 GB CompactFlash card. This facilitated straightforward data retrieval. Data was read from the card into a portable tablet PC in the field using a CompactFlash card reader. Data could also be retrieved

by connecting the portable PC directly to the logger's RS-232 serial port. Data was subsequently transferred to a backed-up fileserver at the earliest opportunity.

The AWS is powered by a PS100E-LA 12 V Lead Acid Power supply (Campbell Scientific, 2009b). This supply incorporates a charging regulator which allows the battery to be recharged and thus continuously power the data logger. The power supply is recharged by means of a single SOP5/X solar panel (Campbell Scientific, 2006). The battery is located alongside the logger inside a weatherproof enclosure. The solar panel is mounted atop the AWS mast and faces south to ensure maximum exposure to incoming solar radiation.

The automatic weather station was located adjacent to the eddy covariance system at Sedge Fen. The weather station was installed at Sedge Fen in June 2008 and has operated continuously since.

3.4. Relative Humidity Stations

Two relative humidity stations were installed outside Sedge Fen. Each station consisted of a HMP45C relative humidity and temperature probe (as described in section 3.2.2.5) connected to a CR200 data logger (Campbell Scientific, 2008c). Each station took measurements at 10 second intervals, from which 30 minute and daily average data were derived and stored on the logger. Data was retrieved by connecting a portable PC to the logger and was subsequently transferred to a backed-up fileserver at the earliest opportunity.

Each relative humidity station is powered by a 12 V rechargeable lead acid battery. Each battery is connected to a SOP5/X solar panel (Campbell Scientific, 2006) to allow recharging. The solar panels are mounted atop the humidity station masts and face south to ensure maximum exposure to incoming solar radiation.

Table 3.1 describes the locations of the relative humidity stations. These stations form a transect with the Sedge Fen AWS, which incorporates a relative humidity probe (section 3.3). The transect was aligned with the prevailing wind direction (south-westerly), placing the instrumentation at Oily Hall upwind of Sedge Fen.

Table 3.1: Locations of relative humidity stations (see also figure 1.3).

Site name	Latitude (°N)	Longitude (°E)	Distance from Sedge Fen (km)	Vegetation description
Adventurer's Fen	52.30	0.27	0.95	Reedbed
Oily Hall	52.27	0.23	5.50	Fallow

3.5. Stomatal Resistance Measurements

Stomatal resistance measurements were made with a CIRAS-1 portable photosynthesis system (PP Systems, 2003). Owing to the manual nature of this procedure, measurements were only possible on specific days, detailed in section 5.2.5. On each day, measurements were made in 30-minute windows so as to synchronise with the eddy covariance data collection interval. Stomatal resistance measurements were taken from eight individual *Phragmites australis* plants located close to the eddy covariance instrumentation. Measurements were taken from three separate leaves on each plant, producing twenty-four measurements of stomatal

resistance for each 30-minute period. Between measurement periods, the CIRAS-1 performed automated calibration routines. All measurements were logged within the CIRAS-1 and retrieved by connecting to a desktop PC and transferring files to a backed-up fileserver at the earliest opportunity.

The CIRAS-1 was powered by a portable 12V rechargeable lead acid battery. Typically, four such batteries were required to power the CIRAS-1 for a complete day. All batteries were fully charged between visits to Sedge Fen. In the event that the available battery power was insufficient, the CIRAS-1 was powered from one of the batteries comprising the eddy covariance power supply (section 3.2.2.6) by means of a customised adaptor lead.

The absorber and desiccant columns used to control the carbon dioxide and water vapour concentrations within the CIRAS-1 were examined following each day of measurements. The chemicals used within all columns were designed to change colour to indicate when they had become exhausted. In the event of exhaustion, the absorber columns were replaced with fresh soda lime or molecular sieve as appropriate. Exhausted desiccant was removed and dried within an oven according to the manufacturer's specifications (PP systems, 2003) before being replaced in the CIRAS-1.

3.6. Leaf Area Index

Leaf area index measurements were made using a Sunscan Canopy Analysis System SS1 (Delta-T Devices, 2008). Leaf area index measurements were taken on days preceding the stomatal resistance measurements. A beam fraction sensor was located close to the eddy covariance system to measure direct solar radiation and care was taken to ensure this sensor was not shaded at any time during the measurement of leaf area index. The beam fraction sensor was connected to the Sunscan probe, which was placed underneath the vegetation canopy at twenty points in the vicinity of the eddy covariance instrumentation. The area of these measurements was limited by the need for the beam fraction sensor and Sunscan probe to remain connected at all times. A portable computer attached to the Sunscan probe logged the incident solar radiation received by the beam fraction sensor and the radiation received within the canopy by the Sunscan probe and thus calculated the radiation attenuated by the canopy and the leaf area index. All data logged on the portable computer were transferred to a backed-up fileserver at the earliest opportunity.

Chapter 4

The Surface Energy Budget at Sedge Fen

4.1. Introduction

4.1.1. Energy Budget Data Quality

Previous studies have described energy budgets for a range of environments, including wetlands. The representativeness and reliability of the data upon which analyses are performed is of critical importance when seeking to define the energy budget at any site. To this end, energy balance studies commonly report flux source areas and energy budget closure.

Flux densities are typically advected towards elevated sensors from an area upwind of the instrumentation, as represented schematically in figure 4.1. Therefore, flux observations are representative of a surface area upwind of the instrumentation rather than the point location at which the instrumentation is sited. In order for the flux data to be considered representative of a surface, the source area should fall within the desired surface type and should ideally be homogeneous.

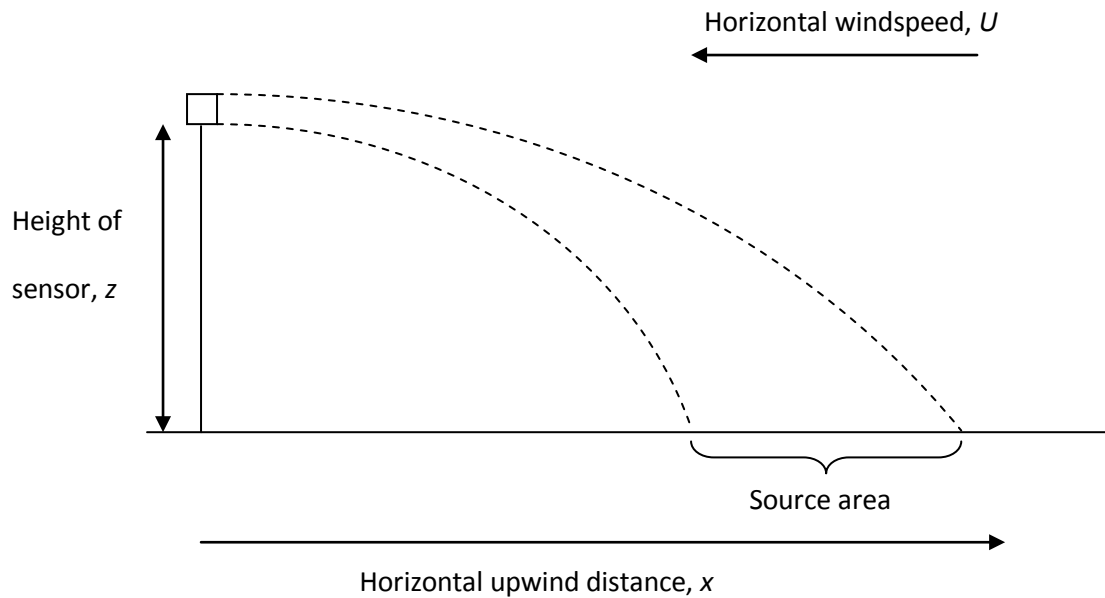


Figure 4.1: Schematic representation of flux source areas

An example of a mathematical description of flux source areas is presented in section 4.2.1. Using such techniques permits the definition of flux source areas in terms of distance upwind of the instrumentation. The concept of fetch is related to that of flux source areas. The fetch is defined as the unobstructed horizontal distance upwind of the instrumentation over which the surface type of interest extends. Ideally, flux source areas should lie within the fetch of the instrumentation. Such calculations allow researchers to demonstrate that the source area modelled for a particular instrumentation system is representative of the surface under consideration (e.g. Gasca-Tucker *et al*, 2007; Gavin and Agnew, 2003). At sites for which modelled source area requirements cannot be fulfilled, flux data may be filtered accordingly so as to remove from consideration fluxes originating over surfaces deemed unrepresentative of that desired (e.g. Kellner, 2001).

Energy budget closure describes the balance between the two sides of the surface energy budget (equation 3.2). As previously described, flux instrumentation systems commonly report unbalanced surface energy budgets and this is attributed to underestimates of the surface fluxes (section 3.2.3.4). Studies of wetland surface energy budgets typically acknowledge the observed shortfall in the energy budget by reporting the closure of the energy budget, describing the ratio of the sum of the sensible and latent heat fluxes to the energy input. Thus the energy budget closure may be considered an independent method of assessing the reliability of energy flux measurements (Finch and Harding, 1998; Li *et al*, 2009; Thompson *et al*, 1999). Whilst most wetland energy budget studies report the energy budget closure, little consideration is given to how the unaccounted energy may be partitioned between the surface fluxes. It is therefore possible that any of the reported surface fluxes may misrepresent the actual rate or quantity of energy transfer. Wohlfahrt *et al* (2009) describe methods by which energy budget closure may be forced (section 4.2.3). However, these recommendations are yet to be widely incorporated within studies of wetland surface energy budgets.

4.1.2. Wetland Surface Energy Budgets

A common feature of wetland surface energy budgets is the tendency for the latent heat flux to account for the dissipation of much of the net radiation receipt. For example, Acreman *et al* (2003) reported that the latent heat flux accounted for over 90% of the net radiation during a five month period at a wet grassland. Similar results were reported for an entire year by Finch and Harding (1998). Li *et al* (2009) reported lower ratios of latent heat flux to net radiation – typically 50 - 60% – for a

reed wetland, although latent heat remained the dominant outgoing surface flux at this site. Eaton *et al* (2001) also note high ratios of latent heat fluxes to net radiation for subarctic wetlands. Comparable observations from non-wetland ecosystems reveal lesser proportions of incident energy converted to latent heat flux. This is attributed to the relatively high moisture availability and low surface resistance to evapotranspiration within wetland environments. Acreman *et al* (2003) provide evidence of a relationship between water availability and surface resistance at a wetland consistent with this explanation.

However, the trends previously described are not necessarily common to all wetland environments. Peacock (2003) reported latent heat fluxes accounting for 32% of net radiation receipt at a reedbed site, approximately half the proportion converted to sensible heat, whilst Kellner (2001) reported approximately equal proportions of received radiation being converted to latent and sensible heat fluxes at a peat mire. Souch *et al* (1996) also reported approximately equal proportions of latent and sensible heat fluxes at a wetland on the shore of Lake Michigan, and identified the suppression of the latent heat flux due to the flow of humid air from the lake. These studies therefore serve to highlight the variations in wetland energy balance characteristics in response to a range of local factors.

Peacock (2003) demonstrated that energy partitioning differs on days with and without rain. On wet days approximately 60% of net radiation was partitioned as latent heat, whilst on dry days this figure was approximately 25%. Thompson *et al* (1999) also noted greater partitioning of energy to latent heat in response to rainfall

for peat bogs. However, these two studies ascribe the variations in energy partitioning to different causes. Peacock (2003) reported that the absolute flux of latent heat remained relatively constant irrespective of whether rain had fallen and that the contrasting partitioning was attributable to fluctuations in the sensible heat flux. Hence, cloudy conditions are associated with low net radiation and consequently lower sensible heat flux. By contrast, Thompson *et al* (1999) argued that vegetation canopies wetted by rainfall events increase the moisture availability and thus enhance the proportion of energy partitioned as latent heat.

Kellner (2001) identified a seasonal variation of energy partitioning, in which a progressively greater proportion of incoming energy was partitioned as latent heat than sensible heat throughout the growing season. This was attributed to the presence of varying quantities of non-transpiring biomass during the growing season. Li *et al* (2009) also note a seasonal variation in energy partitioning related to variations in the water level at their reedbed site. Lafleur *et al* (1997) attributed seasonal variation in energy partitioning at a boreal wetland to the phenology of the vegetation at the site.

4.1.3. Aims

The overall objective of this chapter is to verify the reliability of the eddy covariance flux data. This is of particular importance since the evapotranspiration data derived from latent heat flux measurements are fundamental to analyses in subsequent chapters. This objective will be fulfilled by addressing the following aims:

1. Quantify the fetch and flux source areas of the eddy covariance system at Sedge Fen
2. Ensure the fluxes reported by the eddy covariance system are physically meaningful and consistent with one another
3. Describe the energy budget closure of the Sedge Fen flux data.

4.2. Methods

4.2.1. Flux Source Areas

Within this study, flux source areas are defined as described by Schuepp *et al* (1990), who analytically derive source area parameters from the diffusion equation. Such parameters were shown to compare favourably with numerical simulations and airborne flux measurements. Schuepp *et al* (1990) demonstrate that the relative contribution to the vertical flux, $(1/Q_0) dQ/dx$, at height z (m) from an upwind distance x (m), as represented schematically in figure 4.1, can be derived as:

$$\frac{1}{Q_0} \frac{dQ}{dx} = (-) \frac{U(z-d)}{u_* k x^2} e^{-U(z-d)/k u_* x} \quad (4.1)$$

where

- U = Windspeed (m s^{-1})
- d = Height of zero plane of displacement (m)
- u_* = Friction velocity (m s^{-1})
- k = Von Karman's constant (0.41)

Equation 4.1 produces flux source area predictions such as that shown in figure 4.2.

The area under the graph represents the cumulative contribution to the flux from

within the source area bounded by 0 m and x_L m upwind of the measurement point, and may be expressed as the integral of the right hand side of equation 4.1 between $x = 0$ and $x = x_L$.

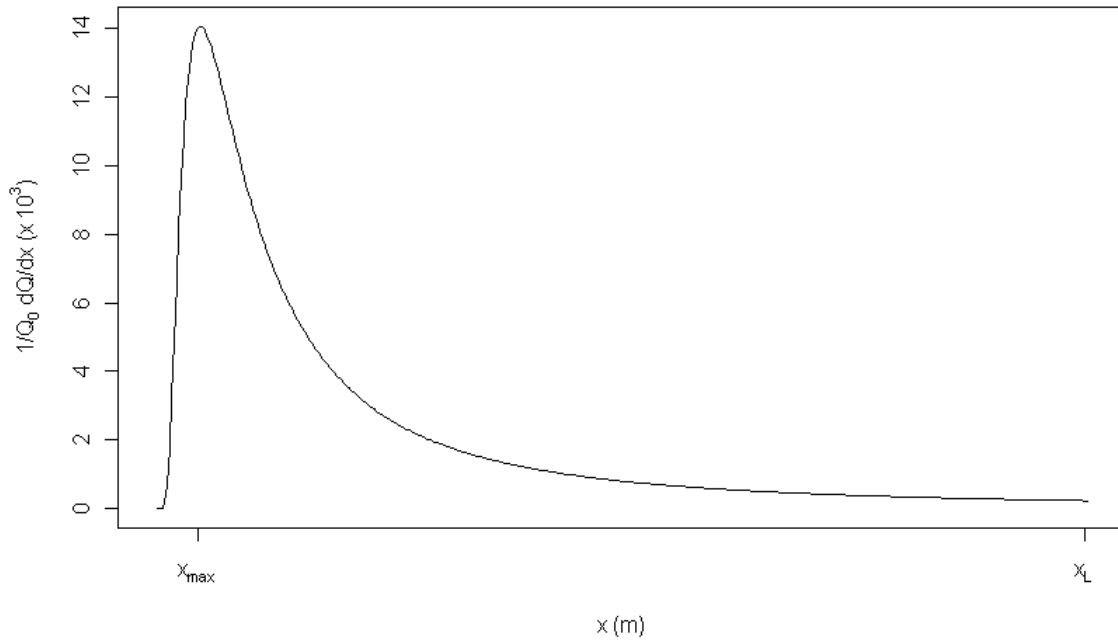


Figure 4.2: Example flux source area prediction demonstrating relative contribution to flux from distance x m upwind of instrumentation according to Schuepp *et al* (1990)

Schuepp *et al* (1990) also demonstrate that the position of the peak of the flux source area, x_{max} (m), representing the area to which the observations are most sensitive can be estimated as:

$$x_{max} = \frac{U (z - d)}{u_* 2k} \quad (4.2)$$

where all terms are as previously defined.

4.2.2. Energy Fluxes

The energy flux data presented within this section are those collected by the eddy covariance system at Sedge Fen (see section 3.2). Flux data has been estimated according to the methods described in section 3.2.3.2 for periods during which flux data was not available. Available energy is defined as the net radiation flux less the ground heat flux.

4.2.3. Energy budget closure

Residual energy is reported as the difference between the terms on each side of equation 3.2, i.e:

$$A_{res} = R_n - G - H - LE - \Delta S \quad (4.3)$$

where:

- A_{res} = Residual energy (MJ m^{-2})
- R_n = Net radiation flux (MJ m^{-2})
- G = Ground heat flux (MJ m^{-2})
- H = Sensible heat flux (MJ m^{-2})
- LE = Latent heat flux (MJ m^{-2})
- ΔS = Energy storage within surface layer (MJ m^{-2})

Wohlfahrt *et al* (2009) note that residual energy may be assigned entirely to either the sensible or latent heat fluxes. These options therefore describe the upper and lower extremes of a range of latent heat data. If the residual energy is assigned to the sensible heat flux, the latent heat flux measured by the eddy covariance system remains unaltered and defines the lower extreme of the possible range of latent heat

flux data, LE_{min} (MJ m^{-2}). The upper extreme of the possible range of latent heat flux data, LE_{max} (MJ m^{-2}), is defined by assigning the residual energy, A_{res} (MJ m^{-2}), to the latent heat flux measured by the eddy covariance system:

$$LE_{max} = LE_{min} + A_{res} \quad (4.4)$$

The mid-point of the latent heat flux range, LE_{mid} (MJ m^{-2}), is used for reporting of some results and statistical analysis. This variable is defined as:

$$LE_{mid} = \frac{LE_{min} + LE_{max}}{2} \quad (4.5)$$

4.2.4. Bowen Ratio

The Bowen ratio, β , describes the proportion of sensible heat flux, H (MJ m^{-2}), to latent heat flux, LE (MJ m^{-2}):

$$\beta = \frac{H}{LE} \quad (4.6)$$

The assignment of residual energy, A_{res} (MJ m^{-2}), to either the sensible or latent heat flux will therefore alter the Bowen ratio. A range of Bowen ratios arising from the assigning of residual energy is therefore defined according to:

$$\beta_{min} = \frac{H}{LE + A_{res}} \quad (4.7)$$

and

$$\beta_{max} = \frac{H + A_{res}}{LE} \quad (4.8)$$

The mid-point of the range of Bowen ratios, β_{mid} , is therefore given by:

$$\beta_{mid} = \frac{\beta_{min} + \beta_{max}}{2} \quad (4.9)$$

4.3. Results

4.3.1. Flux Source Area

The proportion of the flux emanating from within the fetch of the eddy covariance system and the position of the peak footprint was calculated according to the methods described in section 4.2.1. The results for the entire study period are presented in table 4.1. These results demonstrate that for the shortest fetch (to the north of the instrumentation), 70% of the observed flux is estimated to originate within the unobstructed fetch of the instrumentation when a northerly wind is present. Similar flux proportions originating within 150 m of the instrumentation are estimated for all wind directions. 78% of the observed flux is estimated to originate from within the next shortest fetch (to the west of the instrumentation). The second longest fetch is to the south of the instrumentation and extends for 350 m. The prevailing wind direction is southerly during the study period and between 84% and 88% of the observed flux is estimated to originate within the southerly fetch. The longest fetch is to the east of the instrumentation and extends 500 m. 90% of the observed flux is estimated to originate within this fetch when the wind is from the east. The flux proportions originating within a given distance of the eddy covariance instrumentation are similar for all wind directions. The mean position of the peak footprint is also relatively consistent for all wind directions, and lies within even the range of the shortest fetch.

Table 4.1: Summary flux source area characteristics for different wind directions at Wicken Fen, 2009 – 10.

	North (315° - 45°)	East (45° - 135°)	South (135° - 225°)	West (225° - 315°)
Proportion of measurement period (%)	25.76	11.41	40.99	21.85
Fetch (m)	150	500	350	200
Flux proportion from within:				
150 m	0.70	0.72	0.70	0.72
200 m		0.78	0.77	0.78
300 m		0.85	0.84	
400 m		0.88	0.88	
500 m		0.90		
Mean distance to maximum flux (m)	27.00	25.42	26.51	24.64
Standard deviation of distance to maximum flux (m)	14.08	9.83	7.00	5.27

4.3.2. Energy Fluxes at Sedge Fen

The mean weekly energy flux data collected by the eddy covariance system at Sedge Fen are presented in figure 4.3. The net radiation, R_n , can be seen to peak during June and July in both years and subsequently decline. The 2009 data show that the net radiation becomes negative during November and December. The latent heat flux, LE , can be seen to be the greatest flux behind the net radiation. The latent heat flux peaks in July of both years before steadily declining. Unlike the net radiation, the latent heat flux does not become negative at any point during the study periods. In both years the latent heat flux becomes greater than the net radiation in October. The sensible heat flux, H , is generally lower than the latent heat flux, with the exception of

several weeks during April, May and June 2010. During this period, the magnitudes of the sensible and latent heat fluxes are similar to one another. By contrast, for the corresponding period in 2009 the latent heat flux is consistently greater than the sensible heat flux. The sensible heat flux peaks during the April – June period in both years and subsequently declines to negative values by July. During 2009, the sensible heat flux tends to more strongly negative values during October, whilst this onset commences in August during 2010. The ground heat flux, G , is the lesser of all fluxes in figure 4.3, being close to $0 \text{ MJ m}^{-2} \text{ d}^{-1}$ throughout both study periods. The ground heat flux is positive until August and then negative thereafter during both years. Although not shown within figure 4.3, the additional storage terms, ΔS (see section 3.2.3.3), calculated for Sedge Fen were negligible.

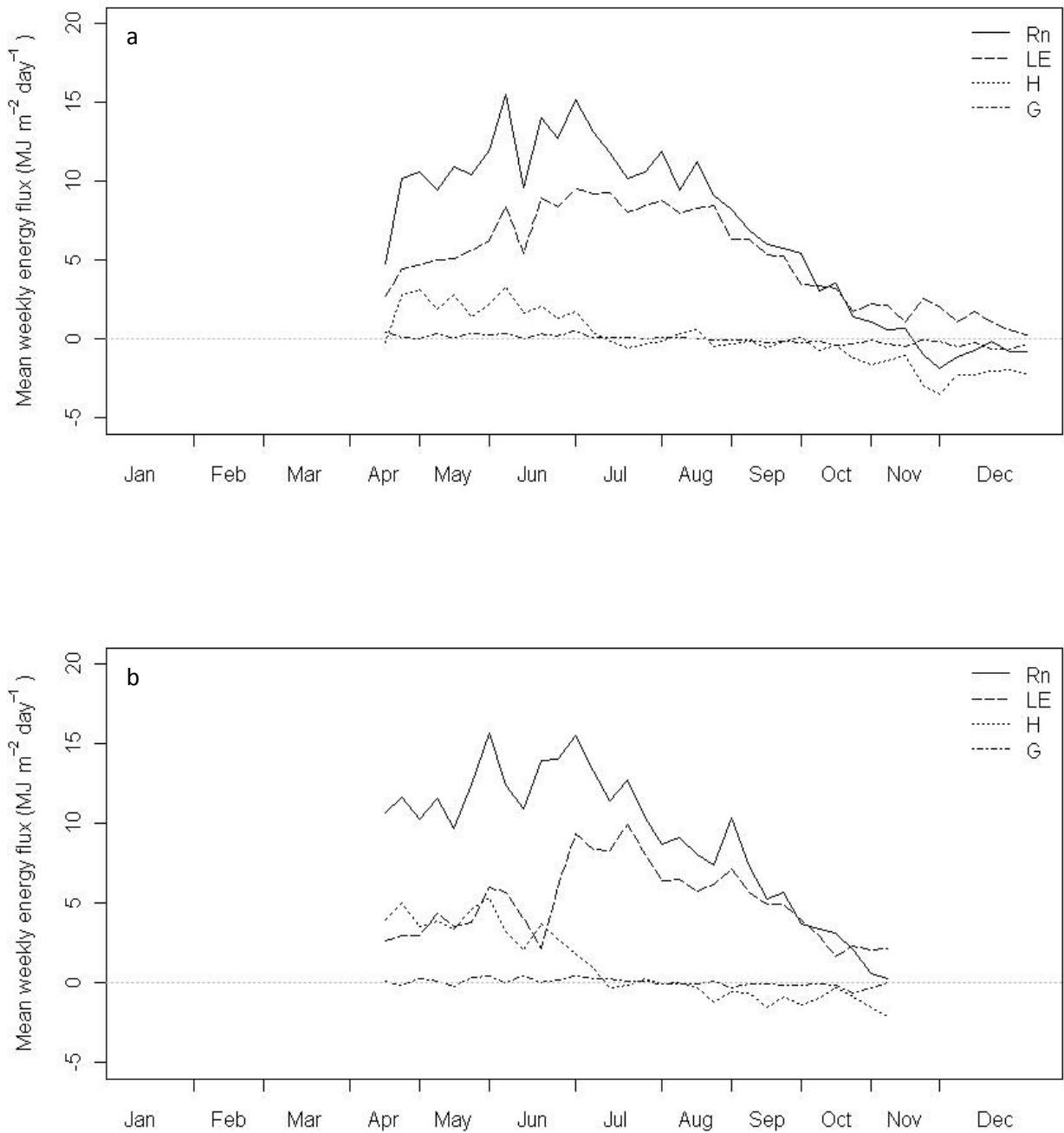


Figure 4.3: Surface energy fluxes recorded at Sedge Fen by the eddy covariance system for: a) 2009 and; b) 2010.

4.3.2.1. Net Radiation

The 2009 net radiation data is presented as net long- and shortwave fluxes in figure 4.4. During 2009, the net short wave radiation is consistently positive, whilst the net

longwave radiation is generally negative, with only one exception during November 2009. The negative net radiation values observed during November and December 2009 therefore result from the magnitude of the negative net longwave radiation flux being greater than that of the positive shortwave radiation flux during these months.

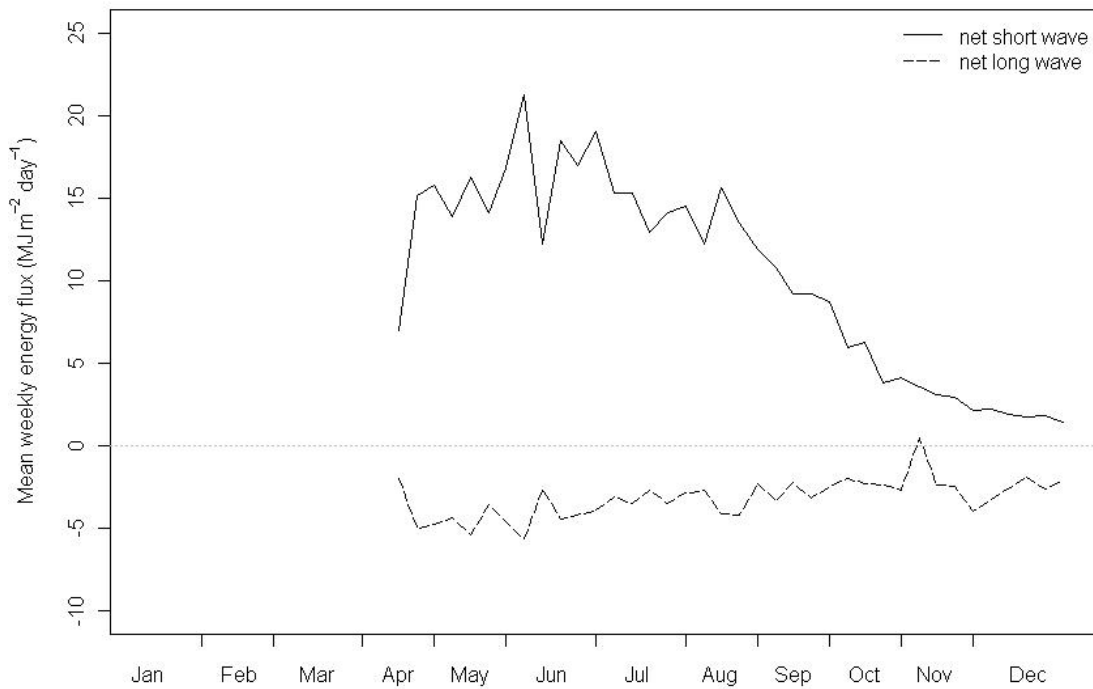


Figure 4.4: Net longwave and shortwave radiation fluxes at Sedge Fen, 2009.

An analysis of variance was invoked upon the monthly net radiation data. Examination of the net radiation data revealed that the data did not conform to a normal distribution. A non-parametric form of analysis of variance was therefore considered appropriate, and the Kruskal-Wallis rank sum test was invoked upon the data (Wheater & Cook, 2000). The null hypothesis was defined as there being no significant difference between the monthly net radiation data during each year and the significance level was set at 0.05. The results for each year were:

2009: $H = 205.24$ (8 df), $p < 0.01$

2010: $H = 122.78$ (6 df), $p < 0.01$

The alternative hypothesis must therefore be accepted. For 2009 and 2010, the monthly variation in net radiation is statistically significant

Dunn's multiple comparison test (Wheater and Cook, 2000) was invoked upon the monthly net radiation data, and the results are described in the form of superscripts in table 4.2. The data for 2009 reveal that the months between April and September are statistically similar to one another. Within this period, the months from May to August are also statistically similar to one another, but not to any other months. September and October are statistically similar to one another, and October also demonstrates a similarity with November and December. The 2010 data show a slightly different pattern, in which the April – August net radiation data are statistically similar to one another, with the April – July data forming another statistically similar subgroup. August and September are statistically similar to one another, and September is also statistically similar to October.

Table 4.2: Monthly mean and standard deviation of daily net radiation fluxes at Sedge Fen, 2009 and 2010. Superscripts indicate values that are not statistically different according to Dunn's multiple comparison test. Results of Mann-Whitney U tests comparing monthly net radiation data from successive years are also presented.

	2009		2010		Mann-Whitney test		
	Mean (MJ m ⁻²)	SD (MJ m ⁻²)	Mean (MJ m ⁻²)	SD (MJ m ⁻²)	U ₂₀₀₉	U ₂₀₁₀	p
April	8.50 ^a	3.77	10.93 ^{e, f}	2.45	145	339	0.02
May	11.42 ^{a, b}	3.76	12.20 ^{e, f}	4.00	411	550	0.33
June	12.91 ^{a, b}	4.21	13.66 ^{e, f}	4.57	402	498	0.49
July	11.78 ^{a, b}	3.20	11.93 ^{e, f}	3.40	461	500	0.79
August	10.05 ^{a, b}	3.06	8.59 ^{e, g}	2.75	608	353	0.07
September	6.10 ^{a, c}	2.17	5.77 ^{g, h}	2.52	492	408	0.54
October	2.26 ^{c, d}	1.53	2.08 ^h	1.73	530	431	0.49
November	-0.80 ^d	1.42					
December	-0.56 ^d	1.05					

The monthly mean net radiation data summarised in table 4.2 follows a similar pattern in both years, peaking in June and declining throughout the subsequent months. The monthly means are generally comparable for the two years, albeit slightly higher for the April – July period and lower for the remaining months during 2010 compared to 2009. So as to assess whether the same months in successive years are statistically comparable, a Mann-Whitney U test was invoked upon monthly net radiation data. For each test, the null hypothesis was defined as there being no significant difference between the monthly data from successive years and the significance level was set at 0.05. These results are also summarised in table 4.2. The Mann-Whitney results indicate that for all months except April, the null hypothesis must be accepted. Therefore, April is the only month for which a statistically significant difference exists between the monthly net radiation data for 2009 and 2010.

4.3.2.2. Ground Heat Flux

A Kruskal-Wallis rank sum test was invoked upon the monthly ground heat flux data, since investigation showed that this data also did not conform to a normal distribution. The null hypothesis was defined as there being no significant difference between the monthly ground heat flux data during each year and the significance level was set at 0.05. The results for each year were:

$$2009: H = 132.39 (8 \text{ df}), p < 0.01$$

$$2010: H = 51.17 (6 \text{ df}), p < 0.01$$

The alternative hypothesis must therefore be accepted. For 2009 and 2010, the monthly variation in the ground heat flux is statistically significant.

Dunn's multiple comparison test was invoked upon the monthly ground heat flux data, and the results are described in the form of superscripts in table 4.3. The results for 2009 indicate that the data for the period April – August are statistically similar. July, August and September are also statistically similar with respect to the ground heat fluxes observed. The August and September ground heat flux data are also statistically similar to those of October. The data for the months September – December form the last group of data that is statistically similar in terms of ground heat flux. During 2010, the months April – September exhibit a statistical similarity with respect to ground heat flux. The period April – July forms a sub-group of months with statistically similar ground heat fluxes. The months of August, September and October also exhibit a statistical similarity with respect to the ground heat flux data.

Table 4.3: Monthly mean and standard deviation of daily ground heat fluxes at Sedge Fen, 2009 and 2010. Superscripts indicate values that are not statistically different according to Dunn's multiple comparison test. Results of Mann-Whitney U tests comparing monthly ground heat flux data from successive years are also presented.

	2009		2010		Mann-Whitney test		
	Mean (MJ m ⁻²)	SD (MJ m ⁻²)	Mean (MJ m ⁻²)	SD (MJ m ⁻²)	U ₂₀₀₉	U ₂₀₁₀	p
April	0.21 ^a	0.25	0.11 ^{e, f}	0.29	288	196	0.29
May	0.31 ^a	0.28	0.15 ^{e, f}	0.40	623	338	0.045
June	0.25 ^a	0.24	0.26 ^{e, f}	0.27	425	475	0.72
July	0.10 ^{a, b}	0.18	0.18 ^{e, f}	0.23	372	589	0.13
August	0.06 ^{a, b, c}	0.24	-0.06 ^{e, g}	0.24	617	344	0.06
September	-0.15 ^{b, c, d}	0.28	-0.11 ^{e, g}	0.25	414	486	0.6
October	-0.21 ^{c, d}	0.30	-0.27 ^g	0.38	501	460	0.78
November	-0.27 ^d	0.27					
December	-0.45 ^d	0.27					

The monthly mean ground heat fluxes in table 4.3 demonstrate a May peak in 2009 and a June peak in 2010. In both years, the monthly mean heat flux declines throughout the subsequent months, becoming negative during September in 2009 and August in 2010. A Mann-Whitney U test was invoked upon the monthly ground heat flux data so as to assess whether corresponding months in the successive years were statistically similar. For each test, the null hypothesis was defined as there being no significant difference between the monthly data from successive years and the significance level was set at 0.05. These results are also summarised in table 4.3. The Mann-Whitney results indicate that for all months except May, the null hypothesis must be accepted. Therefore, May is the only month for which a statistically significant difference exists between the monthly ground heat flux data for 2009 and 2010.

4.3.2.3. Sensible Heat Flux

A Kruskal-Wallis rank sum test was invoked upon the monthly sensible heat flux data, since investigation showed that this data also did not conform to a normal distribution. The null hypothesis was defined as there being no significant difference between the monthly sensible heat flux data during each year and the significance level was set at 0.05. The results for each year were:

$$2009: H = 177.57 (8 \text{ df}), p < 0.01$$

$$2010: H = 149.25 (6 \text{ df}), p < 0.01$$

The alternative hypothesis must therefore be accepted. For 2009 and 2010, the monthly variation in the sensible heat flux is statistically significant.

Dunn's multiple comparison test was invoked upon the monthly sensible heat flux data, and the results are described in the form of superscripts in table 4.4. During 2009, the months between April and September exhibit a statistical similarity. Within this period, May and June are similar to one another but statistically distinct from all other months. The sensible heat flux data for the months between July and October are statistically similar to one another, and the October data also exhibits a similarity to the November and December sensible heat flux data. Within the 2010 sensible heat flux data, there are three groups of months which exhibit statistical similarities; April – June, July – September and August – October.

Table 4.4: Monthly mean and standard deviation of daily sensible heat fluxes at Sedge Fen, 2009 and 2010. Superscripts indicate values that are not statistically different according to Dunn's multiple comparison test. Results of Mann-Whitney U tests comparing monthly sensible heat flux data from successive years are also presented.

	2009		2010		Mann-Whitney test		
	Mean (MJ m ⁻²)	SD (MJ m ⁻²)	Mean (MJ m ⁻²)	SD (MJ m ⁻²)	U ₂₀₀₉	U ₂₀₁₀	p
April	1.93 ^a	2.15	4.12 ^e	1.38	96	388	<0.01
May	2.28 ^{a,b}	1.71	4.15 ^e	1.90	225	736	<0.01
June	1.82 ^{a,b}	1.36	2.77 ^e	1.80	337	563	0.1
July	-0.01 ^{a,c}	0.91	0.24 ^f	0.92	371	590	0.13
August	0.00 ^{a,c}	0.96	-0.51 ^{f,g}	0.95	606	355	0.08
September	-0.19 ^{a,c}	0.90	-1.02 ^{f,g}	1.09	635	265	<0.01
October	-0.97 ^{c,d}	0.97	-0.97 ^g	0.83	479	482	0.99
November	-2.35 ^d	1.17					
December	-2.12 ^d	0.64					

The mean sensible heat flux data in table 4.4 reveal peaks in May during both 2009 and 2010. The sensible heat fluxes subsequently decline throughout the remaining months in both years, becoming negative in July 2009 and in August 2010. The magnitude of the monthly mean sensible heat flux data is generally greater in 2010 than 2009. A Mann-Whitney U test was invoked upon the monthly sensible heat flux data so as to assess whether corresponding months in the successive years were statistically similar. For each test, the null hypothesis was defined as there being no significant difference between the monthly data from successive years and the significance level was set at 0.05. These results are also summarised in table 4.4. The Mann-Whitney results indicate that for all months except April, May and September the null hypothesis must be accepted. Therefore, the months of April, May and

September are the only months for which a statistically significant difference exists between the monthly sensible heat flux data for 2009 and 2010.

4.3.2.4. Latent Heat Flux

A Kruskal-Wallis rank sum test was invoked upon the monthly latent heat flux data, since investigation showed that this data also did not conform to a normal distribution. The null hypothesis was defined as there being no significant difference between the monthly latent heat flux data during each year and the significance level was set at 0.05. The results for each year were:

$$2009: H = 207.28 (8 \text{ df}), p < 0.01$$

$$2010: H = 115.12 (6 \text{ df}), p < 0.01$$

The alternative hypothesis must therefore be accepted. For 2009 and 2010, the monthly variation in the latent heat flux is statistically significant.

Dunn's multiple comparison test was invoked upon the monthly latent heat flux data, and the results are described in the form of superscripts in table 4.5. During 2009, the April latent heat flux data exhibits a statistical similarity to that of May, September, October and November. The latent heat flux data for all months within the period between May and September are statistically similar to one another, and the data for July and August are also statistically similar to each other. The latent heat flux data from the months between October and December also exhibit a statistical similarity. During 2010, the months of April, May and October exhibit statistically similar latent

heat flux data, as do May, June, August and September. The July and August latent heat flux data are statistically similar to each other, as are the August and September data.

Table 4.5: Monthly mean and standard deviation of daily latent heat fluxes at Sedge Fen, 2009 and 2010. Superscripts indicate values that are not statistically different according to Dunn's multiple comparison test. Results of Mann-Whitney U tests comparing monthly latent heat flux data from successive years are also presented.

	2009		2010		Mann-Whitney test		
	Mean (MJ m ⁻²)	SD (MJ m ⁻²)	Mean (MJ m ⁻²)	SD (MJ m ⁻²)	U ₂₀₀₉	U ₂₀₁₀	p
April	3.96 ^a	1.23	2.93 ^e	0.53	364	120	<0.01
May	5.86 ^{a,b}	1.60	4.60 ^{e,f}	1.48	709	252	<0.01
June	8.00 ^b	2.54	5.35 ^f	3.95	629	271	<0.01
July	8.91 ^{b,c}	2.19	8.61 ^g	2.21	507	454	0.72
August	8.05 ^{b,c}	1.99	6.36 ^{f,g,h}	1.37	725	236	<0.01
September	5.18 ^{a,b}	1.29	4.97 ^{f,h}	1.26	498	402	0.49
October	2.60 ^{a,d}	1.57	2.22 ^e	0.88	607	354	0.08
November	1.81 ^{a,d}	1.05					
December	0.94 ^d	0.75					

The monthly mean latent heat flux data presented in table 4.5 reveal that the latent heat flux peaks in July in both years. During 2009, the monthly mean latent heat flux is greater than that in 2010. A Mann-Whitney U test was invoked upon the monthly latent heat flux data so as to assess whether corresponding months in the successive years were statistically similar. For each test, the null hypothesis was defined as there being no significant difference between the monthly data from successive years and the significance level was set at 0.05. These results are also summarised in table 4.5. The Mann-Whitney results indicate that the null hypothesis must be accepted for July,

September and October. Therefore, for all months except July, September and October a statistically significant difference exists between the monthly latent heat flux data for 2009 and 2010.

4.3.2.5. Bowen Ratio

A Kruskal-Wallis rank sum test was invoked upon the monthly Bowen ratio data, since investigation showed that this data also did not conform to a normal distribution. The null hypothesis was defined as there being no significant difference between the monthly Bowen ratio data during each year and the significance level was set at 0.05. The results for each year were:

$$2009: H = 163.79 (8 \text{ df}), p < 0.01$$

$$2010: H = 146.03 (6 \text{ df}), p < 0.01$$

The alternative hypothesis must therefore be accepted. For 2009 and 2010, the monthly variation in the Bowen ratio is statistically significant.

Dunn's multiple comparison test was invoked upon the monthly Bowen ratio data, and the results are described in the form of superscripts in table 4.6. During 2009, the Bowen ratio data for all months between April and September exhibit a statistical similarity. Within this period, the May and June Bowen ratio data are statistically similar to one another, as are the June, July and August data. The Bowen ratio data for the months between July and October are statistically similar to one another. October, November and December are the final group of months to exhibit a

statistical similarity with respect to the 2009 Bowen ratio data. During 2010, the April and May Bowen ratio data are statistically similar, as are the May and June data. June and July exhibit a statistical similarity with respect to the Bowen ratio data, as do July, August and September. August, September and October also exhibit a statistical similarity between the Bowen ratio data.

Table 4.6: Monthly mean and standard deviation of daily Bowen ratio at Sedge Fen, 2009 and 2010. Superscripts indicate values that are not statistically different according to Dunn's multiple comparison test. Results of Mann-Whitney U tests comparing monthly Bowen ratio data from successive years are also presented.

	2009		2010		Mann-Whitney test		
	Mean (MJ m ⁻²)	SD (MJ m ⁻²)	Mean (MJ m ⁻²)	SD (MJ m ⁻²)	U ₂₀₀₉	U ₂₀₁₀	p
April	0.33 ^a	0.60	1.40 ^f	0.41	27	457	<0.01
May	0.37 ^{a, b}	0.27	0.92 ^{f, g}	0.40	139	822	<0.01
June	0.22 ^{a, b, c}	0.16	-0.49 ^{g, h}	5.96	268	632	<0.01
July	-0.01 ^{a, c, d}	0.11	0.02 ^{h, i}	0.10	376	585	0.14
August	-0.01 ^{a, c, d}	0.11	-0.09 ^{i, j}	0.16	617	344	0.06
September	-0.06 ^{a, d}	0.21	-0.24 ^{i, j}	0.26	634	266	<0.01
October	-0.47 ^{d, e}	0.72	-0.50 ^j	0.46	536	425	0.44
November	-1.93 ^e	2.25					
December	9.55 ^e	70.88					

The monthly mean Bowen ratio data presented in table 4.6 reveals that during 2009, the Bowen ratio peaks in May and subsequently declines. The high value of 9.55 recorded in December 2009 was investigated and found to be the result of a Bowen ratio of 355 on 24th December 2009, caused by a near-zero value of latent heat flux on this date. The removal of this value results in a monthly mean Bowen ratio of -2.36 for December 2009. Since the flux data for 24th December 2009 does not appear to be

in error, it was retained for use in the subsequent analyses. During 2010, the mean monthly Bowen ratio declines from a peak in April to a low in June. This value prompted an investigation of the June 2010 data, and was found to be the result of a Bowen ratio of -31.67 on 17th June 2010 resulting from a near-zero value of latent heat flux on this date. The removal of this value results in a monthly mean Bowen ratio of 0.59 for June 2010. Since the flux data for 17th June 2010 does not appear to be in error, it was retained for use in subsequent analyses. The Bowen ratio data for 2010 recovers in July and then declines throughout the remaining months, reaching a low in October comparable with that reached in June. A Mann-Whitney U test was invoked upon the monthly Bowen ratio data so as to assess whether corresponding months in the successive years were statistically similar. For each test, the null hypothesis was defined as there being no significant difference between the monthly data from successive years and the significance level was set at 0.05. These results are also summarised in table 4.6. The Mann-Whitney results indicate that the null hypothesis must be accepted for July, August and October. Therefore, for all months except July, August and October a statistically significant difference exists between the monthly Bowen ratio data for 2009 and 2010.

4.3.2.6. Residual Energy

The residual energy arising from the imbalance of the surface energy fluxes recorded by the eddy covariance system (see section 3.2.3.4) for 2009 and 2010 is presented in figure 4.5. The residual energy peaks during June in both years, and declines through the subsequent months. During 2010 the June peak is approximately three times greater than that for 2009, and there is also a secondary peak in early September.

During November 2009 negative residual energy values are observed, implying fluxes in excess of the available energy recorded by the eddy covariance system.

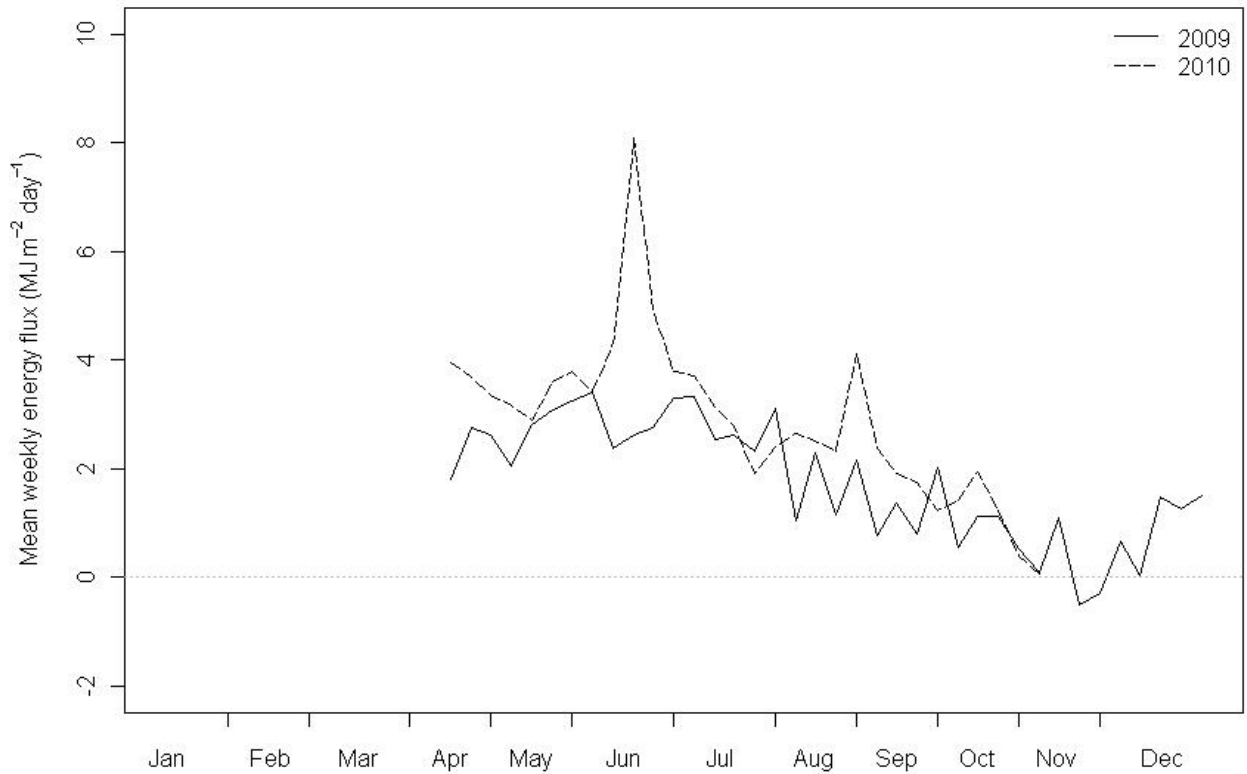


Figure 4.5: Residual energy at Sedge Fen, 2009 and 2010.

The residual energy data is presented as monthly proportions of available energy (defined as the difference between net radiation and ground heat flux) in table 4.7. The residual energy is typically approximately 30% of the monthly available energy. An obvious exception is the large negative value reported for December 2009, implying that approximately ten times more energy is leaving the surface than is received. This result arises due to the definition of available energy adopted, which does not include sensible heat flux. During December 2009, there is a negative total sensible heat flux of -63.45 MJ m^{-2} . During the same period, the available energy is

-3.23 MJ m⁻² and the residual energy 31.28 MJ m⁻². The negative sensible heat flux is therefore sufficient to account for the residual energy and the observed latent heat flux (28.10 MJ m⁻²) during December 2009.

Table 4.7: Residual energy as proportion of available energy at Sedge Fen

	Residual energy as proportion of available energy ($R_n - G$) (%)	
	2009	2010
April	29.32	35.39
May	27.11	27.87
June	22.72	39.75
July	23.96	24.87
August	19.63	32.46
September	20.20	32.61
October	33.87	46.57
November	2.36	
December	-969.74	
Total	26.07	32.57

A Kruskal-Wallis rank sum test was invoked upon the monthly residual energy data, since investigation showed that this data also did not conform to a normal distribution. The null hypothesis was defined as there being no significant difference between the monthly residual energy data during each year and the significance level was set at 0.05. The results for each year were:

2009: $H = 114.71$ (8 df), $p < 0.01$

2010: $H = 93.25$ (6 df), $p < 0.01$

The alternative hypothesis must therefore be accepted. For 2009 and 2010, the monthly variation in the residual energy is statistically significant.

Dunn's multiple comparison test was invoked upon the monthly residual energy data, and the results are described in the form of superscripts in table 4.8. The results for 2009 indicate that the months from April until August share statistically similar residual energy data. August, September, October and December exhibit statistically similar residual energy data. The residual energy data from September, October, November and December also exhibit a statistical similarity. During 2010, the months between April and August demonstrate a statistical similarity with respect to the residual energy data. Within this group, the residual energy data for April and May demonstrate a similarity to one another, but not with that of any other months. Two other statistically similar groups exist within the 2010 monthly residual energy data: July – September and; September and October.

The monthly mean residual energy data presented in table 4.8 reveals that there is a peak in May 2009 and June 2010. In both years, the residual energy declines in the subsequent months. During November 2009, the mean residual energy is slightly negative, implying that marginally more energy is leaving the surface at Sedge Fen than is received. A Mann-Whitney U test was invoked upon the monthly residual energy data so as to assess whether corresponding months in the successive years were statistically similar. For each test, the null hypothesis was defined as there being

no significant difference between the monthly data from successive years and the significance level was set at 0.05. These results are also summarised in table 4.8. The Mann-Whitney results indicate that the null hypothesis must be accepted for May, July and October. Therefore, for all months except May, July and October a statistically significant difference exists between the monthly residual energy data for 2009 and 2010.

Table 4.8: Monthly mean and standard deviation of daily residual energy at Sedge Fen, 2009 and 2010. Superscripts indicate values that are not statistically different according to Dunn's multiple comparison test. Results of Mann-Whitney U tests comparing monthly residual energy data from successive years are also presented.

	2009		2010		Mann-Whitney test		
	Mean (MJ m ⁻²)	SD (MJ m ⁻²)	Mean (MJ m ⁻²)	SD (MJ m ⁻²)	U ₂₀₀₉	U ₂₀₁₀	p
April	2.43 ^a	1.18	3.83 ^{d,e}	1.31	103	381	< 0.01
May	3.01 ^a	1.29	3.36 ^{d,e}	1.13	384	577	0.18
June	2.88 ^a	0.99	5.33 ^d	2.57	135	765	< 0.01
July	2.80 ^a	1.32	2.92 ^{d,f}	1.29	438	523	0.56
August	1.96 ^{a,b}	2.03	2.81 ^{d,f}	1.73	290	671	< 0.01
September	1.26 ^{b,c}	1.18	1.92 ^{f,g}	1.11	287	613	0.02
October	0.84 ^{b,c}	1.68	1.09 ^g	1.27	409	552	0.32
November	-0.01 ^c	1.13					
December	1.04 ^{b,c}	1.26					

4.3.3. Forced Closure of Energy Budget

The residual energy data reported within section 4.3.2.6 represents a significant proportion of the available energy, raising the possibility that the sensible and latent

heat flux data reported in sections 4.3.2.3 and 4.3.2.4 are underestimates of the actual values. Closure may be forced upon the eddy covariance energy data by apportioning the residual energy either to the sensible or latent heat flux. Figure 4.6 presents the maximum ranges of latent heat flux data defined as described in section 4.2.3, and translates the latent heat flux data into units of evapotranspiration. The lower extremes of the latent heat flux ranges are defined by the latent heat flux data presented in figure 4.3, whilst the upper boundary represents the addition to the lower values of the residual energy data presented in figure 4.5. The range of the latent heat flux and evapotranspiration data thus reflects the behaviour of the residual energy commented upon in section 4.2.3.6.

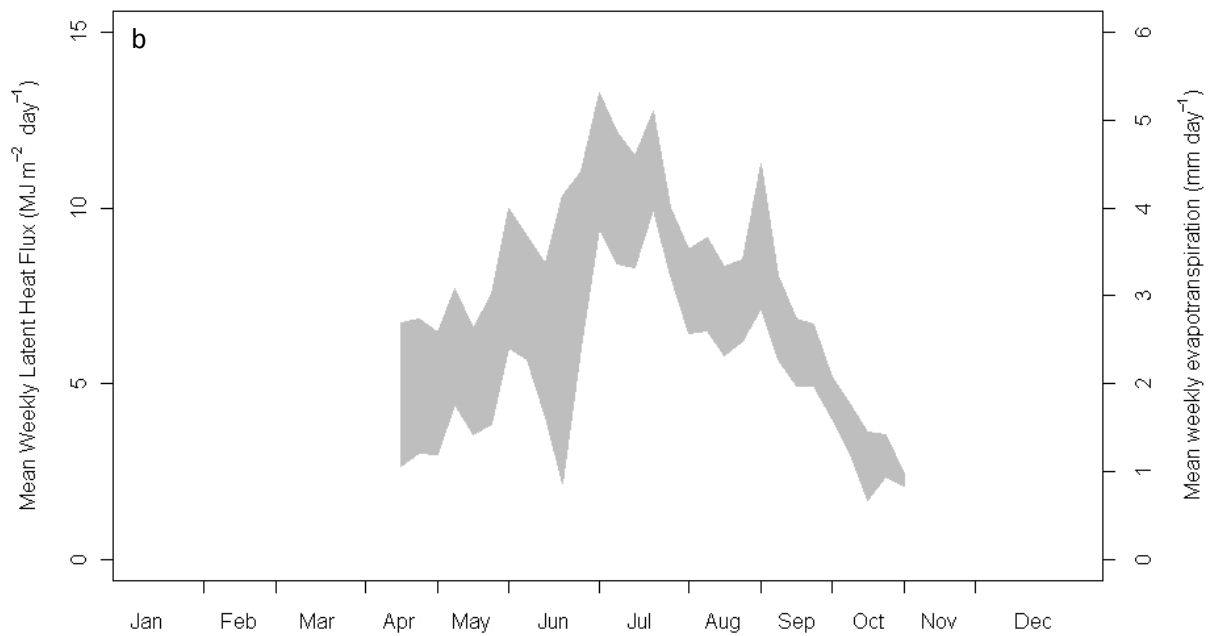
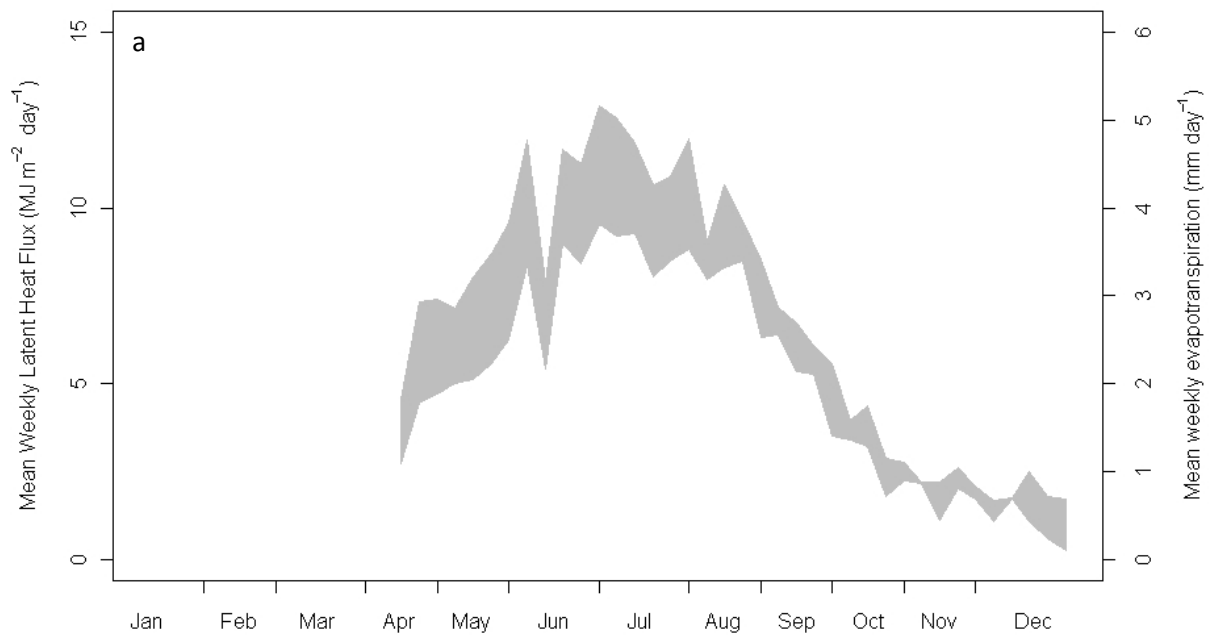


Figure 4.6: Ranges of latent heat flux and actual evapotranspiration estimates derived by the apportioning of residual energy described in section 4.2.3 for: a) 2009 and; b) 2010.

4.3.3.1. Revised Latent Heat Fluxes

In order to evaluate the range of latent heat fluxes presented within figure 4.6, the mid-point of the monthly fluxes were defined as described in section 4.2.3. A Kruskal-Wallis test was invoked upon the latent heat flux mid-point data. The null hypothesis was defined as there being no significant difference between the monthly mid-point of latent heat flux range data during each year and the significance level was set at 0.05. The results for each year were:

$$2009: H = 214.62 (8 \text{ df}), p < 0.01$$

$$2010: H = 117.86 (6 \text{ df}), p < 0.01$$

The alternative hypothesis must therefore be accepted. For 2009 and 2010, the monthly variation in the latent heat flux mid-point is statistically significant.

Dunn's multiple comparison test was invoked upon the monthly latent heat flux mid-point data, and the results are described in the form of superscripts in table 4.9. During 2009, April, May, September and October exhibit a statistical similarity with respect to the latent heat flux mid-point. The months in the period May – September exhibit a statistical similarity, within which the months of June, July and August form a distinct sub-group. The latent heat flux mid-point data for October, November and December are also statistically similar to one another. The results for 2010 indicate that April is statistically similar to September and October with respect to latent heat flux mid-point data. May, June, August and September are also statistically similar to one another, as are June, July, August and September. July and August exhibit a

statistical similarity to one another with respect to latent heat flux mid point data, but not to any other months.

Table 4.9: Monthly mean and standard deviation of daily latent heat flux mid-point at Sedge Fen, 2009 and 2010. Superscripts indicate values that are not statistically different according to Dunn's multiple comparison test. Results of Mann-Whitney U tests comparing monthly latent heat flux mid-point data from successive years are also presented.

	2009		2010		Mann-Whitney test		
	Mean (MJ m ⁻²)	SD (MJ m ⁻²)	Mean (MJ m ⁻²)	SD (MJ m ⁻²)	U ₂₀₀₉	U ₂₀₁₀	p
April	5.18 ^a	1.55	4.84 ^e	1.02	282	202	0.36
May	7.37 ^{a, b}	1.93	6.28 ^f	1.77	657	304	0.01
June	9.44 ^{b, c}	2.82	8.01 ^{f, g}	3.37	558	342	0.11
July	10.31 ^{b, c}	2.32	10.07 ^{g, h}	2.53	490	471	0.90
August	9.03 ^{b, c}	2.11	7.77 ^{f, g, h}	1.87	662	299	0.01
September	5.81 ^{a, b}	1.35	5.93 ^{e, f, g}	1.50	427	473	0.74
October	3.02 ^{a, d}	0.99	2.77 ^e	0.90	577	384	0.18
November	1.81 ^d	0.81					
December	1.46 ^d	0.66					

The monthly mean latent heat flux mid-point data presented in table 4.9 reveals that there is a July peak in latent heat flux during both years. The mean monthly latent heat flux mid-point is generally greater during 2009 than 2010, with the only exception being the values for September. A Mann-Whitney U test was invoked upon the monthly latent heat flux mid-point data so as to assess whether corresponding months in the successive years were statistically similar. For each test, the null hypothesis was defined as there being no significant difference between the monthly

data from successive years and the significance level was set at 0.05. These results are also summarised in table 4.9. The Mann-Whitney results indicate that the null hypothesis must be rejected for May and August. Therefore, May and August are the only months for which a statistically significant difference exists between the monthly latent heat flux mid-point data for 2009 and 2010.

4.3.3.2. Revised Bowen Ratio

The use of a range of latent heat flux values will produce a range of Bowen ratio data, the extremes of which are defined by equations 4.7 and 4.8. The Bowen ratio data presented within section 4.3.2.5 demonstrated that large individual daily values, whilst correct, may exert considerable influence over the monthly average Bowen ratio. Revised Bowen ratios were therefore derived using monthly total energy data according to equations 4.7 - 4.9. The monthly Bowen ratio mid-points are presented in table 4.10. When presented in this manner, the monthly Bowen ratio mid-points can be seen to decline throughout each study period. During 2009, the decline is most marked during the periods April – July and October – December. During the period between July and September the monthly Bowen ratio mid points are relatively stable. These patterns are repeated in 2010, although the values of the Bowen ratio mid-points are generally greater than the equivalent months in 2009, especially in the period between April and June.

Table 4.10: Monthly Bowen ratio mid points.

	2009	2010
April	0.70	1.66
May	0.58	1.08
June	0.38	0.89
July	0.16	0.19
August	0.12	0.15
September	0.09	0.02
October	-0.16	-0.12
November	-1.30	
December	-1.11	

A Mann-Whitney test was invoked upon the monthly Bowen ratio mid-point data presented in table 4.10 so as to assess whether the data from each year were statistically similar. For each test, the null hypothesis was defined as there being no significant difference between the data from successive years and the significance level was set at 0.05. These results are:

$$U_{2009} = 19, U_{2010} = 44, p = 0.21$$

The null hypothesis must therefore be accepted. There is no statistically significant difference between the Bowen ratio mid-point data from 2009 and 2010.

4.4. Discussion

The flux source area results presented in section 4.3.1 indicate that the prevailing wind during the study period is from the south. Northerly winds are marginally more common than westerly winds, whilst easterly winds were the least frequently observed. These results become important when viewed within the context of the unobstructed fetch of the eddy covariance instrumentation. The system is bounded to the north by woodland, which also partially bounds the system to the east. A drainage ditch lies 200 m to the west of the system, which divides Sedge Fen from Verrall's Fen, an area consisting of several vegetation communities (Mountford *et al*, 2005). The southern boundary of the unobstructed fetch is defined by Wicken Lode, beyond which lie the reedbeds of Adventurer's Fen. The flux source area data can therefore be used to indicate how representative of Sedge Fen the eddy covariance data are.

The results presented in section 4.3.1 demonstrate that the flux proportions estimated to originate within a specified distance of the instrumentation are consistent for all wind directions. The distances to the peak source area also demonstrate a consistency between all wind directions. Taken together, these results are indicative of a homogeneous surface surrounding the instrumentation within the unobstructed fetches defined in table 4.1. Crucially, the peak source area lies within the unobstructed fetches for all wind directions, reinforcing that high proportions of the observed fluxes are likely to originate within the unobstructed fetch of the instrumentation.

It is acknowledged that these results are applicable to situations of neutral atmospheric stability. In stable conditions the source area will increase in size, whilst unstable conditions will produce a smaller source area. While this implies a smaller proportion of fluxes originating within the fetch of the eddy covariance system in stable atmospheric conditions, active evapotranspiration will be associated with neutral or unstable conditions (Acreman *et al*, 2003). The source area estimates for Sedge Fen compare favourably with those reported by Acreman *et al* (2003) and Thompson *et al* (1999). Acreman *et al* (2003) estimated that for neutral conditions 70% of the observed flux originated from within the shortest fetch, whilst Thompson *et al* (1999) estimated that 80% of the observed flux was derived from within the shortest fetch for unstable conditions. The large proportion of fluxes derived from within the fetch of the eddy covariance system and the apparent homogeneity of the surface suggests that the eddy covariance data are representative of the surface fluxes at Sedge Fen. The actual evapotranspiration estimates derived by the eddy covariance system are therefore adjudged to accurately represent the evaporative loss from the surface at Sedge Fen.

The mean weekly energy flux data presented in section 4.3.2 demonstrates the net radiation to be the dominant input of energy to the surface at Sedge Fen during 2009 and 2010. Although the net radiation is observed to be negative during November and December 2009, consideration of the short- and longwave radiation fluxes during 2009 confirm that this is not due to instrumental error. Rather, during these months the magnitude of the negative longwave flux is greater than that of the positive shortwave flux, resulting in the observed negative net radiation fluxes. Despite the negative net radiation flux observed during November and December 2009, a positive

latent heat flux is maintained during this period. The data presented within figure 4.3 show that this coincides with a sustained period of negative sensible heat fluxes, implying that energy is being advected from outside the source area of the eddy covariance instrumentation. Whilst negative sensible heat fluxes are observed during much of the study period, the coincidence with lesser negative net radiation fluxes results in the advected sensible heat being the dominant energy input at Sedge Fen during November and December 2009. This advected energy serves to sustain the latent heat flux, and thus evapotranspiration during this period.

The monthly net radiation data displays a statistically significant variation between months according to the results of the Kruskal-Wallis and Dunn's multiple comparison tests. In both years, a peak value is reached in June, followed by a subsequent decline. The groupings of months with statistically similar net radiation suggest a distinct seasonality in net radiation fluxes. The Mann-Whitney test compared the net radiation data from the same months in successive years. The results demonstrated that only for April did a statistically significant difference exist between the monthly net radiation data during the period April – October. This suggests that the net radiation flux at Sedge Fen may be characterised as a repeating annual cycle, although a longer data record would be required in order to better define representative values. When considered alongside the results presented in figure 4.4, it becomes evident that the variation of the net radiation flux during 2009 is driven by the fluctuation in the net shortwave radiation flux, since the net longwave flux exhibits little variation through the year. These results are therefore consistent with the expected variation of net radiation expected within the mid-latitudes of the northern hemisphere.

The monthly ground heat flux data also exhibits a statistically significant variation between months. There is a tendency for the ground heat flux to be positive for much of the summer, indicating the transfer of energy from the surface layer to deeper soil layers during this period. During late summer/early autumn, the ground heat flux becomes negative and the magnitude progressively increases throughout the remainder of the study period. This is indicative of a reversal of the summer observations, implying that energy is being transferred to the surface layer from underlying soil layers. Overall, the ground heat flux data implies that energy is being transferred to and stored within subsurface layers during the first half of each study period and released from storage during the latter months of each study period. Thus the ground heat flux represents an energy sink or source dependent on the time of year. The Mann-Whitney test results indicate that this behaviour is statistically consistent in the April – October period of each year, with the May ground heat flux data being the only exception. However, figure 4.3 highlights that the magnitudes of the ground heat fluxes during 2009 and 2010 are likely to be of little consequence in the context of the overall surface energy budget.

The sensible and latent heat fluxes also exhibit statistically significant monthly variations, although these contrast with one another. The sensible heat flux peaks in May in both years, and becomes consistently negative from September in 2009 and August in 2010. By contrast, the latent heat flux is positive throughout each study period, reaching a peak in July in both years. Mann-Whitney tests of monthly sensible heat fluxes in the successive years demonstrate that there are statistically significant differences between the April, May and September data. The same test applied to the latent heat flux data demonstrates statistically significant differences for

all months except July, September and October. This suggests that these fluxes are not as consistent as the net radiation and ground heat flux fluxes from year to year. This is also reflected in the Bowen ratio data presented in section 4.3.2.5. Consideration of the Bowen ratio reinforces the finding that the latent heat flux is typically larger than the sensible heat flux at Sedge Fen. The near-zero values of Bowen ratio observed in July and August imply that these are the months in which the magnitudes of the sensible and latent heat fluxes differ most. The negative Bowen ratios observed during the latter months of each year arise as a result of the negative sensible heat fluxes previously commented upon and their increasing magnitudes are indicative of the increasing magnitudes of the negative sensible heat fluxes and decreasing latent heat fluxes observed during these periods. Taken together, these results suggest that the partitioning of available energy into sensible and latent heat fluxes at Sedge Fen is not consistent from year to year. Accurate evapotranspiration estimates cannot therefore be based upon empirical estimates of typical latent heat fluxes at Sedge Fen.

The sensible heat flux exhibits a consistent seasonal trend in both years, falling from a peak in the early summer period to negative values by the late summer (figure 4.3). The negative sensible heat fluxes have been cited as evidence of the advection of energy from outside the eddy covariance system's source area, which serves to sustain evapotranspiration and thus implies that the flux data is reliable. The implications of this scenario must be considered within the context of the wider landscape in which Wicken Fen is situated. Wicken Fen is a small wetland area surrounded by agricultural land (figure 1.3), and so energy advected from outside the flux source area of the eddy covariance instrumentation will have originated from the land under

agricultural management. This implies that the sensible heat flux outside the Fen is greater than that within the Fen during the late summer and winter periods, hence the advection of excess energy manifested by the negative sensible heat fluxes recorded at the Fen. The seasonal nature of the sensible heat flux gradient may be indicative of differing water regimes operating at Sedge Fen and the agricultural land. Relative to Sedge Fen, the agricultural land is likely to become drier throughout the growing season as the available water is removed from the soil by the vegetation. Although some of this loss will be replaced by irrigation to maximise crop yields, economic and regulatory factors will ensure that there is a net loss of water from the agricultural land throughout the summer. The gradual drying of the agricultural land will therefore result in progressively lower proportions of energy being partitioned as latent heat in response to there being less water available for evaporation. The harvesting of crops is likely to exacerbate this trend by reducing the contribution of transpiration to the latent heat flux. The reduction of the latent heat flux generated by the agricultural land is likely to be compensated for by an increase in the sensible heat flux, which is advected towards Sedge Fen. By contrast, Sedge Fen remains relatively wet throughout the growing season, and thus the sensible heat flux is suppressed in favour of the latent heat flux. The lack of turbulent convective motion resulting from a weak sensible heat flux at Sedge Fen would likely prohibit dissipation of the energy advected from the agricultural land and so this energy is transferred to the surface at Sedge Fen. The sensible heat flux behaviour observed at Sedge Fen in the latter half of each year is therefore likely to be indicative of energy balance processes operating at the regional, rather than local, scale.

The eddy covariance flux data was shown not to completely close the surface energy budget in section 4.3.2.6. Surface storage terms were calculated as described in section 3.2.3.3 but were found to be negligible and therefore do not account for the incomplete closure of the surface energy budget at Sedge Fen. The monthly residual energy within the surface energy budget typically represented approximately 30% of the available energy. However, the monthly variation in the residual energy was shown to be statistically significant, thus precluding the possibility of applying a constant uncertainty margin to all flux data. Since incomplete closure is a widely acknowledged limitation of the eddy covariance technique (Foken *et al*, 2004; Oncley *et al*, 2007; Wilson *et al*, 2002), the residual energy reported within section 4.3.2.6 is not considered to be indicative of a flaw within the eddy covariance instrumentation deployed at Sedge Fen or within the processing routines applied to the data. However, the incomplete closure raises uncertainty regarding the accuracy of the latent heat fluxes, and thus the evapotranspiration estimates, reported by the eddy covariance system.

Closure was therefore forced upon the surface energy budget data reported by the eddy covariance system following the recommendations of Wohlfahrt *et al* (2009); the residual energy was assigned to either the latent or sensible heat fluxes. Thus a range of latent heat flux data was defined, the lower extreme of which represents the latent heat flux data recorded by the eddy covariance system and the upper extreme representing the addition of the residual energy to the measured latent heat flux. Whilst it remains unknown precisely where within this possible range the actual latent heat flux lies, the definition of the range represents the best available estimate of the likely limits of the actual latent heat flux. Consideration was also given to another

recommendation of Wohlfahrt *et al* (2009); that of apportioning the residual energy between the sensible and latent heat fluxes so as to preserve the Bowen ratio. This methodology would have produced a specific estimate of latent heat flux for each timestep. Given the relatively low Bowen ratios reported for much of the study periods, much of the residual energy would have been assigned to the latent heat flux and thus produced estimates in the upper part of the latent heat flux ranges described in figure 4.6. However, given that there is no evidence to either support or contradict the underlying assumption of Bowen ratio preservation it was deemed inappropriate to derive specific latent heat flux estimates using this method.

The mid-point data was derived from the range of latent heat flux resulting from forced closure of the energy budget for use in analysis. By basing the estimated range of latent heat flux on the latent heat fluxes recorded by the eddy covariance system, the monthly variation of the latent heat flux data previously described is preserved. Furthermore, comparison of months from successive years is also improved, with only the latent heat flux mid-point data during May and August exhibiting a statistically significant difference according to the Mann-Whitney test. It may therefore be possible to generate empirical monthly estimates of latent heat fluxes, although further data and analysis is necessary to validate this approach. When forcing closure upon the surface energy budget using these methods, consideration must be given to the effect this will have on the Bowen ratio. Unless explicitly preserved, the Bowen ratio will be altered by varying the amounts of energy assigned to the sensible and latent heat fluxes as the residual energy is apportioned to either surface flux. This has been addressed by defining a range of Bowen ratios, the upper and lower extremes of which define whether the residual energy has been assigned to the sensible or latent heat fluxes, respectively. The mid-points of the Bowen ratio range thus defined for

each year show similar values during the period July – October, suggesting that these values may be used to characterise surface energy partitioning at Sedge Fen during this period. Again, analysis of further observations will serve to assess the validity of this proposal.

4.5. Conclusions

The fetch of the eddy covariance system at Sedge Fen has been defined for all wind directions. The majority of the observed fluxes are estimated to have originated within the unobstructed fetch for all wind directions and thus the observed fluxes are believed to be representative of the surface at Sedge Fen.

The observed fluxes have been scrutinised and are adjudged to be consistent with one another. Negative net radiation fluxes have been shown to be the result of outgoing longwave radiation exceeding the input of both long- and shortwave radiation at the surface. Negative sensible heat fluxes represent the advection of energy from outside the flux source area of the eddy covariance instrumentation, and are the dominant energy source during periods of negative net radiation. The latent heat flux is the dominant loss of energy from Sedge Fen, and thus indicates that evapotranspiration is maintained throughout the year.

Consideration has been given to the closure of the surface energy budget, and a methodology described in which closure is forced by assuming the residual energy represents an underestimate of either the sensible or latent heat fluxes. This produces

a range of possible latent heat flux data from which a range of evapotranspiration estimates may be derived. These ranges represent the best available estimate of the inherent uncertainty of latent heat flux estimates derived from eddy covariance measurements.

Chapter 5

Surface Controls on Evapotranspiration at Sedge Fen

5.1. Introduction

5.1.1. Wetland Evapotranspiration Measurements and Estimates

Previous studies have demonstrated a range of wetland evapotranspiration rates when employing the eddy covariance or Bowen ratio techniques. For example, sedge meadows in South Africa were found to evaporate between 0.6 and 9.8 mm d⁻¹ during the summer, whilst nearby reedbed evaporation was found to be between 0.2 and 3.3 mm d⁻¹ during the same period (Smithers *et al*, 1995). Within the UK, extreme values for reeds of 13.39 mm d⁻¹ have been reported (Fermor, 1997) although lower values between 0.5 and 5 mm d⁻¹ were found for reedbeds by Peacock and Hess (2004). For UK wet grasslands typical maximum rates between 0.6 mm d⁻¹ during a very wet period to 6.4 mm d⁻¹ during a hot dry spell have been reported from the Pevensey Levels, Sussex (Gasca-Tucker and Acreman, 2000) and 1 to 5.5 mm d⁻¹ at Yarnton Mead, Oxfordshire (Gardner, 1991). Acreman *et al* (2003), reported evaporation rates from a reedbed to be 14% higher than that of a nearby wet grassland over a five month period. Mould *et al* (2010) recorded up to 5.5 mm d⁻¹ from Otmoor floodplain in Oxfordshire. Thus evapotranspiration rates vary between wetlands.

The variation in observed wetland evapotranspiration rates may be partly attributable to differences in meteorological variables between sites. Empirical approaches to

estimating evaporative fluxes, such as the Penman or Penman-Monteith equations, attempt to describe the evaporative loss as a function of meteorological variables. In the case of the Penman-Monteith equation, surface parameters are standardised to represent a hypothetical reference surface akin to grass thus producing estimates of reference evapotranspiration (section 2.2.4). When applied within wetland environments, estimated values of evaporative loss contrast with measured values. Finch and Harding (1998) found that measured evapotranspiration agreed well with reference evapotranspiration estimates at the seasonal scale, likely due to the reference surface closely approximating the grass surface at the study site. Acreman *et al* (2003) reported a similar finding, noting a good agreement between Penman evaporation estimates and measurements of evapotranspiration for a wet grassland. However, reedbed evapotranspiration was shown to exceed Penman evaporation estimates. Thompson *et al* (1999) reported evapotranspiration rates lower than the equilibrium evaporation rate estimated from meteorological data for dry days at a peat bog. Whilst the studies summarised here utilise differing methodologies to estimate the evaporative flux, it is interesting to note the contrasting relationships with measurements of evapotranspiration. This suggests that consideration of meteorological parameters does not sufficiently describe all factors controlling evapotranspiration.

5.1.2. Surface Characteristics

The control of non-meteorological factors over evapotranspiration is acknowledged within the formulation of reference evapotranspiration by the definition of a reference surface. Therefore, evapotranspiration measurements may not be consistent with

reference evapotranspiration estimates in environments where the surface characteristics differ from those specified for the reference surface. Reference evapotranspiration estimates are commonly adjusted to represent evapotranspiration from particular vegetation communities by means of crop coefficients. Crop coefficients are defined as the ratio of actual to reference evapotranspiration, and thus require some measurement of evapotranspiration. Crop coefficients may vary seasonally for particular species as well as between species (Borin *et al*, 2011; Mao *et al*, 2002). Wetland vegetation communities may be composed of numerous species, thus complicating the application of a coefficient representing a monocultural vegetation stand to estimate the evaporative flux. Shuttleworth (1993) notes that evapotranspiration estimation practices may be further developed by exploring the potential of a “one-step” estimation procedure based upon investigation of individual surface parameters rather than relying on the adjustment of reference evapotranspiration estimates by means of crop coefficients.

Previous studies have focussed on surface variables in attempting to explain the discrepancies observed between measurements and estimates of the evaporative flux. Acreman *et al* (2003) investigated the aerodynamic and surface resistance terms within the Penman-Monteith equation (Appendix B) for a wet grassland and a reedbed. The roughness length for momentum (describing the effects of a vegetation surface on atmospheric turbulence) was shown to be approximately five times larger at the reedbed. Surface resistance was derived by use of evapotranspiration and meteorological measurements within an inverted form of the Penman-Monteith equation and was shown to remain close to zero for the reedbed and fluctuate between positive values and zero for the wet grassland. These findings were consistent with

the higher evaporative flux measured at the reedbed and were attributed to the assemblage of tall vegetation and open water at this site being more conducive to evapotranspiration. Mao *et al* (2002) also noted contrasting values of canopy resistance between two wetland vegetation species. Burgin (2006) derived surface resistance at a wet grassland site from measurements of stomatal resistance, leaf area index and vegetation cover. The mean surface resistances were shown to be lower than the 70 s m^{-1} adopted in the definition of the reference surface. However, whilst the application of the measured surface resistance values within the Penman-Monteith equation was shown to improve evapotranspiration estimates relative to eddy covariance measurements, there remained a discrepancy between estimates and measurements of evapotranspiration. Aerodynamic resistance at a reedbed was also investigated by Peacock (2003). Assumptions regarding the relationship between the zero plane displacement and vegetation height were shown to be accurate for this site. However, the relationship between vegetation height and aerodynamic roughness length for momentum transfer was shown to differ from that assumed within the Penman-Monteith equation. Thus the reedbed surface studied by Peacock (2003) may be regarded as inducing a greater degree of atmospheric turbulence than the reference surface. Lafleur *et al* (1997) found that albedo at a boreal wetland varied in response to the phenology of the vegetation. Kim and Verma (1996) also noted a variation in albedo at a *Sphagnum* fen, attributable to variations in soil water level. Both Lafleur *et al* (1997) and Kim and Verma (1996) observed albedo values lower than that assumed for the reference surface throughout the growing season.

The variation of the surface parameters incorporated within evapotranspiration estimation methods is therefore well established. It is likely that the standardisation

of albedo, aerodynamic resistance and surface resistance values in deriving reference evapotranspiration estimates is partly responsible for the contrasts reported between such estimates and evapotranspiration measurements. However, there is no substantial progress towards Shuttleworth's (1993) recommendation regarding evapotranspiration estimation procedures explicitly incorporating variable surface parameters.

5.1.3. Aims

The overall objective of this chapter is to quantify and model the evapotranspiration flux at Sedge Fen. This objective shall be fulfilled by addressing the following aims:

1. Comparison of evapotranspiration measurements at Sedge Fen to reference evapotranspiration estimates
2. Investigation of surface parameters (i.e. albedo, aerodynamic resistance and surface resistance) at Sedge Fen so as to allow comparison with those assumed for the reference surface
3. Application of Sedge Fen surface parameters within the Penman-Monteith equation so as to assess the potential for improving evapotranspiration estimation techniques.

5.2. Methods

The data used within this section was collected by the eddy covariance system and the automatic weather station described in chapter 3. Data was collected between 9th

April – 31st December 2009 and 9th April – 3rd November 2010. Data was not available during the period 1st January – 8th April 2010 due to a power shortage. The solar radiation available during this period was insufficient to recharge the eddy covariance system's power supply, resulting in the instrumentation shutting down.

5.2.1. Reference Evapotranspiration

Daily maximum and minimum temperature and average relative humidity and wind speed data were summarised from the 30 minute averaged data collected by the automatic weather station (see section 3.3). Solar radiation data were taken from the eddy covariance system (see section 3.2.), and gaps were filled according to the procedure described in section 3.2.3.2. The daily meteorological data were then used to derive daily reference evapotranspiration, ET_0 (mm), using the AWSET software (Hess, 2002) according to the equations described in Appendix B.

5.2.2. Albedo

The albedo, α , of a surface describes the proportion of incident solar radiation reflected by the surface. The albedo at Sedge Fen was calculated using the incoming, $R_{SW\downarrow}$ (W m^{-2}), and reflected, $R_{SW\uparrow}$ (W m^{-2}), solar radiation data from the CNR1 radiometer (section 3.2.2.1), according to:

$$\alpha = \frac{R_{SW\uparrow}}{R_{SW\downarrow}} \quad (5.1)$$

The daily albedo was calculated using radiation data for the 30-minute period ending at midday. Where midday data was unavailable, the values for the 30-minute period

ending at 1130 or 1230 were used instead. If radiation data was unavailable for all these periods, the daily albedo was not calculated.

5.2.3. Aerodynamic Resistance

The aerodynamic resistance, r_a ($s\ m^{-1}$), of a surface describes the role of atmospheric turbulence in the evaporation process (Oke, 1987). The aerodynamic resistance is a function of surface roughness and windspeed and may be derived as described in Appendix B (equations B.5 – B.8)

The zero plane displacement, d , was introduced to the wind profile equation (equation 5.2) so as to retain the logarithmic form of the profile where measurements are made within the roughness sublayer above tall vegetation. If the logarithmic profile obtained from wind speed measurements in such situations were extrapolated downwards, the flow would be seen to behave as if the surface were located within the vegetation stand rather than at ground level. Therefore the zero plane displacement represents the elevated position of the active surface and is thus indicative of the bulk drag exerted on the air by the vegetation (Garratt, 1992; Oke, 1987). The aerodynamic roughness length governing momentum transfer, z_o , is defined as the height at which the logarithmic wind profile extrapolates to a zero wind speed. The aerodynamic roughness length is a function of surface geometry parameters such as roughness element height, shape and density distribution (Garratt, 1992; Oke, 1987).

In order to calculate the aerodynamic resistance for Sedge Fen according to equation B.5, the values of the d , z_{oh} and z_o terms must be derived. The height of the zero plane displacement may be solved by considering the logarithmic wind profile for conditions of neutral stability:

$$u = \frac{u^*}{k} \ln\left(\frac{z-d}{z_o}\right) \quad (5.2)$$

where u^* = friction velocity (m s^{-1}) and all other terms as defined in Appendix B.

Measurement of the wind profile therefore requires measurements of wind speed (u_1 , u_2 , u_3) at a minimum of three different heights (z_1 , z_2 , z_3). If such data are available, equation 5.2 may be rearranged to give:

$$\frac{u_1 - u_2}{u_1 - u_3} = \frac{\ln(z_1 - d) - \ln(z_2 - d)}{\ln(z_1 - d) - \ln(z_3 - d)} \quad (5.3)$$

The value of d may therefore be derived from equation 5.3 by iteration.

Further consideration of the logarithmic wind profile (equation 5.2) allows for the definition of z_o . It follows from equation 5.2 that u and $\ln(z - d)$ are linearly related to one another. Therefore $\ln(z_o)$ is represented by the additive constant within the linear relationship between u and $\ln(z - d)$ since the wind speed, u , will be 0 m s^{-1} when $\ln(z_o)$ is equal to $\ln(z - d)$: i.e. when the measurement height above the active surface is equal to the height at which the wind speed is zero. The roughness length governing heat and vapour transport, z_{oh} , is calculated as $0.1z_o$ following the recommendations of Brutsaert (2005).

Consideration of equation B.5 reveals aerodynamic resistance to be a function of both wind speed and the aerodynamic parameters of the surface over which the wind travels. Therefore, variations in atmospheric turbulence as described by the aerodynamic resistance may be the result of variations in either the surface and/or the wind speed. Since the surface characteristics are of interest within this chapter, the turbulent effects of variable wind speed are removed by considering the aerodynamic impedance to turbulent fluxes. Aerodynamic impedance is defined as the product of the derived aerodynamic resistance and wind speed, and is thus dimensionless and solely representative of the effects of the surface on atmospheric turbulence (see equation B.5). Aerodynamic impedance may be regarded as analogous to the “smoothness” of a surface; the smoother the surface, the less turbulence it will induce and thus the higher the value of the aerodynamic impedance.

The second cup anemometer required for defining the logarithmic wind profile was installed at Sedge Fen during June 2009, and thus the methods described within this section could only be applied from June 2009.

5.2.4. Daily Mean Surface Resistance

Daily mean surface resistance, r_s (s m^{-1}) was calculated according to Alves and Pereira (2000):

$$r_s = r_a \left(\frac{\Delta}{\gamma} \beta - 1 \right) + \frac{\rho C_p D}{\gamma L E} \quad (5.4)$$

where

r_a	=	Aerodynamic resistance (s m^{-1})
Δ	=	Slope of saturation vapour pressure curve ($\text{Pa } ^\circ\text{C}^{-1}$)
γ	=	Psychrometric constant ($\text{Pa } ^\circ\text{C}^{-1}$)
β	=	Bowen ratio
ρ	=	Air density (kg m^{-3})
C_p	=	Specific heat of moist air ($1013 \text{ J kg}^{-1} ^\circ\text{C}^{-1}$)
D	=	Vapour pressure deficit (Pa)
LE	=	Latent heat flux density (W m^{-2})

For those variables derived from meteorological data, daily averages were used. The procedures described by Hess (2002) were used to define the variables Δ , γ , ρ and D . Monthly aerodynamic resistances calculated for Sedge Fen (see sections 5.2.3 and 5.3.2.2) were used within the derivation of surface resistance according to equation 5.4. Latent heat flux density data was converted from units of $\text{MJ m}^{-2} \text{ d}^{-1}$ to W m^{-2} . In order to address the lack of energy budget closure by the eddy covariance data (see section 3.2.3.4), maximum and minimum Bowen ratio data were derived as described in section 4.2.4 and subsequently used within equation 5.4 to generate maximum and minimum daily surface resistance data, r_{smax} and r_{smin} , respectively. The residual energy flux term, A_{res} (W m^{-2}), was added to the latent heat flux term, LE (W m^{-2}), within equation 5.4 to produce the minimum daily surface resistance, r_{smin} . The daily mean surface resistance, r_{smean} (s m^{-1}), is defined as:

$$r_{smean} = \frac{r_{smax} + r_{smin}}{2} \quad (5.5)$$

The use of monthly aerodynamic resistance data derived for Sedge Fen within the calculation of surface resistance according to equation 5.4 results in surface resistance

values only being derived for periods when aerodynamic resistance data were available; i.e. from June 2009 (see section 5.2.3).

5.2.5. Stomatal Resistance Measurements

Stomatal resistance, r_l ($s\ m^{-1}$), data were collected and processed as described in section 3.5. Data were collected at 30-minute intervals on five days during 2009 and seven days during 2010, as summarised in table 5.1. Although the intention was to record stomatal resistance data throughout the daylight period, this was not always possible. Since the porometry technique requires a dry canopy in order to produce reliable measurements, recording had to be suspended if dew was present on the leaves or following periods of rain in order to allow the canopy to dry naturally. The presence of water within the vegetation canopy accounts for the majority of the missing data detailed in table 5.1. Daily mean stomatal resistance values were computed as the average of all stomatal resistance observations collected within a day.

Table 5.1: Summary of stomatal resistance data collection periods

Year	Date	Time periods data available (30 min period ending GMT)
2009	22 nd July	0830 – 1400; 1500 - 1600
	11 th August	0930 - 1830
	26 th August	1100 – 1530; 1730
	8 th September	0900 – 0930; 1030 - 1800
	29 th September	0930 - 1700
2010	25 th May	0900 - 1800
	10 th June	0930 - 1730
	29 th June	1100 - 1800
	20 th July	0900 - 1800
	17 th August	1500 - 1800
	7 th September	1130 – 1200; 1500 - 1700
	28 th September	1300 - 1600

5.2.6. Leaf Area Index Measurements

Leaf Area Index (LAI) measurements were collected as described in section 3.6. During the 2010 field campaign, the SunScan system developed a fault that could not be rectified before the end of the season. Since the dominant vegetation on Sedge Fen undergoes an annual cycle of growth and senescence, the development of LAI was assumed to be similar in both years. Both the 2009 and 2010 LAI were therefore used to generate a composite dataset describing the development of LAI during the period 25th May – 29th September. LAI values for days between observations were generated by linear interpolation between the days either side of the date in question for which observations were made.

Following the recommendations of Allen *et al* (1998), the LAI observations were used to define the active leaf area index, LAI_{active} :

$$LAI_{active} = 0.5LAI \quad (5.6)$$

The derivation of the active leaf area index acknowledges that generally only the upper portion of a dense canopy contributes to surface water vapour transfer.

5.2.7. Bulk Surface Resistance Estimates

Bulk surface resistance, r_c ($s\ m^{-1}$), was calculated using the stomatal resistance, r_l ($s\ m^{-1}$), and active leaf area index, LAI_{active} , data described in the preceding sections according to the recommendations of Allen *et al* (1998):

$$r_c = \frac{r_l}{LAI_{active}} \quad (5.7)$$

5.2.8. Penman-Monteith Evapotranspiration Estimates

Evapotranspiration estimates were recalculated for Sedge Fen using the surface variables described in the previous sections. Reference evapotranspiration estimates derived using observed albedo data were used within a rearranged form of equation B.1 to derive the ET_{rad} term, which is independent of surface or aerodynamic resistance (see equation B.2) and thus constant. The derived values of daily mean surface resistance, r_s ($s\ m^{-1}$), and aerodynamic resistance, r_a ($s\ m^{-1}$), were then used to derive the ET_{aero} and γ^* terms according to equations B.3 and B.4, respectively. The

Penman-Monteith evapotranspiration estimates for Sedge Fen, ET_{SF} (mm), were then calculated according to equation B.1.

5.3. Results

5.3.1. Actual and Reference Evapotranspiration

The monthly evapotranspiration estimates from the eddy covariance data are compared to the reference evapotranspiration estimates in Table 5.2. For the purposes of this comparison, the mid-point of the range of estimates provided by the eddy covariance data (section 4.3.3.1) is presented within Table 5.2. The actual evapotranspiration estimates are greater than the reference evapotranspiration estimates for all months with the exception of April 2010. The totals for each year reveal that the mean actual evapotranspiration estimates are greater than the reference evapotranspiration estimates by 188.6 mm between April and December 2009 and by 110.3 mm between April and October 2010.

Table 5.2: Monthly evapotranspiration estimates from eddy covariance data (Actual ET) and reference evapotranspiration estimates (ET_O) from AWS data for Sedge Fen, 2009 and 2010. N/A indicates months for which data were not available.

	2009			2010		
	Actual ET	ET _O	Ratio	Actual ET	ET _O	Ratio
	(mm)	(mm)		(mm)	(mm)	
April	45.2	40.7	1.11	42.1	46.4	0.91
May	90.8	80.9	1.12	77.1	76.1	1.01
June	112.8	86	1.31	95.6	88.2	1.08
July	127.6	81.4	1.57	124.6	95.8	1.30
August	111.7	76.4	1.46	96.2	62.7	1.53
September	69.6	46.7	1.49	71.2	41.0	1.74
October	37.5	21	1.79	34.4	20.7	1.66
November	22.0	11.4	1.93	N/A	N/A	N/A
December	17.8	2.0	8.91	N/A	N/A	N/A
Total	635.1	446.5		541.2	430.9	
(Apr – Oct)	(595.3)	(433.1)				

The monthly ratio of actual to reference evapotranspiration varies on a monthly basis during both 2009 and 2010. The values are closest to unity during the early part of the growing season. As the growing season progresses, the actual evapotranspiration becomes progressively larger than the reference evapotranspiration. During 2009 this trend is reversed in August, when the ratio shows a slight decline before rising again during the successive months. The ratio for December 2009 is particularly striking,

being the largest within the data. The trend during 2010 differs slightly, in that the ratio is below unity during April and rises to a peak in September before declining slightly in October.

The high ratio of actual to reference evapotranspiration observed for December 2009 warrants further consideration. The reference evapotranspiration estimate for this month is particularly low and exhibits the largest proportional decline relative to the preceding month within the evapotranspiration data presented in table 5.2. A regression of monthly total reference evapotranspiration against the monthly total radiation absorbed at the surface (i.e. $(1-\alpha)R_{SW\downarrow}$) is presented in figure 5.1. These two variables demonstrate a clear linear relationship, with the high R^2 value indicating that 97% of the variation in monthly reference evapotranspiration can be explained by the monthly variation in energy absorbed at the surface. The low value of reference evapotranspiration reported for December 2009 is therefore attributable to the low energy receipt at the surface during this month.

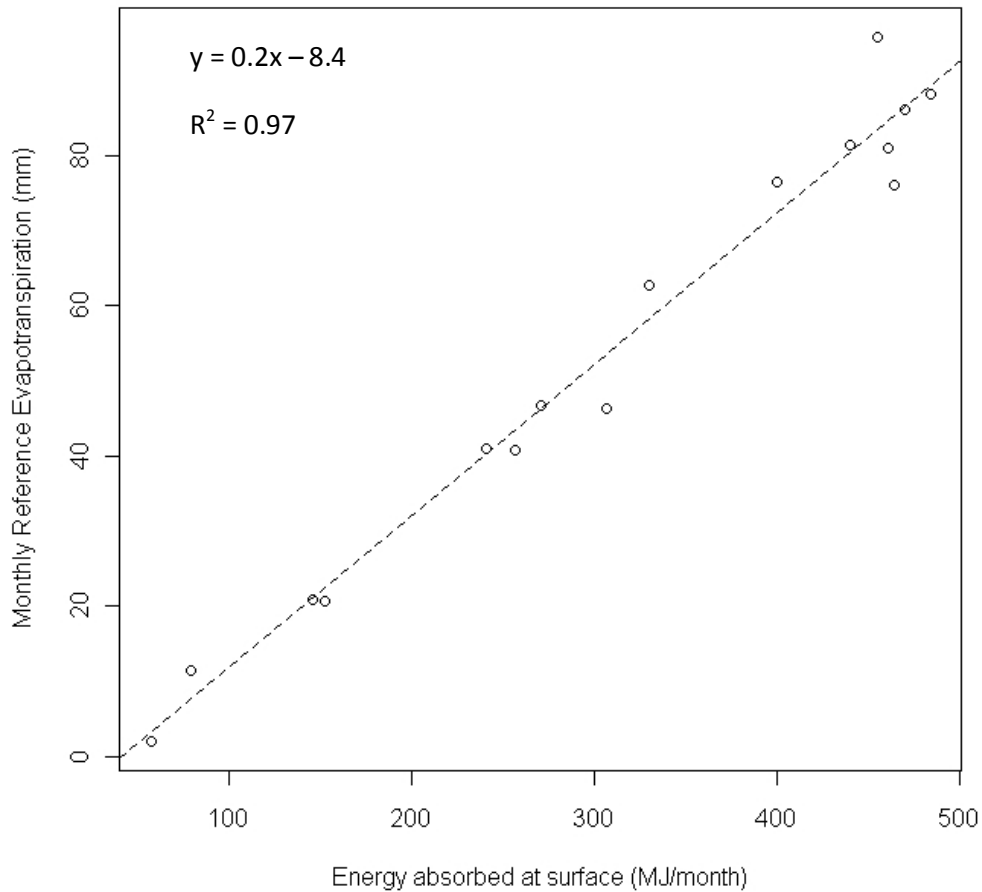


Figure 5.1: Relationship between surface energy absorption and reference evapotranspiration

The mean weekly actual and reference evapotranspiration data for 2009 and 2010 are shown in figure 5.2. The grey areas in each plot represent the energy unaccounted for by the eddy covariance system, and thus the closure of the energy balance (as described in section 4.3.3). The lower boundary of the range is defined by the evapotranspiration estimate as derived from the latent heat flux measured by the eddy covariance system. The upper boundary represents the evapotranspiration estimate derived by assigning the unaccounted energy to latent heat flux. The grey areas therefore define the range within which the actual evapotranspiration is likely to lie. The evapotranspiration ranges are greatest between April and August in both years, and decrease during the autumn months. This indicates a greater amount of

unaccounted energy during the summer according to the measurements gathered by the eddy covariance system.

These plots serve to highlight the aforementioned tendency for the actual evapotranspiration estimates to be greater than the reference evapotranspiration estimates. However, the reference evapotranspiration estimates lie within the range of the actual evapotranspiration estimates during April and May 2009 and between April and June 2010. After these periods the actual evapotranspiration estimates are greater than the reference evapotranspiration estimates. In 2009, the absolute difference between the actual and reference estimates is greatest in July and August and the two estimates can be seen to converge during the subsequent months, although the actual evapotranspiration estimates remain greater than the reference estimates. A similar pattern is observed in 2010, although slightly later in the year, with the greatest difference between the evapotranspiration estimates being observed in August and September.

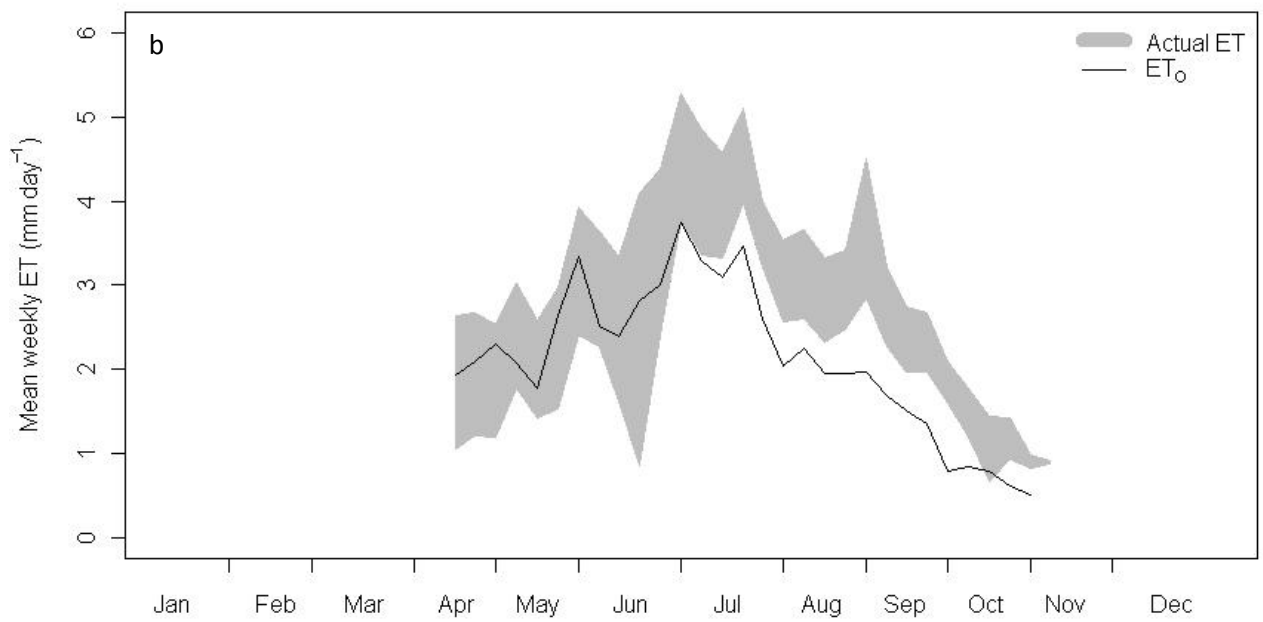
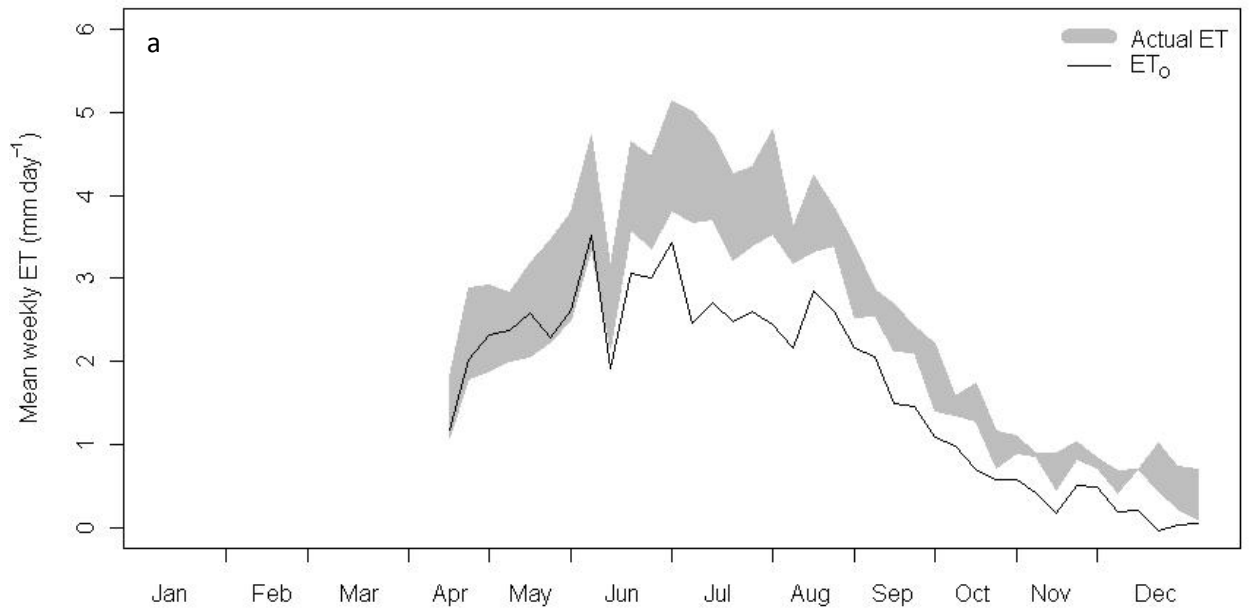


Figure 5.2: Mean weekly actual and reference evapotranspiration estimates for: a) 2009 and; b) 2010.

5.3.2. Surface Parameterisations

The data presented in section 5.3.1 indicates a tendency for the actual evapotranspiration estimates to be greater than the reference evapotranspiration estimates. Within this section, surface parameters are derived for Sedge Fen and compared to those of the reference surface.

5.3.2.1. Albedo

Daily albedo values were calculated as described in section 5.2.2 and are summarised as weekly averages for 2009 and 2010 in figure 5.3. Overall, the values are relatively stable. There is a small rise in albedo during June and July and a slight fall during September and October. There is a large peak in December 2009. Closer investigation revealed a sudden rise in albedo on 18th December 2009 to a value of 0.44. Albedo subsequently declined during the remainder of December but remained above 0.25 until 27th December 2009. The initial rise in albedo coincided with widespread snowfall in Cambridgeshire during the latter part of 17th December 2009^{1,2}. It would therefore seem that lying snow during December 2009 is responsible for increasing albedo values for the latter part of this month. Since the snowfall exerts an influence over the albedo data, the December 2009 data was omitted from the following analyses relating to the albedo at Sedge Fen.

¹ <http://www.metoffice.gov.uk/corporate/pressoffice/2009/ht20091223.html>

² http://news.bbc.co.uk/local/cambridgeshire/hi/people_and_places/newsid_8421000/8421387.stm

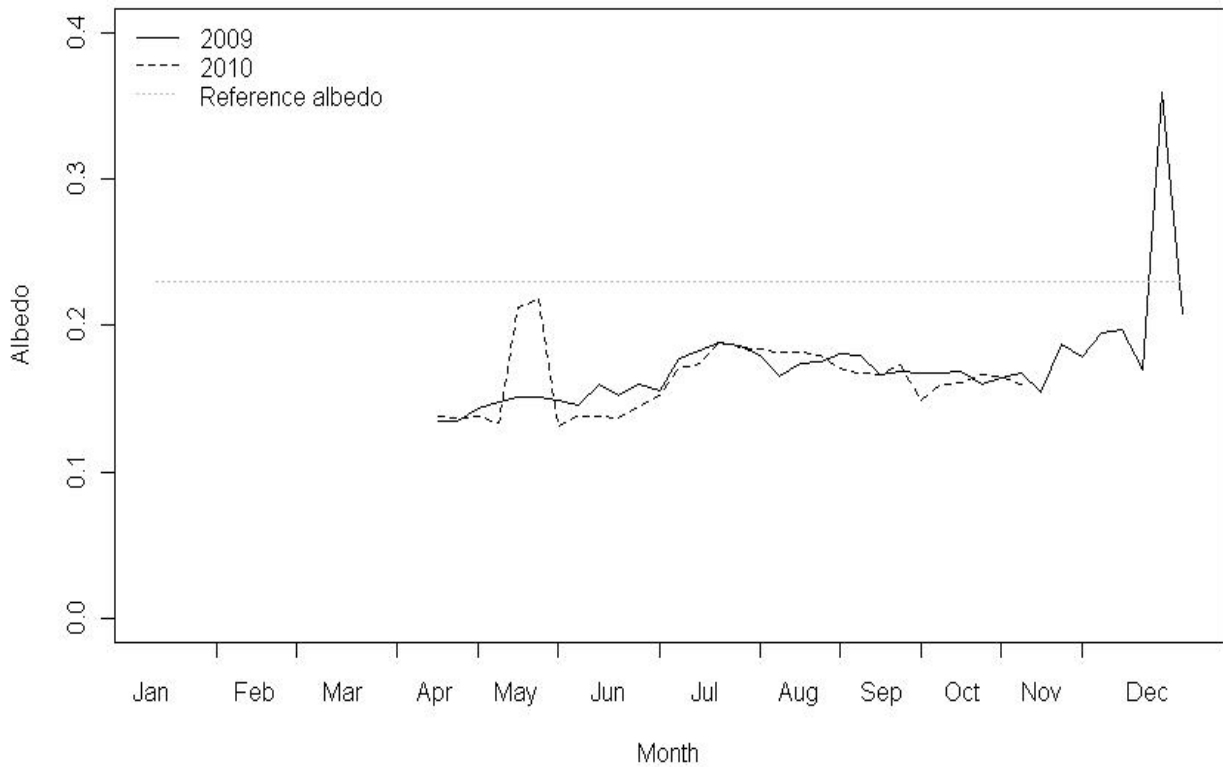


Figure 5.3: Mean weekly albedo at Sedge Fen, 2009 and 2010.

The mean monthly albedo data are presented in table 5.3 and serve to highlight the trends previously commented on. A Kruskal-Wallis rank sum test (Wheater and Cook, 2000) was invoked upon the monthly albedo data, with the null hypothesis being that there was no significant difference between months and the significance level set at 0.05. The results for each year were:

$$2009: H = 118.31 (7 \text{ df}) p < 0.01$$

$$2010: H = 106.52 (6 \text{ df}) p < 0.01$$

The alternative hypothesis therefore has to be accepted. For 2009 and 2010, the monthly variation in albedo is statistically significant.

So as to assess whether each month is statistically different from all other months within a year, Dunn's multiple comparison test (Wheater and Cook, 2000) was invoked upon the monthly albedo data, and the results are summarised as superscripts in table 5.3. Those months with a common notation show no significant difference from one another. The results for 2009 indicate that the albedo data for April and May show no statistically significant difference from one another. Likewise the albedo data from May and June may be regarded as statistically similar. June, October and November show a statistical similarity with respect to the monthly albedo data, as do July, August and September. The final group of months exhibiting no statistically significant difference with respect to albedo data are August, September, October and November. During 2010, the albedo data for April, May and June exhibit a statistical similarity with one another. The May, June, September and October albedo data exhibit no statistically significant difference. The July, August and October albedo data exhibit a statistical similarity with one another, as do the September and October data.

A Mann-Whitney U test was also invoked upon the monthly albedo data so as to assess whether corresponding months in the successive years were statistically similar. For each test the null hypothesis was defined as there being no significant difference between the monthly data from successive years and the significance level was set at 0.05. These results are also summarised in table 5.3. The Mann-Whitney results indicate that the null hypothesis must be accepted for all months except May, June and August. Therefore, May, June and August are the only months for which a statistically significant difference exists between the monthly albedo data for 2009 and 2010.

Table 5.3: Monthly mean and standard deviation of albedo at Sedge Fen, 2009 and 2010. Superscripts indicate mean albedo values that are not statistically different according to Dunn’s multiple comparison test

	2009		2010		Mann-Whitney test		
	Mean	Standard deviation	Mean	Standard deviation	U ₂₀₀₉	U ₂₀₁₀	p
April	0.14 ^a	0.0070	0.14 ^f	0.0030	231	209	0.794
May	0.15 ^{a, b}	0.0060	0.17 ^{f, g}	0.0960	621	340	0.048
June	0.16 ^{b, c}	0.0100	0.14 ^{f, g}	0.0100	766	134	<0.010
July	0.18 ^d	0.0083	0.18 ^h	0.0100	551	348	0.136
August	0.17 ^{d, e}	0.0070	0.18 ^h	0.0080	244	626	<0.010
September	0.17 ^{d, e}	0.0080	0.16 ^{g, i}	0.0130	559	311	0.061
October	0.17 ^{c, e}	0.0190	0.16 ^{g, h, i}	0.0170	444	393	0.699
November	0.18 ^{c, e}	0.0400					

5.3.2.2. Aerodynamic Impedance

The mean monthly values of zero plane displacement, d , and roughness length, z_o , calculated for Sedge Fen as described in section 5.2.3 are summarised in table 5.4. The zero plane displacement may be seen to be relatively constant during both years, lying within the range 0.90 m – 1.05 m, although monthly fluctuations are evident. The mean monthly roughness length data are lower and more variable during 2009 and 2010.

Table 5.4: Monthly mean of zero plane displacement, d , and roughness length, z_o , at Sedge Fen, calculated as described in section 5.2.3.

	2009		2010	
	d (m)	Z_o (m)	d (m)	Z_o (m)
April			0.98	0.46
May			1.03	0.45
June	0.97	0.63	0.99	0.48
July	0.95	0.60	0.99	0.52
August	0.92	0.76	0.91	0.53
September	1.05	0.59	1.00	0.53
October	0.90	0.71	0.97	0.53
November	0.90	0.59		
December	0.98	0.50		

The zero plane displacement and roughness length data were used to derive aerodynamic impedance data as described in section 5.2.3. The aerodynamic impedance data are summarised as monthly means in table 5.5. The data show some variation on a monthly basis and have large standard deviations, suggesting a considerable variation in surface roughness parameters within months. However, all the monthly mean values are lower than that of the reference surface, calculated as 240.81, and lie between 17 - 44% of the value for the reference surface. The evolution of the aerodynamic impedance at Sedge Fen does not show a consistent trend in each year. During 2009, the monthly mean aerodynamic impedance fluctuates during the summer months and shows a general upward trend through the autumn months, with a peak in November. The 2010 monthly mean aerodynamic impedance values peak in May with a general downward trend apparent in the

subsequent months. The monthly means show a greater stability during the months of July, August and September 2010 than at any other time during the year.

A Kruskal-Wallis rank sum test was invoked upon the monthly aerodynamic impedance data, with the null hypothesis being that there was no significant difference between months and the significance level set at 0.05. The results for each year were:

$$2009: H = 30.08 (6 \text{ df}) p < 0.01$$

$$2010: H = 22.33 (6 \text{ df}) p < 0.01$$

The alternative hypothesis therefore has to be accepted. For 2009 and 2010, the monthly variation in aerodynamic impedance is statistically significant.

Dunn's multiple comparison test was invoked upon the mean monthly aerodynamic impedance data, and the results are described in the form of superscripts in table 5.5. The 2009 data reveal that the June aerodynamic impedance data are statistically similar to all other months during this year. The July aerodynamic impedance data exhibits a statistical similarity with all months during the period September – December. August, September and October also exhibit a statistical similarity with respect to the aerodynamic impedance data. The October and December aerodynamic impedance data also exhibit a statistical similarity. By contrast, the 2010 data are divided into two groups. The aerodynamic impedance data for April exhibits a statistical similarity with all other months. Within this group, the aerodynamic impedance data for all months within the period May – September was found to be statistically similar.

Table 5.5: Monthly mean and standard deviation of aerodynamic impedance at Sedge Fen, 2009 and 2010. Superscripts indicate values that are not statistically different according to Dunn's multiple comparison test.

	2009		2010		Mann-Whitney test		
	Mean	Standard deviation	Mean	Standard deviation	U ₂₀₀₉	U ₂₀₁₀	p
April			97.27 ^e	107.02			
May			104.94 ^{e, f}	114.61			
June	42.02 ^a	47.83	84.96 ^{e, f}	98.21	2391	3889	0.02
July	63.77 ^{a, b}	68.29	69.19 ^{e, f}	71.76	27492	30276	0.361
August	44.33 ^{a, c}	52.10	68.38 ^{e, f}	73.92	15081	24935	<0.01
September	52.86 ^{a, b, c}	54.85	65.42 ^{e, f}	75.74	14215	17033	0.143
October	65.96 ^{a, b, c, d}	105.66	50.14 ^e	52.13	17735	21705	0.085
November	94.87 ^{a, b}	130.19					
December	73.37 ^{a, b, d}	94.41					

A Mann-Whitney U test was also invoked upon the monthly aerodynamic impedance data so as to assess whether corresponding months in the successive years were statistically similar. For each test the null hypothesis was defined as there being no significant difference between the monthly data from successive years and the significance level was set at 0.05. These results are also summarised in table 5.5. The Mann-Whitney results indicate that the null hypothesis must be accepted for all months except June and August. Therefore, June and August are the only months for which a statistically significant difference exists between the monthly aerodynamic impedance data for 2009 and 2010.

5.3.2.3. Surface Resistance

The daily mean surface resistance data were calculated as described in section 5.2.4 and are summarised as weekly averages for 2009 and 2010 in figure 5.4. During both years, the daily mean surface resistance exhibits a greater range during the autumn months. The 2010 surface resistance data exhibits a similar large range during April and May. The narrowest range of daily mean surface resistance estimates occurs during the June – September period in both years. During this period, much of the range of daily mean surface resistance estimates lies below the reference value of surface resistance. In July and August 2009 the upper limit of the daily mean surface resistance estimates is lower than the reference value of surface resistance. This also occurs during 2010, albeit for brief rather than sustained periods. During the spring and autumn months, this trend is typically reversed and much of the range of estimated daily mean surface resistance is greater than the reference value of surface resistance.

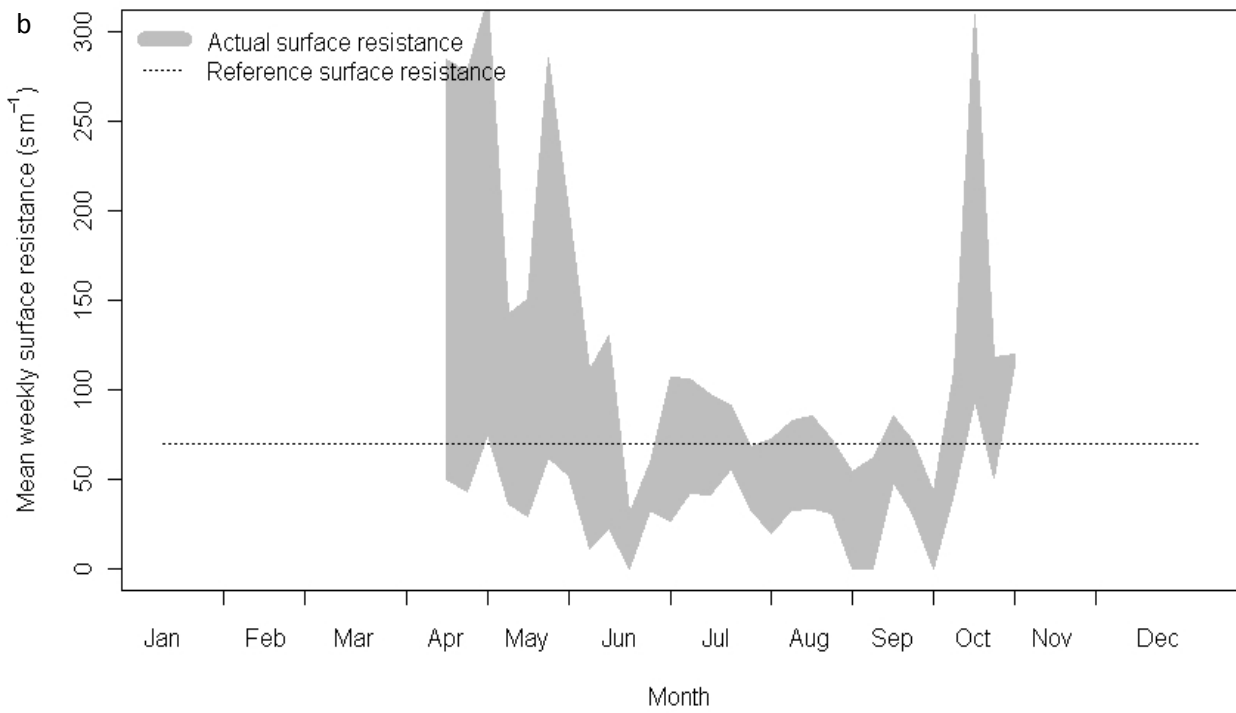
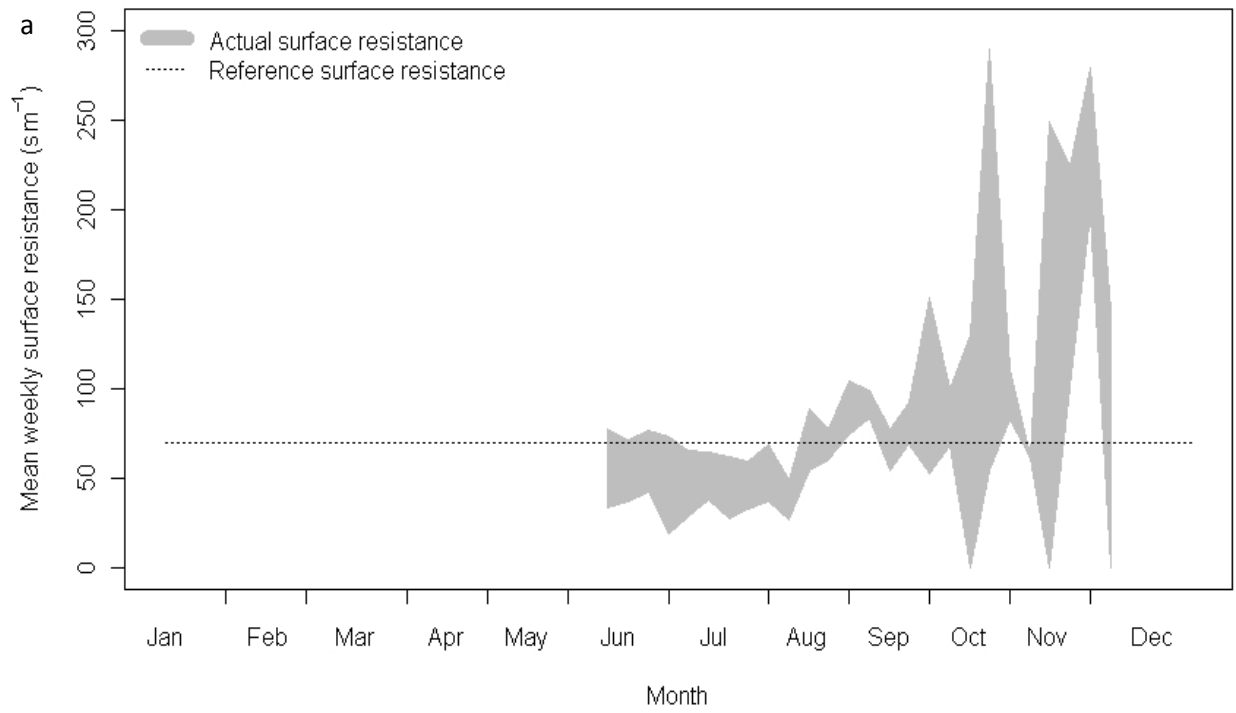


Figure 5.4: Weekly mean surface resistance estimates for Sedge Fen: a) 2009 and; b) 2010

The mean daily surface resistance, r_{smean} , (equation 5.5) data for the June – October period in 2009 was compared to the mean daily surface resistance data for the same period in 2010 by means of a Mann-Whitney U-test. This nonparametric test was considered appropriate as examination of the mean daily surface resistance data revealed that in neither year did the data approximate a normal distribution. The null hypothesis was defined as there being no significant difference between the mean daily surface resistance data for the two years and the significance level was set at 0.05. The result was:

$$U_{2009} = 10714, U_{2010} = 12695, p = 0.2$$

The null hypothesis therefore has to be accepted. For 2009 and 2010, the mean daily surface resistance data show no statistically significant difference.

5.3.3. Surface Resistance Measurements

5.3.3.1. Stomatal Resistance

The mean daily stomatal resistance data (see section 5.2.5) gathered during 2009 and 2010 are presented in figure 5.5. The 2009 data reveals that the mean daily stomatal resistances were typically lower than the reference value of 70 s m^{-1} . The 2010 data were much greater than the 2009 values and displayed a greater range.

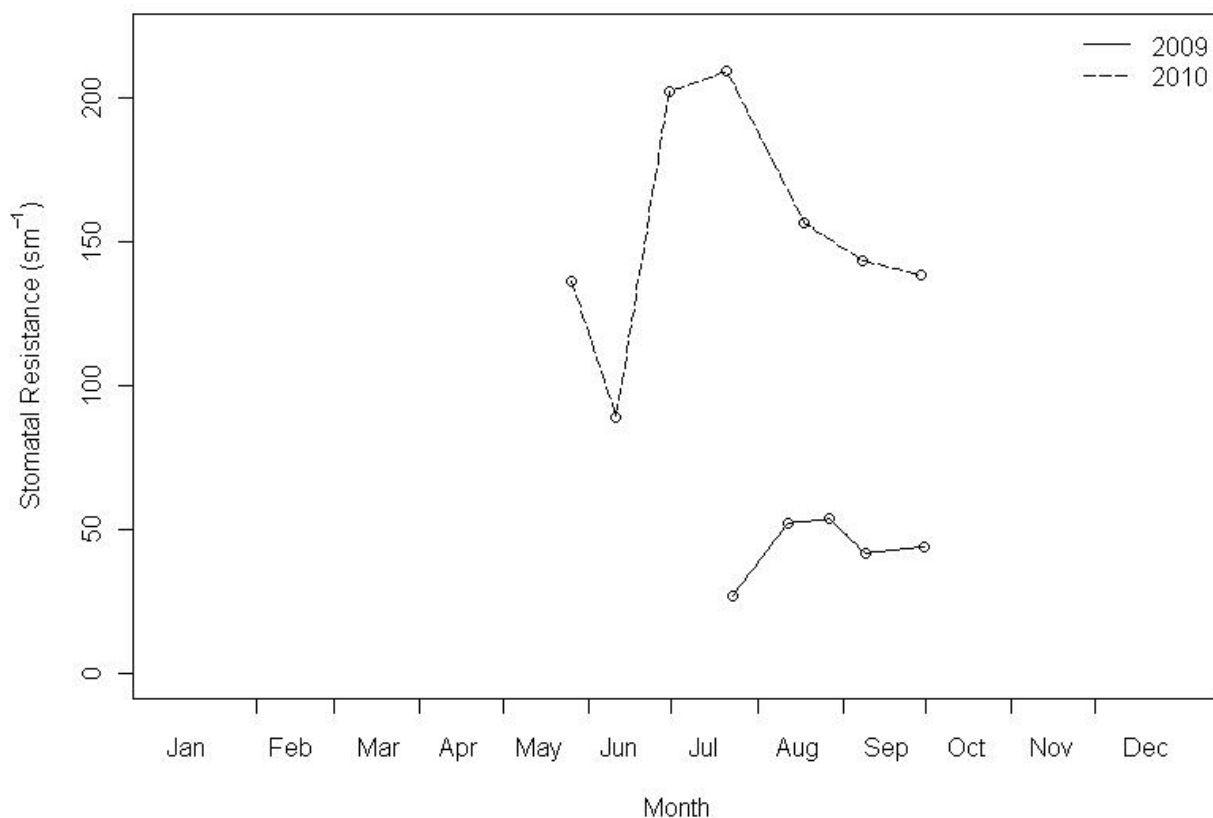


Figure 5.5: Mean daily stomatal resistance data recorded by porometer for 2009 and 2010.

The stomatal resistance data gathered during each year were compared by means of a Mann-Whitney U test so as to assess whether they were from the same population. The null hypothesis was defined as there being no significant difference between the mean daily stomatal resistance data during each year and the significance level was set at 0.05. The results were:

$$U_{2009} = 0, U_{2010} = 35, p < 0.01$$

The alternative hypothesis must therefore be accepted. The difference in stomatal resistance data for 2009 and 2010 is statistically significant.

Stomatal resistance is known to be controlled by solar radiation, temperature and vapour pressure deficit (section 2.2.2). The total solar radiation, mean temperature and mean vapour pressure deficit were therefore calculated according to the formulae detailed by Hess (2002) for each day on which stomatal resistance data were recorded and the data from 2009 and 2010 compared by means of a Mann-Whitney U test. For all comparisons the null hypothesis was defined as there being no significant difference between the data for each year and the significance level was set at 0.05. The results are presented in table 5.6.

Table 5.6: Results of Mann-Whitney U tests applied to meteorological variables taken on days of porometry measurements

	U ₂₀₀₉	n	U ₂₀₁₀	n	p
Total solar radiation	18	5	17	7	1
Mean temperature	24	5	11	7	0.34
Mean vapour pressure deficit	23	5	12	7	0.43

The results in table 5.6 indicate that the null hypothesis must be accepted for each test. Therefore there is no statistically significant difference between the meteorological parameters analysed between 2009 and 2010.

The relationships between stomatal resistance and meteorological variables were also examined by means of Pearson's product moment correlation coefficient, r (Wheater and Cook, 2000). For all applications of the test, the null hypothesis was that there is no relationship between stomatal resistance and the meteorological variable of interest and the significance level was set at 0.05. The results are presented in Table 5.7.

Table 5.7: Results of Pearson’s product moment correlation coefficient applied to stomatal resistance and meteorological data recorded on days of porometry measurements

		r	df	R ²	p
2009	Total solar radiation	-0.27	3	0.07	0.67
	Mean temperature	0.16	3	0.03	0.80
	Mean vapour pressure deficit	-0.15	3	0.02	0.81
2010	Total solar radiation	0.54	5	0.29	0.21
	Mean temperature	0.88	5	0.77	< 0.01
	Mean vapour pressure deficit	0.83	5	0.69	0.02

For 2009, none of the r values were significant. There is therefore no statistically significant relationship between mean daily stomatal resistance and total daily solar radiation, mean daily temperature or mean vapour pressure deficit during 2009. For 2010, the r value describing the relationship between mean daily stomatal resistance and total solar radiation was also not statistically significant. However, the r values comparing stomatal resistance to mean daily temperature and mean daily vapour pressure deficit demonstrate statistically significant positive relationships.

5.3.3.2. Leaf Area Index

The leaf area index data (see section 5.2.6) gathered during 2009 and 2010 is presented in figure 5.6. The leaf area index curve rises to a peak in late August and subsequently declines for the remainder of the study period.

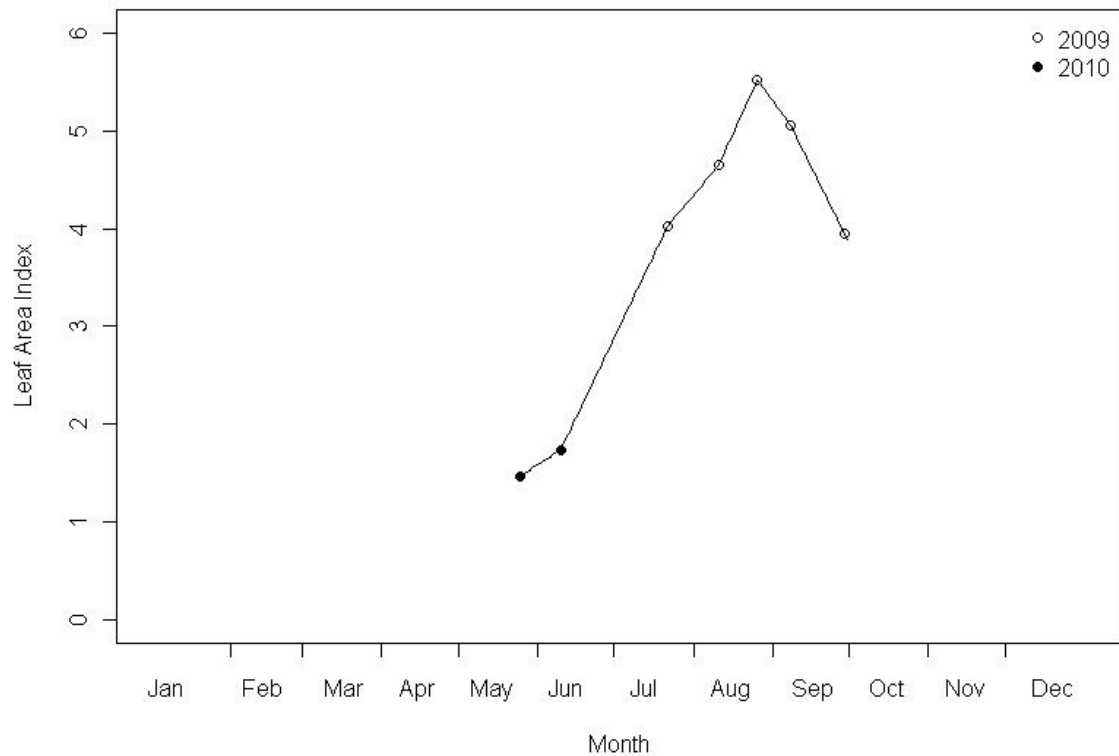


Figure 5.6: Leaf area index curve compiled from 2009 and 2010 LAI data.

5.3.3.3. Bulk Surface Resistance

The bulk surface resistance was calculated as described in section 5.2.7. The bulk surface resistance data were compared to the mean daily surface resistance data generated according to the Alves & Pereira (2000) method (see section 5.3.2.3) for the days described in table 5.1 by means of Mann-Whitney U tests. For each test, the null hypothesis was defined as there being no statistically significant difference between the bulk surface resistance and mean daily surface resistance data and the significance level was set at 0.05. The results were:

$$2009: U_{rs} = 25, U_{rc} = 0, p < 0.01$$

$$2010: U_{rs} = 16, U_{rc} = 33, p = 0.32$$

For 2009, the null hypothesis may be rejected; the bulk surface resistance and mean daily surface resistance data show a statistically significant difference. By contrast, the null hypothesis must be accepted for 2010; the bulk surface resistance and mean daily surface resistance data show no statistically significant difference.

5.3.4. Penman-Monteith Evapotranspiration Estimates for Sedge Fen

Sedge Fen evapotranspiration estimates were calculated as described in section 5.2.8 to account for the variations in albedo, aerodynamic impedance and mean daily surface resistance described in section 5.3.2. The reference surface values of albedo and aerodynamic impedance used to derive the data presented in section 5.1 were substituted for the mean monthly values detailed in tables 5.3 and 5.5, respectively. The mean daily surface resistance was calculated according to equation 5.4 using the mean of the mean monthly latent heat flux data presented in table 4.9 and the monthly mean of the Bowen ratio data presented in table 4.10. The mean daily surface resistance calculated in this manner was used in place of the reference surface value of surface resistance. The resulting evapotranspiration estimates therefore account for the differences in these parameters between the reference surface and the surface present at Sedge Fen, and are referred to as the Sedge Fen Penman-Monteith evapotranspiration estimates, ET_{SF} . These estimates are compared to the actual evapotranspiration estimates in figure 5.7.

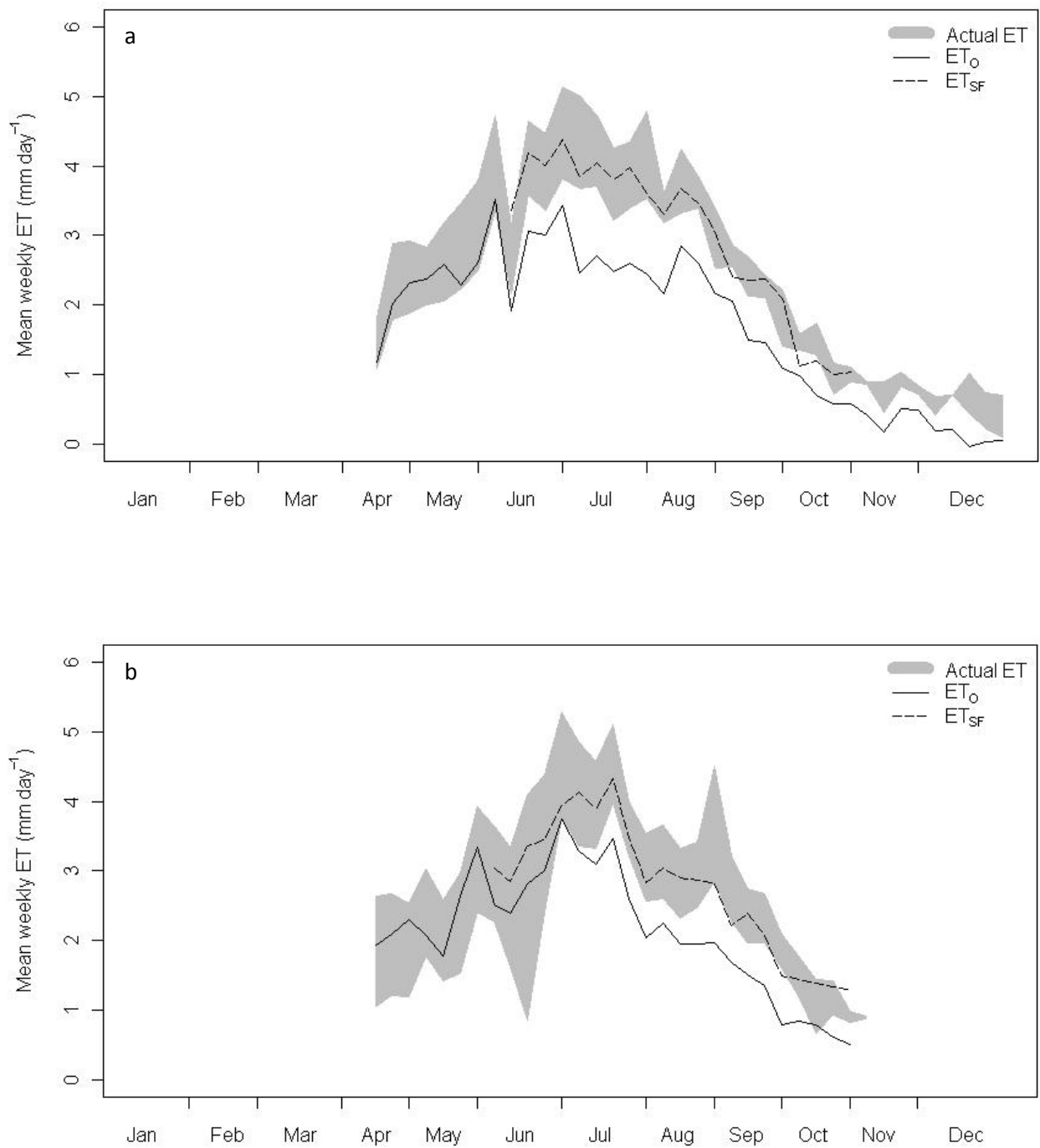


Figure 5.7: Mean weekly actual, reference and Sedge Fen Penman-Monteith evapotranspiration for: a) 2009 and; b) 2010.

The use of surface parameters based on observations at Sedge Fen produces evapotranspiration estimates within the range of actual evapotranspiration estimates.

5.4. Discussion

The comparison of actual and reference evapotranspiration estimates (section 5.3.1) reveals a tendency for the actual evapotranspiration to be greater than the reference evapotranspiration. During the period April – October, the ratio of actual to reference evapotranspiration is 1.37 for 2009 and 1.26 for 2010. The difference between the ratios for the two years is primarily attributable to a 53.9 mm difference in the actual evapotranspiration totals for the April – October periods. During the same period, the reference evapotranspiration estimates for 2009 and 2010 are in good agreement with one another, differing by only 2.2 mm. Given the well-established relationships between meteorological variables incorporated within the Penman-Monteith equation and evapotranspiration highlighted in section 5.1, the greater variation observed in actual compared to reference evapotranspiration estimates may be attributable to seasonal variations in surface parameters that are not accounted for by the constant hypothetical reference surface assumed in the derivation of reference evapotranspiration estimates.

The ratio of actual to reference evapotranspiration displays variation on a monthly basis during 2009 and 2010. Although there is a tendency for the ratio to increase as the growing season progresses, there is little agreement between individual months for the two years. Caution must therefore be exercised in applying crop correction factors to Sedge Fen reference evapotranspiration estimates. The high ratio of actual to reference evapotranspiration observed during December 2009 is a result of a low reference evapotranspiration total for this month. Further investigation revealed a strong dependence of reference evapotranspiration on absorbed solar radiation,

consistent with the findings of previous works cited in section 5.1 (Eaton and Rouse, 2001; Izadifar and Elshorbagy, 2010; Kellner, 2001; Lafleur and Roulet, 1992; Souch *et al.*, 1996). Thus the low reference evapotranspiration value for December 2009 is attributable to low energy absorption by the surface at Sedge Fen during this month, which is consistent with the high albedo values attributed to lying snow (section 5.3.2.1). The value of actual evapotranspiration derived by the eddy covariance system was believed to be accurate despite the low energy receipt, and may be explained by the presence of a negative sensible heat flux serving as a sufficient energy input to sustain a positive latent heat flux, and thus evapotranspiration (see chapter 4).

When considered within the context of the possible range of actual evapotranspiration estimates from the eddy covariance system, the reference evapotranspiration estimates show some agreement with the actual evapotranspiration estimates. The general trends of the actual and reference evapotranspiration estimates are similar during the measurement periods, confirming the importance of meteorological factors in influencing evapotranspiration. However, the range of actual evapotranspiration estimates display a tendency to be greater than the reference evapotranspiration estimates from early summer onwards. The initial agreement between the actual and reference evapotranspiration estimates during the periods April – May 2009 and April – June 2010 suggests that the reference surface is an adequate approximation of the surface for the purposes of estimating evapotranspiration at Sedge Fen during these periods. By contrast, the discrepancy between the evapotranspiration estimates during the periods June – December 2009 and July – October 2010 appear to confirm the

aforementioned suspicion that deviations from reference surface parameters exert an influence over the actual evapotranspiration at Sedge Fen.

Further investigation of the influence of surface parameters on the actual evapotranspiration at Sedge Fen focussed on the surface parameterisations utilised in the derivation of reference evapotranspiration, namely the albedo, aerodynamic resistance and surface resistance of the reference surface. Given the variations in these parameters previously reported for different surfaces (see section 5.1.2), it was considered prudent to evaluate whether the reference surface parameters are an adequate representation of those at Sedge Fen, and if not whether the differences explain the discrepancies observed between actual and reference evapotranspiration.

The albedo data for Sedge Fen were shown to be consistently lower than the reference albedo during the measurement periods. The only exception was associated with snowfall at Sedge Fen during December 2009. A pattern was discernable within the albedo data, whereby peaks were observed in July, followed by a gradual decline during subsequent months. This pattern is consistent with those reported for a boreal sedge fen by Lafleur *et al* (1997), who attribute this pattern to the phenology of the vegetation. Statistical analyses of the albedo data served to demonstrate statistically significant differences between monthly albedo during each year, and also suggested that for some months the albedo data were statistically similar for successive years. This raises the possibility that monthly variations in albedo may be defined as an annual cycle, although further data would be required to better define typical monthly

albedo averages. The average albedo at Sedge Fen is therefore lower than that assumed for the reference surface, and also prone to variation on monthly timescales.

The aerodynamic properties of the surface at Sedge Fen were calculated from wind profile measurements as described in section 5.2.3. The monthly means of the zero plane displacement were shown to be approximately 1 m (table 5.4), indicating that the wind profile observations are consistent with an active surface approximately 1 m above ground level. The zero plane displacement data is relatively consistent during both 2009 and 2010, suggesting the vegetation canopy exerts a constant drag on the air above. There appear to be no clear trends within the zero plane displacement data, suggesting that this variable is independent of the annual canopy phenology. This is consistent with both the management regime and phenology of the vegetation at Sedge Fen. Although some harvesting takes place at Sedge Fen during the late summer, this is typically in isolated patches and leaves the majority of the canopy standing. Following senescence, the moribund stems of the vegetation remain in an upright position, thus maintaining a vegetative canopy outside of the growing season. Thus, the consistency of the zero plane displacement is likely a reflection of the constant exertion of drag on the air by an aerodynamically consistent canopy. By contrast, the roughness length data exhibit less consistency, showing greater and more varied values in 2009 than 2010. This may be due to the roughness length being determined by factors such as the height, shape and density distribution of the surface roughness elements. These variables may be expected to vary during the growing season as individual stems develop and senesce within the pre-existing canopy of previous years' growth. It is also possible that the harvesting of specific areas at Sedge Fen influences the density distribution of roughness elements at the surface.

Whilst such factors may account for the variations in roughness length, further detailed investigations are required in order to demonstrate whether this is the case.

Zero plane displacement, d (m), and roughness length, z_o (m), are generally estimated as a function of vegetation height, h (m), for the purposes of calculating reference evapotranspiration (Appendix B). Back-calculation of heights from the zero plane displacement and roughness length data using equations B.6 and B.7 reveals that the back-calculated vegetation heights are not equal. The heights derived from the roughness length data are typically greater than those based upon the zero plane displacement data by a factor of 3 – 4. Aerodynamic parameters derived using crop heights will therefore differ from those derived from wind profile measurements. Thus the definition of aerodynamic parameters is an important consideration when attempting to derive evapotranspiration estimates using the Penman-Monteith equation.

The aerodynamic parameters derived from wind profile measurements were used to calculate the aerodynamic impedance of the surface at Sedge Fen as described in section 5.2.3. The monthly aerodynamic impedance data presented in section 5.3.2.2 were shown to be lower than that for the reference surface. The monthly aerodynamic impedance data for 2009 and 2010 did not exhibit a consistent seasonal pattern, although statistical analyses demonstrated significant monthly variations in the mean values. The variations in the monthly aerodynamic impedance data may be explained in terms of the zero plane displacement and roughness length data previously described. That the aerodynamic impedance derived from the wind profile

measurements is lower than the reference value of aerodynamic impedance is consistent with the actual evapotranspiration estimates being greater than the reference evapotranspiration estimates. The surface at Sedge Fen promotes greater atmospheric turbulence than the reference surface, thus promoting the turbulent transportation of water vapour within the atmosphere, permitting greater evapotranspiration.

It is acknowledged that the analysis of aerodynamic factors is based upon the implicit assumption of conditions of neutral stability prevailing at Sedge Fen. In either stable or unstable atmospheric conditions, the wind profile will not conform to the logarithmic form assumed as convective and mechanical considerations serve to enhance or suppress atmospheric buoyancy, and thus the structure of turbulent eddies. Given the lesser role of the sensible heat flux within the surface energy budget (see chapter 4), unstable conditions are likely to be rare at Sedge Fen since the energy required to generate convective motion within the atmosphere is utilised instead in the evaporative process in the form of the latent heat flux. Although the stability conditions at Sedge Fen are not explicitly addressed, the agreement between Penman-Monteith evapotranspiration and actual evapotranspiration estimates observed in section 5.3.4 implies that the assumption of neutral stability is sufficient for the purposes of deriving the zero plane displacement and roughness length of the surface at Sedge Fen.

Much of the range of estimated mean daily surface resistance was shown to be lower than the reference surface resistance applied within the calculation of reference

evapotranspiration. Statistical comparison of the mean daily surface resistance data from each year revealed no statistically significant difference between the two data sets. This suggests that the mean daily surface resistance at Sedge Fen exhibits a regular cycle, although data collected over several years would serve to verify this apparent trend. The existence of cyclical daily mean surface resistance is likely to reflect the trends of the meteorological variables from which it is derived (equation 5.4), which is consistent with the statistical similarity exhibited by meteorological data from selected days in 2009 and 2010 presented in section 5.3.3.1.

Surface resistance was also examined by using porometry measurements. Stomatal resistance data gathered during 2009 was shown to be statistically different from that gathered in 2010, with higher values recorded in 2010. Statistical comparisons showed that the meteorological variables known to influence stomatal resistance demonstrated no statistically significant differences between the two years. Furthermore, the stomatal resistance data were shown to be correlated with mean daily temperature and mean daily vapour pressure deficit in 2010, but not in 2009. Consequently, bulk surface resistance estimates derived from the stomatal resistance data is likely a reflection of the dependence of both variables on the same meteorological parameters. However, the contrast between the values and relationships of the 2009 and 2010 stomatal resistance data are interesting. The implication is that either the 2009 stomatal resistance data are responding to non-meteorological factors, or are erroneous. Without further investigation, it is impossible to identify which of these scenarios is most likely. Given the doubts that remain over the veracity of the 2009 stomatal resistance data, it would not be prudent to base any parameterisation of surface resistance at Sedge Fen on these data.

Given the difference between the albedo, aerodynamic impedance and mean daily surface resistance parameters defined for the reference surface and those observed at Sedge Fen, the reference surface is not an accurate representation of the surface characteristics of Sedge Fen for much of the growing season. So as to assess whether the discrepancies in these surface parameters are responsible for the disagreements observed between reference and actual evapotranspiration, an evapotranspiration estimate incorporating the reported albedo, aerodynamic resistance and mean daily surface resistance values was derived. The Penman-Monteith evapotranspiration for Sedge Fen was calculated using the same methodology and data as the reference evapotranspiration. However, the reference albedo and aerodynamic resistance parameters were replaced by the monthly values derived in section 5.3.2. Mean daily surface resistance was calculated for all days using the available meteorological data within equation 5.4. The use of monthly mean latent heat flux and Bowen ratio data within the derivation of mean daily surface resistance was justified on the basis of operational applicability of the method. Daily eddy covariance data may not be available in many wetland environments, so some degree of parameterisation of these variables may be necessary. The modified latent heat flux and Bowen ratio data presented in section 4.3.3 demonstrated some similarity, thus offering the potential to parameterise these data as monthly means.

The Penman-Monteith Sedge Fen evapotranspiration estimates showed an increase relative to the reference evapotranspiration estimates. This is consistent with the reduced albedo, aerodynamic impedance and surface resistance data reported within this chapter. A reduced albedo implies a greater proportion of incident solar radiation is absorbed at the surface and thus is available as an energy input to the evaporative

process. A reduction in aerodynamic impedance may be interpreted as a rougher surface, capable of inducing enhanced boundary layer turbulence to aid the vertical transportation of water vapour. Reduced surface resistance is representative of a surface more conducive to evapotranspiration than the reference surface. It is possible that the lower surface resistance of the vegetation at Sedge Fen is indicative of greater transpiration than for the hypothetical reference surface, which is regarded to be analogous to grass. However, further experimentation would be necessary to address the transpiration characteristics of these vegetation types. The Penman-Monteith Sedge Fen evapotranspiration estimates lie within the range of the actual evapotranspiration estimates for much of the study period. This suggests that the methods applied within this chapter generate evapotranspiration estimates more representative of the actual evapotranspiration at Sedge Fen than the reference evapotranspiration.

5.5. Conclusions

Actual evapotranspiration estimates for Sedge Fen show agreement with reference evapotranspiration estimates during the early part of the growing season, but are subsequently greater than reference evapotranspiration. Investigation of Sedge Fen surface parameters demonstrated that these parameters were generally lower than those assumed for the reference surface, thus explaining the discrepancy between actual and reference evapotranspiration estimates. Use of the Sedge Fen surface parameters within the Penman-Monteith equation produces evapotranspiration estimates in agreement with the actual evapotranspiration estimates. Therefore evapotranspiration estimates generated using surface parameters derived largely from

the available meteorological data represent an improvement to reference evapotranspiration estimates at Sedge Fen.

Chapter 6

Sedge Fen Microclimate

6.1. Introduction

6.1.1. Wetland Microclimates

Few studies have sought to identify the existence of wetland microclimates. Přibáň and Ondok (1978) observed lower air temperatures within two wet grassland communities than outside the wetlands. Contrasts also existed between the two wetlands; for example, surface temperature and relative humidity was shown to differ at each wetland site. Brom and Pokorný (2009) compared meteorological data gathered at wetlands in the Czech Republic to that collected within drained pastures. Smaller diurnal temperature variations and temperature amplitudes were observed at the wetlands. Li *et al* (2009) measured atmospheric variables at a 900 km² reed wetland and an arable plantation. Enhanced air temperatures at the wetland were reported, averaging 0.3°C over the course of a year, contrasting with the findings of Přibáň and Ondok (1978). Li *et al* (2009) also examined vapour pressure deficits and demonstrated that during the growing season the atmosphere at the reed wetland was more humid than that at the arable site by an average of 0.07 kPa.

These works attributed the observed microclimatic differences to environmental conditions unique to each site. For example, Přibáň and Ondok (1978) observed differences between the energy partitioning at their wetland sites. One site

experienced lower ground heat fluxes than the other, and associated differences in the sensible heat flux were also observed. The differing ground heat fluxes were attributed to differences in soil water levels and soil thermal conductivities at the two sites. The surface relative humidity and temperature differences were attributed to energy storage within a litter layer of low thermal conductivity present at only one of the sites. Li *et al* (2009) attributed the enhanced wetland air temperatures to stronger heat exchange between surface and atmosphere at their wetland site than at the arable plantation. The seasonal patterns of heat exchange observed at each site were attributed to phenological factors and, in the case of the wetland, summer inundation. Thus surface factors may influence energy partitioning, resulting in atmospheric conditions in wetlands that contrast with those outside.

Whilst all measurements reported by the previously cited studies are recorded according to consistent methodologies, no consideration is given to the possibility that the measurements may be affected by instrumental bias. Given the low magnitudes of the differences in atmospheric variables observed, the assumption that all sensors operate to identical sensitivities ideally requires confirmation. Examination of data gathered by exposing the sensors to identical atmospheric conditions would ascertain whether individual instruments were biased relative to others. Any bias shown to exist may then be removed from the field measurements, thus reducing the potential for erroneously identifying the existence of wetland microclimates. Furthermore, whilst Brom and Pokorný (2009) and Přibáň and Ondok (1978) record measurements at sites in close proximity to one another, Li *et al* (2009) report measurements taken at sites 60 km apart. The results reported by Li *et al* (2009) may represent synoptic scale atmospheric differences rather than the existence of a wetland microclimate.

Therefore, scope exists for further investigations into the existence of wetland microclimates.

6.1.2. Microclimatic Influences on Estimates of the Evaporative Flux

The existence of wetland microclimates may influence the evaporative flux from the wetland. Meteorological controls on evapotranspiration are well established (section 2.2) and so atmospheric conditions unique to wetlands may be expected to produce characteristic evaporative fluxes. Previous studies provide potential evidence of wetland microclimates influencing evaporative fluxes. For example, Gardner (1991) found monthly potential evaporation totals were up to 25 mm higher when using meteorological data from outside the wetland compared to potential evaporation estimates based on meteorological data collected at the wetland. Gasca-Tucker *et al* (2007) report a similar finding, in which potential evaporation estimated using meteorological data from outside a wetland is higher than that estimated using meteorological data from within the wetland for evaporation rates over 2 mm d⁻¹. Both these studies acknowledge that the meteorological data may be subject to inconsistencies in data collection or calculation procedures and thus cannot be presented as definitive evidence of wetland microclimates. However, the contrasts between wetland and non-wetland evaporation estimates demonstrate that differences between meteorological data gathered inside and outside wetlands will produce differing estimates of the evaporative flux. If significant, the potential for inaccuracies in evaporative flux estimates may be of interest to wetland managers.

6.1.3. Aims

The overall objective of this chapter is to assess whether a wetland microclimate can be said to exist at Sedge Fen and whether any such microclimate influences evapotranspiration estimates. This objective shall be fulfilled by addressing the following aims

1. Comparison of sensors so as to minimise the effects of instrumental bias
2. Comparison of temperature and relative humidity data measured within and outside Sedge Fen so as to determine whether a wetland microclimate exists with respect to these variables
3. Comparison of reference evapotranspiration estimates based on meteorological data gathered within and outside Sedge Fen.

6.2. Methods

30-minute averages of temperature and relative humidity were gathered using HMP45C temperature and relative humidity probes as described in section 3.4. The probes were located within a wetland (Sedge Fen), on the edge of a wetland (Adventurer's Fen) and on former arable land outside the wetland (Oily Hall).

6.2.1. Calibration of probes

Prior to deployment, the three HMP45C probes were installed adjacent to one another within the Centre for Ecology and Hydrology's meteorological compound at Wallingford (51.60°N, 1.11°W). The probes logged 30 minute average temperature

and relative humidity data for a 2 day period (5th and 6th June 2008). The 30 minute data from the Adventurer's Fen and Oily Hall probes were then compared to that from the Sedge Fen probe by means of linear regression so as to ensure consistency. Any difference between the data recorded by the probes would therefore be indicative of an instrumental bias, which would need to be accounted for before comparing the data gathered in the field by the three probes. If significant differences were identified, the regression equations defined by the comparison of the probes would provide the means by which to adjust the data from the Adventurer's Fen and Oily Hall probes.

6.2.2. Regression Confidence Intervals

The regressions applied to the Adventurer's Fen and Oily Hall temperature and relative humidity data (see sections 6.2.1 and 6.3.1) have an inherent error which may be quantified. The mean square error, *MSE*, is defined as:

$$MSE = \frac{\sum(y - y_i)^2}{n - 2} \quad (6.1)$$

where:

y = variable measured by Sedge Fen probe during calibration

y_i = variable predicted from Adventurer's Fen or Oily Hall probe during calibration

n = number of calibration measurements

The mean square error is then used to derive the confidence interval, *CI*, according to:

$$CI = \pm t_{(n-2)} \sqrt{MSE \left[1 + \frac{1}{n} + \frac{(y_k - \bar{y})^2}{\sum (y_i - \bar{y})^2} \right]} \quad (6.2)$$

where:

y_k = variable measured by probes at Adventurer's Fen or Oily Hall

\bar{y} = mean of variable predicted during calibration

$t_{(n-2)}$ = t-statistic for $n-2$ degrees of freedom at the 95% confidence limit

Thus the confidence intervals derived define the region within which observed differences between the Sedge Fen and Adventurer's Fen or Oily Hall data may be attributable to errors within the regressions applied to the data from the probes at Adventurer's Fen and Oily Hall. Any differences lying outside of these confidence intervals are likely to indicate actual differences in the variable of interest at the two sites under consideration.

6.2.3. Temperature data

Mean air temperature, T_{mean} (°C), is calculated for each day from the daily minimum, T_{min} (°C), and maximum, T_{max} (°C), air temperatures according to:

$$T_{mean} = \frac{T_{min} + T_{max}}{2} \quad (6.3)$$

6.2.4. Vapour Pressure data

The saturation vapour pressure, $e_s(T)$ (kPa), at temperature T (°C), is calculated as:

$$e_s(T) = 0.6107e^{\frac{17.27T}{T+273.3}} \quad (6.4)$$

The mean daily vapour pressure, e (kPa), is therefore derived using the minimum and maximum daily temperature, T_{min} and T_{max} (°C), and the mean daily relative humidity, RH (%), according to:

$$e = \frac{RH}{100} \left(\frac{e_s(T_{min}) + e_s(T_{max})}{2} \right) \quad (6.5)$$

6.2.5. Radiation Data

Daily solar radiation, R_s (MJ m⁻² d⁻¹) was calculated for Sedge Fen using the Hargreaves method as described by Allen *et al* (1998). The formulae for deriving daily solar radiation according to this method are detailed in Appendix C. Given that incident solar radiation is not affected by the presence of the wetland and the close proximity of the stations, the solar radiation estimated at Sedge Fen was assumed to be representative of all sites.

6.2.6. Windspeed data

30 minute averages of windspeed were measured by a cup anemometer at a height of 3.08 m at Sedge Fen (see section 3.3.2). Windspeed data were not available for the Adventurer's Fen or Oily Hall sites, and so the windspeed was assumed to be constant for all sites.

6.2.7. Reference Evapotranspiration Estimates

Daily reference evapotranspiration, ET_0 (mm), was calculated according to the methodology described in Appendix B using the daily temperature, relative humidity, solar radiation and windspeed data described in sections 6.2.3 – 6.2.6.

6.2.8. Anomalies

The temperature and vapour pressure data for Adventurer's Fen and Oily Hall are presented as weekly mean anomalies relative to the Sedge Fen data, representing the difference in the variable of interest between the site of interest and Sedge Fen.

6.3. Results

6.3.1. Calibration Results

The results of the comparison of temperature and relative humidity data measured by both the Adventurer's Fen and Oily Hall probes with that measured by the Sedge Fen probe (see section 6.2.1) are detailed in table 6.1. The regressions demonstrate that the gradients derived for all temperature and relative humidity are statistically significant at the 0.01 level, although all gradients show minimal deviation from unity. Only the temperature data exhibit statistically significant values for the y-intercept. The high R^2 values indicate that almost all of the variance in data between the probe at Sedge Fen and those at Adventurer's Fen and Oily Hall are explained by the linear relationships detailed in table 6.1. The temperature and relative humidity data from Adventurer's Fen and Oily Hall were therefore corrected using the

appropriate parameters from table 6.1 so as to remove the effects of systematic errors from subsequent analyses of the data.

Table 6.1: Results of comparison of half-hourly temperature and relative humidity data from HMP45Cs at Adventurers' Fen and Oily Hall, relative to that installed on Sedge Fen

	Adventurers' Fen		Oily Hall	
	Temperature	Relative Humidity	Temperature	Relative Humidity
Gradient	1.024	1.003	1.024	0.999
Standard error	0.005	0.004	0.004	0.004
p-value	<0.01	<0.01	<0.01	<0.01
y-intercept (°C / %)	-0.284	-0.330	-0.341	-0.028
Standard error	0.058	0.332	0.052	0.307
p-value	<0.01	0.327	<0.01	0.928
R ²	0.999	0.999	0.999	0.999

As noted in section 6.2.2, the corrections applied to the Adventurer's Fen and Oily Hall may themselves act as a source of error. 95% confidence intervals were therefore calculated according to equations 6.1 and 6.2 for the entire study period. The key parameters on which these calculations are based are summarised in table 6.2. The mean square errors are larger for the temperature data than the vapour pressure data at both sites, indicating that larger confidence intervals may be expected with the corrections of the temperature data. The confidence intervals derived using these parameters is plotted with the appropriate anomaly data in the subsequent sections for ease of comparison.

Table 6.2: Parameters used for calculating confidence intervals associated with the regressions detailed in table 6.1. These parameters act as inputs to equation 6.2

	Adventurer's Fen		Oily Hall	
	Temperature	Vapour Pressure	Temperature	Vapour Pressure
n	41	41	41	41
$t_{(n-2)}$	2.02	2.02	2.02	2.02
MSE	0.0119	$2.66 \cdot 10^{-5}$	0.0093	$2.57 \cdot 10^{-5}$

6.3.2. Solar Radiation

The daily solar radiation estimates for Sedge Fen were compared to the solar radiation measurements made by the eddy covariance system by means of linear regression, and the results are summarised in figure 6.1. The Hargreaves estimates exhibit a good approximation to the eddy covariance measurements of solar radiation. Although there is some disagreement, the use of the Hargreaves solar radiation estimates allows for the generation of an uninterrupted record of solar radiation data during 2009 and 2010. The use of solar radiation estimates to generate reference evapotranspiration data will not adversely affect subsequent analyses within this chapter, since it is the differences in reference evapotranspiration estimates between the three sites that are of interest rather than the absolute values.

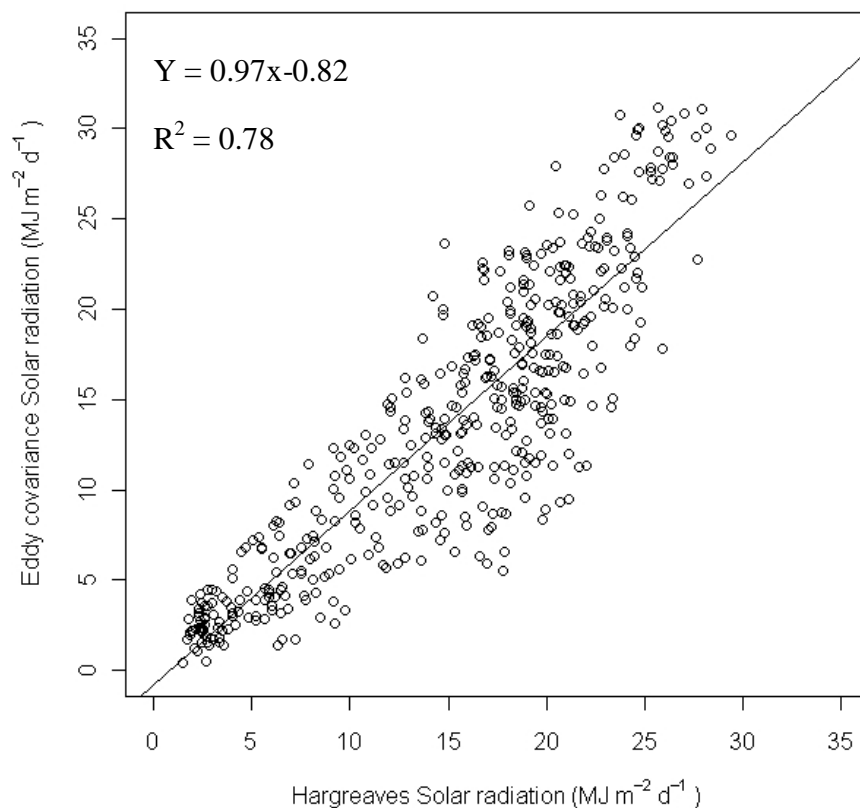


Figure 6.1: Comparison of Hargreaves solar radiation estimates and eddy covariance solar radiation measurements

6.3.3. Temperature Comparison

The weekly mean temperature data from Adventurer’s Fen and Oily Hall are presented as anomalies relative to the Sedge Fen temperature data in figure 6.2. Similar trends are observed at both Adventurer’s Fen and Oily Hall. The temperatures at each site are slightly higher than those at Sedge Fen during the summer months (June – October) and slightly lower during the winter months (November – May). Although the general trends at Adventurer’s Fen and Oily Hall are similar, the temperatures at Oily Hall exhibit greater positive anomalies during summer and greater negative anomalies during the winter than those at Adventurer’s Fen relative to the temperatures at Sedge Fen. The Adventurer’s Fen temperature data show a greater tendency to fall within the confidence interval than the Oily Hall

temperature data, particularly during the winter period. Only during the summer periods do the temperature anomalies for both stations lie outside the confidence intervals for sustained periods.

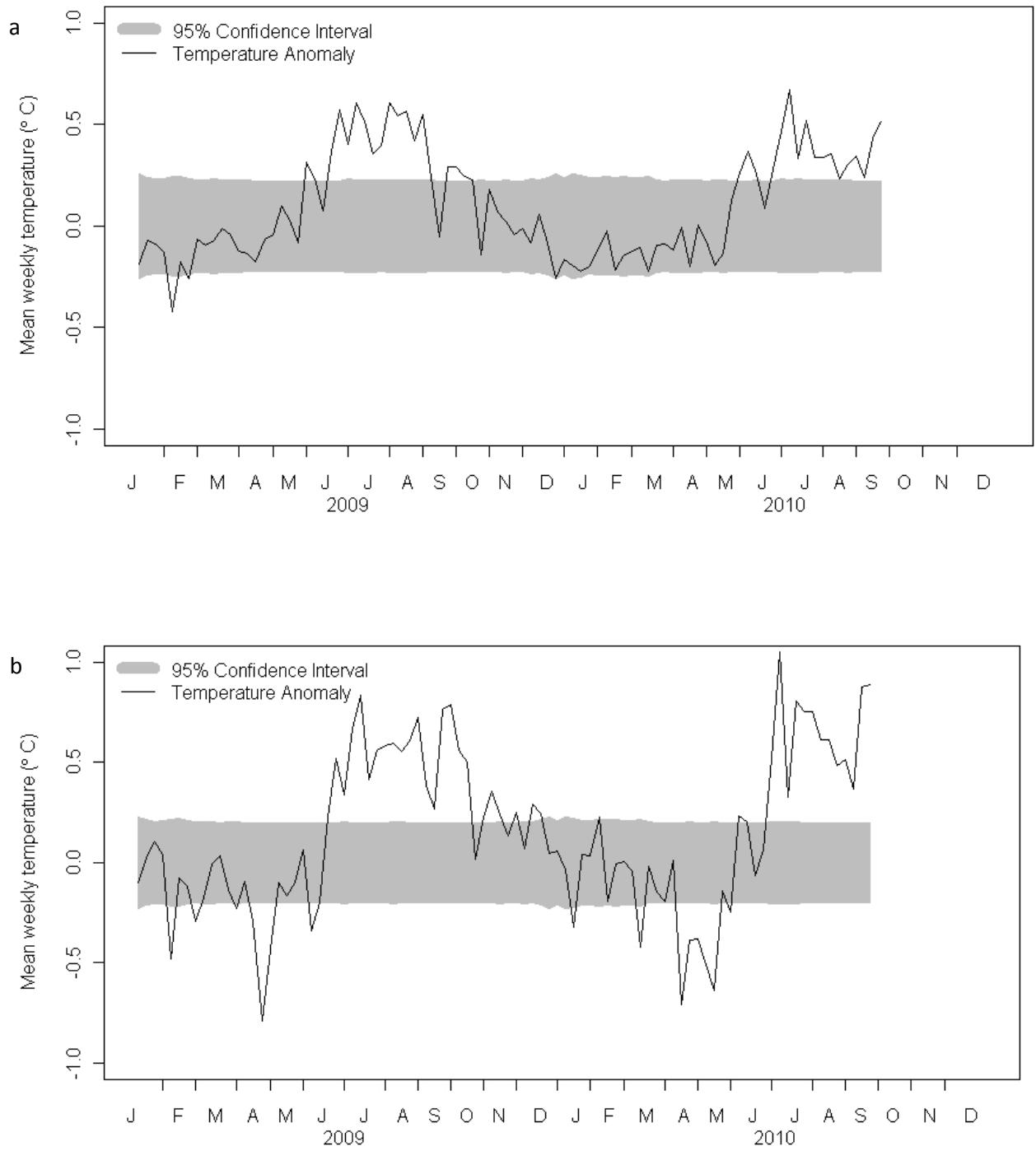


Figure 6.2: Weekly mean temperature anomalies relative to Sedge Fen at:
a) Adventurer's Fen and; b) Oily Hall

The daily mean temperature data from Adventurer’s Fen and Oily Hall were compared to the daily mean temperature data from Sedge Fen by means of a paired Mann-Whitney U test. The null hypothesis was defined as there being no significant difference between the paired daily mean temperature data from the two stations, and the significance level was set at 0.05. The results are summarised in table 6.3 and demonstrate that the alternative hypothesis must be accepted for all tests. Therefore the differences in the mean daily temperature at both Adventurer’s Fen and Oily Hall are statistically significant.

Table 6.3: Results of comparisons of daily mean temperature data from Adventurer’s Fen and Oily Hall to that at Sedge Fen by means of the Mann-Whitney U test.

	Adventurer’s Fen		Oily Hall	
	2009	2010	2009	2010
U ₁	23944	13345	21150	14008
U ₂	42486	23240	45280	22577
P	<0.01	<0.01	<0.01	<0.01

30-minute mean temperature anomalies at Adventurer’s Fen and Oily Hall relative to Sedge Fen are presented in figure 6.3. The 30-minute temperature anomalies for Adventurer’s Fen demonstrate that the temperature at Adventurer’s Fen exceeds that at Sedge Fen between approximately 1600 – 0600. For the remainder of the day, the Sedge Fen temperature is higher than the temperature at Adventurer’s Fen. Most of the 30-minute Adventurer’s Fen anomalies lie within the 95% confidence interval, the exceptions being the anomalies between approximately 1800 – 0000 which lie just outside the confidence interval. The Oily Hall 30-minute temperature anomalies

exhibit the same trends as the Adventurer's Fen anomalies. However, the Oily Hall anomalies demonstrate a larger amplitude, resulting in much of the data lying outside the confidence interval. The positive anomalies (indicating that the Oily Hall temperature exceeds that at Sedge Fen) lie outside the confidence interval between approximately 1700 and 0500, whilst the negative anomalies (indicating that the Sedge Fen temperature exceeds that at Oily Hall) lie outside the confidence interval between approximately 0700 and 1500.

The mean weekly diurnal temperature ranges for Adventurer's Fen and Oily Hall are summarised as anomalies relative to those at Sedge Fen in figure 6.4. A general seasonal trend is evident in which the diurnal temperature range at Sedge Fen is greater than that at Adventurer's Fen during the summer, but similar in the winter. The diurnal temperature range at Sedge Fen is generally greater than that at Oily Hall throughout the year, although the differences during the winter are lower than those observed during the winter.

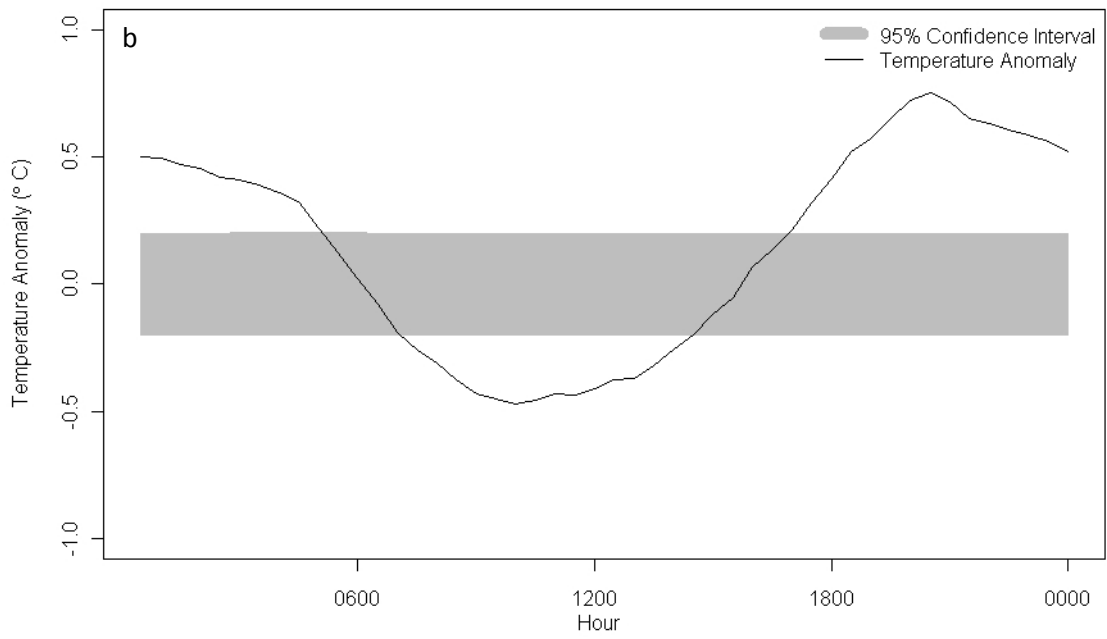
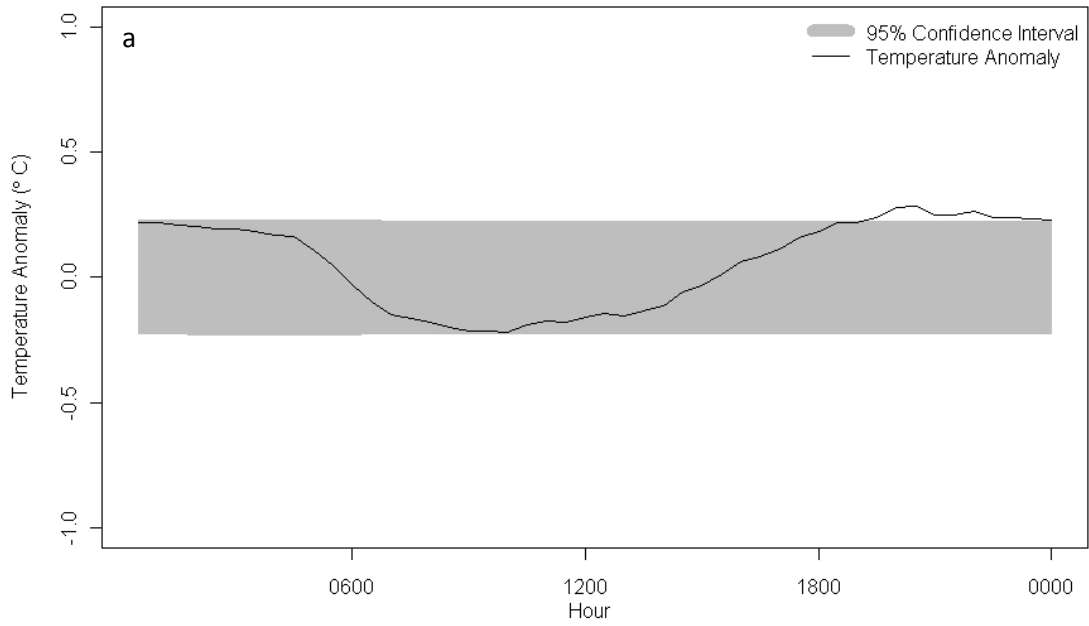


Figure 6.3: 30-minute mean temperature anomalies relative to Sedge Fen at:
 a) Adventurer's Fen and; b) Oily Hall

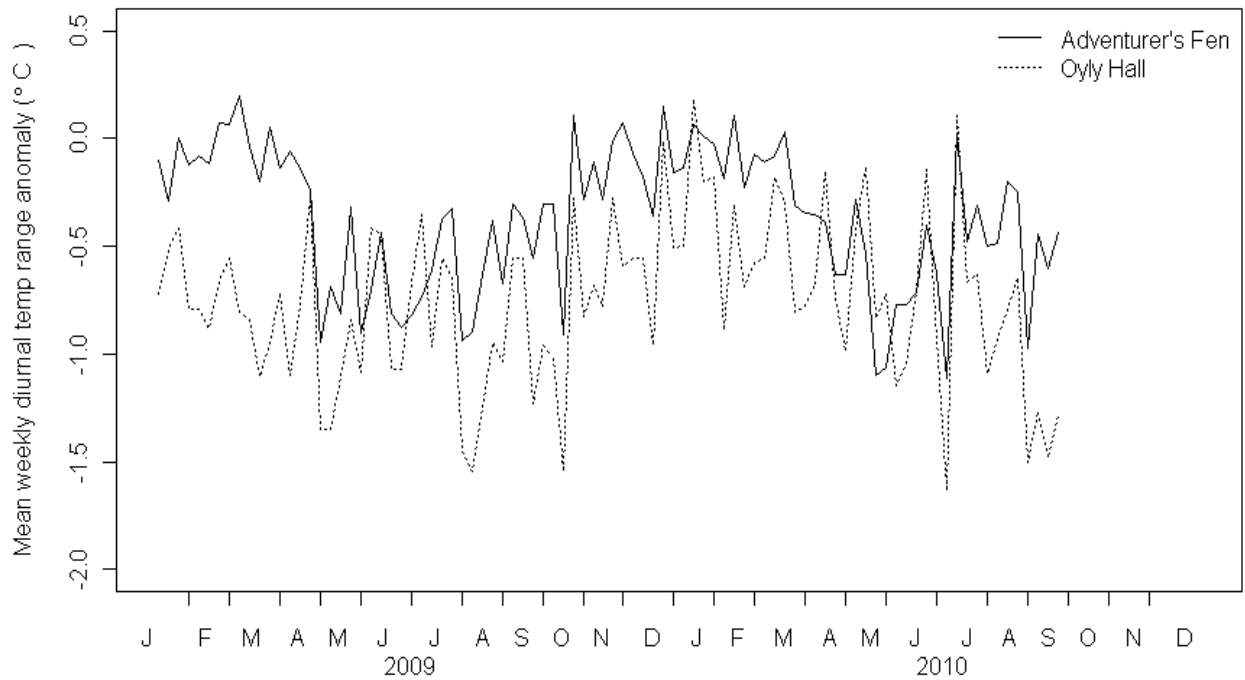


Figure 6.4: Weekly mean diurnal temperature range anomalies relative to Sedge Fen at Adventurer's Fen and Oily Hall

6.3.4. Vapour Pressure Comparison

The weekly mean vapour pressure data from Adventurer's Fen and Oily Hall are presented as anomalies relative to the Sedge Fen vapour pressure data in figure 6.5. The vapour pressures at Adventurer's Fen are typically slightly lower than those at Sedge Fen, although the Adventurer's Fen anomalies generally lie within the confidence interval. The anomalies only lie outside the confidence interval for a sustained period from March to May 2010. By contrast, the vapour pressure at Oily Hall is consistently lower than that at Sedge Fen, and typically lies outside the confidence interval. During 2010, the negative vapour pressure anomaly observed at Oily Hall is greater than that observed during 2009.

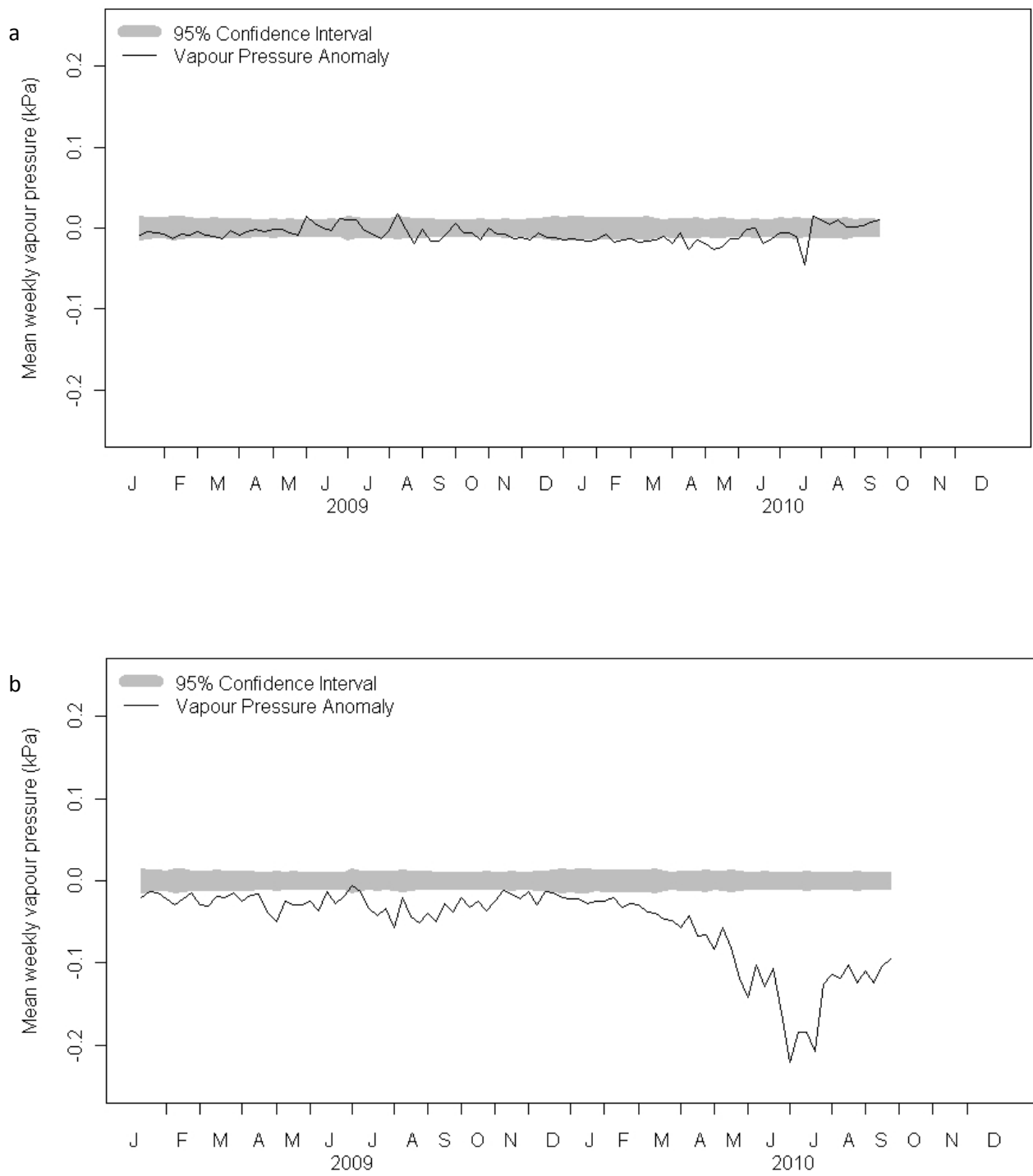


Figure 6.5: Weekly vapour pressure anomalies relative to Sedge Fen at:
a) Adventurer's Fen and; b) Oily Hall

The daily mean vapour pressure data from Adventurer’s Fen and Oily Hall were compared to the daily mean vapour pressure data from Sedge Fen by means of a paired Mann-Whitney U test. The null hypothesis was defined as there being no significant difference between the paired daily mean vapour pressure data from the two stations, and the significance level was set at 0.05. The results are summarised in table 6.4 and demonstrate that the alternative hypothesis must be accepted for all tests. Therefore the differences in the mean daily vapour pressure at both Adventurer’s Fen and Oily Hall are statistically significant.

Table 6.4: Results of comparisons of daily mean vapour pressure data from Adventurer’s Fen and Oily Hall to that at Sedge Fen by means of the Mann-Whitney U test.

	Adventurer’s Fen		Oily Hall	
	2009	2010	2009	2010
U ₁	48154	29067	62791	36581
U ₂	18276	7518	3639	4
P	<0.01	<0.01	<0.01	<0.01

6.3.5. Reference Evapotranspiration Comparison

Weekly mean reference evapotranspiration estimates for Adventurer’s Fen and Oily Hall are presented as anomalies relative to Sedge Fen reference evapotranspiration estimates in figure 6.6. The reference evapotranspiration at both Adventurer’s Fen and Oily Hall is generally greater than that at Sedge Fen. The reference evapotranspiration anomalies peak during the summer at both sites. The reference evapotranspiration estimates at Oily Hall are greater than those at Adventurer’s Fen

for most of the observation period. The only exceptions are in the April – June period, when the Oily Hall reference evapotranspiration estimates are lower than those for Adventurer’s Fen. The largest anomalies are observed at Oily Hall during summer 2010.

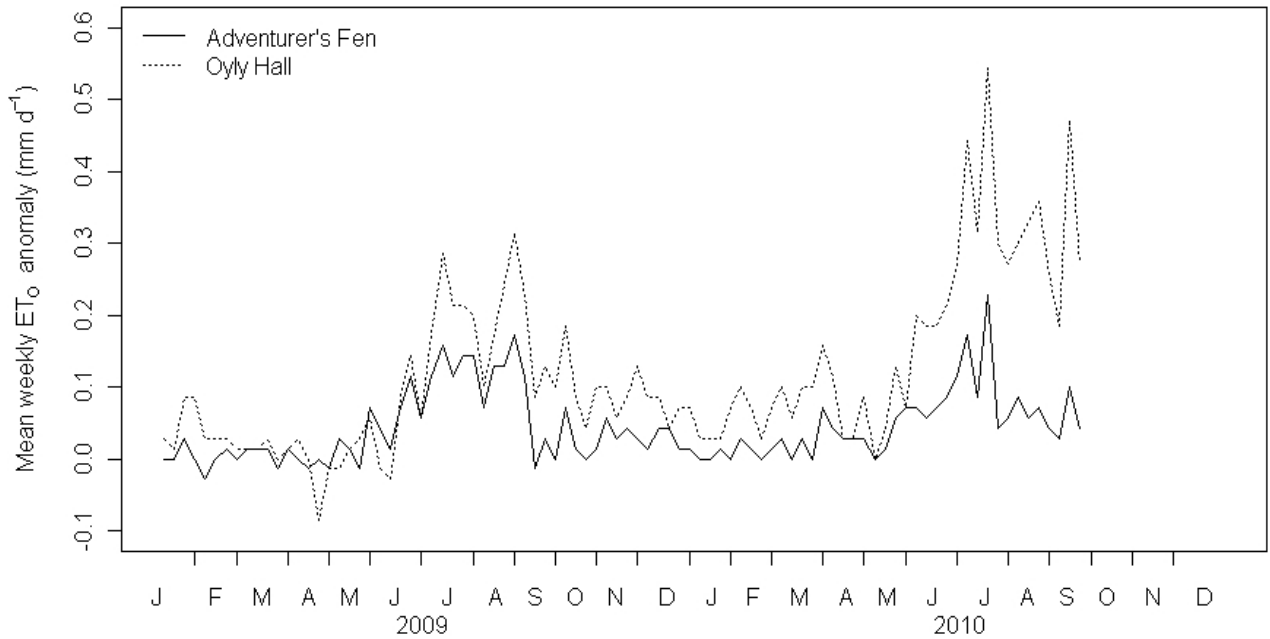


Figure 6.6: Weekly mean reference evapotranspiration anomalies relative to Sedge Fen at Adventurer’s Fen and Oily Hall.

The annual reference evapotranspiration totals for each site are summarised in table 6.5. The total reference evapotranspiration is lowest at Sedge Fen during both years, whilst Oily Hall experiences the highest.

Table 6.5: Summary of reference evapotranspiration data at all stations, 2009 and 2010.

	Sedge Fen		Adventurer's Fen		Oily Hall	
	2009	2010	2009	2010	2009	2010
Total ET _O (mm)	603.6	533.9	618.4	547.1	633.3	580.7

6.4. Discussion

The three temperature and relative humidity probes used to gather the data for this chapter were compared by deploying all probes at the same location. Examination of the data collected by each probe demonstrated that statistically significant differences existed between temperature and relative humidity data gathered by different probes. Linear regression of the calibration data from the Adventurer's Fen and Oily Hall probes relative to the data from the Sedge Fen probe demonstrated that most of the variation observed between the data collected by a pair of probes could be explained by simple linear relationships. Instrumental error was therefore removed from the data by adjusting the Adventurer's Fen and Oily Hall temperature and relative humidity data according to the linear relationships defined in table 6.1. However, it is acknowledged that the application of linear regression may introduce errors into the adjusted data. These errors are quantified as 95% confidence intervals for both temperature and vapour pressure data, as described in sections 6.2.2 and 6.3.1. Any differences between data from a pair of probes lying within the confidence intervals may be attributable to errors associated with the regression applied to one of the data sets. However, any differences lying outside the 95% confidence interval is unlikely to be attributable to errors arising from the regression, and thus is indicative of a genuine difference in the variable of interest between sites. The application of this

methodology therefore explicitly addresses the possibility that differences in temperature and vapour pressure between sites may arise as a result of instrumental bias rather than the existence of microclimates.

The temperature data presented in section 6.3.3 reveal the weekly mean temperatures at Adventurer's Fen and Oily Hall to be higher than those at Sedge Fen during the summer period (June – October), by averages of 0.34°C and 0.48°C, respectively. During the winter, this trend is reversed, with Sedge Fen exhibiting temperatures 0.08°C and 0.11°C higher than those at Adventurer's Fen and Oily Hall, respectively. Statistical comparison of the daily mean temperatures showed the data from Adventurer's Fen and Oily Hall to be significantly different from those at Sedge Fen. The temperature anomalies at Adventurer's Fen exhibit a tendency to lie within the 95% confidence interval during the winter period and to lie outside the confidence interval for a sustained period only during the summer. This suggests that Sedge Fen only experiences a summer microclimate relative to Adventurer's Fen, in which temperatures are suppressed at Sedge Fen. The anomalies at Oily Hall exhibit a greater amplitude than those at Adventurer's Fen, as well as an enhanced tendency to lie outside the confidence interval. These results reinforce the aforementioned suggestion of suppressed summer temperatures at Sedge Fen as well as indicating that Sedge Fen temperatures may be enhanced relative to those at Oily Hall during the late winter period (i.e. April and May).

The 30-minute mean temperature anomalies at Adventurer's Fen and Oily Hall relative to Sedge Fen demonstrate that temperatures at Sedge Fen are higher than

those at the other sites during much of the daylight period and lower overnight. These findings are therefore indicative of a larger diurnal temperature range at Sedge Fen than either Adventurer's Fen or Oily Hall. However, only the Oily Hall 30-minute anomalies lie outside the 95% confidence intervals for much of the day. Therefore, the diurnal temperature ranges at Sedge Fen and Adventurer's Fen cannot be definitively said to be different, since the observed anomalies may be attributable to the linear corrections applied to the Adventurer's Fen temperature data. The similar diurnal temperature ranges at these sites may be a reflection of the location of Adventurer's Fen on the edge of the wetland site. Since many of the Oily Hall 30-minute temperature anomalies lie outside the confidence intervals, it is reasonable to conclude that the diurnal temperature range at Sedge Fen is greater than the range at Oily Hall. This contrasts with the findings of Brom and Pokorný (2009), who reported narrower temperature ranges at wetland sites relative to drained pastures. This suggests that reduced temperature ranges are not a universal feature of wetland microclimates, although further investigation will be required in order to ascertain the mechanisms controlling diurnal temperature ranges in wetlands.

The diurnal temperature range anomalies relative to Sedge Fen exhibit a seasonal pattern. During the summer months the diurnal temperature range at Sedge Fen is greater than that at Adventurer's Fen and Oily Hall. The weekly mean temperatures previously commented upon indicated a tendency for Adventurer's Fen and Oily Hall to be slightly warmer than Sedge Fen during the summer. When considered in the context of larger diurnal temperature ranges at Sedge Fen than the other sites, it would seem that the summer daily minimum temperatures are lower at Sedge Fen than either of the other sites. Thus, overnight cooling within the wetland is greater than outside

during the summer months, whilst the daytime maxima at all sites during the summer are similar. This may be indicative of overnight temperatures being stabilised by the release of stored heat within the surface layer outside of the wetland, implying that incident energy is either not stored within the surface layer at the wetland or that stored energy is not released overnight at the wetland. However, surface energy budget measurements at all three sites would be required in order to further investigate these possible explanations.

The vapour pressure anomalies presented in section 6.3.4 indicate a more humid atmosphere at Sedge Fen than at Adventurer's Fen and Oily Hall. During the summer months, the vapour pressure at Sedge Fen is greater than that at Adventurer's Fen and Oily Hall by averages of 0.003 kPa and 0.077 kPa, respectively. During the winter months, the vapour pressure is greater at Sedge Fen by averages of 0.011 kPa and 0.036 kPa than the vapour pressures at Adventurer's Fen and Oily Hall, respectively. Thus, the vapour pressure anomalies at Adventurer's Fen are consistently less than those at Oily Hall. The vapour pressure anomalies at Adventurer's Fen lie within the confidence interval for most of the observation period, so cannot definitively be said to differ from the vapour pressures observed at Sedge Fen. In contrast, the Oily Hall vapour pressure anomalies lie outside the confidence intervals for almost the entire duration of the observation period, and are therefore indicative of heightened atmospheric vapour pressures within the wetland compared to outside. Unlike the temperature anomalies, the magnitude of the Oily Hall vapour pressure anomaly differs in successive years, with the 2010 average vapour pressure anomaly being 0.064 kPa greater than that during 2009. Investigation of the vapour pressure data from all sites revealed that the vapour pressures at Sedge Fen and Adventurer's Fen

are comparable in both years, whilst the vapour pressure at Oily Hall is lower in 2009 than 2010. Therefore, the differences observed in the Oily Hall vapour pressure anomalies are attributable to annual differences in the Oily Hall vapour pressure data. This may suggest the vapour pressure is more stable on an annual basis within the wetland than outside. However, it may also imply that the relative humidity probe at Oily Hall has drifted from the calibration parameters defined in section 6.3.1. A further calibration will confirm whether instrumental drift has occurred, and until this has been performed the 2010 vapour pressure data should be regarded with caution. The generally higher vapour pressures observed at the wetland may represent the greater availability of water for evaporation at this site. If actual evapotranspiration is greater within the wetland than outside, this may account for the more humid atmosphere observed at Sedge fen compared to that at Oily Hall.

The meteorological data therefore suggest a wetland microclimate exists at Sedge Fen, in which winter temperatures are higher than those outside the wetland and summer temperatures are lower than those outside. Vapour pressures are also higher within the wetland than outside, particularly in the summer months. In general, the anomalies at Oily Hall are greater than those observed at Adventurer's Fen. This is likely to be indicative of the location of Adventurer's Fen on the edge of the wetland. The summer temperature trends agree with the findings of Přibáň and Ondok (1978). However, they are contrary to the findings of Li *et al* (2009), who reported enhanced wetland air temperatures. Furthermore, the diurnal temperature variations observed at the three sites within this study contradict the findings of Brom and Pokorný (2009), who identified smaller diurnal temperature variations within wetland than outside. The summer vapour pressure anomalies at Oily Hall are consistent with the findings

of Li *et al* (2009). Whilst these studies all agree on the existence of wetland microclimates, there remains disagreement regarding the temperature characteristics of the wetland microclimate relative to areas outside the wetland. This raises the possibility that individual wetlands have unique microclimates with respect to air temperature.

The reference evapotranspiration estimates based on the meteorological data from each site previously described demonstrate that higher reference evapotranspiration estimates can be expected at Adventurer's Fen and Oily Hall than at Sedge Fen. The reference evapotranspiration at Adventurer's Fen is 2.5% higher than that at Sedge Fen during both 2009 and 2010, whilst the reference evapotranspiration estimated at Oily Hall is 4.9% and 8.8% higher than that at Sedge Fen during 2009 and 2010, respectively. This is consistent with the enhanced summer mean temperatures and lower vapour pressures observed at Oily Hall. That the proportional ET_0 increase at Oily Hall relative to Sedge Fen is greater in 2010 than 2009 is indicative of a particular sensitivity to the vapour pressures at each site, which were shown to exhibit the greatest difference during 2010. Therefore variations in temperature and vapour pressure within and outside wetlands produce varying estimates of reference evapotranspiration. For the sites examined within this chapter, warmer and drier atmospheres outside the wetland stimulate a greater atmospheric demand for evapotranspiration by enhancing the vapour pressure deficit term within the Penman-Monteith equation and thus result in higher estimates of reference evapotranspiration for sites outside the wetland.

6.5. Conclusions

A wetland microclimate has been identified at Sedge Fen, characterised by lower summer mean temperatures, higher winter mean temperatures and a larger diurnal temperature range at Sedge Fen than at nearby sites outside the wetland. The vapour pressure is also consistently higher at Sedge Fen than at the other locations. The issue of instrumental bias has been addressed, lending credence to the assertion that these differences are indicative of a local climate amelioration function. Although small, these meteorological differences produce varying estimates of reference evapotranspiration.

This creates a dilemma for wetland evapotranspiration studies. When seeking to calculate reference evapotranspiration, meteorological data should ideally be collected within wetlands so as to accurately capture microclimate effects. However, in situations where this is not possible, meteorological data sourced from locations outside the wetland may not be sufficiently proximate to adequately represent atmospheric conditions at the wetland.

Chapter 7

The Hydrology of Sedge Fen

7.1. Introduction

7.1.1. Hydrological Studies of Sedge Fen

Much of the understanding of the hydrological functioning of Sedge Fen is based upon the work of Godwin (1931). Using purpose-built automated water level recorders, this study described the behaviour of the soil water levels at Sedge Fen. Examination of seasonal data revealed a tendency for a lowering of water levels in summer. The lack of an equivalent seasonality in rainfall data led Godwin (1931) to propose that enhanced summer transpiration from vegetation was responsible for the lowering of water levels observed during the summer months. Diurnal water level fluctuations were examined and revealed a rapid fall in water levels during daylight hours followed by a partial overnight recovery. This was consistent with the proposal that summer water levels were responding to the loss of water by transpiration. Comparison with water level data gathered from an area of bare soil lent further credence to this proposal. Overnight rises in water levels were attributed to the inflow of water from the ditch network. Ditch water levels were shown not to exhibit fluctuations corresponding to those of the soil water level, suggesting that soil water level fluctuations were not controlled by changes in ditch water levels.

Godwin and Bharucha (1932) further investigated the behaviour of Sedge Fen soil water levels by monitoring water levels across the fen. This investigation revealed that at locations close to open ditches, soil water levels responded to the ditch water levels. Following heavy spring rainfall the soil water levels close to ditches rapidly dropped as water drained from the soil into the open ditches, in which water levels were lower than those in the soil. By contrast, high soil water levels persisted within the fen interior (i.e. at locations distant from the ditch network) implying little drainage to the ditch network from these locations. Throughout the summer lower water levels were observed at the interior of the Fen than at the ditch margins, indicating that the ditch water levels were acting to stabilise soil water levels immediately adjacent to the ditch network. Godwin and Bharucha (1932) therefore considered Sedge Fen to comprise of two hydrological regions; one small area defined as extending 25 m from open ditches and another comprising the remainder of the Fen.

The seasonal variation of relative water levels in the soil and ditch network results in the ditches serving alternating hydrological functions. During winter, soil water levels are typically higher than ditch water levels. Thus the ditches act to drain water from the soil immediately adjacent to the ditch network whilst soil water levels in the interior areas remain high. As a consequence, the Sedge Fen water table adopts a slightly convex shape. During the summer, soil water levels drop below ditch water levels as a result of enhanced transpiration and so the ditches function as irrigation channels, stabilising water levels in the region adjacent to ditches whilst water levels in the interior of the Fen continue to fall. The Fen water table therefore adopts a slightly concave shape during the summer.

More recent studies of Sedge Fen water levels were undertaken by Gowing (1977) and Gilman (1988). Both of these studies confirmed the findings of Godwin and Godwin and Bharucha (1932) regarding the seasonal behaviour and shape of the water table at Sedge Fen. Therefore, fluctuations of soil water levels across most of Sedge Fen are commonly assumed to be in response to precipitation and evapotranspiration. Exchanges of water with subterranean water sources are not expected to influence soil water levels as Sedge Fen is underlain by an impervious layer of clay (Friday and Rowell, 1997). The only surface water at Sedge Fen is within open ditches and is believed to have a limited range of influence on soil water levels. However, Gowing (1977) notes that the assumption that ditch water levels do not influence the soil water levels at the Fen interior may be misleading as it implies there is no exchange of water between the ditches and the fen interior. Given the existence of a hydraulic gradient, it is probable that water does move between the ditches and the Fen interior. However, the volumes involved are insufficient to exert a significant influence over soil water levels at the Fen interior.

7.1.2. Evapotranspiration Estimates from Sedge Fen Water Balance

Given the relative simplicity of the hydrological budget of Sedge Fen, in which soil water levels respond to precipitation and evapotranspiration across much of the Fen, estimates of any hydrological flux are possible if the other fluxes may be quantified. McCartney *et al* (2001) adopted this methodology to derive evapotranspiration estimates for Sedge Fen based on measurements of precipitation and soil water level change. McCartney *et al* (2001) adopted Godwin and Bharucha's (1932) conceptualisation of Sedge Fen, assuming no lateral movement of soil water at

distances greater than 50 m from ditches. The evapotranspiration calculated for the interior region of the Fen was assumed to be representative of the region adjacent to the ditch network and so lateral soil water movement was quantified as the residual of the water budget described by soil water level change, precipitation and evapotranspiration.

In order to convert changes in soil water level to changes in soil water storage, the soil water level change must be multiplied by the specific yield of the soil. The specific yield describes the volume of water that can freely drain from a soil under the influence of gravity, and is expressed as a proportion of the total volume of the aquifer (Ward and Robinson, 1990). Gilman (1988) determined the specific yield of the peat soil at Sedge Fen by investigating the response of the soil water level to precipitation events. Gilman derived a specific yield of 0.12 according to this method, and this value was adopted by McCartney *et al* (2001) in deriving evapotranspiration estimates for Sedge Fen. McCartney *et al* (2001) found that summer evapotranspiration estimates based upon the Sedge Fen water budget were lower than potential evaporation estimates, and attributed this to the effects of a summer soil moisture deficit at Sedge Fen.

7.1.3. Aims

The objective of this chapter is to assess the accuracy of evapotranspiration estimates derived from the Sedge Fen water budget so as to further understanding of the

hydrological functioning of Sedge Fen. This objective will be fulfilled by addressing the following aims:

1. Describe the precipitation and soil water levels in 2009 and 2010 and deriving evapotranspiration estimates according to the model described by McCartney *et al* (2001)
2. Comparing evapotranspiration estimates based on the Sedge Fen water budget to evapotranspiration measurements gathered by the eddy covariance system.
3. Investigating any difference between evapotranspiration estimates and measurements within the context of the assumptions made by the McCartney *et al* (2001) model.

7.2. Methods

7.2.1. Soil Water Level

Water levels at Sedge Fen have been monitored by the National Trust since 1994. A network of dipwells was established across Sedge Fen, and the locations of the dipwells are reported by McCartney *et al* (2001). All dipwells are read manually at monthly intervals.

From 2006, automated water level recorders were installed across Wicken Fen by Anglia Ruskin University¹ to monitor hourly water level fluctuations. On Sedge Fen,

¹ Dipwell data were provided by Dr. Francine Hughes (Anglia Ruskin University), Peter Stroh (Anglia Ruskin University), The Environment Agency (Anglian Region) and the National Trust at Wicken Fen.

automatic recorders were installed at dipwells 9 and 10. These dipwells form part of a transect adjacent to Christy's Drove. Dipwell 9 is located approximately 80 m from the ditch network, whilst Dipwell 10 is located adjacent to a ditch at the junction of Christy's Drove and Gardiner's Drove (see figure 7.1). The 2009 and 2010 data from these dipwells are used within this chapter to compile weekly and monthly mean water levels for use in water balance calculations and comparison with the longer-term water level data.

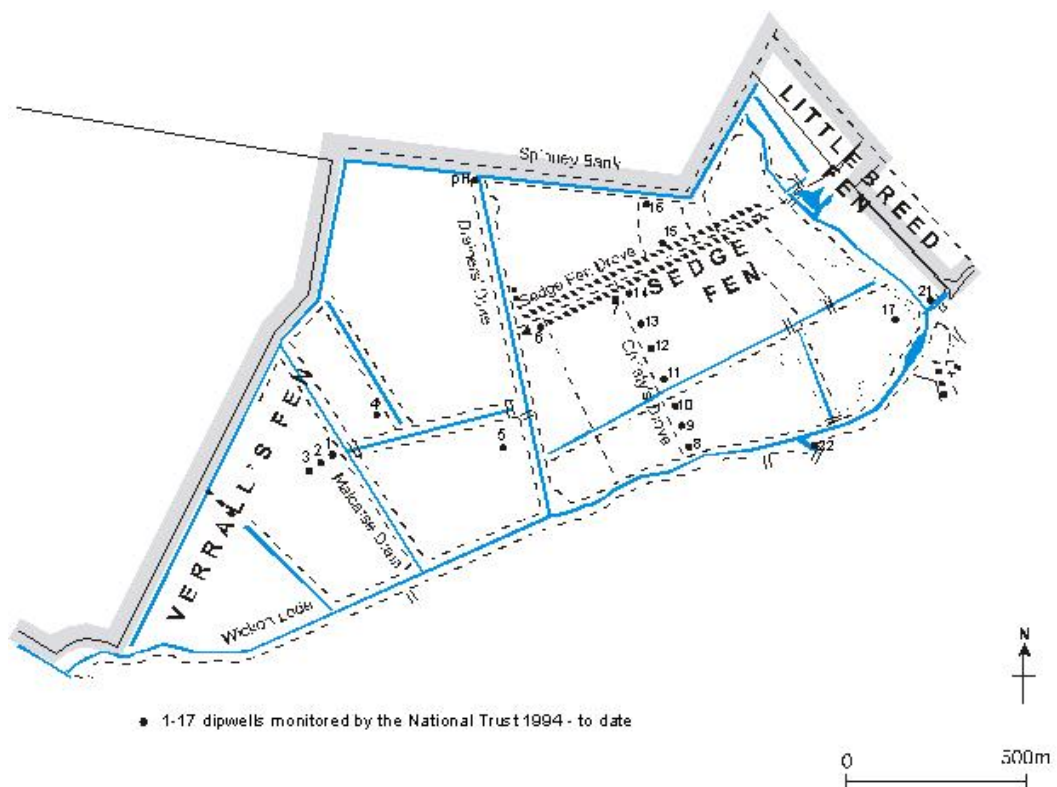


Figure 7.1: Map of Sedge Fen showing locations of dipwells (from McCartney *et al*, 2001)

7.2.2. Precipitation data

Precipitation data have been collected by the National Trust at Wicken Fen since 1996. Until early 2003 an automated rain gauge was located in a field near the Wicken Fen visitor's centre. In early 2003, a new automated rain gauge was installed

on the roof of the Wicken Fen visitors centre (figure 7.2) (Lester, pers. comm.). The automated rain gauge currently in use logs cumulative rainfall at 5 minute intervals.



Figure 7.2: Location of Sedge Fen automated rain gauge atop Wicken Fen Visitor's Centre.

The automated rain gauge at Wicken Fen may be susceptible to a degree of sheltering from the raised section of roof adjacent to it (figure 7.2). Daily rainfall totals were therefore acquired from the British Atmospheric Data Centre (2011) for nearby rain gauges at Upware Pumping Station and Stretham. The details of these stations are summarised in table 7.1. The rainfall data at these stations were recorded at 0900, and so the data from the automated rain gauge at Sedge Fen were aggregated to daily values so as to synchronise with the Upware and Stretham gauges. Long-term average rainfall data measured at a rain gauge in Cambridge during the period 1971 –

2000 was also acquired from the UK Meteorological Office². Comparison of the long-term data with the observations at individual rain gauges provided another means to assess the quality of the rainfall data upon which subsequent analyses were based.

Table 7.1: Summary of rain gauges

Rain gauge	Station Number	Location (decimal degrees)	Elevation (m)	Distance from Sedge Fen (km)
Wicken Fen		52.310, 0.291		
Upware Pumping Station	184863	52.304, 0.256	2	2.6
Stretham	180704	52.334, 0.227	4	5.4
Cambridge: NIAB	183799	52.245, 0.102	26	14.8

So as to enable comparisons of the Sedge Fen, Upware and Stretham precipitation data, the data from the rain gauges located at Upware, P_{Upware} , and Stretham, $P_{Stretham}$, was averaged according to:

$$P_{average} = \frac{P_{Upware} + P_{Stretham}}{2} \quad (7.1)$$

The monthly cumulative average rainfall from Upware and Stretham, $P_{average}$, was then compared to the rainfall at Sedge Fen by means of a double mass curve. The monthly rainfall data collected at Sedge Fen was also compared to the monthly average rainfall recorded at Upware and Stretham by least squares regression.

² <http://www.metoffice.gov.uk/climate/uk/averages/19712000/sites/cambridge.html>

7.2.3. Sedge Fen Water Budget

The water budget proposed by McCartney *et al* (2001) was adopted to describe the hydrological fluxes and stores at Sedge Fen. This model is described as:

$$s\Delta h = P - ET \pm D \quad (7.2)$$

The left hand side of equation 7.2 describes the change in the amount of water stored within the soil. This is related to the change in elevation of the soil water level, Δh (mm), by the specific yield, s , which represents an integral of soil properties in both the saturated and unsaturated zones. McCartney *et al* (2001) adopted a specific yield value of 0.12 to represent the peat soil of Sedge Fen. This value was originally proposed by Gilman (1988) and was derived by relating soil water level rises to rainfall events (section 7.1.2).

The right hand side of equation 7.2 describes the input of water in the form of precipitation, P (mm), and removal by evapotranspiration, ET (mm). The remaining term represents the flow of water to or from Sedge Fen, D (mm), and hence may be assigned either a positive or negative value. Since the movement of surface water is confined to ditches and Sedge Fen is known to be isolated from subterranean water sources by a layer of impervious clay (Friday and Rowell, 1997), the flow term must therefore represent the exchange of water between the Sedge Fen soil and the ditch network. McCartney *et al* (2001) assumed that this such exchange was limited to an area within 50 m of ditches, thus dividing Sedge Fen into two zones; a small zone adjacent to ditches in which the lateral movement of water within the soils affects water levels, and a larger zone covering most of Sedge Fen in which there is no lateral

flow within the soil. The water budget for much of Sedge Fen may therefore be described by precipitation input and evaporative output according to McCartney *et al* (2001).

7.2.4. Evapotranspiration Estimates

Evapotranspiration estimates for Sedge Fen were determined according to the McCartney *et al* (2001) water budget by rearranging equation 7.2. Evapotranspiration estimates based on the water budget, ET_{WB} (mm), were calculated at daily intervals during 2009 and 2010. Each day is defined as a 24 hour period ending at 0900, as dictated by standardised recording practices employed in the collection of the precipitation data.

7.2.5. Actual Evapotranspiration

The actual evapotranspiration data reported within this chapter were derived from the eddy covariance instrumentation as described in section 3.2.3. Since the precipitation data were reported at 0900 each day, ET_{WB} will also represent 24-hour data ending at 0900. For comparison, the actual evapotranspiration data were recomputed to represent 24-hour totals ending at 0900. The actual evapotranspiration data reported within this chapter will therefore differ from that reported in chapter 5, which was calculated for 24-hour periods ending at midnight.

7.3. Results

7.3.1. Soil Water Level

The monthly soil water data for 2009 and 2010 are presented and compared to the maxima and minima for the period 1994 – 2008 in figure 7.3. The monthly water levels are above the 1994 – 2008 maximum during January – April 2009, January – May 2010 and October and November 2010. For all other months, both the 2009 and 2010 water level data lie within the range observed during the period 1994 – 2008. During 2009, the water level undergoes a steady decline from April to July before stabilising at approximately 0.55 m below ground level until August. The water level then declines to approximately 0.90 m below ground level in September. From October 2009, the water level rapidly rises to near-surface levels typical of the winter period. During 2010, the water level exhibits a more rapid decline between June and July than that observed during 2009. A 2010 minimum water level of approximately 0.70 m below ground level is observed during July and August, followed by a rise in subsequent months.

The 2009 and 2010 weekly mean soil water level data from the automated dipwells are compared to the weekly mean surface resistance data (see section 5.3.2.3) in figure 7.4. No relationship between the two data sets is evident. The surface resistance exhibits a consistent pattern in both years, in which the lowest values and ranges are observed in the summer period. By contrast the water level data exhibits different patterns in the two years, with the minimum level observed in 2009 being approximately 0.15 m lower and occurring almost two months later than that in 2010.

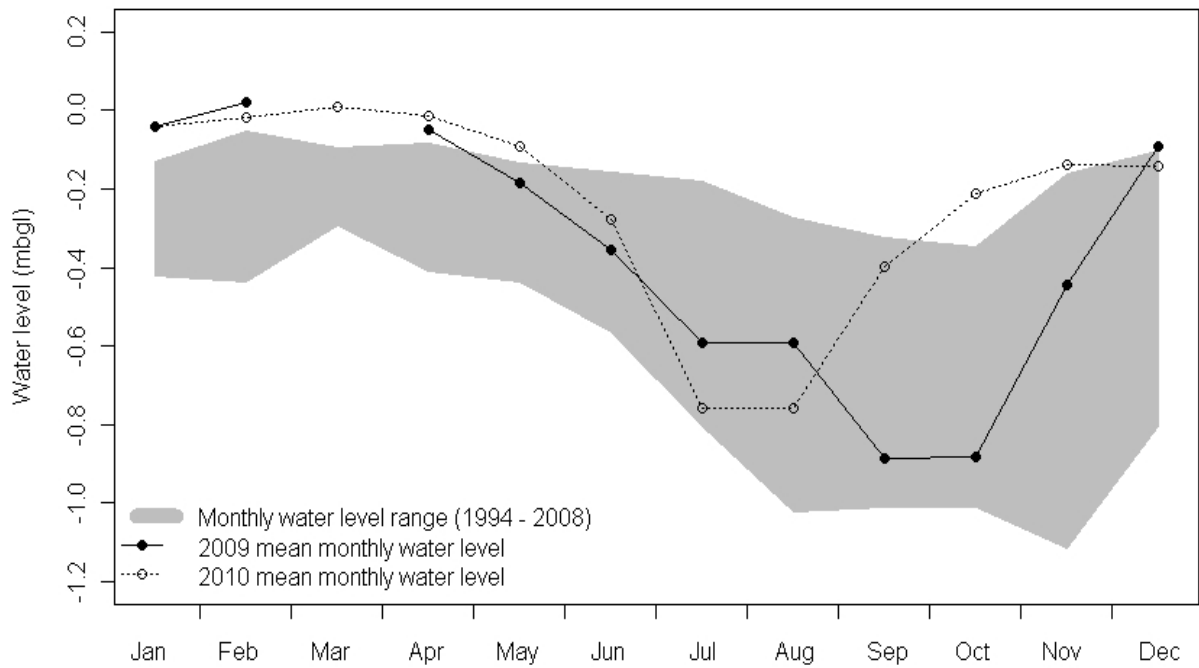


Figure 7.3: Monthly water level range 1994 – 2008 and 2009 and 2010 monthly mean water levels at dipwell 9 on Sedge Fen.

The water levels at dipwell 10 are higher than those at dipwell 9 for much of the study period. This trend is reversed in October during both years, when the water levels in dipwell 9 become higher than those in dipwell 10. The greatest difference between the water levels recorded at dipwells 9 and 10 occurs in July and August during both years.

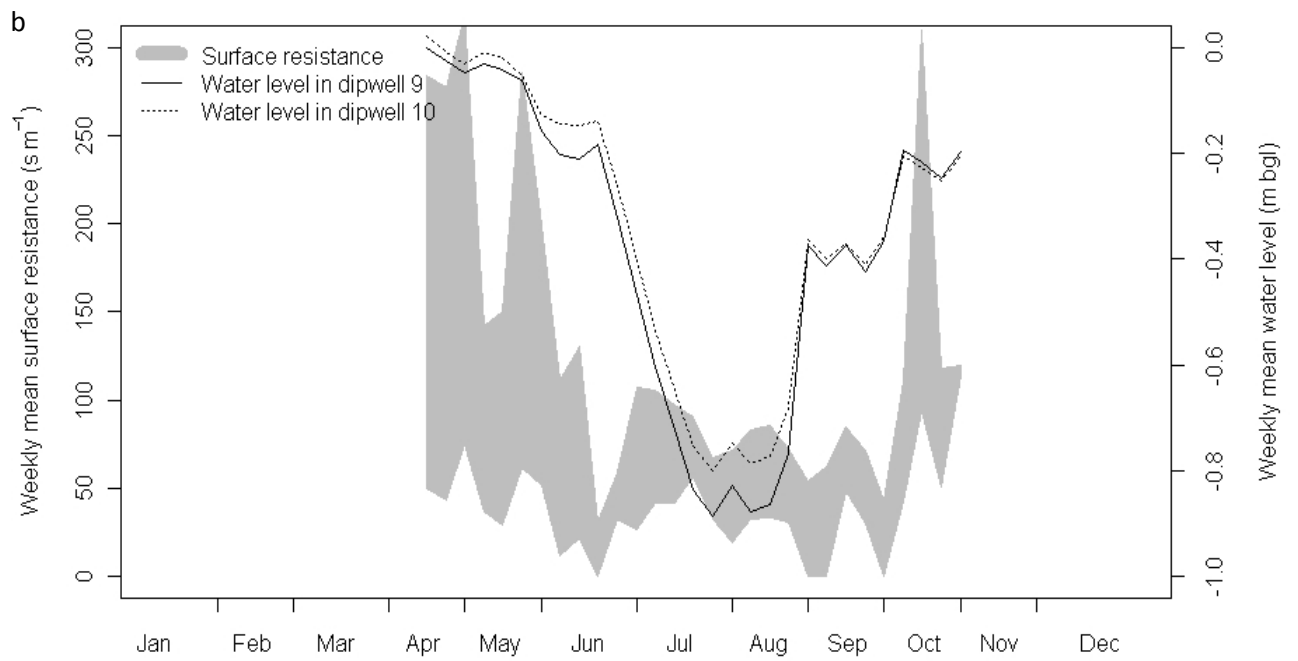
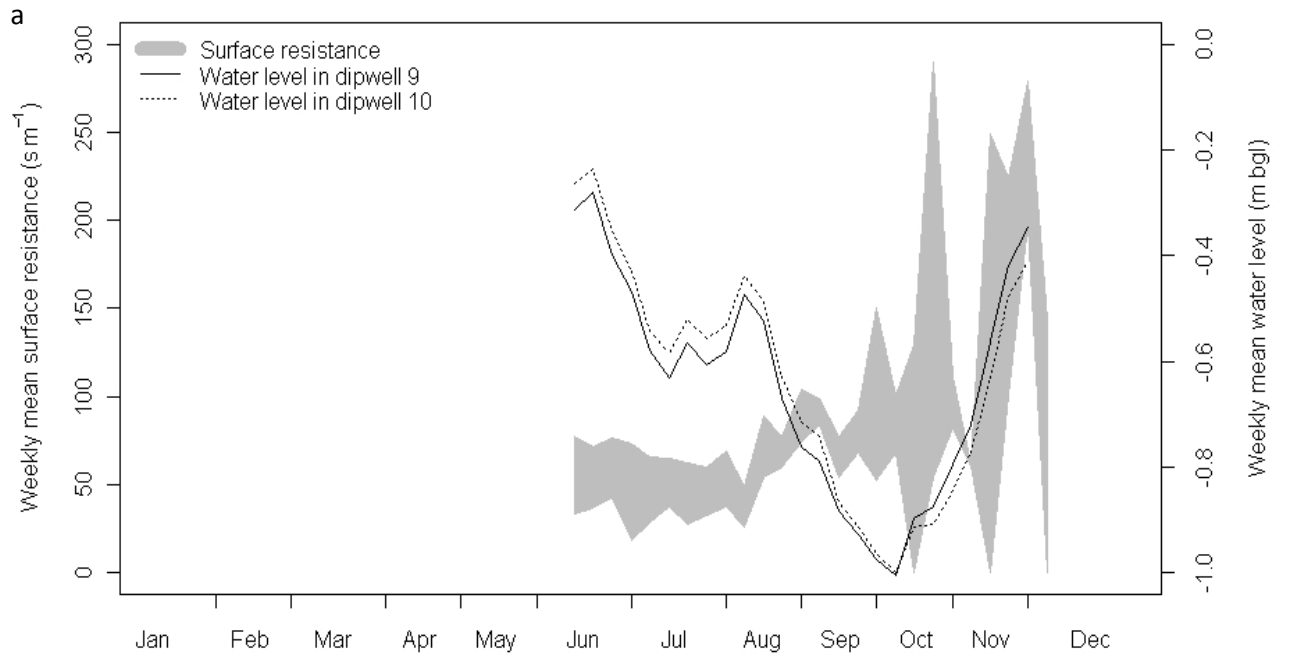


Figure 7.4: Weekly mean surface resistance and water levels at Sedge Fen during a) 2009 and; b) 2010

7.3.2. Precipitation

The rainfall totals from the Sedge Fen gauge (figure 7.5) show a good agreement with those from the Upware and Stretham gauges until 2002. From 2003 onwards, the precipitation data from Sedge Fen underestimate those from Upware and Stretham.

During the period 1996 – 2002 the Sedge Fen monthly rainfall totals exhibit a good relationship with the monthly averages from Upware and Stretham (table 7.2). A similar relationship was observed during the period 2003 – 2008, in which most regression parameters were similar to those derived for the 1996 – 2002 period. However, the gradient was lower in the latter period than in the former.

These results are indicative of the Sedge Fen rain gauge underestimating the actual rainfall receipt, and are considered further in section 7.4. For the purposes of the subsequent analyses, precipitation data from Upware is assumed to be representative of precipitation at Sedge Fen.

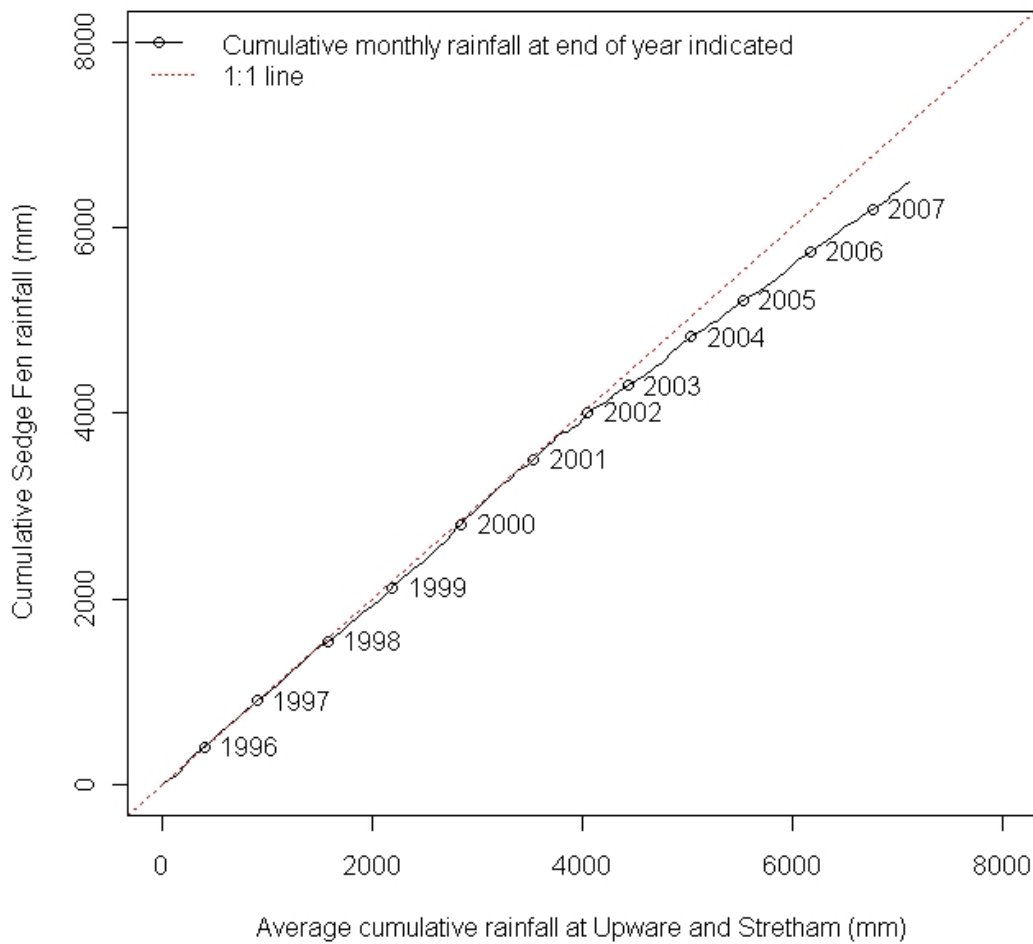


Figure 7.5: Comparison of rainfall data from Sedge Fen and Upware, 1996 – 2008.

Table 7.2: Results of comparison of monthly rainfall totals at Sedge Fen to the average of monthly rainfall recorded at Upware and Stretham

	1996 - 2002	2003 - 2008
Gradient	1.03	0.84
Standard error	0.05	0.04
p-value	<0.01	<0.01
y-intercept	-1.81	-1.87
Standard error	2.67	2.20
p-value	0.50	0.40
R^2	0.86	0.87

The average monthly rainfall at Upware for the period 1994 – 2008 is compared to the average monthly rainfall at Cambridge during the period 1971 - 2000 in table 7.3. The rainfall at Upware is evenly distributed throughout the year, and is representative of that at Cambridge.

Table 7.3: Mean monthly rainfall at Upware (1994 - 2008) and Cambridge (1971 – 2000)

Month	Upware mean (1994 – 2008)	Cambridge mean (1971 – 2000) ³
January	46.6	45.0
February	34.4	32.7
March	34.1	41.5
April	41.5	43.1
May	51.1	44.5
June	47.5	53.8
July	52.5	38.2
August	55.5	48.8
September	49.1	51.0
October	57.7	53.8
November	51.2	51.1
December	45.6	50.0
Total	566.8	553.5

³ <http://www.metoffice.gov.uk/climate/uk/averages/19712000/sites/cambridge.html>

The monthly rainfall totals for 2009 and 2010 are compared to the range of data over the period 1994 – 2008 in figure 7.6. The monthly rainfall data for 2009 are at the lower end of the range defined during the period 1994 – 2008 for most months. Only the July and August data lie within the middle of the range. The 2010 data exhibit the same general trend as the 2009 data, although with higher rainfall occurring in February and August. The August 2010 peak is particularly notable as it represents the largest August rainfall total within the data record

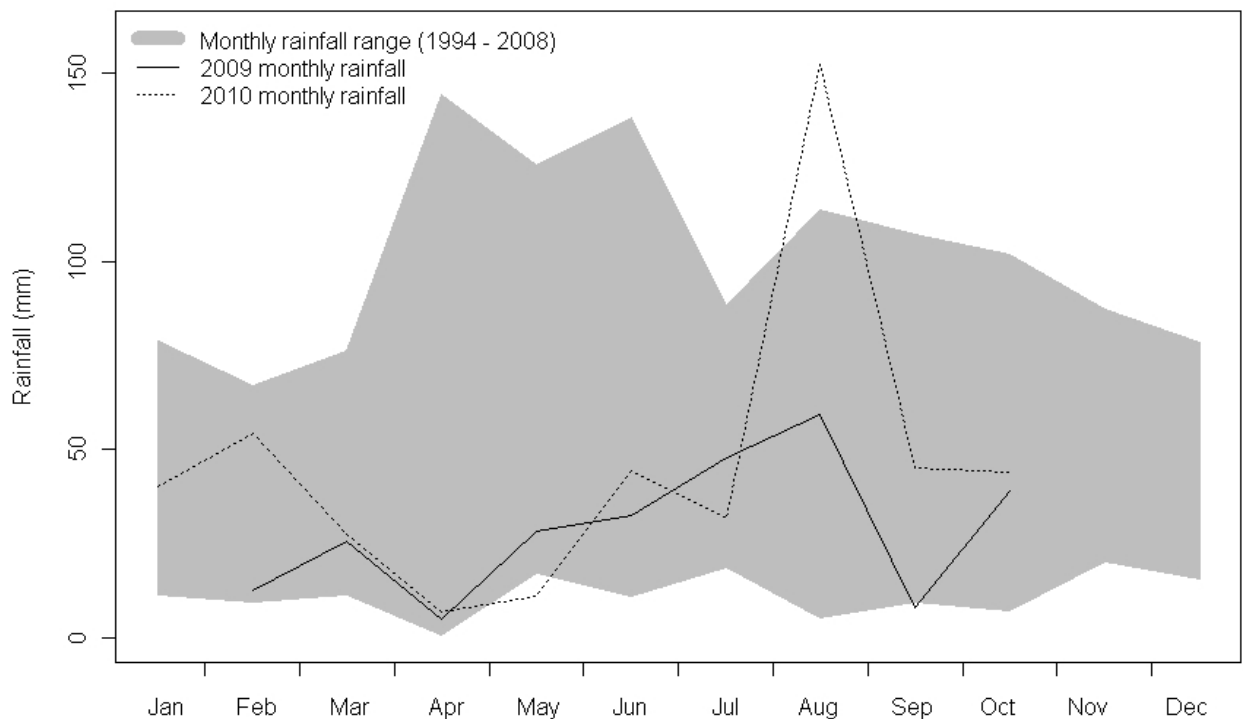


Figure 7.6: Monthly rainfall range 1994 – 2008 and monthly rainfall totals for 2009 and 2010 at Upware. Data courtesy of BADC (2011).

7.3.3. Evapotranspiration

The weekly mean actual and water balance evapotranspiration data for 2009 and 2010 are shown in figure 7.7. During 2009, the evapotranspiration calculated from the

water balance at Sedge Fen generally underestimates the actual evapotranspiration as calculated by the eddy covariance instrumentation. Only for three weeks in 2009 do the two methodologies produce evapotranspiration estimates in agreement with one another. A similar tendency is observed during 2010, although the water balance estimates of evapotranspiration are occasionally greater than the actual evapotranspiration.

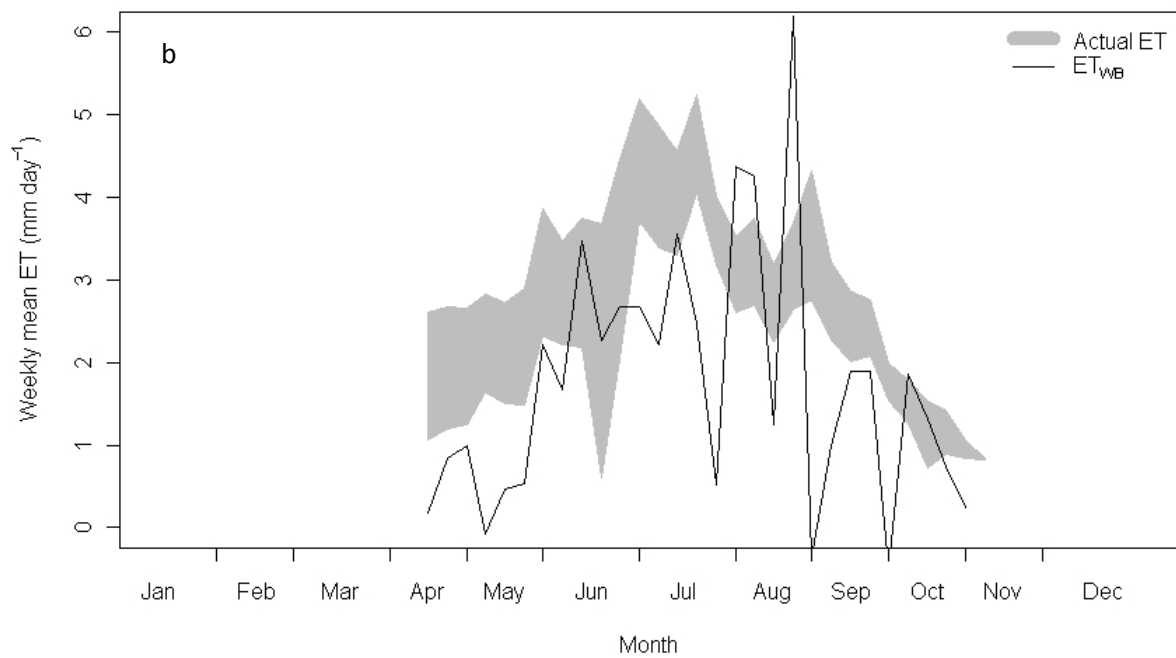
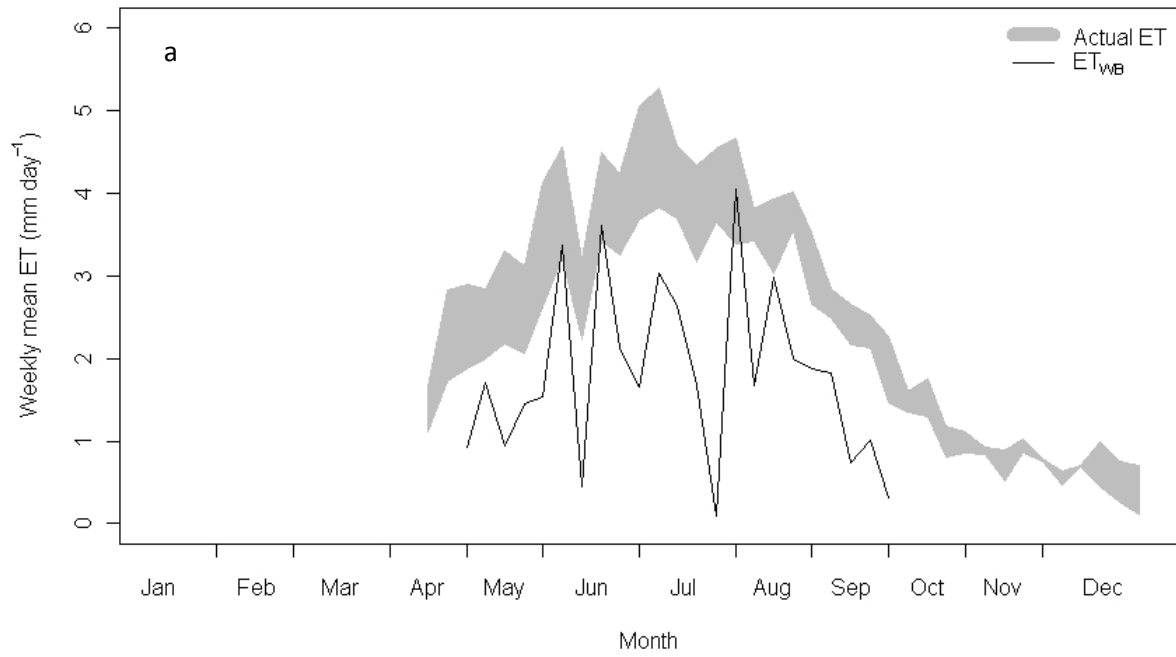


Figure 7.7: Weekly mean actual evapotranspiration as derived by eddy covariance system and estimated evapotranspiration calculated as the residual of the water balance for: a) 2009 and; b) 2010.

The total monthly actual and water balance evapotranspiration data for 2009 and 2010 are summarised in table 7.4. The water balance evapotranspiration estimates are typically lower than actual evapotranspiration calculated by the eddy covariance system, the only exception occurring in August 2010. For most months, the evapotranspiration calculated from the water balance is approximately half that of the actual evapotranspiration, although good approximations to actual evapotranspiration are evident in August and October 2010. During the periods examined, the water balance estimates of evapotranspiration are lower than the actual evapotranspiration data by 241 mm in 2009 and 178.7 mm in 2010.

Table 7.4: Monthly evapotranspiration estimates from eddy covariance system and water balance.

	2009			2010		
	Rainfall	Actual ET	ET _{WB}	Rainfall	Actual ET	ET _{WB}
	(mm)	(mm)	(mm)	(mm)	(mm)	(mm)
April	7.5	21.3	12.1	7.0	42.2	15.5
May	23.2	91.0	48.8	10.9	76.9	29.7
June	32.3	113.1	61.0	44.5	96.0	80.1
July	59.0	127.9	69.4	31.7	124.2	68.2
August	48.2	110.9	69.3	152.2	96.6	101.8
September	8.0	69.3	31.4	46.8	70.8	33.6
October				42.5	32.1	30.5
Total	178.2	533.5	292.0	335.6	538.2	359.5

7.3.4. Sedge Fen Water Budget

The discrepancy between the evapotranspiration data recorded by the eddy covariance system and that derived from the water balance suggests that the Sedge Fen water balance as modelled by McCartney *et al* (2001) is not representative of the actual water balance at Sedge Fen. This may be due to the validity of the assumptions relating to either the value of the specific yield or the movement of water at Sedge Fen. Each of these assumptions is briefly explored within this section.

7.3.4.1. Inflow of Water

The excess of water may be indicative of the movement of water within the soil, implying a flow towards the point at which the dipwell is located. So as to identify whether such an inflow exists at Sedge Fen, the water budget was examined over periods exhibiting no net change in the soil water level. It follows from equation 7.2 that any difference between precipitation and actual evapotranspiration derived by the eddy covariance system over the same period is indicative of either inflow to or discharge from Sedge Fen, depending on the sign of the difference. The results of this analysis are summarised in table 7.5.

Table 7.5: Hydrological fluxes during periods of zero net soil water level change.

Start Date	End Date	No. Days	Precipitation (mm)	Actual Evapotranspiration (mm)	Flow (mm)
5/9/09	31/10/09	55	39.0	95.2	+56.2
2/6/10	30/9/10	121	273.7	383.8	+110.1

During both periods of zero net change in soil water level total evapotranspiration was greater than total precipitation, thus indicating an inflow of water to Sedge Fen. The average rate of inflow was approximately 1 mm d^{-1} during both periods.

Soil water levels on days without rain were also scrutinised. There were 261 dry days between April and September during 2009 and 2010. The water levels on dry days are summarised as hourly mean changes in water level in figure 7.8, and indicate a general trend of falling water levels during the daytime and overnight recovery. The rises in water levels equate to approximately 5 mm d^{-1} .

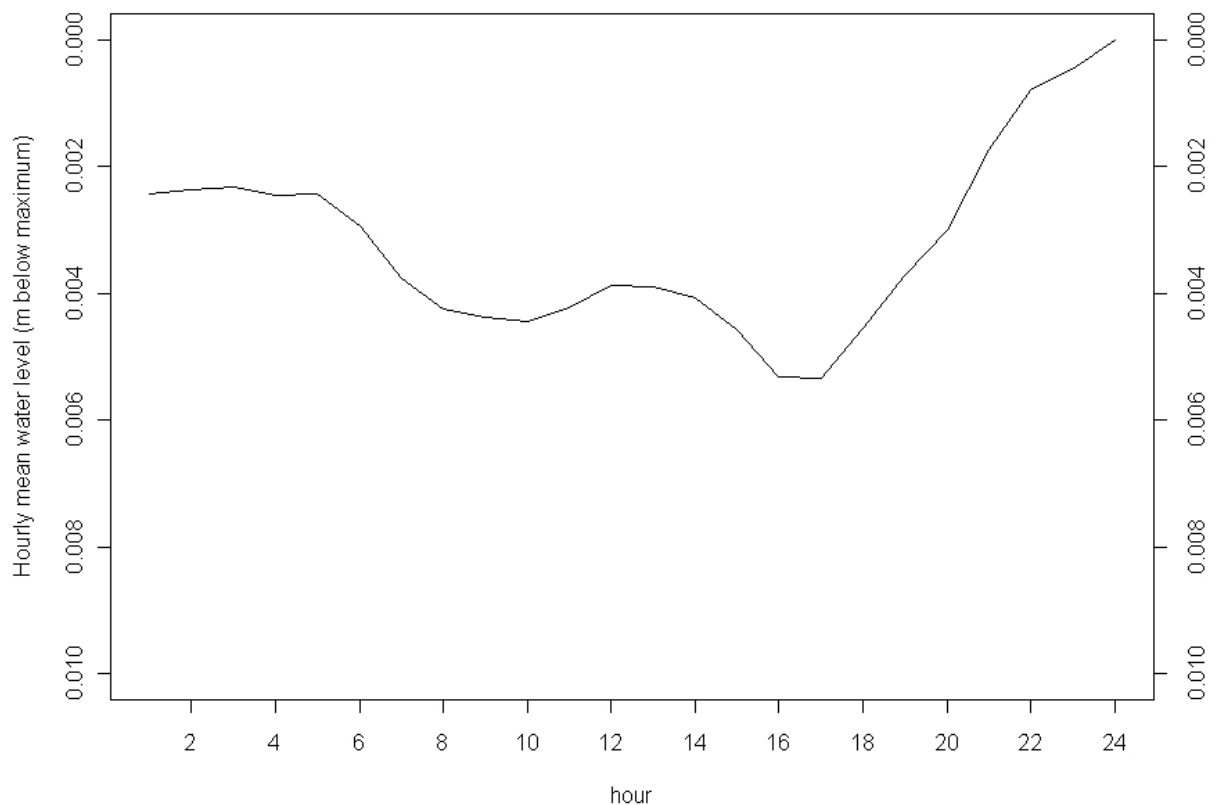


Figure 7.8: Mean hourly water levels at Sedge Fen, April – September 2009 and 2010.

7.3.4.2. Specific Yield

Daily specific yield data were calculated for a 26 day period in September 2009 using a rearranged form of equation 7.2. Evapotranspiration was assumed to be that measured by the eddy covariance system and inflow was assumed to be 1 mm d^{-1} , as derived in section 7.3.4.1. The daily specific yield data derived according to this procedure are shown in figure 7.9. The specific yield values show a large degree of variation and have an average value of 0.21.

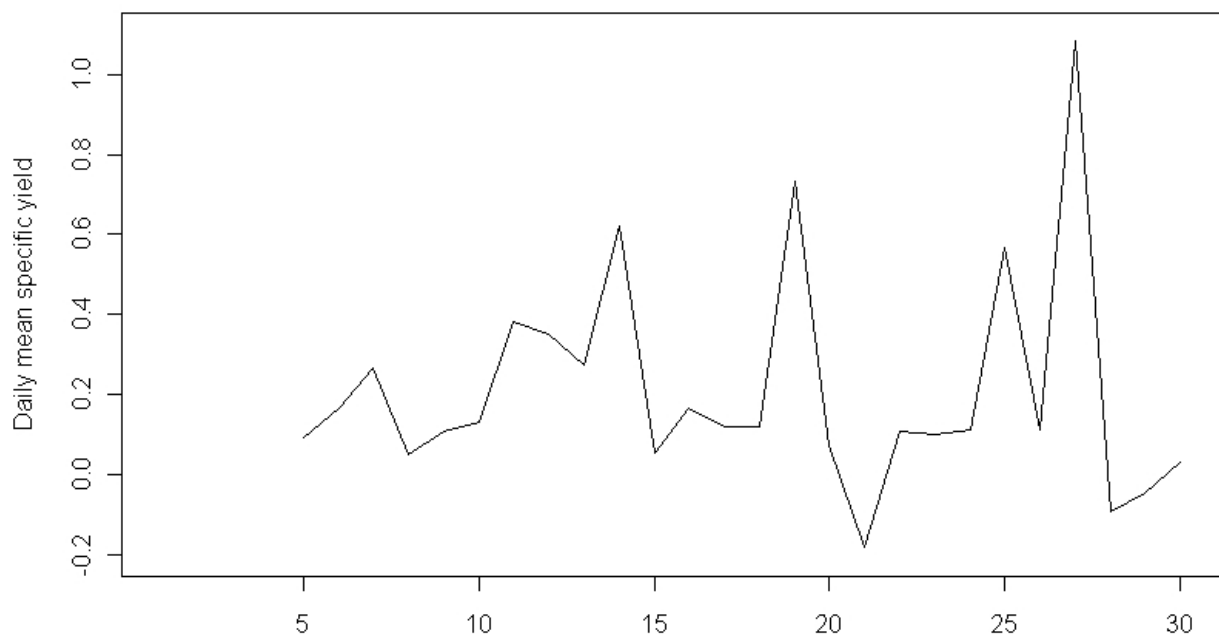


Figure 7.9: Daily specific yield at Sedge Fen, September 2009

7.3.4.3. Revised Evapotranspiration Estimates

The mean rate of inflow and mean specific yield data derived in sections 7.3.4.1 and 7.3.4.2 were used to generate revised estimates of evapotranspiration, $ET_{WB,R}$, based on the Sedge Fen water budget (equation 7.2). These evapotranspiration estimates are

presented alongside those derived from the water balance adopting the assumptions of McCartney *et al* (2001) relating to inflow and specific yield, ET_{WB} (see section 7.3.3) and actual evapotranspiration as measured by the eddy covariance system in table 7.6. The revised water balance evapotranspiration estimates are typically closer to the actual evapotranspiration data than estimates derived according to the assumptions of McCartney *et al* (2001). The revised evapotranspiration estimates are 1.6 mm higher than the data gathered by the eddy covariance system during the period May – September 2009, and 32.8 mm higher during the period April – September 2010.

Table 7.6: Actual evapotranspiration, water balance evapotranspiration estimates according to McCartney *et al* (2001), ET_{WB} , and revised water balance evapotranspiration estimates accounting for inflow and specific yield findings of previous sections, ET_{WB_R} .

	2009			2010		
	Actual ET (mm)	ET_{WB} (mm)	ET_{WB_R} (mm)	Actual ET (mm)	ET_{WB} (mm)	ET_{WB_R} (mm)
April				42.2	15.5	51.9
May	91.0	48.8	98.9	76.9	29.7	74.9
June	113.1	61.0	112.5	96.0	80.1	136.9
July	127.9	69.4	108.3	124.2	68.2	126.5
August	110.9	69.3	116.2	96.6	101.8	95.0
September	69.3	31.4	78.0	70.8	33.6	53.7
Total	512.2	279.9	513.8	506.1	329.0	538.9

7.4. Discussion

The soil water levels for 2009 and 2010 presented within section 7.3.1. reveal that during both years, the behaviour of the water levels is broadly consistent with long term observations, although subject to annual variation. Consideration of monthly rainfall in each year (figure 7.6) reveals an exceptionally large volume of rainfall in August 2010, relative to the long-term averages for both the immediate vicinity and the East Anglian region. It is therefore likely that this large input of water has served to prevent further decline of the Sedge Fen soil water level and to initiate a subsequent recovery. By contrast, the lack of an equivalent rainfall input in 2009 permits further lowering of the water level, a trend which is not reversed until October. This scenario is consistent with the present hydrological understanding of Sedge Fen, in which precipitation is a major input of water to Sedge Fen.

The soil water levels were compared to the surface resistance data described in chapter 5. No relationship was evident from the seasonal behaviour of these two variables, suggesting that the soil water level exerts little or no control over the surface resistance. This contrasts with the findings of Acreman *et al* (2003), who reported a rise in surface resistance as water levels declined for a wet grassland. This may imply that the soil water level does not decline below the root zone of the vegetation at Sedge Fen during 2009 and 2010, and thus drought stress is not experienced. There is therefore no physiological response from the vegetation and so surface resistance is a function of atmospheric variables.

Investigation of precipitation data demonstrated that data collected at Wicken Fen was lower than that observed at nearby rain gauges from 2003 onwards. This coincides with the relocation of the Wicken Fen rain gauge. The current situation of the Wicken Fen rain gauge leaves it susceptible to sheltering by an adjacent section of raised roof (see figure 7.2), providing a possible explanation for the lower rainfall observed at Wicken Fen than at other sites within the locality since 2003. The Upware and Stretham gauges have remained in their present locations since 1983⁴ and 1871⁵, respectively, and are located in accordance with the Met Office guidelines (BADC, 2011). The underestimate is therefore not believed to reflect any changes relating to the situation of either of these gauges. Subsequent analyses within this chapter have proceeded on the assumption that the quality of the Wicken Fen precipitation data is compromised, and so rainfall data from Upware have been used instead of data from the Wicken Fen rain gauge.

Evapotranspiration estimates derived according to the McCartney *et al* (2001) Sedge Fen water budget were shown to underestimate the actual evapotranspiration flux measured by the eddy covariance system. As noted in section 7.3.3, the exception to this trend occurs in August 2010. This exception is attributable to the soil water level change observed during August 2010 not balancing the large quantity of rainfall deposited. Therefore, estimates of evapotranspiration calculated from McCartney *et al*'s (2001) Sedge Fen water budget are likely to underestimate the actual evapotranspiration flux. If the rainfall, soil water level data and actual

⁴ http://badc.nerc.ac.uk/cgi-bin/midas_stations/station_details.cgi.py?id=4510&db=midas_stations

⁵ http://badc.nerc.ac.uk/cgi-bin/midas_stations/station_details.cgi.py?id=4436&db=midas_stations

evapotranspiration data are accepted as being accurate, this suggests that the McCartney *et al* (2001) water budget does not sufficiently describe all hydrological fluxes at Sedge Fen. The relative simplicity of the McCartney *et al* (2001) water budget indicates that inaccuracies can only therefore arise as a result of the application of an inappropriate value of specific yield or the omission of a hydrological input.

Closure of the McCartney *et al* (2001) Sedge Fen water budget was not demonstrated for periods during which there was no net soil water level change, thus implying an inflow of water to Sedge Fen. Any such flow must occur within the peat soil given the general lack of surface water and hydrological isolation of Sedge Fen highlighted in section 7.2.3. The McCartney *et al* (2001) water budget explicitly discounts the existence of water movement within the peat at distances of more than 50 m from ditches. This condition is based upon earlier work at Sedge Fen reported by Godwin and Bharucha (1932) which concludes that water levels are not markedly influenced by ditch water levels at distances of more than 50 m. However, as noted by Gowing (1977), this statement does not imply that there is no flow of water within the peat, rather that the flow that does occur is insufficient to balance the lowering of soil water levels due to evaporative loss. Thus, a transect of Sedge Fen water levels in summer may adopt a concave shape, with the highest levels occurring immediately adjacent to ditches and lowering with increasing distance from the ditch network. Water may flow down this gradient, but in insufficient volume to raise water levels across the entire Fen owing to the low hydraulic conductivity of the peat soil (Godwin and Bharucha, 1932; Gowing, 1977).

Evidence for the existence of a hydraulic gradient at Sedge Fen is revealed by consideration of the water levels in dipwells 9 and 10 (figure 7.4). Dipwell 9 is located approximately 80 m from a ditch and exhibits lower water levels during the summer period than dipwell 10, which is adjacent to the ditch nearest dipwell 9. This is consistent with the concave shape of the summer water table at Sedge Fen described by Godwin and Bharucha (1932). During October 2009 and 2010, water levels in dipwell 9 were shown to be higher than those in dipwell 10. This may be the early part of the winter water level regime described by Godwin and Bharucha (1932), in which the Sedge Fen water table adopts a convex shape. Consequently, the hydraulic gradient is reversed and the ditches serve to drain the interior areas of Sedge Fen. The 2009 and 2010 water level data therefore indicate that seasonal water levels at Sedge Fen still behave as described by Godwin and Bharucha (1932), and therefore provide the hydraulic gradient that is the precondition for the movement of water within the soil.

Consideration of hourly mean water levels on days without rain would seem to support the suggestion of water movement within the soil at Sedge Fen. The filtering of soil water level data to exclude days with rain serves to minimise the likelihood of any rises being attributable to rainfall. However, observed water level rises may occur as the result of gradual infiltration by rainfall deposited on days omitted from the analyses, and this potential source of error must be acknowledged. The mean hourly water level data exhibit a diurnal cycle of drawdown and recovery in both 2009 and 2010. If the drawdown is assumed to represent daily uptake, and subsequent transpiration of, soil water by vegetation, then the recovery must be at least partially representative of the inflow of soil water. Despite this apparent inflow

of water, the soil water level continues to decline due throughout much of the summer (as indicated by figure 7.4). Thus the replenishment of soil water levels due to subsurface inflow is insufficient to replace that lost to vegetative uptake, which is consistent with the assertions of Godwin and Bharucha (1932) and Gowing (1977).

The assumption that the specific yield of the peat soil at Sedge Fen may be represented by a value of 0.12 was also examined, and the average specific yield during September 2009 was calculated as 0.21. The use of this specific yield value within the McCartney *et al* (2001) Sedge Fen water budget (equation 7.2) therefore results in an enhanced sensitivity to the change in soil water levels. As a consequence, evapotranspiration estimates based on the water budget are slightly higher when using a specific yield of 0.21, typically by a magnitude of the order of 20 mm month⁻¹. Consideration of the actual evapotranspiration and estimated evapotranspiration totals presented in table 7.4 demonstrates that the increases in evapotranspiration estimates based on the water budget attributable to the increased specific yield value are insufficient to generate estimates approximating the actual evapotranspiration measurements for most months. Therefore, whilst the estimation of evapotranspiration using the McCartney *et al* (2001) water budget is sensitive to the value of specific yield selected, the response of the evapotranspiration estimates to a higher value of specific yield does not account for the differences between estimated and measured evapotranspiration.

It is acknowledged that the methodology employed within this study to derive a specific yield value differs from that adopted by Gilman (1988), whose value was

subsequently used by McCartney *et al* (2001). Despite this, the specific yield results reported in section 7.3.4.2 are broadly consistent with those reported by Gilman (1988). Gilman (1988) also noted a variation in specific yield values of the Sedge fen peat, with most of the values falling within the range 0.1 – 0.2. An average value of 0.15 was determined by discounting the higher values of specific yield (defined as those values above 0.3) as these were believed to be representative of high water level conditions, in which the open structure of the unhumified peat found near the surface affects the results. Such screening was not performed within this study since the water levels did not approach the surface during the period under consideration (figure 7.4). Gilman (1988) subsequently revised the mean specific yield downwards to 0.12 so as to account for the tendency of the methodology employed to overestimate the derived value of specific yield. Additionally, it was proposed that this value of specific yield be applied only when the soil water level was lower than 0.15 m below ground level. For water levels above this depth, Gilman (1988) assumed specific yield to rise linearly with depth to a value of 0.2 at the surface so as to reflect the increase in soil porosity near the surface. Neither McCartney *et al* (2001) or this study adopted a depth-dependent specific yield. Since much of the evapotranspiration occurs during the months when soil water levels are considerably lower than the critical depth adopted by Gilman (1988), the use of a constant value of specific yield is believed to adequately represent the porosity of the deeper peat soil.

The specific yield value of 0.21 derived within this study therefore describes a more porous soil profile than that of Gilman (1988). This may be attributable to the differing locations on Sedge Fen at which measurements were made – Gilman's (1988) data were recorded in the vicinity of dipwell 15 (figure 7.1) – or due to

structural changes within the peat during the intervening period. However, the differing specific yield values may also be attributed to different methodologies. Ideally, specific yield would be determined by laboratory tests using peat cores removed from Sedge Fen, although the protected status of the site (section 1.1.2) precludes this possibility. All estimates of specific yield must therefore be based on *in situ* measurements and are subject to the associated uncertainties. That the specific yield value derived within this study represents a more porous soil than that derived by Gilman (1988) is consistent with, and a function of, the inflow of water highlighted in section 7.3.4.1.

The lack of closure of the Sedge Fen water budget and consequent underestimation of the actual evapotranspiration when applying the model described by McCartney *et al* (2001) may therefore be attributable to inappropriate assumptions relating to the movement of water within the soil and the specific yield. Consideration of the constant inflow of water from ditches throughout the entire extent of Sedge Fen (as represented by a daily average value) and a higher specific yield results in evapotranspiration estimates consistent with those measured by the eddy covariance system. This result is expected for those periods of zero net soil water level change, since actual evapotranspiration data were used to estimate the mean inflow (table 7.5). Thus the derivation of evapotranspiration estimates based upon the revised water balance represents the inversion of the calculation procedure during these periods. However, the agreements observed between actual evapotranspiration and evapotranspiration estimates based upon the revised water balance between May and August 2009 and April and May 2010 are not subject to this consideration and suggest that the derived value of mean inflow is applicable throughout the study period.

An alternative explanation for the unclosed water budget may be offered by considering the unsaturated zone. This may be defined as the region within the soil above the water table, in which soil pores may retain, but are not filled by, water. The unsaturated zone at Sedge Fen displays a seasonal variation, extending through a greater depth of the soil profile during summer than winter in response to the water levels described in figure 7.4. The vegetation at Sedge Fen may be accessing water stored within the unsaturated zone, and therefore producing evapotranspiration totals higher than anticipated by the water budget approach, which considers only fluxes of water. It is likely that water stored within the unsaturated zone accounts for at least a part of the enhanced evapotranspiration observed at Sedge Fen. Whilst this does not invalidate the proposed revisions to the procedure for estimating evapotranspiration based on the water budget, it does necessitate a reappraisal of the inflow term within the water budget. If some of the additional water is drawn from the unsaturated zone, then the magnitude of the inflow term must be reduced and an additional term included representing vegetative water uptake from the unsaturated zone in order for the Sedge Fen water budget to accurately describe the hydrological functioning of Sedge Fen.

It is acknowledged that the water balance calculations presented within this chapter are based on water level data from a single dipwell. It would be desirable to repeat the analyses performed within this chapter using data from multiple dipwells located at least 50 m from ditches across Sedge Fen. Such an exercise would serve to confirm the validity of the hypothesis relating to subsurface water movement at Sedge Fen. Furthermore, questions relating to the comparability of point evapotranspiration estimates generated from the water budget to the area-averaged eddy covariance

evapotranspiration estimates may be addressed with additional dipwells. However, the only automated dipwell currently recording hourly water level data at Sedge Fen is that from which the data used within this chapter are sourced. Much scope therefore remains for further work based on the methodology applied within this chapter.

7.5. Conclusions

The Wicken Fen rain gauge was shown to underestimate precipitation when compared with gauges located nearby. This is believed to be a systematic error arising from the situation of the rain gauge at Wicken Fen. Water budget calculations for Sedge Fen should therefore be performed using rainfall data from the alternative gauges until such time as the Wicken Fen gauge is appropriately relocated.

Sedge Fen evapotranspiration estimates derived from a simple water budget underestimated actual evapotranspiration data compiled by the eddy covariance system. This deficit may be attributable to assumptions made within the formulation of the water budget; those of no lateral water movement within the peat and the value of specific yield. Examination of the water budget during periods of zero net change in water level provides evidence of inflow, presumably resulting from the water level gradient between areas adjacent to and remote from the ditch network. Further evidence of inflow resulted from the examination of hourly dipwell data. Specific yield values for Sedge Fen were found to be higher than those derived by previous work. Accounting for the mean daily subsurface inflow and specific yield was shown to improve the water budget closure for both 2009 and 2010, although an excess of

water resulted for 2010. Seasonal evapotranspiration estimates for Sedge Fen may therefore be improved by considering the subsurface movement of water.

Chapter 8

Conclusions

This chapter summarises the research undertaken in this thesis and draws conclusions. This is done within the framework of the research questions outlined in section 1.3. Each research question is individually discussed. Consideration is also given to the potential for further research raised by the findings of this study.

8.1. Answering the Research Questions

8.1.1. What is the energy balance at Sedge Fen?

8.1.1.1. Flux Source Area

The flux source areas of the eddy covariance system were modelled and shown to be mostly within the unobstructed fetch at Sedge Fen. For example, 70% of the measured fluxes were estimated to originate within the shortest fetch. This analysis acted as a quality control procedure, serving to confirm that the energy fluxes reported by the eddy covariance system were representative of the Sedge Fen surface. Had large proportions of the flux source areas lain outside the fetch, then this procedure would have allowed for the filtering of data so as to minimise the likelihood of analyses being performed on unrepresentative data.

8.1.1.2. Surface Energy Balance

The energy balance at Sedge Fen was described during 2009 and 2010. A typical wetland energy balance was shown to exist at Sedge Fen, in which most of the incoming radiation was partitioned as latent heat. The latent heat flux accounted for 74% of net radiation flux in 2009 and 54% in 2010. The latent heat flux reflected the seasonal trends of the net radiation. However, data from November and December 2009 revealed that a positive latent heat flux was maintained despite a negative net radiation flux. The negative net radiation flux was not believed to be erroneous but indicative of the emission of longwave radiation from the surface being greater than the shortwave solar radiation receipt. That these observations coincided with negative sensible heat fluxes suggests that the latent heat flux is sustained by energy advected from outside the flux source area. Since the flux source areas encompass most of Sedge Fen, it is likely that energy is being advected in to Sedge Fen from the surrounding land. This effect may therefore act to sustain the evaporative flux (as represented by the latent heat flux) during a period in which no evapotranspiration is often assumed to occur.

The seasonal variations of all fluxes were shown to be statistically significant. The net radiation and ground heat fluxes were shown to behave consistently during the two years for which data were available, suggesting that these fluxes may be characterised as repeating annual cycles and thus predicted. By contrast the sensible and latent heat fluxes did not show consistent annual behaviour, thus negating the potential for reliable prediction of energy partitioning, and thus evapotranspiration, at Sedge Fen according to a prescribed cyclical regime.

8.1.1.3. Energy Budget Closure

The flux data were shown not to close the surface energy budget for Sedge Fen, even when surface storage terms are accounted for. The surface fluxes accounted for 74% of the available energy in 2009 and 67% in 2010. Whilst incomplete energy budget closure is a known limitation of the eddy covariance technique, this has implications for determining the evaporative loss. It is likely that a proportion of the unaccounted energy represents latent heat flux, although the nature of this proportion is impossible to quantify. This was addressed by using the residual energy to define a range of possible latent heat fluxes. This was deemed acceptable within the context of this study as the focus of the investigation was the evaporative flux. It is acknowledged that the same range of uncertainty may equally be applied to the sensible heat flux. Whilst explaining the partitioning of the residual energy is beyond the scope of this study, the assigning of the residual energy to the latent heat flux provides an explicit acknowledgement of the uncertainty associated with the evapotranspiration measurements used within subsequent analyses.

8.1.2. What is the actual evaporative loss from Sedge Fen?

The actual evaporative flux was quantified as the mid-point of the range of evapotranspiration data derived from the latent heat flux. The values defined in this manner were 635.1 mm for the period between April and December 2009 and 541.2 mm between April and October 2010. These values approximate the long-term average annual rainfall for the East Anglian region (table 7.3) and exceed the rainfall measured during the study period (table 7.4). This emphasises the importance of evapotranspiration as a major hydrological flux at Sedge Fen.

8.1.3. How accurately can the evaporative loss at Sedge Fen be modelled?

Eddy covariance evapotranspiration measurements were shown to be higher than reference evapotranspiration estimates at Sedge Fen for most of the study period. Evapotranspiration measurements were 188.6 mm higher than reference evapotranspiration estimates during 2009 and 110.3 mm higher during 2010. The ratio of actual to reference evapotranspiration varies between months and years, averaging 1.42 in 2009 and 1.26 in 2010, thus complicating the application of crop coefficients to reference evapotranspiration estimates at Sedge Fen. However, the trends of the reference evapotranspiration data mirror those of the eddy covariance evapotranspiration measurements, reflecting the known dependence of evapotranspiration on the meteorological variables incorporated within the Penman-Monteith equation. Consideration of the surface variables affecting evapotranspiration (section 8.1.4) results in improved estimates of evapotranspiration relative to the eddy covariance measurements.

Evapotranspiration at Sedge fen has also been modelled as the residual of a simple water balance (section 7.2.3). Evapotranspiration estimates based on the water balance were also shown to underestimate the actual evaporative loss reported by the eddy covariance system by 241.5 mm in 2009 and 178.7 mm in 2010. These differences are comparable with the differences between evapotranspiration measurements and reference evapotranspiration estimates. This has implications for the assumptions made regarding the Sedge Fen water balance (section 8.1.6). Further investigations revealed that the consideration of lateral soil water movement resulted in improved evapotranspiration estimates for Sedge Fen.

8.1.4. What are the controls on the evaporative loss at Sedge Fen, and how can they be modelled?

The meteorological controls on evapotranspiration are well established and are incorporated within the Penman-Monteith equation used to derive reference evapotranspiration estimates within this study. By contrast, the surface controls on evapotranspiration have received little consideration within the literature and are commonly standardised to represent a hypothetical reference surface. Within this study, values of albedo, aerodynamic impedance and bulk surface resistance were derived from meteorological data for Sedge Fen. The average values of albedo and aerodynamic impedance were shown to be lower than those assumed for the reference surface (table 8.1). Although the average values of surface resistance for Sedge Fen were higher than the reference value, the Sedge Fen surface resistance values have been distorted by large values at either end of the growing season (figure 5.4). For much of the growing season, the surface resistance at Sedge Fen is lower than that assumed for the reference surface. This is not surprising since the hypothetical reference surface is parameterised to represent a short uniform grass surface rather than the wetland vegetation community found at Sedge Fen. However, the difference between the Sedge Fen surface characteristics and those of the reference surface offered a possible explanation for the difference between reference evapotranspiration estimates and eddy covariance measurements. The application of the Sedge Fen surface parameters within the Penman-Monteith equation produced evapotranspiration estimates consistent with the eddy covariance measurements.

Table 8.1: Reference surface parameters and average values of surface parameters at Sedge Fen.

	Reference	Sedge Fen	
	Surface	2009	2010
Albedo	0.23	0.17	0.16
Aerodynamic impedance	240.81	62.45	77.19
Surface resistance ($s\ m^{-1}$)	70.00	75.59	75.63

It therefore appears that the potential exists for direct parameterisation of surface variables based upon simple meteorological data. This is advantageous to wetland managers as it allows for improved evapotranspiration estimates utilising data that is likely already being collected. The techniques applied within this study are universally applicable and so are not necessarily limited to wetland environments. It is acknowledged that the techniques used to derive surface parameters require validation for a variety of surfaces. However, their successful derivation and application so as to improve evapotranspiration estimates at Sedge Fen would appear to be an important first step towards Shuttleworth's (1993) proposed "one-step" method of evapotranspiration estimation.

8.1.5. Does Sedge Fen experience a microclimate relative to the surrounding area

which may affect estimates of the evaporative loss?

A wetland microclimate was shown to exist, characterised by lower summer temperatures (by 0.48°C), a larger diurnal temperature range (by 1°C) and higher summer vapour pressures (by $0.08\ \text{kPa}$) at Sedge Fen than outside the wetland. Consideration was given to the possibility of instrumental bias, demonstrating that the

difference in these meteorological variables was not attributable to instrumental factors. The existence of the wetland microclimate results in lower reference evapotranspiration estimates when using meteorological data collected at Sedge Fen compared with those generated using meteorological data from the surrounding area. Although the differences in the reference evapotranspiration are relatively small – being of the order of 30 – 50 mm yr⁻¹ – it would be advisable for hydrological managers to use meteorological data sourced within wetlands when attempting to model wetland evapotranspiration based on meteorological data. Not only will this serve to minimise errors introduced by microclimatic differences, it will also provide data from which representative wetland surface parameters may be modelled (section 8.1.4).

8.1.6. How does the actual evaporative loss affect the current hydrological understanding of Sedge Fen?

Actual evapotranspiration data were used within a simple water budget model of Sedge Fen that described water level fluctuations as a function of rainfall input and evaporative loss. The model was shown to be unbalanced during periods of zero net water level change, indicating the presence of another hydrological flux. The imbalance was attributed to the lateral movement of water within the peat soil, which was previously assumed to be negligible at distances of more than 50 m from irrigation ditches. The lateral movement of soil water was estimated to be equivalent to a rate of 1 mm d⁻¹ towards the interior of the fen.

The lateral movement of soil water at Sedge Fen is likely to be of interest to those attempting to manage the hydrology at this site. Ditch water levels are likely to be more important for stabilising summer soil water levels across Sedge Fen than previously acknowledged. In turn, this will have implications for the desired vegetation community, and so the nature and control of the lateral soil water movements may be fundamental to ongoing conservation efforts at Sedge Fen.

8.2. Conclusions

This study has demonstrated that Sedge Fen exhibits a typical wetland surface energy budget, in that much of the incident energy is partitioned as latent heat flux due to the relatively high moisture content of the surface layer. However, the tendency of the sensible heat flux to become negative during mid-summer indicates the advection of energy towards Sedge Fen. This additional energy input helps to sustain a positive latent heat flux during the autumn and winter months. Therefore, the evapotranspiration at Sedge fen is partially driven by the exchange of energy with the surrounding landscape. This is likely a manifestation of the relatively small areal extent of Sedge Fen (figure 1.3). Larger wetlands will also be subject to such energy exchanges with the surrounding landscape, although this may only occur in peripheral zones. These considerations lead to questions relating to differential energy partitioning at different locations within larger wetlands and whether a threshold wetland area exists at which such effects may become manifest. Such questions are of particular importance within the context of East Anglia given the landscape-scale wetland restoration objectives of projects such as the Wicken Fen Vision and the Great Fen Project.

It has also been demonstrated that evapotranspiration totals are similar during 2009 and 2010, despite a large variation in the precipitation receipt (table 7.4). This suggests that the vegetation at Sedge Fen did not experience drought stress arising from the lower precipitation during 2009 and therefore implies that precipitation is not the principal hydrological input to Sedge Fen. If the assumption of the hydrological isolation of Sedge Fen from a groundwater supply is valid, then abstraction from the River Cam must represent the primary source of water at Sedge Fen. This serves to highlight the importance of hydrological management in fulfilling the wetland conservation objectives at Sedge Fen. Hydrological models of Sedge Fen implicitly incorporate this water supply as a soil water level variable. However, rather than responding to precipitation input soil water levels are principally controlled by the volume of water abstracted from the Cam and made available within the ditch network. At longer timescales this may mean that the water levels, and thus the evapotranspiration loss, at Sedge Fen will not alter in response to changing precipitation climatology provided current management practices continue, although the evapotranspiration loss may vary in response to alterations in other meteorological parameters.

Although precipitation may not be the principal hydrological input at Sedge Fen, the amount of water available within the ditch network may be indirectly dependent on precipitation. Since the Sedge Fen water levels depend on abstraction from the River Cam, the quantity of water available for transfer into the Sedge Fen ditch network will be a function of catchment-scale precipitation input. Although the present

precipitation climatology and catchment-scale hydrology ensure the availability of sufficient quantities of water to satisfy all demands, this may not be the case in a scenario of reduced regional rainfall. The future availability of water resources therefore requires strategic consideration as does the allocation of limited water resources if a shortfall is identified. Such considerations have implications for wetland management and expansion as these undertakings may face stiffer competition from agricultural, industrial and residential demands for the allocation of water resources. Contingency wetland management practices may therefore need to consider the tolerance of the desired communities to alterations in the hydrological regime or even the deliberate realignment of vegetation communities in response to reduced water availability.

8.3. Recommendations for Further Research

In order to further the findings of this study, outstanding research questions remain to be addressed.

The most basic of these is to continue the collection of evapotranspiration data at Sedge Fen. This will permit the findings of this study to be validated for a range of conditions over a longer timescale than the two years presented here. Ultimately, this will serve to improve the robustness of the results. The National Trust and the Centre for Ecology and Hydrology have expressed a desire to retain the eddy covariance system and automatic weather station at Sedge Fen, and it is to be hoped that the data

gathered contributes to further valuable insights into the nature of the evaporative loss from, and the hydrological functioning of, Sedge Fen.

The procedure by which improved evapotranspiration estimates were derived should be applied to other wetland environments. Such an investigation would reveal whether these techniques are universally applicable for the estimation of wetland evapotranspiration. If this inquiry were to be undertaken, archived data from previous studies may be utilised, negating the need for further field measurement campaigns.

The microclimate shown to exist within this study is only representative of the situation at Sedge Fen. Therefore any studies attempting to model wetland evapotranspiration as a function of meteorological data should establish whether a wetland microclimate exists at the study site and whether any microclimate has a significant effect on derivations of reference evapotranspiration. Collectively, such investigations would form a body of research describing the nature of wetland microclimates and whether factors such as wetland type or size affect observed microclimates. Any such studies should give consideration to issues of instrumental bias and ideally instruments located outside of wetlands should be sufficiently near so as not to report climatic differences likely to be attributable to synoptic factors.

The large vapour pressure anomalies observed at Oily Hall during 2010 may be the result of instrumental drift. In order to address this issue, the temperature and relative humidity probes will be retrieved from their field locations and subjected to a further

calibration procedure as described in section 6.2.1. This calibration will form an addendum to this study and provide the context for interpreting the meteorological data gathered at Oily Hall during 2010.

This study has identified the lateral movement of water within the soil at Sedge Fen. However, much work remains to be undertaken in order to describe the magnitude and behaviour of this flux across the entire extent of Sedge Fen. Detailed water level measurements should be taken at several locations across Sedge Fen in order to establish whether the water level data presented within this study are representative of Sedge Fen as a whole. National Trust staff have expressed a desire to expand the current water level monitoring network by deploying automated loggers, and it is to be hoped that the resulting data are of use in informing future modelling of the hydrological functioning of Sedge Fen.

References

- Aboukhaled, A., Alfaro, A. and Smith, M., 1982. *Lysimeters*. FAO Irrigation and Drainage Paper 39.
- Acreman, M. And José, P., 2000. Wetlands. in Acreman, M. (ed). *The Hydrology of the UK: A Study of Change*. Routledge.
- Acreman, M.C., Harding, R.J., Lloyd, C.R. and McNeil, D.D., 2003. Evaporation characteristics of wetlands: Experience from a wet grassland and a reedbed using eddy correlation measurements. *Hydrology and Earth System Sciences*, **7**, 11 – 21.
- Acreman, M.C., Fisher, J., Stratford, C.J., Mould, D.J. and Mountford, M.O., 2007. Hydrological science and wetland restoration: some case studies from Europe. *Hydrology and Earth System Sciences*, **11**, 158 – 169.
- Alavi, N., Warland, J.S., Berg, A.A., 2006. Filling gaps in evapotranspiration measurements for water budget studies: Evaluation of a Kalman filtering approach. *Agricultural and Forest Meteorology*, **141**, 57 – 66.
- Allen, R.G., Pereira, L.S., Raes, D. and Smith, M., 1998. *Crop Evapotranspiration – Guidelines for computing crop water requirements*. FAO Drainage and Irrigation Paper 56. Food and Agriculture Organisation of the United Nations.
<http://www.fao.org/docrep/X0490E/X0490E00.htm>
- Alves, I. and Pereira, L.S., 2000. Modelling surface resistance from climatic variables? *Agricultural Water Management*, **42**, 371 – 385.
- Anglian Water Services Limited, 2007. *Strategic Direction Statement 2010 – 2035*.
- Auble, D.L. and Meyers, T.P., 1991. An open path, fast response infrared absorption gas analyser for H₂O and CO₂. *Boundary-Layer Meteorology*, **59**, 243 – 256.

Bullock, A. and Acreman, M., 2003. The role of wetlands in the hydrological cycle. *Hydrology and Earth System Sciences*, **7**, 358 – 389.

Borin, M., Milani, M., Salvato, M. and Toscano, A., 2011. Evaluation of *Phragmites australis* (Cav.) Trin. Evapotranspiration in Northern and Southern Italy. *Ecological Engineering*, **37**, 721 – 728.

British Atmospheric Data Centre (2011). UK Meteorological Office MIDAS Land Surface Stations Data (1853 – current). Available from http://badc.nerc.ac.uk/view/badc.nerc.ac.uk__ATOM__dataent_ukmo-midas

Brom, J. and Pokorný, J., 2009 Temperature and humidity characteristics of two willow stands, a peaty meadow and a drained pasture and their impact on landscape functioning. *Boreal Environment research*, **14**, 389-403.

Brustaert, W., 2005. *Hydrology: An Introduction*. Cambridge University press.

Burgin, L., 2006. *Evaporation over Otmoor wetlands*. MSc Thesis. University of Reading.

Campbell Scientific, 2006. *Solar Panels: 5, 10 and 18 Watt Models User Guide*. ftp://ftp.campbellsci.com/pub/csl/outgoing/uk/manuals/solarpan_feb06.pdf

Campbell Scientific, 2008a. *CNRI Net Radiometer Instruction Manual*. ftp://ftp.campbellsci.com/pub/csl/outgoing/uk/manuals/cnr1_dec08.pdf

Campbell Scientific, 2008b. *HFP01 Soil Heat Flux Plate User Guide*. ftp://ftp.campbellsci.com/pub/csl/outgoing/uk/manuals/hfp01_apr08.pdf

Campbell Scientific, 2008c. *CR200 Series Datalogger User's Guide*. ftp://ftp.campbellsci.com/pub/csl/outgoing/uk/manuals/cr200_jan08.pdf

Campbell Scientific, 2009a. *HMP45C Temperature and Relative Humidity Probe User Guide*.

ftp://ftp.campbellsci.com/pub/csl/outgoing/uk/manuals/hmp45c_feb09.pdf

Campbell Scientific, 2009b. *Power Supplies User Guide*.

ftp://ftp.campbellsci.com/pub/csl/outgoing/uk/manuals/power_supplies_feb09.pdf

Conway, V.M., 1936. Studies in the Autecology of *Cladium mariscus* R. Br. I. Structure and Development. *New Phytologist*, **35**, 177 – 204.

Conway, V.M., 1938. Studies in the Autecology of *Cladium mariscus* R. Br. V. The Distribution of the Species. *New Phytologist*, **37**, 312 – 328.

Corbet, S.A., Dempster, J.P., Bennett, T.J., Revell, R.J., Smith, C.C., Yeo, P.F., Perry, I., Drane, A.B. and Moore, N.W., 1997. Insects and their Conservation. in Friday, L.E. (ed). *Wicken Fen: The Making of a Wetland Nature Reserve*. Harley. 123 – 143.

Crawford, T.M. and Duchon, C.E. 1999. An Improved Parameterization for Estimating Effective Atmospheric Emissivity for Use in Calculating Daytime Downwelling Longwave Radiation. *Journal of Applied Meteorology*, **38**, 474 – 480.

Crill, P.M., Butler, J.H., Cooper, D.J. and Novelli, P.C., 1995. Standard analytical methods for measuring trace gases in the environment. in Matson, P.A. and Harriss, R.C. (eds). *Biogenic Trace Gases: Measuring Emissions from Soil and Water*. Blackwell. 164 – 205.

Cuerva, A., Sanz-Andrés, A., Navarro, J., 2003. On multiple-path sonic anemometer measurement theory. *Experiments in Fluids*, **34**, 345 – 357.

Darby, H.C., 1983. *The Changing Fenland*. Cambridge University Press.

DeFelice, T.P., 1998. *An Introduction to Meteorological Instrumentation and Measurement*. Prentice Hall.

- Delta-T Devices, 2008. *User Manual for the SunScan Canopy Analysis System Type SS1*.
- Duever, M.J., 1988. Hydrologic Processes for Models of Freshwater Wetlands. in Mitsch, W.J., Straškraba, M. and Jørgensen, S.E. (Eds). *Wetland Modelling*. Elsevier. 9 – 39.
- Dyer, A.J., 1961. Measurements of evaporation and heat transfer in the lower atmosphere by an automatic eddy-correlation technique. *Quarterly Journal of the Royal Meteorological Society*, **87**, 401 – 412.
- Eaton, A.K. and Rouse, W.R., 2001. Controls on evapotranspiration at a subarctic sedge fen. *Hydrological Processes*, **15**, 3423 – 3431.
- Eaton, A.K., Rouse, W.R., Lafleur, P.M., Marsh, P. and Blanken, P.D., 2001. Surface Energy Balance of the Western and Central Canadian Subarctic: Variations in the Energy Balance among Five Major Terrain Types. *Journal of Climate*, **14**, 3692 - 3703
- Fermor, P., 1997. *Establishment of reed bed within a created surface water fen wetland nature reserve*. PhD thesis. University of Birmingham.
- Finch, J.W. and Harding, R.J., 1998. A comparison between reference transpiration and measurements of evaporation for a riparian grassland site. *Hydrology and Earth System Sciences*, **2**, 129 – 136.
- Foken, Th. and Wichura, B., 1996. Tools for quality assessment of surface-based flux measurements. *Agricultural and Forest Meteorology*, **78**, 83 – 105.
- Foken, T., Göckede, M., Mauder, M., Mahrt, L. Amiro, B. And Munger, W., 2004. Post-field data quality control. in Lee, X., Massman, W. and Law, B. (eds) *Handbook of Micrometeorology. A guide for surface flux measurement and analysis*. Kluwer. 181 – 208.

Friday, L.E. (ed), 1997. *Wicken Fen: The Making of a Wetland Nature Reserve*. Harley.

Friday, L.E. and Harvey, H.J., 1997. Sedge, Litter and Drovers. in Friday, L.E. (ed) *Wicken Fen: The making of a wetland nature reserve*. Harley. 60 – 81.

Friday, L.E., Moore, N.W. and Ballard, S.M., 1997. Ecology, Research and Education at Wicken Fen. in Friday, L.E. (ed). *Wicken Fen: The Making of a Wetland Nature Reserve*. Harley. 255 – 276.

Friday, L.E. and Rowell, T.A., 1997. Patterns and Processes. in Friday, L.E. (ed). *Wicken Fen: The Making of a Wetland Nature Reserve*. Harley. 11 – 21.

Gangopadhyaya, M., Harbeck, G.E., Nordenson, T.J., Omar, M.H. and Uryvaev, V.A., 1966. *Measurement and estimation of evaporation and evapotranspiration*. Technical Note No. 83. World Meteorological Organisation

Gardner, C., 1991. *Water regime of river meadows: Yarnton Mead case study. Report to MAFF*. Institute of Hydrology, Wallingford.

Garratt, J.R., 1992. *The Atmospheric Boundary Layer*. Cambridge University Press.

Gasca-Tucker, D. and Acreman, M., 2000 Modelling ditch water levels on the Pevensey Levels wetland, a lowland wet grassland wetland in East Sussex, UK. *Physical Chemistry of the Earth (B)*, **25**, 593-597.

Gasca-Tucker, D.L., Acreman, M.C., Agnew, C.T. and Thompson, J.R., 2007. Estimating evaporation from a wet grassland. *Hydrology and Earth System Sciences*, **11**, 270 – 282.

Gavin, H. and Agnew, C.T., 2003. Evaluating the reliability of point estimates of wetland reference evaporation. *Hydrology and Earth System Sciences*, **7**, 3 – 10.

- Gill Instruments, 2007. *Windmaster Ultrasonic Anemometer User Manual*.
<http://www.gill.co.uk/data/manuals/WindmasterManual.pdf>
- Gill Instruments Ltd, 2009. *Note on Windmaster (Pro) Firmware Upgrade to v110*.
- Gilman, K., 1988. *The Hydrology of Wicken Fen*. Institute of Hydrology.
- Godwin, H., 1929. The “Sedge” and “Litter” of Wicken Fen. *Journal of Ecology*, **17**, 148 – 160.
- Godwin, H., 1931. Studies in the Ecology of Wicken Fen: I. The Ground Water Level of the Fen. *Journal of Ecology*, **19**, 449 – 473.
- Godwin, H. and Bharucha, F.R., 1932. Studies in the Ecology of Wicken Fen: II. The Fen Water Table and its Control of Plant Communities. *The Journal of Ecology*, **20**, 157 – 191.
- Gowing, J.W., 1977. *The Hydrology of Wicken Fen and its Influence on the Acidity of the Soil*. MSc Thesis. Cranfield Institute of Technology
- Hammer, D.E. and Kadlec, R.H., 1986. A model for wetland surface water dynamics *Water Resources Research*, **22**, 1951-1958.
- Harris, L.E., 1953. *Vermuyden and the Fens: A Study of Sir Cornelius Vermuyden*. Cleaver-Hulme Press.
- Hess, T.M., 2002. *AWSET: Potential Evapotranspiration Program for Automatic Weather Stations. Version 3.0*. Cranfield University.
- Hume, C., 2008. *Wetland Vision Technical Document: overview and reporting of project philosophy and technical approach*. The Wetland Vision Partnership.

- Izadifar, Z. and Elshorbagy, A., 2010. Prediction of hourly actual evapotranspiration using neural networks, genetic programming, and statistical models. *Hydrological Processes*, **24**, 3413 – 3425.
- Jacobs, A.F.G., Heusinkveld, B.G., Holtslag, A.A.M., 2008. Towards Closing the Surface Energy Budget of a Mid-latitude Grassland. *Boundary-Layer Meteorology*, **126**, 125 – 136.
- Jones, H.G., 1992. *Plants and Microclimate: A quantitative approach to environmental plant physiology*. (2nd Edition). Cambridge University Press.
- Kellner, E., 2001. Surface energy fluxes and control of evapotranspiration from a Swedish *Sphagnum* mire. *Agricultural and Forest Meteorology*, **110**, 101 – 123.
- Kim, J. and Verma, S.B., 1996. Surface exchange of water vapour between and open *Sphagnum* fen and the atmosphere. *Boundary-Layer Meteorology*, **79**, 243 – 264.
- Kipp & Zonen, 2006. *CMA series Albedometer and CMP series Pyranometer Instruction Manual*.
[http://www.kippzonen.com/?download/72112/CMP+6,+CMP+11,+CMP+21,+CMP+22+Pyranometers+-+Manual+\(English\).aspx](http://www.kippzonen.com/?download/72112/CMP+6,+CMP+11,+CMP+21,+CMP+22+Pyranometers+-+Manual+(English).aspx)
- Lafleur, P.M. and Roulet, N.T., 1992. A comparison of evaporation rates from two fens of the Hudson Bay Lowland. *Aquatic Botany*, **44**, 59 – 69.
- Lafleur, P.M., McCaughey, J.H., Joiner, D.W., Bartlett, P.A. and Jelinski, D.E., 1997. Seasonal trends in energy, water, and carbon dioxide fluxes at a northern boreal wetland. *Journal of Geophysical Research: Atmospheres*, **102**, 29009 – 29020.
- Lee, X., Finnigan, J. And Paw, K.T., 2004. Coordinate systems and flux bias error. in Lee, X., Massman, W. and Law, B. (eds) *Handbook of Micrometeorology. A guide for surface flux measurement and analysis*. Kluwer. 33 – 66.

Li, Y., Zhou, L., Xu, Z. and Zhou, G., 2009. Comparison of water vapour, heat and energy exchanges over agricultural and wetland ecosystems. *Hydrological Processes*, **23**, 2069 – 2080.

Li-Cor Biosciences, 2007. *LI-7500 CO₂/H₂O Analyzer Instruction Manual*.

ftp://ftp.licor.com/perm/env/LI-7500/Manual/LI-7500Manual_V4.pdf

Lock, J.M., Friday, L.E. and Bennett, T.J., 1997. The Management of the Fen. in Friday, L.E. (ed). *Wicken Fen: The Making of a Wetland Nature Reserve*. Harley. 213 – 254.

Maltby, E., 1986. *Waterlogged Wealth*. Earthscan.

Maltby, E., Ormerod, S., Acreman, M., Blackwell, M., Durance, I., Everard, M., Morris, J., Spray, C., Biggs, J., Boon, P., Brierley, B., Brown, L., Burn, A., Clarke, L., Clarke, S., Diack, I., Duigan, C., Dunbar, M., Gilvear, D., Gurnell, A., Jenkins, A., Large, A., Maberly, S., Moss, B., Newman, J., Robertson, A., Ross, M., Rowan, J., Shepherd, M., Skinner, A., Thompson, J., Vaughan, I. and Ward, R., 2011.

Freshwaters – Openwaters, Wetlands and Floodplains. in UNEP World Conservation Monitoring Centre (eds). *UK National Ecosystem Assessment: Technical report*.

<http://uknea.unep-wcmc.org/Resources/tabid/82/Default.aspx>

Mao, L.M., Bergman, M.J. and Tai, C.C., 2002. Evapotranspiration measurement and estimation of three wetland environments in the upper St. Johns River basin, Florida. *Journal of the American Water resources Association*, **38**, 1271 – 1285.

Mauder, M., Liebenthal, C., Göckede, M., Leps, J.P., Beyrich, F. And Foken, T., 2006. Processing and quality control of flux data during LITFASS-2003. *Boundary-Layer Meteorology*, **121**, 67 – 88.

McCartney, M.P., de la Hera, A., Acreman, M.C. and Mountford, O., 2001. *An Investigation of the Water Budget of Wicken Fen*. Centre for Ecology and Hydrology, Wallingford.

Meteorological Office, 1981. *Handbook of Meteorological Instruments Volume 4: Measurement of Surface Wind*. (2nd Edition). HMSO.

Middleton, W.E.K. and Spilhaus, A.F., 1953. *Meteorological Instruments* (3rd Edition). University of Toronto Press.

Mitsch, W.J. and Gosselink, 2000. *Wetlands* (3rd Edition). John Wiley & Sons.

Monteith, J.L., 1965. Evaporation and the Environment. *Symposium of the Society of Experimental Biology*, **19**, 205 – 243.

Monteith, J.L. and Unsworth, M.H., 1990. *Principles of Environmental Physics* (2nd Edition). Edward Arnold.

Moore, C.J., 1986. Frequency response corrections for eddy correlation systems. *Boundary-Layer Meteorology*, **37**, 17 – 35.

Moore, N.W., 1997. The Fenland Reserves. in Friday, L.E. (ed). *Wicken Fen: The Making of a Wetland Nature Reserve*. Harley. 3 – 8.

Mould, D.J., Frahm, E., Salzmann, Th., Miegel, K., Acreman, M.C., 2010. Using diurnal groundwater fluctuations for estimating evapotranspiration in wetland environments: case studies in southeast England and northeast Germany. *Ecohydrology*, **3**, 294 – 305.

Mountford, O., Colston, A. and Lester, M., 2005. Management for diversity: the sedge and litter vegetation at Wicken Fen NNR in 2004. *Nature in Cambridgeshire*, **47**, 15 – 23.

Oke, T.R., 1987. *Boundary Layer Climates*. (2nd Edition). Routledge.

Oncley, S.P., Foken, T., Vogt, R., Kohsiek, W., DeBruin, H.A.R., Bernhofer, C., Christen, A., van Gorsel, E., Grantz, D., Feigenwinter, C., Lehner, I., Liebethal, C., Liu, H., Mauder, M., Pitacco, A., Ribeiro, L. and Weindinger, T., 2007. The Energy Balance Experiment EBEX-2000. Part I: overview and energy balance. *Boundary-Layer Meteorology*, **123**, 1 – 28.

Peacock, C., 2003. *Reedbed Hydrology and Water Requirements*. PhD Thesis. Cranfield University

Peacock, C.E. and Hess, T.M., 2004. Estimating evapotranspiration from a reed bed using the Bowen ration energy balance method. *Hydrological Processes*, **18**, 247 – 260.

Penman, H.L., 1948. Natural evaporation from open water, bare soil and grass. *Proceedings of the Royal Society of London*, **A193**, 120 – 145.

Penman, H.L., 1956. Estimating evaporation. *Transactions, American Geophysical Union*, **37**, 43 – 50.

PP Systems, 2003. *CIRAS-1 Portable Photosynthesis System Operator's Manual Version 1.30*.

Přibáň, K. and Ondok, J.P., 1978 Microclimate and evapotranspiration in two wet grassland communities. *Folia Geobotanica*, **13**, 113-128.

R Foundation for Statistical computing, 2009. *R Version 2.9.0*. Available from <http://www.r-project.org/> (accessed 25th June 2009).

Reichstein, M., Falge, E., Baldocchi, D., Papale, D., Aubinet, M., Berbigier, P., Bernhofer, C., Buchman, N., Gilmanov, T., Granier, A., Grünwald, T., Havránková, K., Ilvesniemi, H., Janous, D., Knohl, A., Laurila, T., Lohila, A., Loustau, D., Matteucci, G., Meyers, T., Miglietta, F., Ourcival, J-M., Pumpanen, J., Rambal, S., Rotenberg, E., Sanz, M., Tenhunen, J., Seufert, G., Vaccari, F., Vesala, T., Yakir, D. and Valentini, R., 2005. On the separation of net ecosystem exchange into assimilation and ecosystem respiration: review and improved algorithm. *Global Change Biology*, **11**, 1424 – 1439.

Rowell, T.A., 1997. The History of the Fen. in Friday, L.E. (ed). *Wicken Fen: The Making of a Wetland Nature Reserve*. Harley. 187 – 212.

Schuepp, P.H., Leclerc, M.Y., Macpherson, J.I., and Desjardins, R.L., 1990. Footprint prediction of scalar fluxes from analytical solutions of the diffusion equation. *Boundary-Layer Meteorology*, **50**, 355 – 373.

Shaw, E.M., 1994. *Hydrology in Practice* (3rd Edition). Chapman and Hall.

Shuttleworth, W.J., 1993. Evaporation. in Maidment, D.R. (Ed). *Handbook of Hydrology*. McGraw-Hill.

Shuttleworth, W.J., 2007. Putting the ‘vap’ into evaporation. *Hydrology and Earth System Sciences*, **11**, 210 – 244.

Smithers, J.C., Donkin, A.D., Lorentz, S.A. and Schulze, R.E., 1995 Uncertainties in estimating evaporation and the water budget of a southern African wetland. in Petts, G. (ed) *Man’s Influence on Freshwater Ecosystems and Water Use*. IAHS Publication 230. 103 – 112.

Souch, C., Wolfe, C.P. and Grimmond, C.S.B., 1996. Wetland evapotranspiration and energy partitioning: Indiana Dunes National Lakeshore. *Journal of Hydrology*, **184**, 189 – 208.

Strangeways, I., 2003. *Measuring the Natural Environment*. (2nd Edition). Cambridge University Press.

Sutcliffe, J.V. and Parks, Y.P., 1999. *The hydrology of the Nile*. IAHS Special Publication no 5. IAHS.

Swinbank, W.C., 1951. The measurement of vertical transfer of heat and water vapour by eddies in the lower atmosphere. *Journal of Meteorology*, **8**, 135 – 145.

Thompson, M.A., Campbell, D.I. and Spronken-Smith, R.A., 1999. Evaporation from natural and modified raised peat bogs in New Zealand. *Agricultural and Forest Meteorology*, **95**, 85 – 98.

University of Edinburgh, 1999. *EdiRe Data Software Version 1.5.0.9*. Available from <http://www.geos.ed.ac.uk/abs/research/micromet/EdiRe/>

Walters, S.M., 1997. Botanical Records and Floristic Studies. in Friday, L.E. (ed). *Wicken Fen: The Making of a Wetland Nature Reserve*. Harley. 101 – 122.

Wallace, J.M and Hobbs, P.V., 2006. *Atmospheric Science: An Introductory Survey* (2nd Edition). Academic Press.

Wang, K. and Liang, S., 2009. Global atmospheric downward longwave radiation over land surface under all-sky conditions from 1973 to 2008. *Journal of Geophysical Research*, **114**, D19101, doi: 10.1029/2009JD011800

Ward, R.C. and Robinson, M., 2000. *Principles of Hydrology* (4th Edition). McGraw-Hill.

Wentworth-Day, J., 1954. *A History of the Fens*. Harrap.

Wheater, C.P. and Cook, P.A., 2000. *Using Statistics to Understand the Environment*. Routledge.

Wilczak, J.M., Oncley, S.P. and Stage, S.A., 2001. Sonic anemometer tilt correction algorithms. *Boundary-Layer Meteorology*, **99**, 127 – 150.

Williams, M., 1990a. Understanding Wetlands. in Williams, M. (Ed) *Wetlands: A Threatened Landscape*. Blackwell. 1 – 41.

Williams, M., 1990b. Agricultural Impacts in Temperate Wetlands. in Williams, M. (Ed) *Wetlands: A Threatened Landscape*. Blackwell. 181 – 216.

Williams, M., 1990c. Protection and Restrospection. in Williams, M. (Ed) *Wetlands: A Threatened Landscape*. Blackwell. 323 – 353.

Wilson, K., Goldstein, A., Falge, E., Aubinet, M., Baldocchi, D., Berbigier, P., Bernhofer, C., Ceulemans, R., Dolman, H., Field, C., Grelle, A., Ibrom, A., Law, B.E., Kowalski, A., Meyers, T., Moncrieff, J., Monson, R., Oechel, W., Tenhunen, J., Valentini, R. and Verma, S., 2002. Energy balance closure at FLUXNET sites. *Agricultural and Forest Meteorology*, **113**, 223 – 243.

Wohlfahrt, G., Haslwanter, A., Hörtnagl, L., Jasoni, R.L., Fenstermaker, L.F., Arnone, J.A. and Hammerle, A., 2009. On the consequences of the energy imbalance for calculating surface conductance to water vapour. *Agricultural and Forest Meteorology*, **149**, 1556 – 1559.

Appendix A

Eddy Covariance System Comparison

A.1. Introduction

An eddy covariance system measures the transfer of energy between the earth's surface and the atmosphere in the form of sensible and latent heat fluxes. The evapotranspiration rate may be derived from the latent heat flux. Alternatively, the transfer of chemical species such as carbon dioxide or methane may be measured by such systems. The theory upon which eddy covariance systems are based requires instrumentation capable of measuring high frequency fluctuations in the variables of interest. The key components of an eddy covariance system are therefore a sonic anemometer to record fluctuations in vertical windspeed and air temperature and an infra-red gas analyser (IRGA) to record fluctuations in chemical species of interest (Oke, 1987).

This paper is concerned with investigating the effects of a faulty sonic anemometer on the sensible and latent heat fluxes derived by an eddy covariance system. Following the release of Gill's "Windmaster" sonic anemometer model, anecdotal evidence emerged of abnormally low sensible heat fluxes collected by an eddy covariance system incorporating a Windmaster anemometer. Subsequent investigation by the manufacturer confirmed initial suspicions of averaging of high frequency (10 Hz and 20 Hz) data to be correct. A firmware coding error was discovered which resulted in the application of a low pass filter to high frequency speed of sound data, and hence

the irretrievable loss of high frequency temperature data. As a response, the firmware was updated to remove the error, although any data collected with the original firmware should be considered suspect (Evans, pers. comm; Gill, 2009).

In June 2008 an eddy covariance system incorporating a Windmaster sonic anemometer was deployed at Wicken Fen, Cambridgeshire. The issues relating to the Windmaster anemometer and the potential effects on derived sensible and latent heat fluxes were therefore of interest and warranted further investigation. This paper reports experimental work attempting to:

- characterise any errors introduced to sensible and latent heat fluxes arising from the use of a faulty sonic anemometer;
- quantify any errors introduced to evapotranspiration rates by use of a faulty sonic anemometer;
- establish whether any suspect flux data collected using a faulty sonic anemometer may be corrected so as to recover representative flux data; and
- independently verify the effectiveness of Gill's firmware upgrade.

A.2. Methods

A.2.1. Experimental set-up

In order to compare the performance of eddy covariance systems incorporating different models of sonic anemometer, three systems were established adjacent to one another at Chimney Meadows, Oxfordshire. The instrumentation was located at

51.72° N, 1.48° W. The vegetation at the site is a mixture of grass and reeds and is used for grazing in the summer months. The eddy covariance systems were sited so as to have the greatest uninterrupted upwind fetch (> 500 m) to the south west, i.e. into the prevailing wind at the site. Although the fetch in all directions is not ideal for micrometeorological measurements, being as short as 40 m to the north, this was not thought to compromise the comparative nature of the experiment since the proximity of the systems ensured that they would be capturing fluxes from the same upwind source area. Data was collected during the period 20th August – 27th September, 2009.

So as to be comparable the eddy covariance systems were identical to one another insofar as possible, with the exception of the model of sonic anemometer used. Table A.1 summarises the constituent sensors of each system. The systems incorporating original and upgraded Windmaster anemometers were compared to a reference system incorporating a Gill R3 anemometer. The R3 is an older sonic anemometer model than the Windmaster. The R3 used within the experiment has been used in several measurement campaigns without report of fault. The calibration history of the R3 was provided and exhibits a consistent response throughout the operational lifetime of the anemometer. The R3 is therefore believed to be a suitable instrument for inclusion in a reference eddy covariance system. There was only one IRGA available for use in this comparison. However, it was possible to merge the high-frequency IRGA data from system C into the raw data files from systems A and B prior to processing so as to allow for the derivation of fluxes from all systems.

Table A.1: Eddy covariance system components

System	A	B	C
Anemometer	Gill R3	Original Windmaster	Upgraded Windmaster
IRGA			LiCor Li-7500
Temp and relative humidity probe	Vaisala HMP45C	Vaisala HMP45C	Vaisala HMP45C
Logger	Campbell CR1000	Campbell CR3000	Campbell CR3000

All loggers ran similar programs to co-ordinate the collection and storage of data from all three systems. The only differences between the programs were the adjustment coefficients and offsets resulting from the sonic temperature calibration described in section A.2.2. The sampling frequency of each system was set at 10 Hz and data were automatically written to CompactFlash cards for ease of retrieval. All three eddy covariance systems shared a common power supply, comprising sixteen 12 V batteries recharged by photovoltaic panels.

A.2.2. Calibration

Prior to the experiment, all anemometers were calibrated by comparing their temperature measurements with those of an independent control thermometer within an environmental chamber. For each anemometer, observations were made between -10 °C and 40 °C, with calibration data being recorded at approximately 5 °C intervals. The instruments were allowed to stabilise for approximately 30 minutes prior to the recording of calibration data. Although this does not span the complete operating range of the anemometers, the calibration range was sufficient for the temperature range expected during the experiment.

The results of the anemometer calibrations are summarised in table A.2. Following the calibration, each logger program was altered to include the appropriate coefficient and offset in order to automatically adjust the temperature readings to account for the response of the respective instruments.

Table A.2: Anemometer temperature calibration results

System	A	B	C
Anemometer	R3	Original Windmaster	Upgraded Windmaster
Multiplier	0.8266	0.7554	0.9969
Offset	-0.8943	3.426	-3.1416
R ²	0.9928	0.9938	0.9849

A.2.3. Post-processing

Those systems without an IRGA did not have the data required to perform the online calculations necessary for the derivation of heat fluxes. The 10 Hz IRGA data from system C was therefore merged into the 10 Hz files of systems A and B by matching the timestamps of the appropriate records. The merged 10 Hz files were then used in a post-processing routine to derive the 30 minute average sensible and latent heat fluxes.

The post-processing routine was validated using data collected at Wicken Fen between 2nd and 29th September, 2008. It should be noted that although these fluxes are based on erroneous Windmaster data (see section A.1), the intention was to ensure that the post-processing of high frequency data replicated that performed onboard the

eddy covariance system and the resulting comparison is therefore independent of the accuracy of the input data.

Table A.3 compares the fluxes derived by post-processing the 10 Hz data to the fluxes compiled online by the eddy covariance system. It can be seen for both the sensible and latent heat fluxes that the post-processed fluxes accurately represent those compiled online. Therefore, the post-processing procedure employed was considered to be free from error and the resulting data an accurate proxy for flux data computed online.

Table A.3: Results of post-processing verification

	Sensible Heat	Latent Heat
Multiplier	1	0.998
Offset	-0.0019	0.0115
R ²	1	1

A.3. Results

A.3.1. Sensible Heat Fluxes

Figure A.1 compares the sensible heat fluxes derived from the original Windmaster system and the upgraded Windmaster system to those derived by the R3 system. The original Windmaster system (system B; figure A.1a) underestimates the sensible heat flux relative to the R3 system (system A). This is consistent with the original reports of inaccuracies in Windmaster sensible heat flux data (see section A.1). The upgraded Windmaster system (system C; figure A.1b) closely agrees with the R3 system,

suggesting that the firmware upgrade has rectified the initial problems with the Windmaster.

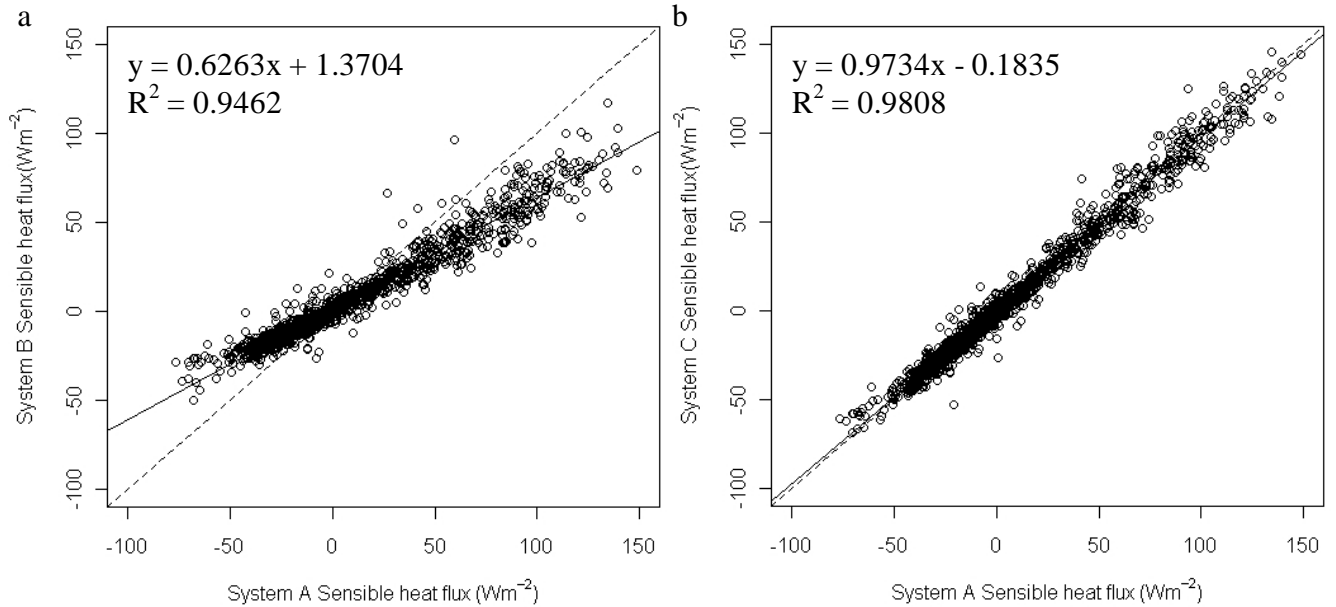


Figure A.1: Comparison of 30-minute averaged sensible heat fluxes from R3 eddy covariance system and: a) Original Windmaster system; b) Upgraded Windmaster system. The solid line represents the line of best fit and the dashed line the 1:1 line.

A.3.2. Latent Heat Fluxes

The latent heat fluxes derived from the original and upgraded Windmaster systems are compared to those derived from the R3 system in figure A.2. The latent heat fluxes from the upgraded Windmaster system (figure A.2b) show a closer agreement with the R3 system than those from the original Windmaster system (figure A.2a). However, the value of the coefficient of determination between the latent heat fluxes of the upgraded Windmaster and R3 systems is not as high as that observed between the sensible heat fluxes derived by these systems.

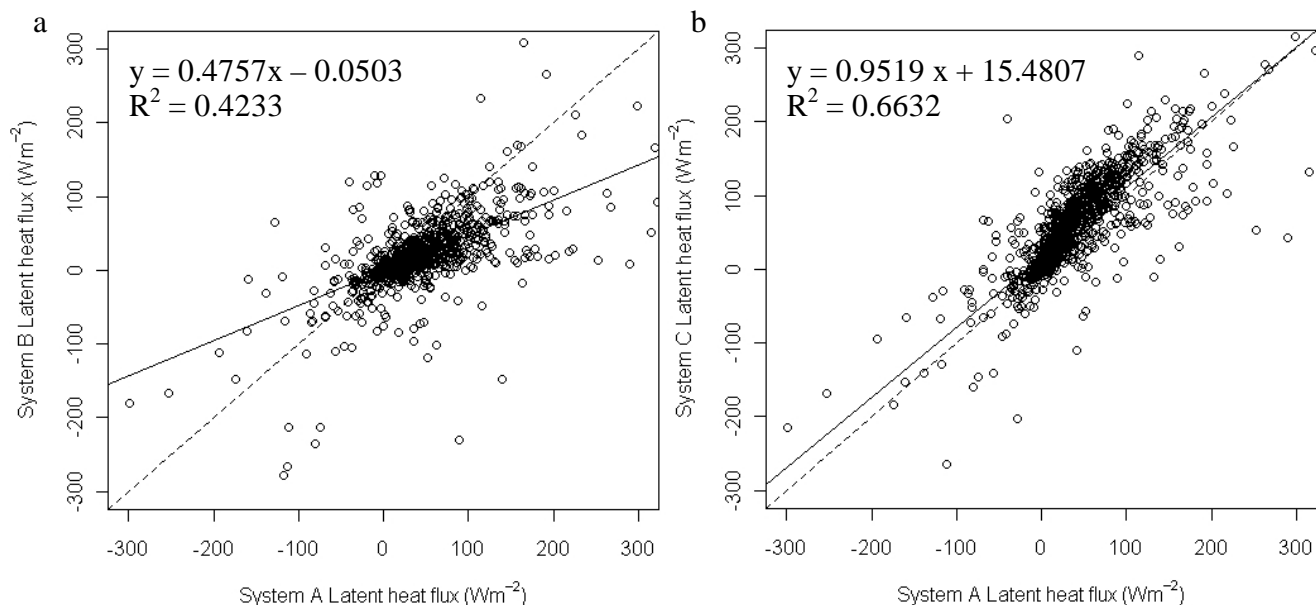


Figure A.2: Comparison of 30-minute averaged latent heat fluxes from R3 eddy covariance system and: a) Original Windmaster system; b) Upgraded Windmaster system. The solid line represents the line of best fit and the dashed line the 1:1 line.

A.3.3. Evapotranspiration Rates

Figure A.3 compares the cumulative daily evapotranspiration totals from all three systems. The evapotranspiration data derived by the original Windmaster underestimate those derived by the R3 system, resulting in a cumulative underestimate of 15.1 mm. The upgraded Windmaster system records higher evapotranspiration rates than both the R3 and original Windmaster systems, resulting in a cumulative overestimate of 16.9 mm relative to the R3 system.

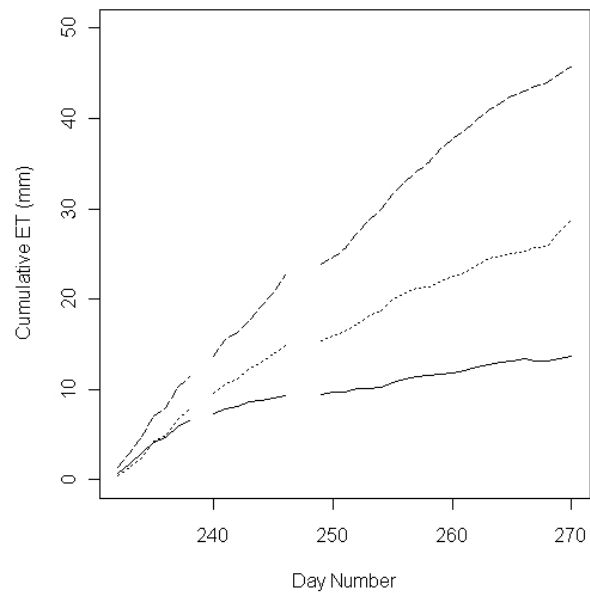


Figure A.3: Cumulative evapotranspiration rates from the K5 system (dotted line), original Windmaster system (solid line) and upgraded Windmaster system (dashed line).

A.3.4. Data Correction

Figure A.4 compares the sensible heat fluxes from the original and upgraded Windmaster systems to one another. There is a statistically significant correlation between the fluxes from each system.

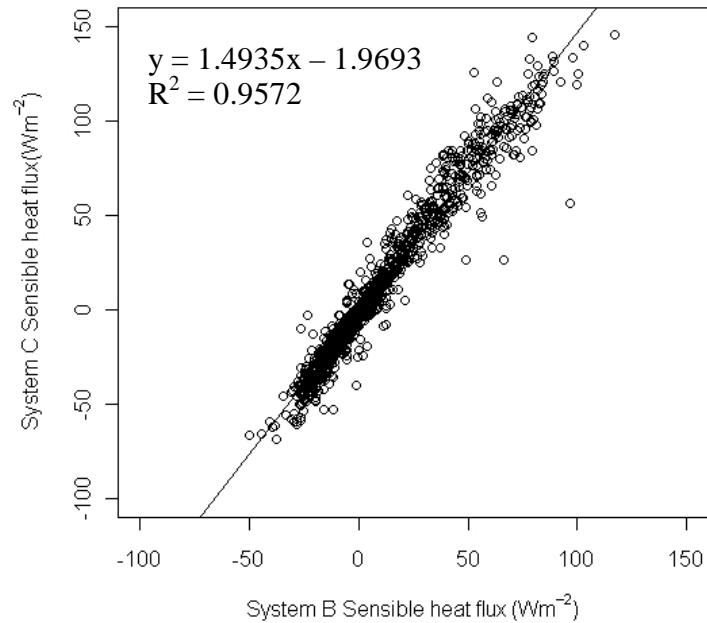


Figure A.4: Comparison of 30-minute averaged sensible heat fluxes from original and upgraded Windmaster eddy covariance systems. The line represents the line of best fit.

Table A.4 presents the cumulative evapotranspiration data displayed as a time series in figure A.4 as comparisons between individual systems. Both the Windmaster systems show distinct and statistically significant relationships with the R3 system.

Table A.4: Results of comparison of cumulative daily evapotranspiration totals with R3 system (system A).

System	B	C
Multiplier	0.4211	1.6875
Offset	2.5566	-1.2132
R ²	0.9677	0.9924

A.4. Conclusions

The disagreement between the sensible and latent heat fluxes collected by the R3 and original Windmaster eddy covariance systems indicates the inaccuracies introduced to flux data by the firmware coding error within the original release of the Windmaster

sonic anemometer. The magnitude of these fluxes is typically underestimated by the original Windmaster system relative to the R3 system. Flux data collected using an original Windmaster should therefore be considered unrepresentative relative to systems incorporating other models of sonic anemometer.

By contrast, the flux data collected by the upgraded Windmaster system compares favourably with the fluxes from the R3 system. In the case of the sensible heat fluxes, the relationship between the two systems is nearly a 1:1 relationship. This finding may be considered an independent verification of Gill's firmware upgrade, and implies systematic error is responsible for the underestimation of sensible heat fluxes by the original Windmaster system. However, despite an improved correlation between latent heat fluxes from the upgraded Windmaster and R3 systems this is not as strong as the correlation between the sensible heat fluxes from the two systems.

The systematic error in sensible heat flux measured by systems incorporating an original Windmaster may be removed using a simple linear correction. This correction offers the possibility of utilising any sensible heat flux data collected using an eddy covariance system incorporating an original Windmaster anemometer. Before applying such a correction, it is advisable to independently verify the above findings so as to ascertain that they are not unique to the instruments or averaging period used within this comparison.

The cumulative evapotranspiration data derived from the latent heat fluxes shows a considerable disagreement between the three systems. The original Windmaster system underestimates the evapotranspiration total derived by the R3 system. This is consistent with the original Windmaster system's tendency to underestimate the latent heat flux. However, the upgraded Windmaster system overestimates the cumulative evapotranspiration total derived by the R3 system. This suggests that despite the firmware modification, evapotranspiration data derived by the upgraded Windmaster system does not accurately approximate that derived by an R3 system.

Whilst it is impossible to assess which of the three systems has generated the most accurate evapotranspiration data on the basis of the data presented here, this finding has implications for the comparability of evapotranspiration data derived by eddy covariance systems incorporating different sonic anemometers. Further work will be necessary so as to determine whether this is a consistent effect, and whether it manifests itself in the other chemical fluxes detected by eddy covariance systems.

This report therefore concludes that flux data derived by eddy covariance systems incorporating an original Windmaster were subject to systematic errors. In the case of sensible heat fluxes, these have been rectified by the firmware upgrade. Furthermore, sensible heat flux data collected using an original Windmaster system may be retrospectively corrected so as to be comparable to upgraded Windmaster sensible heat fluxes and thus allowing the salvaging of previously suspect flux data. However, the differences between cumulative evapotranspiration data suggest that there is another source of systematic disagreement that has not been accounted for. Further

work is recommended in order to further investigate this discrepancy between eddy covariance systems and its implications for the comparability of evapotranspiration data.

Appendix B

The Penman-Monteith Equation

The Penman-Monteith equation applied within this study is as defined by Hess (2002):

$$ET_o = \frac{1}{\Delta + \gamma^*} [ET_{rad} + ET_{aero}] \quad (B.1)$$

$$ET_{rad} = \Delta \left(\frac{R_n - G}{\lambda} \right) \quad (B.2)$$

$$ET_{aero} = \frac{86.4}{\lambda} \frac{\rho C_p}{r_a} (e_a - e_d) \quad (B.3)$$

$$\gamma^* = \gamma \left(1 + \frac{r_s}{r_a} \right) \quad (B.4)$$

Estimates of reference evapotranspiration are explicitly formulated for a hypothetical reference surface defined as having an albedo of 0.23, a height of 0.12 m and a bulk surface resistance of 70 s m^{-1} (Allen *et al*, 1994). The crop height, h (m), is used in the derivation of aerodynamic resistance, r_a :

$$r_a = \frac{\ln[(z-d)/z_{oh}] \ln[(z-d)/z_o]}{k^2 u} \quad (B.5)$$

$$d = \frac{2}{3} h \quad (B.6)$$

$$z_o = 0.12h \quad (B.7)$$

$$z_{oh} = 0.1z_o \quad (B.8)$$

where:

- Δ = Slope of saturation vapour pressure curve (kPa °C⁻¹)
- λ = Latent heat of vapourisation (MJ kg⁻¹)
- ρ = Atmospheric density (kg m⁻³)
- C_p = Specific heat of moist air (1.013 kJ kg⁻¹ °C⁻¹)
- r_a = Aerodynamic resistance (s m⁻¹)
- e_a = Daily mean saturation vapour pressure (kPa)
- e_d = Daily mean vapour pressure (kPa)
- R_n = Net radiation flux (MJ m⁻² d⁻¹)
- G = Ground heat flux (MJ m⁻² d⁻¹)
- γ = Psychrometric constant (kPa °C⁻¹)
- r_s = Bulk surface resistance (s m⁻¹)
- z = Height of windspeed measurement (m)
- d = Height of zero plane displacement (m)
- z_{oh} = Roughness length governing heat and vapour transfer (m)
- z_o = Roughness length governing momentum transfer (m)
- k = Von Karman's constant (0.41)
- u = Windspeed (m s⁻¹)

Appendix C

The Hargreaves Radiation Formulae

$$R_S = K_{R_S} \sqrt{T_{\max} - T_{\min}} R_a \quad (\text{C.1})$$

where:

$$R_a = \frac{24(60)}{\pi} G_{SC} d_r [\omega_S \sin(\varphi) \sin(\delta) + \cos(\varphi) \cos(\delta) \sin(\omega_S)] \quad (\text{C.2})$$

$$d_r = 1 + 0.033 \cos\left(\frac{2\pi}{365} J\right) \quad (\text{C.3})$$

$$\delta = 0.0409 \sin\left(\frac{2\pi}{365} J - 1.39\right) \quad (\text{C.4})$$

$$\omega_S = \arccos[-\tan(\varphi) \tan(\delta)] \quad (\text{C.5})$$

and:

- φ = Latitude (radians)
- J = Julian day number
- δ = Solar declination (radians)
- ω_S = Sunset hour angle (radians)
- d_r = Inverse relative Earth-Sun distance
- G_{SC} = Solar constant ($0.0820 \text{ MJ m}^{-2} \text{ min}^{-1}$)
- R_a = Extraterrestrial radiation ($\text{MJ m}^{-2} \text{ day}^{-1}$)
- R_S = Solar radiation ($\text{MJ m}^{-2} \text{ day}^{-1}$)
- k_{R_S} = Empirical adjustment coefficient ($0.16^\circ\text{C}^{-0.5}$)
- T_{\max} = Daily maximum temperature ($^\circ\text{C}$)
- T_{\min} = Daily minimum temperature ($^\circ\text{C}$)

Appendix D

Relative Humidity Probe Comparison

D.1. Introduction

It has been noted that the enhanced vapour pressure anomaly observed at Oily Hall during summer 2010 relative to that observed during 2009 may be due to instrumental drift (sections 6.4 and 8.2). This section repeats the relative humidity probe comparison described in sections 6.2.1 and 6.3.1 so as to ascertain whether the regression parameters applied to the Oily Hall probe have changed during the data collection period.

D.2. Methods

The temperature and relative humidity probes at Adventurer's Fen and Oily Hall were relocated so as to be adjacent to the probe at Sedge Fen between 15th and 29th July 2011. The 30-minute data gathered by the probes was subjected to the processing described in section 6.2 to generate the results reported within this section. For ease of description the probes shall be referred to according to their previous locations, as in chapter 6.

D.3. Results

The results of the most recent comparison of temperature and relative humidity data from the Adventurer's Fen and Oily Hall probes to that of the Sedge Fen probe are detailed in table D1. Comparison with the results presented in table 6.1 reveal that the regression parameters of all relationships have changed since the original comparison in June 2008. The greatest differences between the 2008 and 2011 regression parameters are in the y-intercepts, and in particular those of the relative humidity regressions.

Table D.1: Results of comparison of half-hourly temperature and relative humidity data from HMP45C probes at Adventurer's Fen and Oily Hall relative to that installed on Sedge Fen.

	Adventurers' Fen		Oily Hall	
	Temperature	Relative Humidity	Temperature	Relative Humidity
Gradient	0.996	0.955	0.999	0.97
Standard error	0.003	0.004	0.005	0.008
p-value	<0.01	<0.01	<0.01	<0.01
y-intercept (°C / %)	0.073	3.536	0.046	7.785
Standard error	0.051	0.307	0.069	0.589
p-value	0.154	<0.01	0.499	<0.01
R ²	0.993	0.99	0.987	0.99

The weekly vapour pressure anomalies at Adventurer's Fen and Oily Hall were calculated using both the 2008 and 2011 regression data, and are presented in figure D.1. The Adventurer's Fen anomalies based on the 2011 regressions show a general

agreement with those based on the 2008 regressions, differing by an average of 0.0024 kPa during the study period. The obvious exceptions are the large variations in the anomalies based upon the 2011 regressions from March to May 2009. By contrast, the Oily Hall vapour pressure anomalies based on the 2011 regressions show a marked disagreement with those based on the 2008 regressions. For the Oily Hall probe, the vapour pressure anomalies based on the 2011 regressions are on average 0.0833 kPa higher than those based on the 2008 regressions. The magnitude of the summer 2010 vapour pressure anomalies at Oily Hall calculated according to the 2011 regressions are comparable with the magnitudes of the summer 2009 anomalies calculated according to the 2008 regressions.

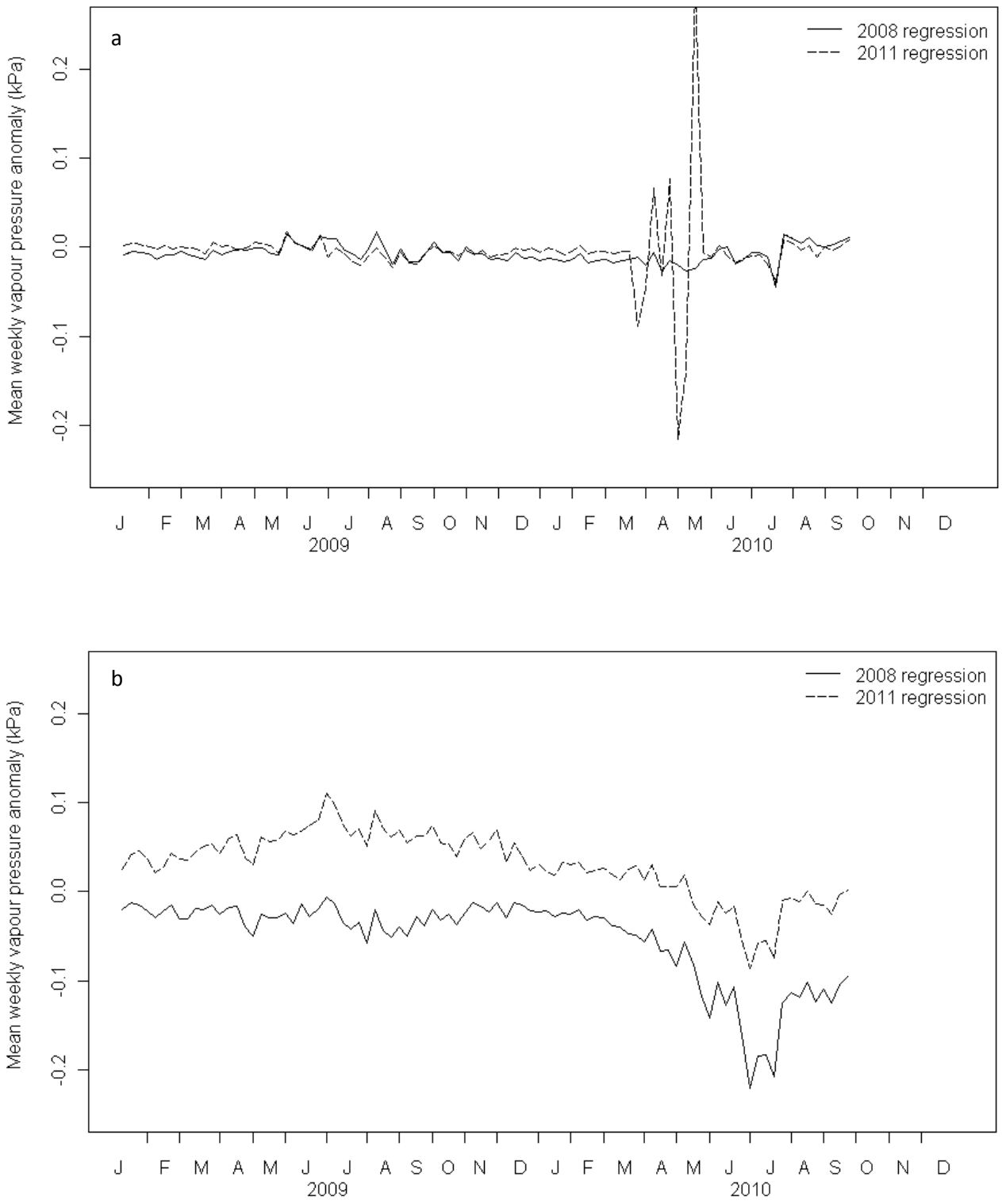


Figure D.1: Comparisons of vapour pressure anomalies relative to Sedge Fen using 2008 regressions (table 6.1) and 2011 regressions (table D.1) for: a) Adventurers Fen and; b) Oily Hall

D.4. Conclusions

The regression parameters derived in chapter 6 to describe the responses of the temperature and relative humidity probes at Adventurer's Fen and Oily Hall relative to the probe at sedge Fen have been shown to alter between 2008 and 2011. This is indicative of an alteration in the response characteristics of either one or both sensors in each pairing during the measurement campaign.

Consideration of the Adventurer's Fen vapour pressure anomalies relative to Sedge Fen reveals that similar anomalies are reported whether the 2008 or 2011 regressions are applied. This indicates that the regression parameters for these probes exhibit stability during the measurement campaign. Overall, this implies that either the response characteristics of both probes remain unaltered, or that the response characteristics of each probe undergo a consistent change. The large variation observed during spring 2010 when applying the 2011 regression to the Adventurer's Fen vapour pressure data coincides with a similar variation in the temperature data when using the same regression parameters. Since the vapour pressure data is derived from temperature data (equations 6.4 and 6.5), it would seem that the large variation of vapour pressure anomalies are attributable to variations of the temperature anomalies.

No such stability is observed within the Oily Hall vapour pressure anomaly data when applying the 2008 and 2011 regression data. The relative responses of the Oily Hall and Sedge Fen probes have therefore altered during the measurement campaign. It is

likely that the response characteristics of the sensors changed gradually, rather than as an instantaneous step change, although positively identifying the rate of this change is impossible on the basis of the data available. Furthermore, the response characteristics may have continued to change between the end of the data collection period in September 2010 and the comparison undertaken in July 2011. However, it is reasonable to assume that the 2008 regression parameters are representative of the earlier part of the data collection period, whilst the 2011 regression parameters are representative of the latter part.

A case may therefore be made for the apparently large negative vapour pressure anomaly observed at Oily Hall during summer 2010 (figure 6.5b) being an artefact of the application of inappropriate regression parameters arising from instrumental drift rather than evidence of a significantly drier atmosphere during this period. This would necessitate the downward revision of the reference evapotranspiration estimate for 2010 at Oily Hall presented in table 6.5 so as to reflect the reduced vapour pressure deficit. However, this does not necessarily imply that the identification of a wetland microclimate at Sedge Fen with respect to summer vapour pressure is erroneous. Given the similarity in the magnitudes of the vapour pressure anomalies at Oily Hall when applying the 2008 regressions to the summer 2009 data and the 2011 regressions to the summer 2010 data, it is feasible that a change in the sensor responses may have occurred during the intervening winter period.